

Understanding the role of *Foxc1* and *Foxc2* in embryonic bone development

by

Asra Almubarak

A thesis submitted in partial fulfillment of the requirements for the degree of

Doctor of Philosophy

Medical Sciences - Medical Genetics  
University of Alberta

© Asra Almubarak, 2022

## Abstract:

Endochondral ossification is a skeletal development process where mesenchymal progenitors differentiate into chondrocytes that will be eventually replaced by bone. Disrupting this process causes skeletal dysplasia. FOXC1 and FOXC2 are two transcription factors of the forkhead box family that express at early stages of endochondral ossification. The similar expression pattern and similar endochondral ossification phenotype observed in *Foxc1* or *Foxc2* mutant mice, indicate a possible compensation between the two genes. Compound *Foxc1* and *Foxc2* mutant mice die *in utero* before any skeletal elements are formed. In order to study the molecular and biological aspects of *Fox1* and *Foxc2* function in endochondral ossification, we employed both *in vitro* and *in vivo* systems. ATDC5 prechondrocytic cells, mouse embryonic stem cells (mESCs) and U2OS osteosarcoma cells were used to investigate molecular function of FOXC1. In addition, we generated two conditional mutant mouse models to study of the role for *Foxc1* and *Foxc2* in skeletal development. First, both *Foxc* genes were deleted in chondrocytes (*Col2-cre;Foxc1<sup>Δ/Δ</sup>;Foxc2<sup>Δ/Δ</sup>*). Second *Foxc1* and *Foxc2* were deleted in condensing limb bud mesenchyme (*Prx1-cre;Foxc1<sup>Δ/Δ</sup>;Foxc2<sup>Δ/Δ</sup>*). Our analysis showed that SRY (sex-determining region Y)-box 9 (SOX9), a master regulatory transcription factor of chondrogenesis directly regulates *Foxc1* expression. We also demonstrated that *Foxc1* overexpression enhances chondrocyte differentiation in mouse embryonic stem cells, while loss of *Foxc1* function inhibits chondrogenesis in ATDC5 cells. Conditional KO of *Foxc1* and *Foxc2* in chondrocytes in mice led to general skeletal dysplasia with preferential abnormality in the axial skeleton including the vertebral column compared to the appendicular skeleton. The long bones were smaller due to a disorganized growth plate, reduced columnar chondrocyte proliferation and impaired mineralization. Moreover, *Col2-cre;Foxc1<sup>Δ/Δ</sup>;Foxc2<sup>Δ/Δ</sup>* mice displayed complete lack of

chondrogenesis in the cervical vertebrae and delayed endochondral development of the thoracic vertebrae. In the intervertebral discs, the anulus fibrosus was not formed and the nucleus pulposus was irregularly shaped.

*Prx1-Cre* conditional deletion of *Foxc1* and *Foxc2* in early limb bud mesenchyme resulted in mice with shorter, bowed limbs that exhibited reduced mineralization, thinner digits, and smaller bone eminences. In the growth plate, absence of both *Foxc* genes impaired the formation of *Ihh* expressing cells which compromised proliferation and lead to a delayed entry into hypertrophy at E14.5. At E16.5, COLX hypertrophic chondrocyte domains were strikingly mineralized and expanded into the primary ossification center of the mutant limb, with disrupted mineralization of the primary ossification center. *Foxc1* and *Foxc2* KO compromised phosphate-regulating gene with homologies to endopeptidases on the X chromosome (*Phex*) expression in the primary ossification center leading to Osteopontin (OPN) stabilization and decreased mineralization.

Previously reported stabilization of  $\beta$ -CATENIN in hypertrophic chondrocytes led to similar growth plate abnormalities to those in *Prx1-cre;Foxc1<sup>Δ/Δ</sup>;Foxc2<sup>Δ/Δ</sup>* mice limbs. *In vitro* analysis addressed the functional association between FOXC1 and  $\beta$ -CATENIN and demonstrated that overexpression of *Foxc1* inhibited  $\beta$ -CATENIN activity in U2OS cells. Moreover, we demonstrate that FOXC1 DNA-binding is required in order to completely inhibit  $\beta$ -CATENIN activity, and not through FOXC1 physical binding with  $\beta$ -CATENIN protein. Our findings suggest that *Foxc1* and *Foxc2* are essential for regulating different aspects of endochondral ossification, and that loss of *Foxc1* and *Foxc2* function impaired the progression of various stages of endochondral ossification in axial and appendicular skeleton.

## **Preface:**

This thesis is an original work by Asra Fouad Almubarak. The research project of which this thesis is a part, received ethics approval from the University of Alberta Animal Policy and Welfare Committee (AUP804). The author has completed all required Lab safety training, in addition to all required animal training set by the Canadian council on Animal care (CCAC) on the care and use of animals in research, teaching and testing.

**Chapter 2** in this thesis has been published under the title “Loss of *Foxc1* and *Foxc2* function in chondroprogenitor cells disrupts endochondral ossification” by the following authors: Asra Almubarak , Rotem Lavy , Nikola Srnica , Yawen Hu , Devi Priyanka Maripuri , Tsutomu Kume, and Fred B. Berry, in the Journal of Biological Chemistry. Volume 297, Issue 3, 101020, September 2021.

Asra Almubarak was responsible for the molecular part in the paper that includes assessing SOX9 overexpression on *Foxc1* and *Foxc2* expression level in mESCs, performing the SOX9 – *Foxc1* enhancers luciferase experiment, *Foxc1* gain of function in mESCs, and *Foxc1* loss of function in ATDC5 cells experiments. Moreover, Asra performed the Western blot, GFP Immunofluorescence and imaging.

Nikola Srnica did the Control, and *Col2-cre* mice skeletal prep. Yawen Hu performed the IF staining of the tibia. Devi Priyanka Maripuri was responsible for analyzing the rib tissue RNA seq data. George Kurian performed ChIP. Tsutomu Kume provided the *Foxc1<sup>fl/fl</sup> ;Foxc2<sup>fl/fl</sup>* mice, and Fred B. Berry was the supervisor, the author, and was responsible for designing the project, performing the RNA scope ISH, and detecting *Foxc1* loss of function via Western blot.

**Chapter 3:** Asra worked on spine sectioning in addition to safranin O staining, Immunofluorescence (IF) and *In situ hybridization*, In addition to the results analysis. Fred Berry collected and dissected the mice.

**Chapter 4:** This chapter is under supervisory revision before submission for publication. This work was mainly performed and written by Asra Almubarak including sections preparation, histological, immunofluorescence, and RNA scope *in situ* hybridization staining. In addition, Asra Almubarak performed all measurements, quantifications and contributed to planning the project and analyzing the results.

Qiuwan Zhang was responsible for the performing, imaging and analyzing *Prx1-cre* skeletal prep work, Cheng-Hai Zhang crossed and generated the *Sox9-Cre* mice and *Prx1-Cre* mice used for preparing the skeletal prep. Andrew B. Lassar is a supervisory author, and he supervised the *Sox9-Cre* and the *Prx1-cre* skeletal prep work. Fred B Berry is a supervisory author, and who dissected some of the *Prx1-cre* mice used in this chapter.

**Chapter 5:** is an original work done by Asra Almubarak and supervised by Fred B Berry.

Christi Li contributed to the pulldown assay with Asra Almubarak.

## **Acknowledgment:**

First and foremost, I would like to express my sincere gratitude to my supervisor Dr. Fred B. Berry for his continuous support, invaluable advice, and patience during my PhD study, particularly during challenging times. His guidance helped me to improve different aspects of my research skills including lab work, writing, presenting, and planing my experiments. I would like to extend my thank to my committee members Professor Daniel Graf, and Dr. Anastassia Voronova for their insightful comments, advice, and continuous support.

Special thank to Professor Andrew J Simmonds for being my candidacy arm's length examiner and allowing me to use his immunofluorescence microscope to show my beautiful and amazing IF results during my work. Many thanks also go to Dr. Jennifer C Hocking for being my candidacy arm's length examiner, and Dr. Rachel Wevrick for being a great graduate students coordinator and my candidacy exam chair.

Many thanks go to Dr. Sarah Hughes for letting me use her LI-COR scanner to visualize all my western blots. I would also like to thank Professor Zhixiang Wang for giving me the opportunity to write a protocol chapter for KI67 IF detection in chondrocytes as part of his book and being the chair of my PhD defence. A special thank to our collaborator professor Andrew B. Lassar and his team for contributing to the *Prx1-Cre* work.

I would like to thank the Ministry of health in Saudi Arabia for sponsoring me financially through the Ministry of Education to help me pursue my PhD degree at the University of Alberta. They provided me with a valuable opportunity to improve my self and grow in a great environment at the University of Alberta.

My heartfelt thanks go to my husband Mohammed Alqanbar for believing and supporting me. My Parents, who encouraged me and provided me with everything I need to reach my goals and become a successful person. Finally, many thanks to my family in law for their continued support and encouragement.

## Table of content:

<b>Abstract</b> .....	<b>ii</b>
<b>Preface</b> .....	<b>iv</b>
<b>Acknowledgments</b> .....	<b>vi</b>
<b>Table of content</b> .....	<b>viii</b>
<b>List of figures</b> .....	<b>xiii</b>
<b>List of Abbreviations</b> .....	<b>xvi</b>
<b>Chapter 1: Introduction</b> .....	<b>1</b>
1.1 literature review .....	1
1.1.1 Skeletal development .....	1
1.1.2 Intramembranous ossification .....	2
1.1.3 Endochondral ossification of the axial skeleton .....	2
1.1.4 Endochondral ossification of the limb .....	3
1.1.5 Signaling pathways involved in Endochondral bone development .....	8
1.1.6 Transcription factors .....	11
1.1.7 The forkhead box family.....	14
1.1.8 The molecular structure of FOXC1 and FOXC2 transcription factors .....	14
1.1.9 FOX transcription factors in skeletal development .....	18
1.1.10 Role of FOXC1 and FOXC2 in developmental disorders .....	19
1.1.11 Skeletal dysplasia .....	21
1.2 Rational and hypothesis .....	23
1.3 Project outline.....	25
<b>Chapter 2: Loss of <i>Foxc1</i> and <i>Foxc2</i> function in chondroprogenitor cells disrupts endochondral ossification</b> .....	<b>26</b>
<b>2.1 Contribution to the experiment</b>	
2.1 Abstract .....	28
2.2 Introduction .....	29

2.3 Results .....	32
2.3.1 SOX9 directly regulates <i>Foxc1</i> expression.....	32
2.3.2 <i>Foxc1</i> regulates chondrocyte differentiation in vitro .....	36
2.3.3 <i>Foxc1</i> and <i>Foxc2</i> are expressed in the perichondrium and the resting zone of the growth plate .....	42
2.3.4 Deletion of <i>Foxc1</i> and <i>Foxc2</i> in chondrocyte progenitors causes skeletal dysplasia .....	46
2.3.5 <i>Foxc1</i> and <i>Foxc2</i> are required for the formation of the growth plate .....	52
2.3.6 Endochondral ossification gene expression is reduced in <i>Col2-cre;Foxc1<sup>Δ/Δ</sup>;Foxc2<sup>Δ/Δ</sup></i> embryos .....	55
2.4 Discussion .....	65
2.5 Experimental procedures .....	71
2.5.1 Cell culture and in vitro differentiation .....	71
2.5.2 RNA isolation and qRT-PCR .....	72
2.5.3 ChIP assays .....	72
2.5.4 Reporter cloning and luciferase assays .....	73
2.5.5 Chondrocyte-differentiation procedures .....	73
2.5.6 Mouse models .....	74
2.5.7 Skeletal preps and analysis .....	75
2.5.8 <i>In situ</i> hybridization .....	75
2.5.9 Immunofluorescence .....	75
2.5.10 RNA-Seq .....	76
2.5.11 Statistical analysis .....	77

<b>Chapter 3: Examination of <i>Foxc1</i> and <i>Foxc2</i> Function in formation of the axial skeleton.....</b>	<b>79</b>
3.1 Introduction .....	81
3.2 Materials and Methods .....	84
3.2.1 Mouse models .....	84
3.2.2 <i>In situ</i> hybridization .....	84

3.2.3	Immunofluorescence .....	84
3.2.4	Safranin O staining .....	84
3.3	Results .....	85
3.3.1	<i>Foxc1</i> and <i>Foxc2</i> expression varies spatially and temporally during embryonic vertebral development .....	85
3.3.2	Conditional <i>Foxc1</i> and <i>Foxc2</i> deletion in the sclerotome blocked initiation of chondrogenesis in the cervical vertebrae .....	88
3.3.3	Delayed endochondral ossification process in the vertebral column by early deletion of <i>Foxc1</i> and <i>Foxc2</i> .....	91
3.3.4	Deletion of <i>Foxc1</i> and <i>Foxc2</i> in the sclerotome compromised vertebral chondrocytes proliferation .....	95
3.4	Discussion .....	98

**Chapter 4: *Foxc1* and *Foxc2* function in osteochondral progenitors for the progression through chondrocyte hypertrophy and mineralization of the primary ossification center** 102

4.1	Abstract .....	104
4.2	Introduction .....	105
4.3	Materials and Methods .....	109
4.3.1	Mouse models .....	109
4.3.2	Tissue preparation .....	109
4.3.3	Safranin O staining .....	110
4.3.4	Alcian blue Von-kossa staining .....	110
4.3.5	TRAP staining .....	110
4.3.6	TUNEL (terminal deoxynucleotidyl transferase dUTP nick end labeling) assay .....	111
4.3.7	<i>In situ</i> hybridization .....	111
4.3.8	Immunofluorescence .....	112
4.4	Results .....	114
4.4.1	Impaired formation of cartilaginous elements in early deletion of	

<i>Foxc1</i> and <i>Foxc2</i> in <i>Sox9-cre</i> expressing cells .....	114
4.4.2 <i>Foxc1</i> and <i>Foxc2</i> regulation of Endochondral ossification varies Spatially and temporally during endochondral bone development .....	121
4.4.3 Loss of <i>Foxc1</i> and <i>Foxc2</i> reduced proliferation activity during early growth plate development .....	124
4.4.4 Loss of <i>Foxc1</i> and <i>Foxc2</i> function expands hypertrophic chondrocyte zone .....	130
4.4.5 Entry and exit from chondrocyte hypertrophy is delayed in <i>Prx1-cre;Foxc1<sup>Δ/Δ</sup>;Foxc2<sup>Δ/Δ</sup></i> mice .....	136
4.4.6 <i>Foxc1</i> and <i>Foxc2</i> are required for proper mineralization and bone formation .....	144
4.4.7 Bone remodeling was compromised by the absence of <i>Foxc1</i> and <i>Foxc2</i> in long bones .....	148
4.4.8 <i>Foxc1</i> is required for <i>Phex</i> expression to maintain bone mineralization .....	152
4.5 Discussion .....	155
4.5.1 <i>Foxc1</i> and <i>Foxc2</i> play overlapping roles in the formation of limb skeleton ....	155
4.5.2 <i>Foxc1</i> and <i>Foxc2</i> function in the limb skeleton preferentially in the distal vs proximal elements .....	156
4.5.3 <i>Foxc1</i> and <i>Foxc2</i> are required at different stages of endochondral ossification	157
4.5.4 <i>Phex</i> expression is reduced in <i>Prx1-cre;Foxc1<sup>Δ/Δ</sup>;Foxc2<sup>Δ/Δ</sup></i> limbs .....	161
<b>Chapter 5: Do <i>Foxc1</i> and <math>\beta</math>-Catenin function together .....</b>	<b>164</b>
5.1 Introduction .....	166
5.2 Materials and Methods .....	170
5.2.1 Cell culture .....	170
5.2.2 Cell transfection and luciferase assay .....	170
5.2.3 Transfection and protein extraction .....	171
5.2.4 Western Blot (Licor Protocol) .....	171
5.2.5 Pulldown assay .....	172
5.2.6 RNA scope <i>in situ</i> hybridization .....	172

5.3 Results .....	173
5.3.1 <i>Foxc1</i> inhibited $\beta$ -CATENIN activity in U2OS cells .....	173
5.3.2 HA-FOXC1 expressing vector activated 6XFOXC1 binding site-luciferase reporter .....	176
5.3.3 FOXC1 inhibited the activity of (non-phosphorylated) active $\beta$ -CATENIN in U2OS cells .....	182
5.3.4 FOXC1 inhibits $\beta$ -CATENIN activity through different means in U2OS cells.	188
5.3.5 GSK inhibition enhanced FOXC1 formation in U2OS cells .....	191
5.3.6 FOXC1 did not bind physically to $\beta$ -CATENIN in U2OS cells .....	194
5.3.7 Loss of FOXC1 function stabilized $\beta$ -CATENIN in ATDC5 cells .....	197
5.3.8 <i>Lef1</i> enhanced activity was identified in E16.5 <i>Prx1-cre;Foxc1<sup>Δ/Δ</sup>;Foxc2<sup>Δ/Δ</sup></i> growth plate .....	200
5.4 Discussion .....	203
<b>Chapter 6: Discussion .....</b>	<b>207</b>
6.1 Discussion and conclusion .....	207
6.2 Limitation and future directions .....	218
<b>References .....</b>	<b>221</b>
<b>Appendices .....</b>	<b>238</b>
Table 2.S1 list of downregulated genes in rib cage RNA isolated from mutant embryos .....	238
Table 2.S2 list of upregulated genes in rib cage RNA isolated from mutant embryos .....	244
Table 2.S3 Statistical analysis of the upregulated genes biological processes .....	266

## List of Figures:

Figure 1.1 Endochondral ossification development process in the growth plate of the limb .....	6
Figure 1.2 FOXC1 and FOXC2 structures .....	16
Figure 2.1. SOX9 regulates expression of <i>Foxc1</i> .....	34
Figure 2.2. Elevated <i>Foxc1</i> promotes chondrocyte differentiation of mouse embryonic stem cells (mES) .....	38
Figure 2.3. Loss of <i>Foxc1</i> expression in ATDC5 cells alters chondrocyte differentiation .....	40
Figure 2.4. <i>Foxc1</i> and <i>Foxc2</i> are expressed in the perichondrium and resting zone of the growth plate .....	44
Figure 2.5. <i>Col2-cre</i> ablation of <i>Foxc1</i> and <i>Foxc2</i> expression in the developing limb .....	48
Figure 2.6. <i>Col2-cre</i> deletion of <i>Foxc1</i> and <i>Foxc2</i> causes skeletal hypoplasia .....	50
Figure 2.7. Disrupted growth plate organization in <i>Col2-cre;Foxc1<sup>Δ/Δ</sup>;Foxc2<sup>Δ/Δ</sup></i> mutants .....	53
Figure 2.8. Loss of <i>Foxc1</i> and <i>Foxc2</i> function in chondrocytes results in a general reduction of mRNA levels of genes expressed throughout endochondral ossification .....	57
Figure 2.9. Altered chondrocyte differentiation in <i>Col2-cre; Foxc1<sup>Δ/Δ</sup>;Foxc2<sup>Δ/Δ</sup></i> Embryos .....	60
Figure 2.10. Impaired mineralization in <i>Col2-cre;Foxc1<sup>Δ/Δ</sup>;Foxc2<sup>Δ/Δ</sup></i> mutants .....	63
Figure 3.1. <i>Foxc1</i> and <i>Foxc2</i> have a similar expression pattern that undergo temporal changes in the vertebrae .....	86
Figure 3.2. Less cartilage formed in the vertebral column in the absence of <i>Foxc1</i> and <i>Foxc2</i> genes .....	89
Figure 3.3 Deletion of <i>Foxc1</i> and <i>Foxc2</i> block endochondral ossification in the cervical vertebrae .....	93
Figure 3.4. Thoracic vertebrae have fewer proliferating cells in the absence of <i>Foxc1</i> and <i>Foxc2</i> function .....	96
Supplementary Figure 4.S1. <i>Foxc1</i> and <i>Foxc2</i> share redundant roles to promote axial chondrogenesis .....	115

Figure 4.1. <i>Foxc1</i> and <i>Foxc2</i> play critical roles in the formation of both the distal regions of the appendicular skeleton and support the growth of the bone eminences .....	119
Figure 4.2. <i>Foxc1</i> and <i>Foxc2</i> expression varies spatially and temporally during embryonic bone development .....	122
Figure 4.3. <i>Foxc1</i> and <i>Foxc2</i> KO cause decreased chondrocytes proliferation at E14.5 .....	125
Figure 4.4. Deletion of <i>Foxc1</i> and <i>Foxc2</i> affected the formation of <i>Ihh</i> expression Chondrocytes .....	128
Supplementary Figure 4.S2. Deletion of <i>Foxc1</i> and <i>Foxc2</i> did not block Chondrogenesis .....	131
Figure 4.5. Early deletion of <i>Foxc1</i> and <i>Foxc2</i> disrupted terminal endochondral ossification process .....	134
Supplementary Figure 4.S3. Absence of <i>Foxc1</i> and <i>Foxc2</i> did not alter the developmental rate of COL2 Positive chondrocytes in the growth plate .....	137
Figure 4.6. Early <i>Foxc1</i> and <i>Foxc2</i> deletion caused a delay in entry and exit from hypertrophy, causing formation of a small primary ossification center at later time points .....	139
Figure 4.7. <i>Foxc1</i> and <i>Foxc2</i> KO did not promote cellular apoptosis within the Growth plate chondrocytes .....	142
Figure 4.8. Lack of <i>Foxc1</i> and <i>Foxc2</i> affected endochondral mineralization and bone formation .....	146
Figure 4.9. Absence of <i>Foxc1</i> and <i>Foxc2</i> in the lateral plate mesoderm had a detrimental effect on bone remodeling process .....	150
Figure 4.10. <i>Phex</i> expression was compromised by the absence of <i>Foxc1</i> and <i>Foxc2</i> .....	153
Figure 5.1. Transfection of FOXC1 expression vector reduced TOPFlash activity.....	174
Figure 5.2. HA-FOXC1 vector activated the 6X FOXC1 binding site-luciferase reporter in U2OS cells .....	177
Figure 5.3 Transfected HA-FOXC1 vector was functional in U2OS cells .....	180
Figure 5.4. Transfected FOXC1 expressing vector inhibited TOPFlash activity in WT- $\beta$ -CATENIN and S33Y transfected U2OS cells .....	183

Figure 5.5 Transfection of FOXC1 vector had a negative effect on FLAG- $\beta$ -CATENIN and FLAG-S33Y protein levels in U2OS cells .....	186
Figure 5.6. FOXC1 needs to bind DNA to block $\beta$ -CATENIN activity .....	189
Figure 5.7. More FOXC1 was made when GSK was inhibited by CHIR .....	192
Figure 5.8. No physical binding between FOXC1 and $\beta$ -CATENIN in U2OS cells .....	195
Figure 5.9 Crisper <i>Foxc1</i> deletion stabilized $\beta$ -CATENIN in ATDC5 pre-chondrocytes treated with CHIR .....	198
Figure 5.10. Absence of FOXC1 function enhanced <i>Lef</i> localization in E16.5 <i>Prx1-cre</i> ; <i>Foxc1</i> <sup><math>\Delta/\Delta</math></sup> ; <i>Foxc2</i> <sup><math>\Delta/\Delta</math></sup> growth plate compared to the control .....	201
Figure 6.1 Summary of <i>Prx1-cre</i> ; <i>Foxc1</i> <sup><math>\Delta/\Delta</math></sup> ; <i>Foxc2</i> <sup><math>\Delta/\Delta</math></sup> growth plate phenotypes .....	212

## List of abbreviations:

AD: Activation domain  
AF: Annulus fibrosus  
APC: Adenomatosis polyposis coli  
AER: Apical ectodermal ridge  
BMP: Bone morphogenetic proteins  
BrdU: Bromodeoxyuridine / 5-bromo-2'-deoxyuridine  
ChIP: Chromatin immunoprecipitation  
CAR: Chimeric antigen receptor  
CC: Columnar chondrocytes  
CCD: Cleidocranial dysostosis or Cleidocranial dysostosis  
crFOXC1: Crispr mutated Foxc1  
COL2/Col2a: Collagen type II alpha 1  
COLX/Col10 : Collagen, type X, alpha 1  
CXCL12: C-X-C Motif Chemokine Ligand 12  
DHH: Desert hedgehog  
DKK: Dkkopf  
DNA: Deoxyribonucleic acid  
Dox: Doxycycline  
Dpc: Days post coitum  
E: embryonic day  
EDTA: Ethylenediaminetetraacetic acid  
EGFP: Enhanced GFP  
ERK1/2: Extracellular signal-regulated kinase type 1 and 2  
EV: Empty vector  
FBS: Fetal bovine serum  
FGF: Fibroblast growth factor  
*Fgfr1*: Fibroblast Growth Factor Receptor 1  
*Fgfr3*: Fibroblast Growth Factor Receptor 3  
FHD: fork-head domain

*Fkh*: fork-head  
FOX, fork-head box  
FRS2 $\alpha$ : FGFR substrate 2 $\alpha$   
Fzd: Transmembrane receptors Frizzled  
GSK3 $\beta$ : Glycogen synthase kinase 3 $\beta$   
HC/H: Hypertrophic chondrocytes  
IF: Immunofluorescence  
ID: inhibition domain  
IDT: Integrated DNA Technologies  
IHH: Indian hedgehog  
I-Smad: Inhibitory Smad  
*Ibsp*: Integrin Binding Sialoprotein  
KI67: Marker of Proliferation Ki-67  
KO: Knockout  
*Krm*: Kremen  
LEF1: Lymphoid Enhancer Binding Factor 1  
LRP-5 : Receptors lipoprotein-related protein 5  
LRP-6: Receptors lipoprotein-related protein 6  
MAPK: A mitogen-activated protein kinase  
mESCs: Mouse embryonic stem cells  
Mmp13: Matrix metalloproteinase 13  
mTOR: Mammalian target of rapamycin  
NP: Nucleus pulposus  
OMIM: Online Mendelian Inheritance in Man  
OSX/SP7: Osterix  
OPN: Osteopontin  
P38 MAPK: p38 mitogen-activated protein kinases  
PBS: Phosphate-buffered saline  
PBST: Phosphate-buffered saline with tween 20  
PBSX Phosphate-buffered saline with triton x-100  
PHC: Pre-hypertrophic chondrocytes

PHEX: Phosphate Regulating Endopeptidase Homolog X-Linked  
PI3K: Phosphatidylinositol 3-kinase  
PLC $\gamma$ : Phospholipase C Gamma  
POC: Primary ossification center  
Ptch1: Multitransmembrane protein Patched type 1  
Ptch 2: Multitransmembrane protein Patched type 2  
Pth1r: Type 1 receptor for parathyroid hormone  
PTHrP: Parathyroid hormone-related protein  
qRTPCR: Quantitative reverse transcriptase PCR  
RNA: Ribonucleic acid  
RNA-seq: Ribonucleic acid sequencing  
R-Smad: regulatory Smad  
Runx2: Runt related transcription factor 2  
RZ: Resting zone  
SDS-PAGE  
SHH: Sonic hedgehog  
STAT1: Signal transducer and activator of transcription 1  
SMO: Smoothened  
SOX5/6/9: SRY (sex-determining region Y)-box 5/6/9  
*Spp1*: Secreted Phosphoprotein 1  
SUMO: Small Ubiquitin-related Modifier protein  
TUNEL: Terminal deoxynucleotidyl transferase dUTP nick end labeling  
TBS: Tris-buffered saline WB: western blot  
TCF: T-cell factor  
TGF: Transforming growth factor  
TGFR: Transforming growth factor receptor  
TRAP: Tartrate resistant acid phosphatase  
Tris-HCL: Tris hydrochloride  
VEGFA: Vascular endothelial growth factor A  
WIF-1: Wnt inhibitory factor 1  
WNT: Wingless-related integration sit

## **Chapter 1:**

### **1.1 Literature review:**

#### 1.1.1 Skeletal development:

The skeletal system is one of the main and important organ systems that support the body and allows our movement. It acts as a protective layer for vital organs such as the brain, the spinal cord, bone marrow and the heart. Additionally, it acts as the main reservoir for many minerals such as calcium, and phosphorus(Su et al., 2019). In vertebrates, skeletal development proceeds through two mechanisms: endochondral or intramembranous ossification. Cranial bones of the skull, flat bones of the face, and the clavicles forms through intramembranous ossification where bones are formed directly from the differentiation of mesenchyme progenitors into osteoblasts (Franz-Odendaal, 2011). On the other hand, the hip bone, ribs, vertebrae and limb bones such as tibia, femur, and radius, develop through endochondral ossification (Yeung Tsang et al., 2014).

The cells that form the skeleton arise from a number of developmental sources. Skeletal development starts during embryonic development. In this process, the double layered blastula will first develop into a triple-layered gastrula consisting of the endoderm, the mesoderm, and the ectoderm in a process called gastrulation(Docherty, 2007). At this time, the notochord will form and will be surrounded by additional mesoderm cells that will separate into three regions: the paraxial, intermediate, and lateral plate mesoderm. The intermediate mesoderm will form the urogenital organ system. The lateral plate mesoderm will contribute to the formation of many other system including the pulmonary, cardiac and the limb skeleton. The paraxial mesoderm on the other hand is responsible for developing the axial skeleton, including the ribs and the vertebra, as well as the trunk musculature and dermis (DeSai et al., 2022). Moreover, neural crest cells will

form the neural plate border after the ectoderm layer folds to form the neural tube during neurulation. Neural crest cells are located between the dorsal neural tube and the ectoderm. These cells will migrate to the periphery and form various tissues including most of the skull bone elements (Docherty, 2007; Kalamchi and Valle, 2022; Williams et al., 2019).

#### 1.1.2 Intramembranous ossification:

Intramembranous ossification forms the flat bones in the skull. During early embryogenesis, mesenchymal cells originating from the cephalic paraxial mesoderm and the neural crest will multiply and condense into dense nodules where they will differentiate into bone progenitor cells called osteoblasts (Couly et al., 1992). Then, osteoblasts produce a collagen-proteoglycan matrix that binds to calcium. Calcium binding will facilitate calcification of the pre-boned matrix (osteoid). Some osteoblasts will be trapped in the calcified matrix and become mature bone cells (osteocytes) that will help the bone to ossify. Other osteoblasts will flank the ossified layer with an osteoid matrix they form. The calcified matrix will be coated with mesenchymal cells that will form a membranous layer called the periosteum, where the inner part of the mesenchymal cells differentiates into more osteoblasts that will form a parallel layer to the previously made calcified spicules. This process allows the formation of many protective layers of bone in the skull (Berendsen and Olsen, 2015).

#### 1.1.3 Endochondral ossification of the axial skeleton

The paraxial mesoderm flanks and develops simultaneously with the neural that will form the central nervous system, during early fetal development. Here, the paraxial mesoderm will develop pairs of somites that forms along both sides of the neural tube in a craniocaudal direction

(Docherty, 2007; Kaplan et al., 2005; Williams et al., 2019). The somites will then convert into dermomyotome, sclerotome and syndetome. The dermomyotome will contribute to the formation of the skin and muscles, the syndetome will form tendons, while the sclerotome cells will migrate as two different groups of cells around the notochord. The vertebral body forms when the cranial side of a sclerotome merges with the nearby caudal sclerotome cluster. Moreover, sclerotome cells also surround and fuse to the dorsal side of the neural tube to form the vertebral arches that act as a protective layer of the spinal cord (Kalamchi and Valle, 2022; Kaplan et al., 2005). Between each vertebra is an intervertebral disc composed of the nucleus pulposus and annulus fibrosus, formed from the notochord and from the sclerotome, respectively (Ward et al., 2018).

#### 1.1.4 Endochondral ossification of the limb

Long bones develop from the lateral plate mesoderm cells that convert into condensing mesenchymal progenitors with the limb bud that will divide into multiple distinctive cell populations (Mangiavini et al., 2016). A SOX9-positive population differentiates into chondroprogenitor cells to form a cartilaginous template. RUNX2-positive osteoprogenitors surround the SOX9 population and contribute to the formation of the perichondrium and the periosteum (Colnot et al., 2004). The chondroprogenitor cells will differentiate and form an organized structure composed of layers of cells called the growth plate (Fig 1). The first layer is called the resting zone, which is located at both ends of the bone and consists of chondrocyte progenitors enclosed by cartilaginous extra cellular matrix consisting of different collagens, such as COL2a1 and proteoglycans, such as Aggrecan (Hallett et al., 2021; Lauing et al., 2014). These cells will differentiate to proliferative columnar chondrocytes that become flattened and organize into columns, and they have a role in maintaining longitudinal bone growth. Columnar

chondrocytes will further differentiate into a third layer consisting of pre-hypertrophic cells where they exist from the cell cycle. Next these cells will enlarge and mature, forming hypertrophic chondrocytes (HC). These cells secrete another form of collagen, COL10a1, that will contribute to the formation of a mineralized matrix and will help establish the final bone properties (Arseni et al., 2018; Kishimoto et al., 2010). Finally, hypertrophic chondrocytes will either differentiate into osteoblasts that form the bone, or will undergo apoptosis to make a space for the bone marrow (Fig 1)(Sun and Beier, 2014; Yang et al., 2014). The full image of how hypertrophic chondrocytes remodeling is being regulated during terminal endochondral ossification is still not clear, and further investigation is needed. In addition to the contribution of the growth plate HCs in bone formation, other cell lineages such as the perichondrium derived osteoprogenitor and the newly identified borderline chondrocytes, that have also been reported to participate in establishing the primary ossification center through differentiating into osteoblasts (Matsushita et al., 2020; Mizuhashi et al., 2019; Park et al., 2015; Yang et al., 2014).

Hypertrophic chondrocytes (HC) are large chondrocyte cells with a 10–20mm diameter and have a role in cartilage calcification, and remodelling, in addition to stimulating vascular invasion for bone formation. HC express Type X collagen (*Coll10a1*), which supports endochondral ossification through compartmentalizing matrix elements and manipulating matrix mineralization (Lefebvre and Smits, 2005; Shen, 2005). In addition, mature HC secretes vascular endothelial growth factor A (VEGF<sub>A</sub>) that attracts endothelial cells to form vessels in the primary ossification center (Gerber et al., 1999; Zelzer et al., 2004) with the help of matrix metalloproteinase 13 (*Mmp13*), an enzyme that degrades extracellular matrix to facilitate mineralization and vascular invasion (Inada et al., 2004). While some HCs undergo apoptosis (Aizawa et al., 1997; Farnum

and Wilsman, 1987; Gibson, 1998), the majority of these cells were observed to transdifferentiate into osteoblasts and other types of cells that facilitate formation of the primary ossification center. (Hu et al., 2017; Park et al., 2015).

Osteoprogenitor cells in the perichondrium also differentiate into osteoblasts in the periosteum, where they form a collar of compact bone that lines the diaphysis region. Other cell populations such as the borderline chondrocytes between the growth plate and the perichondrium were also reported to form osteoblasts that contribute to the development of the trabecular bone (Colnot et al., 2004; Mizuhashi et al., 2019). Osteoblasts form a calcified bone matrix that ossify and trap some osteoblasts. These trapped cells become mature and form osteocytes. Osteoblasts secrete VEGF to maintain angiogenesis within the ossification center. Vascular endothelial cells also stimulate other factors including VEGF that enhance osteogenesis in bone. Osteoblasts also secrete receptor activator of nuclear factor kappa-B ligand (RANKL) to stimulate the differentiation of osteoclasts that have a role in degrading the bone matrix. Together with osteoblasts, osteoclasts will work together to remodel bone to maintain its integrity (Sivaraj and Adams, 2016). The primary ossification center will grow into the proximal and distal ends of the long bone. After birth, blood vessels will also invade the epiphyses (ends) region of the bone and will facilitate the formation of a secondary ossification center in a similar way, but without forming the medullary cavity (Sivaraj and Adams, 2016; Walzer et al., 2014).

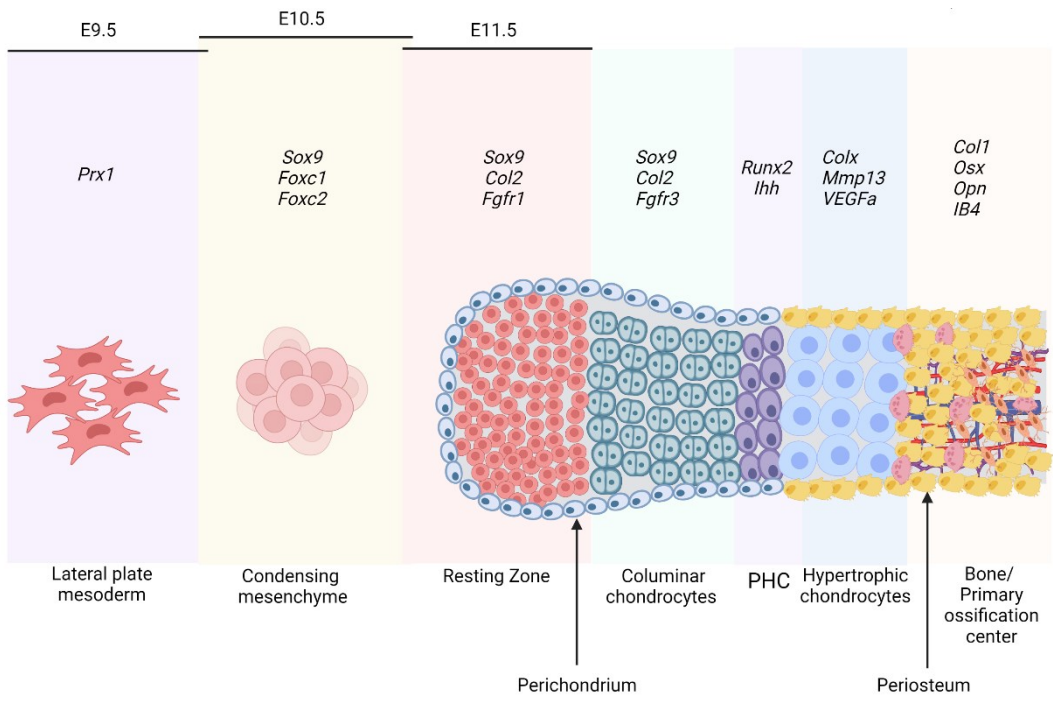


Fig 1.1 Endochondral ossification in the growth plate of the limb.

Schematic diagram of the growth plate developmental stages highlighting distinctive markers of each chondrocyte differentiation stage during the embryonic endochondral ossification process.

This illustration was made using <https://biorender.com>

### 1.1.5 Signaling pathways involved in Endochondral bone development:

Many signaling pathways function together in a complex environment to ensure proper development of the growth plate. The Transforming Growth Factor (TGF- $\beta$ ) family consists of many active members that function to regulate different stages of skeletogenesis, including TGF- $\beta$ s, Bone Morphogenic Proteins (BMPs) and Activins (Akhurst and Padgett, 2015). In this signaling pathway, binding of ligands to the transmembrane serine/threonine receptors will stimulate the formation of a heteromeric receptor ligand complex. At this point, type II ligand bound receptor will phosphorylate type I receptor that will in turn phosphorylate and activate regulatory Smad factors (R-Smads), that bind to Smad4. This Smad complex will translocate into the nucleus and bind DNA to simulate target genes. TGF- $\beta$  mainly activates R-Smads, Smad2, and Smad3, while BMPs recruits Smad1, Smad5, and Smad8 to stimulate the expression of target genes. The TGF- $\beta$ /BMP signaling activity is controlled by inhibitory Smads (I-Smads). BMPs have an essential role in bone formation and joint development (Salazar et al., 2016). In the growth plate, many BMPs function to regulate different stages of endochondral ossification. For example: BMP2 and 4 function together to regulate chondrocyte differentiation and maturation, while BMP7 stimulates osteogenic differentiation (Bandyopadhyay et al., 2006; McBride-Gagyti et al., 2015; Shu et al., 2011). Most importantly, TGF- $\beta$  and BMP signaling are required to stimulate SOX9 expression, a master regulatory transcription factor of chondrogenesis (Pan et al., 2008).

Fibroblast Growth Factor (FGF) signaling pathways contribute to bone formation (Su et al., 2014). The FGF family consists of 18 ligands binds to four distinctive FGF isoform receptors (FGFR 1-4). FGF ligand binding will lead to homodimerization and trans-auto-phosphorylation of the FGFRs. Next, they will phosphorylate FGFR substrate 2 $\alpha$  (FRS2 $\alpha$ ) that will activate many

downstream signaling cascades including Mitogen-Activated Protein Kinase (MAPKs), Phospholipase C Gamma (PLC $\gamma$ ), Phosphatidylinositol 3-kinase (PI3K), in addition to JAK-STAT(Ornitz and Marie, 2015). Several FGFs such as FGF4, FGF8 and FGF10 function at early stage of embryonic development to stimulates limb bud formation and regulates its patterning. FGF9 and FGF18 work together and independently in controlling osteogenesis and chondrocytes proliferation and hypertrophy respectively (Hung et al., 2016). Moreover, FGFR3 signaling stimulates signal transducer and activator of transcription 1 (STAT1), p38 mitogen-activated protein kinases (p38 MAPK) and Extracellular signal-regulated kinase type 1 and 2 (ERK1/2) to control columnar chondrocyte formation and ossification of the primary spongiosa (Ornitz and Marie, 2015).

Another signaling pathway involved in early skeletal development is the Wingless-related integration site (WNT) family, which consists of 19 different ligands. In the canonical  $\beta$ -CATENIN WNT signaling pathway, WNT ligands bind to seven transmembrane receptors, such as the Frizzled (Fzd) family, and receptors Lipoprotein-Related Protein 5 and 6 (LRP-5 and LRP6) (MacDonald et al., 2009). In the absence of WNT ligands,  $\beta$ -CATENIN binds to a destruction complex that consist of glycogen synthase kinase 3 $\beta$  (GSK3 $\beta$ ), adenomatosis polyposis coli (APC) and Axin. Formation of this complex will facilitate  $\beta$ -CATENIN phosphorylation by GSK3 $\beta$  that will then trigger  $\beta$ -CATENIN ubiquitination and degradation (Clevers, 2006; MacDonald et al., 2009). Binding of WNTs to receptors will stabilize  $\beta$ -CATENIN and it translocate to the nucleus to function as a co-activator for T-cell factor/lymphoid enhancer factor (TCF/LEF) transcription factors. Wnt signaling can be controlled by members of the Dikkopf (DKK) family, Wnt inhibitory factor 1 (WIF-1), and secreted Frizzled-related proteins (sFRP) (Kawano and Kypta, 2003).

Various studies reported the involvement of WNT signaling in skeletal development. For instance,  $\beta$ -CATENIN and SOX9 factors antagonize each other during early chondrogenesis to control chondrocytes differentiation in the growth plate (Dao et al., 2012). In addition, balanced activation of  $\beta$ -CATENIN helps in maintaining normal growth plate development including chondrocytes differentiation and hypertrophic maturation, bone formation and remodeling (Houben et al., 2016).

Hedgehog (Hh) signaling is also important in early bone formation (Yang et al., 2015). This group of factors consists of three HH ligands: Sonic hedgehog (SHH), Indian hedgehog (IHH), and Desert Hedgehog (DHH). IHH and SHH participate at different stages during bone development. IHH is a primary ligand that brings the cells into chondrogenesis, while SHH is a key factor in skeletal morphogenesis, as it directs limb patterning, and growth (Alman, 2015; Tickle and Towers, 2017; Yang et al., 2015). In endochondral ossification HH ligands bind to two Patched homolog receptors (Patched1 and Patched2). In the absence of HH ligands, the G protein coupled receptor Smoothed (Smo) is hindered by the Patched receptors. However, upon HH binding the Patched receptor will release Smo and activate the GLI transcription factors (GLI1, GLI2 and GLI3) (Ohba, 2016), that have a role in regulating bone formation and the growth plate developmental patterns (Hui & Angers, 2011). Furthermore, IHH ligand will also promote PTHrP (*Pthlh*) activity located in the resting zone to enhance chondrocyte proliferation. As part of IHH regulatory process, PTHrP binds PTHR1 receptor in the pre-hypertrophic chondrocytes to negatively regulate IHH activity (Brown et al., 2003; Kobayashi et al., 2002; Yan et al., 2016).

Additional signaling pathways, such as Notch, Retinoic acid, Mammalian target of rapamycin (mTOR), and Insulin like growth factor signaling, and many others also participate in

establishing and maintaining skeletal development (J. Chen et al., 2014; Green et al., 2018; Xu et al., 2022).

#### 1.1.6 Transcription factors:

Transcription factors play major roles in regulating expression of genes that control the progression through endochondral ossification events and are thus an important feature to study in order to understand skeletal development. Several transcription factors were reported to play important roles in stimulating chondrocyte differentiation and maintaining regular endochondral ossification. For instance, SOX9, SOX5 and SOX6, regulate many fetal developmental processes including endochondral skeletal development and initiation of chondrogenesis in the condensing mesenchyme of the limb bud and the somite (Bi et al., 1999; Lefebvre et al., 2001). They also play a role in maintaining chondrocyte proliferation and differentiation in the growth plate. SOX9 acts as the master regulatory gene in cartilage development stimulating the expression of a wide range of chondrocyte genes such as *Aggrecan*, *Col2a1*, *Col9a1*, and many others during embryonic bone development (Czarny-Ratajczak et al., 2001; Ovchinnikov et al., 2000; Takimoto et al., 2019). Mutations in the *SOX9* gene lead to Campomelic Dysplasia in humans, an autosomal sex reversal (CD/SRA), characterized by skeletal abnormalities such as: short legs with clubfeet (feet turning inward and upward), abnormal cervical vertebrae, 11 pairs of ribs instead of 12, underdeveloped shoulder blades and displaced hip bone (Barone et al., 2014; Hill-Harfe et al., 2005). *SOX5* mutations in humans cause Lamb-Shaffer syndrome (LSS) which usually results in behavioral problems, speech delay to mild skeletal phenotypes such as short stature (Gkirgkinoudis et al., 2020), while *SOX6* mutations causes a general developmental delay with distinctive skeletal phenotypes such as craniosynostosis, mild facial dysmorphism and multiple osteochondromas

(Tolchin et al., 2020). In mice, *Sox5* single mutation causes the formation of a cleft palate, short chondrocranium, bell-shaped thoracic cage with short ribs, in addition to reduce mineralization in the vertebral bodies, nasal, and presphenoid bones. *Sox6* mutant mice developed short sternum, bent inwards, with ectopically mineralized intersternebrae joints. Most *Sox6* mutant mice die shortly after birth, with surviving ones developing dwarfism within the first week after birth (Tolchin et al., 2020). However, double knockout (KO) of *Sox5* and *Sox6* in mice revealed severe skeletal chondrodysplasia with short vertebral columns and underdeveloped thoracic cages (Lefebvre et al., 2001; Tolchin et al., 2020).

$\beta$ -CATENIN, a transcription factor encoded by the *CTTNB1* gene, is the element of the canonical Wnt/  $\beta$ -CATENIN signaling pathway that translocates to the nucleus after its activation to stimulate the expression of Wnt downstream target genes (Clevers, 2006; Dao et al., 2012; Maupin et al., 2013).  *$\beta$ -Catenin* is associated with the development of the apical ectodermal ridge (AER), maintaining the dorsal–ventral axis of the limbs, and synovial joints formation (Guo et al., 2004; Rodda and McMahon, 2006; Soshnikova et al., 2003). Although there is no known related human skeletal disorder associated with  *$\beta$ -Catenin* gene mutation specifically, several studies have reported skeletal abnormalities when  *$\beta$ -Catenin* is mutated in mice skeletal tissue types such as chondrocytes, neural crest, limb bud mesenchymal cells and osteoblasts. For example, conditional KO of the  *$\beta$ -Catenin* exon 3-6 in chondrocyte progenitors using the *Col2a1-Cre* driver resulted in several skeletal phenotypes including the development of domed skulls, short limbs, and a failure in forming tarsal synovial joints (Guo et al., 2004). Conditional mutation of  *$\beta$ -Catenin* from the limb ectoderm results in different hindlimbs abnormalities including truncation or absence of tibia, fibula, and some of the digits (Soshnikova et al., 2003). Deletion of  *$\beta$ -Catenin* exon 2-6 in

osteoblasts precursors via *Osx1-Cre-TetOff* system was tested on mice prenatally or postnatally at 2 or 4 months of age. Prenatal KO leads to severe bone defects with lack of mineralization and bone formation due to incomplete osteoblast differentiation. However, mice with postnatal conditional deletion of *β-catenin* lack trabecular bone which was replaced by bone marrow adipocytes at 6 months of age (Rodda and McMahon, 2006; Song et al., 2012). *β-catenin* functional loss in mature osteoblasts on the other hand leads to reduced bone mass and enhanced osteoclast activity, with no change in osteoblast number or formation (Glass et al., 2005).

Runt-related transcription factor 2 (RUNX2) is another crucial transcription factor that controls many aspects of bone development. It expresses in the condensing mesenchyme of the limb to establish the formation of an osteoblast progenitor population in the perichondrium. It also regulates chondrocyte proliferation and differentiation of pre-hypertrophic chondrocytes through controlling *Ihh* expression (Yoshida et al., 2004). RUNX2 also controls expression of *Col10a1*, *Mmp13* in the hypertrophic chondrocytes, and bone matrix proteins such as Secreted Phosphoprotein 1 (*Spp1*), and Integrin Binding Sialoprotein (*Ibsp*) in chondrocytes. Moreover, it helps in promoting chondrocyte exit from the cell cycle, maintaining hypertrophic chondrocytes maturation and remodeling (Yoshida et al., 2004). Moreover, RUNX2 is a pioneer transcription factor for osteoblasts differentiation, in addition to its regulatory role in osteoclastogenesis through stimulating RANKL expression in osteoblasts (Byon et al., 2011). In humans, *RUNX2* mutation leads to Cleidocranial Dysostosis (CCD), characterized by abnormal teeth, slight short stature, open cranial sutures, and hypoplastic clavicles with narrow, sloping shoulders (Machol et al., 1993).

### 1.1.7 The forkhead box (FOX) family:

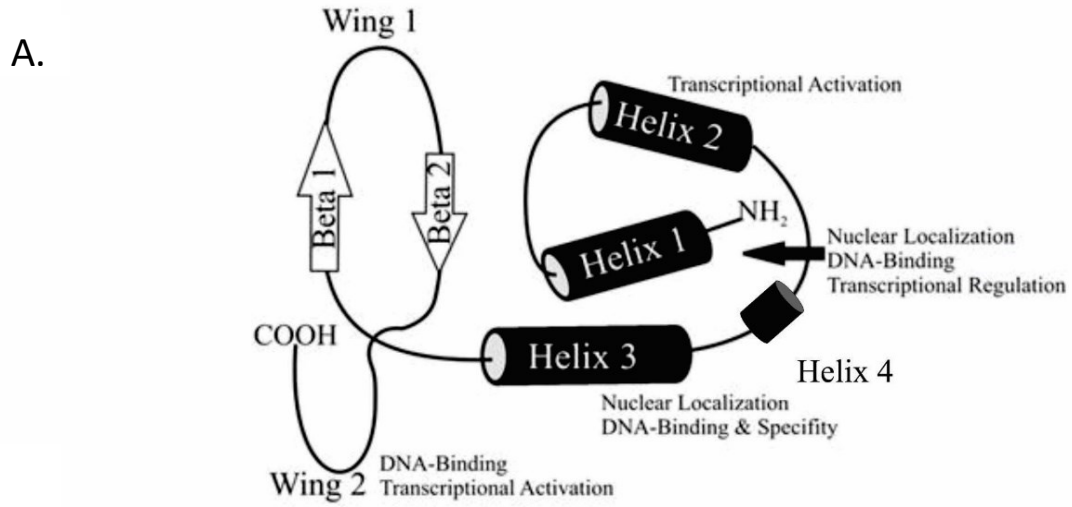
The FOX family consists of a number of different genes identified in eukaryotes from yeast to human, that includes 50 *FOX* genes identified in the human genome with two pseudogenes (*FOXO1B* and *FOXO3B*) and 44 orthologues in mice (Jackson et al., 2010; Katoh and Katoh, 2004; Weigel and Jäckle, 1990). The first forkhead (*fkh*) gene was discovered in 1989 in *Drosophila*. Deletion of this gene gives the fly a fork-headed feature (Weigel et al., 1989). Another group identified *Foxa1* in a rat, where scientists noticed the comparable DNA binding domain between the two transcription factors and decided to name it the fork-head or the winged helix domain (FHD) (Weigel and Jäckle, 1990). This domain was well conserved within all FOX transcription factors. The FHD binding domain consists of 110 amino acids that forms three alpha helices and two beta pleated sheets with the last one surrounded by two loops called the wing region ( Weigel and Jäckle, 1990). The human FOX genes were identified to have a role in the development of various organs such as the kidney, brain, eye, heart and the skeletal system and in cellular functions including germ cell migration, cell proliferation, differentiation, and cellular glucose homeostasis ( Kume et al., 1998; Mattiske et al., 2006; Wilm et al., 2004; Winnier et al., 1999).

### 1.1.8 The molecular structure of FOXC1 and FOXC2 transcription factors:

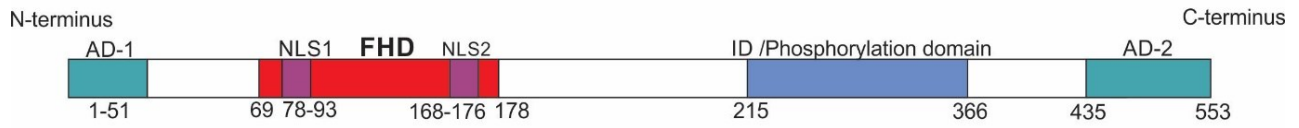
*FOXC1* and *FOXC2* genes were identified in many vertebrate species including humans, mouse, frog, and chicken. Zebrafish has two *Foxc1* genes (*foxc1a*, and *Foxc1b*) (Mansour et al., 1993; Shields et al., 1985; Topczewska et al., 2001; Wilm et al., 2004; Winnier et al., 1999). Both human FOXC1 and FOXC2 transcription factors share a 98% conserved forkhead DNA-binding domain (FHD) that includes three major  $\alpha$ -helices, where helix 3 is known as the DNA-recognition helix, and two anti-parallel  $\beta$ -sheets (Berry et al., 2002, 2005; Tavian et al., 2020). Some FOX

transcription factors such as FOXC1 have a smaller fourth  $\alpha$ -helix located between helix 2 and helix 3. The area between the two  $\beta$ -sheets is surrounded by two loops called the wing region. These two loops wrap around the DNA helix and stabilize the interaction between the transcription factor and the DNA (Fig 1.2A) (Clark et al., 1993).

FOXC1 is generated from a single exon coding region in the *FOXC1* gene located on chromosome 6p25.3 locus (Mears et al., 1998; Nishimura et al., 1998). The FOXC1 protein sequence consists of 553 amino acids with a conserved FHD domain of 110 amino acids located at residues 69 to 178 (Fig 1.2B) (Mears et al., 1998). The FHD consists of two nuclear localization domains NLS1 (78-93) and NLS2 (168-176) residues that are located at the N-terminus and the C-terminus of the FHD. These two nuclear localization domains allow FOXC1 to translocate to the nucleus and bind DNA. FOXC1 also contains two transcription activation domains at the N-terminus (1-51) and the C-terminus (435-553). Finally, the FOXC1 central region is composed of a transcriptional inhibitory domain/ phosphorylation domain (215-366), (Fig 1.2B) (Berry et al., 2002). FOXO3 proteins are known to be regulated by AKT kinase (Brunet et al., 1999). However, FOXC1 lacks a matching sequence to the AKT consensus site, which indicates that it may undergo phosphorylation through a different mechanism such as through protein kinase A or C, or glycogen synthesis kinase 3 (Klenova et al., 2001; Ross et al., 1999). This inhibitory mechanism is necessary to prevent any abnormal developmental effects caused by FOXC1 overactivation, since both FOXC1 overactivation or deletion can cause developmental defects (de Vos et al., 2017; Lehmann et al., 2000; Nishimura et al., 2001).



B.



C.



Fig 1.2. FOXC1 and FOXC2 structures. (A) Schematic diagram of FOXC1 FHD, this image is modified from (Berry et al., 2005). (B) FOXC1 domains, image modified from (Berry et al., 2002) license number: 5333851433633 (C) FOXC2 domains, image modified from (Tavian et al., 2020). AD: Activation domain; ID: Inhibitory domain; NLS: Nuclear localization signal; FHD: Forkhead domain.

FOXC2 is a transcription factor that is also produced from a single exon coding region which is 1.5 Kb long. FOXC2 primary sequence consists of 501 amino acids with a FHD between residue 71 to 162 (Tavian et al., 2020). FOXC2 shares a similar FHD sequence with FOXC1 except for two substitutions of aspartic acid for glutamic acid at sites at the 90 and 100 residues. FOXC2 contains distinctive N- and C-terminal sequences with 56% similarity within the N-Terminus and 30% homology at the C-terminal. FOXC2 has two nuclear localization domains, NLS1 located within the FHD (78-93) and the NLS2 in the central region (168-176) (Tavian et al., 2020). Moreover, FOXC1 also consist of two activation domains, with AD1 located at the N-Terminus (1-71) and AD2 at the C-terminus (395-494) (Danciu et al., 2012; Lam et al., 2013). FOXC2 also has an inhibitory domain that distinctively localized at the very end of the C-terminus region (495-501) (Berry et al., 2005). FOXC2 central region consist of multiple phosphorylation, and SUMOylation sites where Small Ubiquitin-like Modifier (SUMO) can covalently attached to regulate FOXC2 activity (Fig 1.2C) (Berry et al., 2005; Danciu et al., 2012; Tavian et al., 2020). Likewise, negative regulation of FOXC2 transcriptional activity is required, as increase FOXC2 activity was reported to stimulate tumor cell proliferation, metastases, epithelial-mesenchymal transition (EMT), in addition to drug resistance in patents with colorectal or human ovarian cancer (Cui et al., 2015; Li et al., 2016).

#### 1.1.9 FOX transcription factors in skeletal development:

Genetic mutation of many FOX transcription factors was linked to many cancer types and developmental disorders including a wide array of skeletal disorders (Berry et al., 2005; Kume et al., 1998). For instance, *Foxa2* and *Foxa3* play a key role in hypertrophic chondrocytes

differentiation in long bone growth plate, as conditional deletion of *Foxa2* in chondrocytes in a *Foxa3* null background in mice compromised hypertrophic chondrocytes formation and expression of its markers such as COLX and MMP13 (Ionescu et al., 2012). Another study highlighted the importance of *Foxo* family members in maintaining healthy and functional cartilage, since any disruption in *Foxo* expression is associated with cartilage ageing, leading to disk degeneration or osteoarthritis (Akasaki et al., 2014; Alvarez-Garcia et al., 2018). Moreover, *FOXL2* is associated with bone mineralization. *FOXL2* mutation leads to an autosomal dominant disorder called Blepharophimosis, ptosis, and epicanthus inversus syndrome (BPES; OMIM #110100), where patients exhibit reduced bone mineral density (Chawla et al., 2013; Méjécase et al., 2021).

#### 1.1.10 Role of FOXC1 and FOXC2 in developmental disorders:

FOXC1 and FOXC2 are expressed in various types of tissues including skeletal progenitors of the limb, ribs, vertebrae, and the skull (Hiemisch et al., 1998; Kume et al., 1998). Both *Foxc1* and *Foxc2* were reported to have a key regulatory effect in the formation of paraxial versus intermediate mesoderm cell fates during early embryonic development (Wilm et al., 2004). *Foxc1* is involved in the development of various organs such as the heart and blood vessels, eye, meninges of the brain. In addition, *Foxc1* is required for pre chondrogenic mesenchymal cells and endochondral bone development. Chromosomal duplication of the 6p25 locus that includes *FOXC1* gene was reported to affect the development of the anterior chamber of the eye that can lead into glaucoma and iris hypoplasia (Lehmann et al., 2000; Nishimura et al., 2001). Moreover, point mutation of one copy of *FOXC1* in the 6p25.3 locus was identified in type 3 Axenfeld–Rieger syndrome (RIEG OMIM#602482), a rare autosomal dominant disorder. *FOXC1* haploinsufficiency affects mesenchymal cells and neural crest development leading to a number

of developmental phenotypes such as abnormalities in the anterior chamber of the eyes leading to glaucoma, teeth and mid-face hypoplasia, hearing loss and cardiac and abdominal abnormalities (de Vos et al., 2017; Hjalt and Semina, 2005). Similar *FOXC1* haploinsufficiency was also identified in 6p25 deletion syndromes that also show heterozygous deletion of *FOXC1*, which cause an overlapping clinical abnormality with type 3 Axenfeld–Rieger syndrome (de Vos et al., 2017; Kannu et al., 2006).

*FOXC2* truncating mutation leads to lymphedema-distichiasis syndrome (LD) (OMIM# 153400), with lymphedema in limbs and distichiasis (double rows of eyelashes). In addition to the main phenotypes, some people exhibit additional complications such as cardiac defects, extradural cysts, and development of cleft palate (FALLS and KERTESZ, 1964; Fang et al., 2000; Robinow et al., 1970). Moreover, patients with 16q24.1 microdeletion syndrome, where a whole FOX cluster is deleted including *FOXF1*, *MTHFSD*, *FOXC2* and *FOXL1* at 16q24.1, display various systemic abnormalities including axial skeletal defects such as development of butterfly vertebrae and rib fusions (Brice, 2002; Fang et al., 2000; K. Iida et al., 1997; Shaw-Smith, 2010; Stankiewicz et al., 2009).

Genetic studies in the mouse show that *Foxc1* and *Foxc2* have key roles in both intramembranous and endochondral ossification. *Foxc1* homozygous null mutants display severe axial skeleton anomalies. The skull lacks the calvarial bones, basisphenoid bone is malformed, and the maxilla zygomatic process is enlarged (Kume et al., 1998). In the vertebral column, the vertebral bodies and lateral arches are underdeveloped and the dorsal neural arches fail to fuse, the ribs are thin and the ossification center in the sternum is absent. On the other hand, appendicular

skeleton phenotypes are less severe. (Hong et al., 1999; Kume et al., 1998; Winnier et al., 1999). FOXC1 act as a transcription partner of GLI2 that enhance the expression of IHH-GLI2 downstream targets in limbs growth plate (Yoshida et al., 2015a). *Foxc2* null mice exhibited abnormal endochondral and intramembranous axial skeleton development. *Foxc2*<sup>-/-</sup> newborn skull lacks the optic capsule and supraoccipital bones and exhibit abnormal exoccipital and interparietal bones. The presphenoid and palatine bones are absent and result in that lead cleft palate. The thorax ribs are fused and vertebral bodies are small and fail to localize in the center of the vertebral column (Winnier et al., 1997). Compound *Foxc1*<sup>-/-</sup>; *Foxc2*<sup>-/-</sup> mice die around embryonic (E) day 9 due to failure in cardiovascular development (Kume et al., 2001) before any skeletal structures are formed, preventing analysis of the possible association between the two transcription factors in endochondral ossification to be studied.

#### 1.1.11 Skeletal dysplasia:

Disruption of any gene that is expressed during skeletal development can lead to skeletal dysplasia or osteochondrodysplasia. There are a group of disorders that mainly compromise the cartilage and bone formation in addition to other musculoskeletal system elements such as the muscles, joints, tendons and ligaments. Skeletal dysplasia are autosomal dominant, autosomal recessive, X-linked dominant, X-linked recessive, or Y-linked (Bonafe et al., 2015; Warman et al., 2011). Identifying the mode of inheritance of a skeletal dysplasia is important as it conveys information to families and help raise awareness of any possible recurrences in the future (Krakow, 2015). Examples of commonly diagnosed skeletal dysplasia are: Achondroplasia, which includes a number of skeletal disorders, some lethal, that result from mutations in the *FGFR3* gene (Lee et

al., 2017; Shiang et al., 1994). Radiographic diagnostic reports include macrocephaly (large head circumference) with narrow skull based, flat vertebral bodies, long narrow trunk, and small iliac bone elements (Vajo et al., 2000). Another common group of skeletal disorders are the Type II collagenopathies, which result from autosomal dominant mutations of Type II collagen (COL2A1) gene. This group of disorders can be lethal and presents with severe skeletal abnormalities such as development of large skulls, short ribs, absence of mineralization in the vertebrae (Kannu et al., 2012). Other skeletal disorders are characterized by reduction in bone density such as osteogenesis imperfecta or brittle bone disease that can range from mild to severe or perinatal forms. Around 90% of the diagnosed cases of osteogenesis imperfecta are due to dominant mutations in type I collagen, (*COL1A1* and *COL1A2*) (Marini and Blissett, 2013; Sillence, 1981), that lead to defects in collagen assembly while the rest of the cases result from congenital recessive mutations (Marini and Blissett, 2013b). Information about other types of skeletal dysplasia, their causes and patterns of inheritance can be found in the Nosology and Classification of Genetic Skeletal Disorders (Bonafe et al., 2015) and On-line Inheritance in Man (OMIM:[www.omim.org/](http://www.omim.org/)).

## 1.2 Rational and hypothesis:

FOXC1 and FOXC2 are two transcription factors that regulate early development of many organ systems (Hiemisch et al., 1998; Kume et al., 1998; Winnier et al., 1999). In humans, mutation of one *FOXC1* copy was reported to impact neural crest development, which caused several developmental abnormalities such as glaucoma, teeth and mid-face hypoplasia, and hearing loss, in addition to cardiac and abdominal phenotypes (de Vos et al., 2017; Hjalt and Semina, 2005; Mears et al., 1998). In mice, homozygous deletion of *Foxc1* resulted in hydrocephalus and ocular defects, in addition to various skeletal phenotypes such as reduced size of the ribcage, formation of a small vertebral bodies, and absence of the sternum and the cranial vault of the skull (Dressler et al., 2010; Kume et al., 1998). Interestingly, deletion of *Foxc2* in mice lead to a similar range of axial skeletal phenotypes as in *Foxc1* mutants (Winnier et al., 1997). These phenotypic similarities indicate the presence of shared function between the two *Foxc* genes. In order to study this functional similarity, Winnier et al 1999 generated a compound *Foxc1* and *Foxc2* mouse model. Unfortunately, compound *Foxc1* and *Foxc2* null mice weren't viable and die at Embryonic day (E) 9 due to cardiovascular abnormalities, before the onset of skeletogenesis. These mutant mice failed to develop somites, indicating an overlapping role in somitogenesis that contributes to the formation of the axial skeleton (Winnier et al., 1999). Both FOXC1 and FOXC2 transcription factors have highly conserved forkhead domains and can bind similar DNA sequences (Berry et al., 2005). Moreover, both mRNAs showed overlapping expression patterns in various tissue types during early embryonic development (Winnier et al., 1999). These findings support our hypothesis in which ***FOXC1* and *FOXC2* have overlapping transcriptional activity during embryonic skeletal development including their regulatory effect on endochondral ossification.**

There are many questions that need to be answered in order to understand how important *Foxc1* and *Foxc2* are in regulating endochondral ossification. For example, are *Foxc1* and *Foxc2* under similar upstream regulatory controls that stimulates their expression? Do both *Fox* genes express at the same time and in the same types of cells? What types of cells express *Foxc1* and/or *Foxc2* during early growth plate development? What are the downstream targets and signaling pathways that can be regulated by *Foxc1* and *Foxc2*? In my thesis work I will be navigating through various model systems such as ATDC5 pre-chondrocytes cells, mouse embryonic stem cells (mESCs), U2OS osteosarcoma cells in addition to two mouse models (*Col2-cre; Foxc1<sup>Δ/Δ</sup>; Foxc2<sup>Δ/Δ</sup>* and *Prx1-cre; Foxc1<sup>Δ/Δ</sup>; Foxc2<sup>Δ/Δ</sup>*), in order to understand how *Foxc1* and *Foxc2* regulate endochondral bone formation during embryonic development.

### 1.3 Project outline:

In this study we tried to understand how *Foxc1* and *Foxc2* regulate endochondral ossification through addressing the following aims:

1. Identify the molecular roles of *Foxc1* in regulating chondrocyte differentiation *in vitro*
2. Examination of *Foxc1* and *Foxc2* function in formation of the axial skeleton
3. Explore how deletion of *Foxc1* and *Foxc2* before the onset of chondrocyte differentiation disrupts endochondral ossification events
4. Test if *Foxc1* and  $\beta$ -*Catenin* function together.

## **Chapter 2:**

### **Loss of *Foxc1* and *Foxc2* function in chondroprogenitor cells disrupts endochondral ossification**

This chapter was published under the title “**Loss of *Foxc1* and *Foxc2* function in chondroprogenitor cells disrupts endochondral ossification**” by the following authors:

Asra Almubarak<sup>1</sup>, Rotem Lavy<sup>2</sup>, Nikola Sronic<sup>2</sup>, Yawen Hu<sup>1</sup>, Devi Priyanka Maripuri<sup>1</sup>, Tsutomu Kume<sup>3</sup>, and Fred B. Berry, in the Journal of Biological Chemistry. Volume 297, Issue 3, 101020, September 2021.

#### **Contribution to the manuscript:**

Asra worked out the *in vitro* experiments and analysis including the cell culture and genetic transfection, western blot, qRT-PCR and luciferase assays. *Col2-cre;Foxc1<sup>Δ/Δ</sup>;Foxc2<sup>Δ/Δ</sup>* mouse model was generated previously in Berry Lab. Nikola Sronic did the Control, and *Col2-cre* mice skeletal prep. Yawen Hu performed the IF staining of the tibia. Devi Priyanka Maripuri was responsible for analyzing the rib tissue RNA seq data. George Kurian performed CHIP. Tsutomu Kume provided the *Foxc1<sup>fl/fl</sup>;Foxc2<sup>fl/fl</sup>* mice. Fred B. Berry performed the RNA scope ISH and detecting *Foxc1* loss of function via Western blot. This manuscript work was planned, supervised, and written by Fred B. Berry.

# **Loss of *Foxc1* and *Foxc2* function in chondroprogenitor cells disrupts endochondral ossification**

Asra Almubarak<sup>1</sup> , Rotem Lavy<sup>2</sup> , Nikola Srnic<sup>2</sup> , Yawen Hu<sup>1</sup> , Devi Priyanka Maripuri<sup>1</sup> , Tsutomu Kume<sup>3</sup> , and Fred B. Berry<sup>1,2,\*</sup>

From the <sup>1</sup> Department of Medical Genetics and <sup>2</sup> Department of Surgery, University of Alberta, Edmonton, Alberta, Canada; and <sup>3</sup> Feinberg Cardiovascular and Renal Research Institute, Feinberg School of Medicine, Department of Medicine, Northwestern University, Chicago, IL, USA

**Keywords:** Sox9; bone; cell differentiation; chondrogenesis; forkhead box; gene regulation; transcription factor.

---

Crown Copyright © 2021. Published by Elsevier Inc. All rights reserved.

## **Conflict of interest statement**

Conflict of interest The authors declare that they have no conflicts of interest with the contents of this article.

## 2.1 Abstract:

Endochondral ossification initiates the growth of the majority of the mammalian skeleton and is tightly controlled through gene regulatory networks. The forkhead box transcription factors *Foxc1* and *Foxc2* regulate aspects of osteoblast function in the formation of the skeleton, but their roles in chondrocytes to control endochondral ossification are less clear. Here, we demonstrate that *Foxc1* expression is directly regulated by the activity of SRY (sex-determining region Y)-box 9, one of the earliest transcription factors to specify the chondrocyte lineage. Moreover, we demonstrate that elevated expression of *Foxc1* promotes chondrocyte differentiation in mouse embryonic stem cells and loss of *Foxc1* function inhibits chondrogenesis in vitro. Using chondrocyte-targeted deletion of *Foxc1* and *Foxc2* in mice, we reveal a role for these factors in chondrocyte differentiation in vivo. Loss of both *Foxc1* and *Foxc2* caused a general skeletal dysplasia predominantly affecting the vertebral column. The long bones of the limbs were smaller, mineralization was reduced, and organization of the growth plate was disrupted; in particular, the stacked columnar organization of the proliferative chondrocyte layer was reduced in size and cell proliferation was decreased. Differential gene expression analysis indicated disrupted expression patterns of chondrogenesis and ossification genes throughout the entire process of endochondral ossification in chondrocyte-specific *Foxc1/Foxc2* KO embryos. Our results suggest that *Foxc1* and *Foxc2* are required for normal chondrocyte differentiation and function, as loss of both genes results in disorganization of the growth plate, reduced chondrocyte proliferation, and delays in chondrocyte hypertrophy that prevents ossification of the skeleton.

## **2.2 Introduction:**

The majority of the mammalian skeleton forms through a mechanism known as endochondral ossification (Aghajanian and Mohan, 2018; Berendsen and Olsen, 2015). In this developmental event, mesenchymal progenitor cells condense at the sites of newly forming bone and differentiate into chondrocytes. These chondrocytes undergo continued differentiation and organize themselves into cell layers that form the growth plate, which ultimately drives endochondral bone growth. Round resting zone chondrocytes form at the distal ends of long bones. These cells then differentiate inward to become flattened, highly proliferative columnar chondrocytes. Much of the extension of the bone length is achieved by the proliferative activities of these cells. Columnar chondrocytes exit the cell cycle to differentiate into prehypertrophic chondrocytes and then enlarge to form hypertrophic chondrocytes that form a mineralized matrix and sets the foundation for future bone growth. The fate of the hypertrophic chondrocytes is split into a number of outcomes. A portion of these cells will undergo apoptosis and are removed from the bone; alternatively, hypertrophic chondrocytes will transdifferentiate into bone-forming osteoblast cells that contribute to the ossified bone structure (Ono et al., 2014; Yang et al., 2014). Additional osteoblast cells originate from a cell layer, the periosteum, that lines the newly forming bone, and invade into the newly formed marrow spaced along with blood vessels.

The differentiation of chondrocytes to control growth plate functions is a tightly regulated process controlled by multiple signaling networks. In particular, cross-talk between Indian hedgehog (IHH) and parathyroid hormone–related peptide signals coordinate the proliferation of the columnar chondrocytes and their exit from the cell cycle to differentiate into prehypertrophic and hypertrophic chondrocytes (Karp et al., 2000; Kobayashi et al., 2005). In addition, fibroblast growth factor (FGF) signaling networks also regulate growth plate chondrocyte function needed

for proper bone growth (Ornitz and Marie, 2015; Shiang et al., 1994). Disruption to these pathways can affect the formation of the skeleton and result in bone growth disorders in humans (Geister and Camper, 2015).

Campomelic dysplasia (OMIM # 114290) is a lethal skeleton malformation characterized by bowed limb bones and a reduced size of the rib cage (Wagner et al., 1994). Mutations in the transcription factor gene SRY (sex-determining region Y)-box 9 (SOX9) cause campomelic dysplasia, and extensive functional analysis of SOX9 has defined it as a master regulator of the chondrocyte lineage (Bi et al., 1999; Lefebvre et al., 2001; Wagner et al., 1994). SOX9 function regulates multiple stages of chondrocyte differentiation and development including the initial acquisition of the chondrocyte fate, the proliferation of growth plate chondrocytes, and the transition to hypertrophic chondrocytes (Dy et al., 2012; Lefebvre et al., 2001; Lefebvre and Smits, 2005). In addition to its profound role in directing cells down the chondrocyte lineage *Sox9* acts to prevent differentiation toward other lineages (Akiyama et al., 2002; Dy et al., 2012; Shih et al., 2015). Although important in the formation of the chondrocyte lineage, SOX9 is dispensable for the initiation of the chondrogenic lineage and the induction of gene expression patterns associated with this fate (Liu et al., 2018). This finding suggests that additional transcription factors function along with SOX9 to control chondrocyte formation during endochondral ossification.

The forkhead box (FOX) transcription factors are candidates for early regulators of chondrocyte differentiation. Both *Foxc1* and *Foxc2* genes are expressed in the condensing mesenchyme of the presumptive endochondral skeleton (Hiemisch et al., 1998; Kume et al., 1998; Winnier et al., 1997; Yoshida et al., 2015a). Furthermore, *Foxc1* and *Foxc2* are required for proper endochondral ossification as mice deficient for *Foxc1* or *Foxc2* display disruptions to the formation of the endochondral skeleton (Hong et al., 1999; Kume et al., 1998; Winnier et al.,

1997). Homozygous null *Foxc1* mouse mutants die shortly after birth and display small rib cages that lack an ossified sternum (Kume et al., 1998). The neural arches of the vertebral column are not fully mineralized in these mutants. The limbs are shorter in *Foxc1*-deficient mice and *Foxc1* can regulate IHH signaling to control endochondral growth in the limb (Yoshida et al., 2015). *Foxc2* homozygous null mutant mice also die before birth with patterning and ossification defects apparent in the axial skeleton (skull, rib cage, and vertebral column) (Winnier et al., 1997). Although both *Foxc1* and *Foxc2* are expressed at high levels in chondrocytes of the developing limbs (Yoshida et al., 2015), loss of function mutation of either gene results in milder phenotypes than that observed in the axial skeleton. As FOXC1 and FOXC2 proteins have near-identical DNA-binding domains (Berry et al., 2005; Hayashi and Kume, 2008; Pierrou et al., 1994), it is possible that *Foxc1* or *Foxc2* may compensate for the loss of the other. Compound *Foxc1*<sup>-/-</sup>; *Foxc2*<sup>-/-</sup> mice arrest in development before the onset of skeletal formation, and therefore, the combined functions of these genes in endochondral ossification is not known (Kume et al., 2001).

We wished to determine how *Foxc1* and *Foxc2* function in chondrocytes to regulate endochondral ossification. We first used in vitro assays to demonstrate that *Foxc1* expression could be directly regulated by SOX9 activity and that gain or loss of *Foxc1* function could positively or negatively regulate in vitro chondrocyte differentiation, respectively. We also demonstrate that the loss of both *Foxc1* and *Foxc2* function in early chondrocyte cells in the developing mouse disrupts normal endochondral ossification processes. These findings indicate that *Foxc1* and *Foxc2* gene function is required in the chondrocyte cells to correctly form the endochondral skeleton.

## 2.3 Results:

### 2.3.1 SOX9 directly regulates *Foxc1* expression

*Foxc1* and *Foxc2* are expressed in condensing prechondrogenic mesenchyme cells at a time when SOX9 is active (Hiemisch et al., 1998; Kume et al., 1998). Given that their mRNA expression is reduced in Sox9- deficient chondrogenic tissues (Liu et al., 2018), we sought to determine whether *Foxc1* and *Foxc2* were directly regulated by SOX9. First, we used an inducible mouse embryonic stem (mES) cell line that contains a tetracycline-off inducible *Sox9* gene (Nishiyama et al., 2009). Upon the removal of doxycycline (DOX) for 48 h, we observed an elevation of SOX9 protein and mRNA levels (Fig. 2.1A) as well as an increase in collagen, type II, alpha 1 (*Col2a*) mRNA, a known SOX9 target of transcriptional regulation (Bell et al., 1997). Expression of *Foxc1* was also elevated in response to SOX9 induction, but levels of *Foxc2* mRNA remain unchanged (Fig. 2.1A). We next examined previously published SOX9 chromatin immunoprecipitation (ChIP)-seq data (Ohba et al., 2015) and identified four SOX9-binding peaks near the mouse *Foxc1* gene. Three peaks were located upstream of *Foxc1*, which we termed distal A (mm10 chr13:31,764,541-31,764,717), B (mm10 chr13:31,765,465-31,765,623), and C (mm10 chr13:31,779,560-31,779,803), respectively, and one peak located downstream of *Foxc1*, which we termed distal D (mm10 chr13:31,820,626-31,820,791). No peaks were found in proximity to the *Foxc2* gene. We verified SOX9 binding to these sites using ChIP in ATDC5 cells and found SOX9 was associated with all four regulatory elements as well as the known SOX9-binding site in the intron 1 enhancer of the *Col2a* gene (Fig. 2.1B). Next, we cloned each regulatory region into a luciferase reporter that contains a basal promoter and tested for activation by SOX9 in ATDC5 cells. We found that only distal C was activated in response to SOX9. Although distal B was not activated by SOX9, we did detect elevated activity in ATDC5 cells compared with the

empty reporter vector, suggesting this element may confer *Sox9*-independent chondrocyte regulatory activity for *Foxc1* expression. Together, these findings indicate that *Foxc1* is a direct target of SOX9 transcriptional regulatory activity.

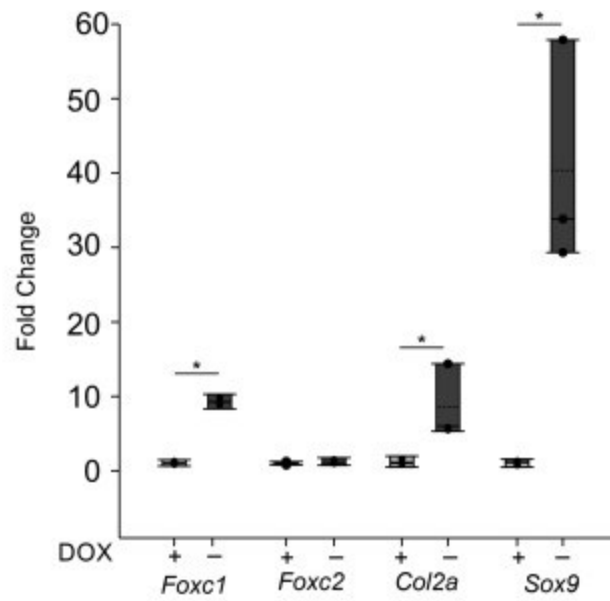
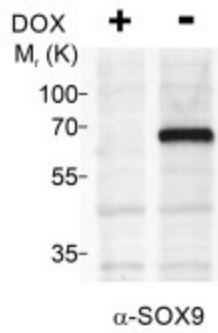
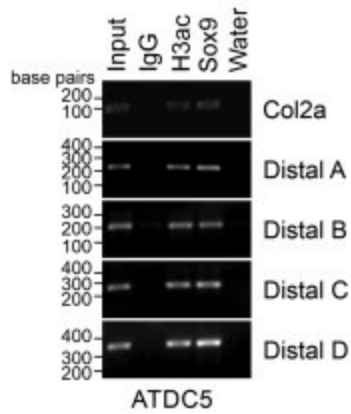
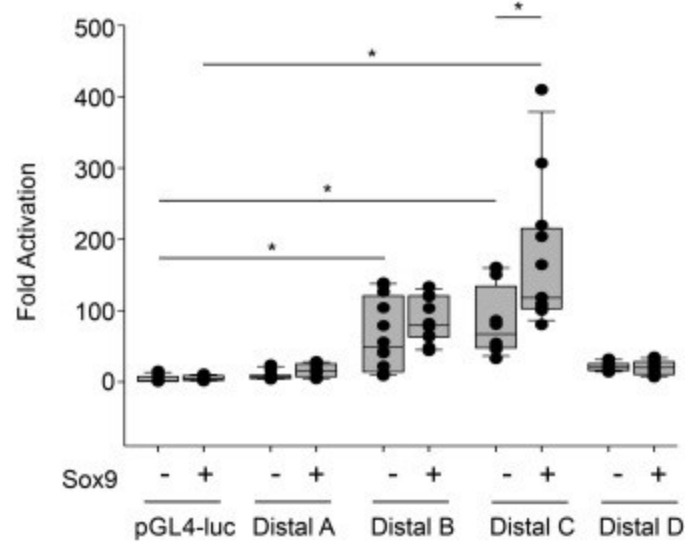
**A****B****C**

Figure 2.1. SOX9 regulates expression of *Foxc1*. A, SOX9 expression was induced in mouse embryonic stem cells containing a doxycycline (Dox)-inducible cassette. Expression was induced for 48 h by removal of Dox. Expression of *Foxc1*, *Foxc2*, *Col2a*, and *Sox9* mRNA was determined by qRT-PCR. Data are presented from three independent experiments. Error bars represent SD. B, SOX9 binding to regulatory elements in *Col2a* and *Foxc1* was determined by chromatin immunoprecipitation (ChIP) in ATDC5 chondrocyte cells. Four *Sox9*-binding sites in the regulatory region of *Foxc1* (distal A-D) were identified from previous ChIP-seq experiments (29). C, *Foxc1* distal regulatory elements were cloned into pGL4-luciferase reporters and transfected along with *Sox9* in ATDC5 cells. Only *Foxc1*-distal C was activated by *Sox9*. Data presented are all data points generated from three biological replicates with each containing three technical replicates. The bottom and top boundaries of each box represent the 25th and 75th percentiles, respectively, whereas the upper and lower error bars represent the 90th and 10th percentiles, respectively. The solid bar inside the box represents the median value, whereas the dashed line represents the mean. Dots indicate each data point. Statistical analysis was performed using one-way ANOVA with Holm–Sidak pairwise multiple comparisons. \*p value < 0.05. *Col2a*, collagen, type II, alpha 1; qRT-PCR, quantitative reverse transcriptase PCR; SOX9, SRY (sex-determining region Y)-box 9.

### 2.3.2 *Foxc1* regulates chondrocyte differentiation in vitro

Next, we examined whether *Foxc1* functions in regulating chondrocyte differentiation. First, we used a *Foxc1*-inducible mES cell line (Correa-Cerro et al., 2011) to assess whether *Foxc1* overexpression influences chondrocyte differentiation. We used a chondrocyte differentiation protocol outlined in Figure 2A and described in (Kawaguchi et al., 2005). Dox was removed from mES cells 2 days before chondrocyte differentiation, and we confirmed that FOXC1 protein levels were elevated by Dox removal (Fig. 2.2B). Expression of SRY (sex-determining region Y)-box 6 (*Sox6*), *Col2a*, runt related transcription factor 2 (*Runx2*), and collagen, type X, alpha 1 (*ColX*) mRNA was elevated in response to FOXC1 protein induction at 21 days of differentiation compared with that of uninduced controls. These results indicate that enforced *Foxc1* expression could enhance the differentiation capacity of mES cells.

To examine whether loss of *Foxc1* function affected chondrocyte differentiation, we used Crispr–Cas9 to mutate the *Foxc1* gene in ATDC5 cells. We generated a cell line (crisprmutated *Foxc1* [crFOXC1]) that introduced a premature stop codon that would truncate FOXC1 protein after helix 2 in the forkhead domain. Given that this truncation occurred before helix 3, the DNA recognition helix, this mutation would result in a nonfunctioning protein. Reduced FOXC1 protein levels were observed in this cell line (Fig. 2.3A). We then induced chondrocyte differentiation by supplementing the culture media with insulin, transferrin, and selenium to initiate chondrocyte differentiation. After 21 days of differentiation, we detected reduced Alcian blue–stained chondrogenic nodules in the crFOXC1 cells (Fig. 2.3B). Furthermore, loss of *Foxc1* function reduced levels of genes expressed in early chondrocyte (*Col2a*, *Sox9*), proliferating chondrocytes (*Fgfr3*), prehypertrophic chondrocytes (*Ihh*), and hypertrophic chondrocytes (*ColX* and matrix

metallopeptidase 13 [*Mmp13*]). Together, these findings indicate an impairment of chondrocyte differentiation when *Foxc1* function is lost.

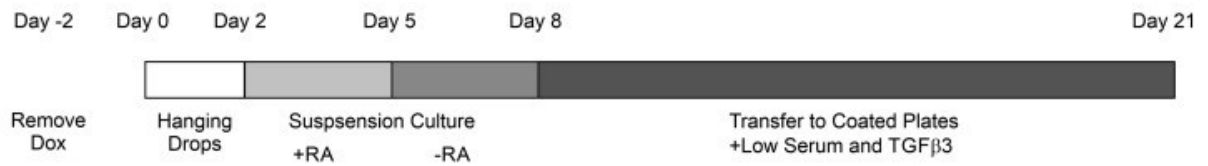
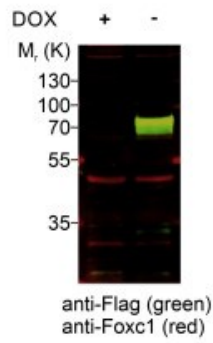
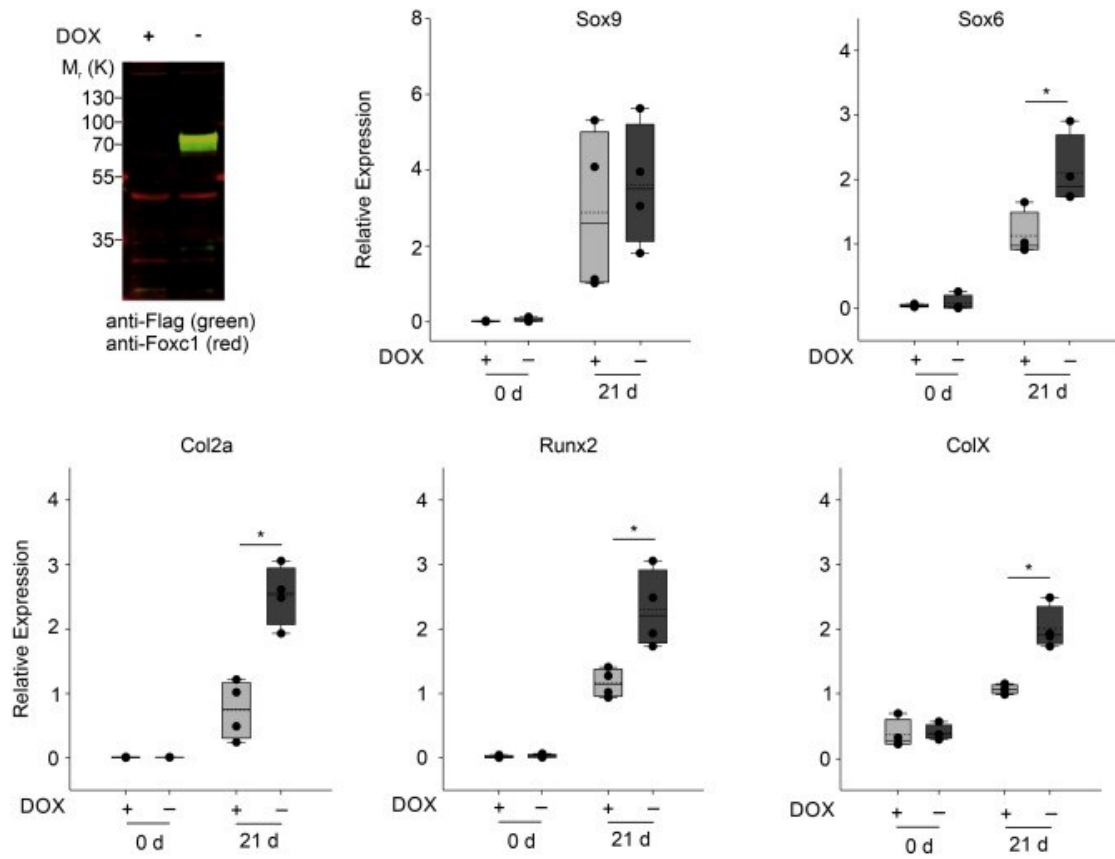
**A****B****C**

Figure 2.2. Elevated *Foxc1* promotes chondrocyte differentiation of mouse embryonic stem cells (mES). A, schematic of chondrocyte differentiation protocol for mES cells (31). B, expression of FOXC1 was confirmed in mES cells containing a Dox-inducible flag-tagged *Foxc1* expression cassette. C, chondrocyte differentiation in mES cells was monitored by measuring expression of *Sox9*, *Sox6*, *Col2a*, runt related transcription factor 2, and *ColX* expression. Data presented are from four biological replicates. The bottom and top boundaries of each box represent the 25th and 75th percentiles, respectively, whereas the upper and lower error bars represent the 90th and 10th percentiles, respectively. The solid bar inside the box represents the median value, whereas the dashed line represents the mean. Dots indicate each data point. Statistical analysis was performed using one-way ANOVA with Holm– Sidak pairwise multiple comparisons. \*p-value < 0.05; \*p-value < 0.05. *Col2a*, collagen, type II, alpha 1; *ColX*, collagen, type X, alpha 1; DOX, doxycycline; *Sox6*, SRY (sex-determining region Y)-box 6; SOX9, SRY (sex-determining region Y)-box 9.

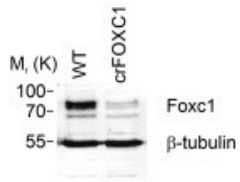
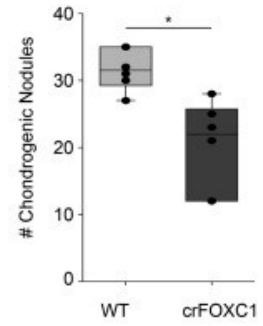
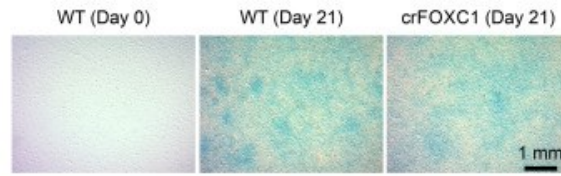
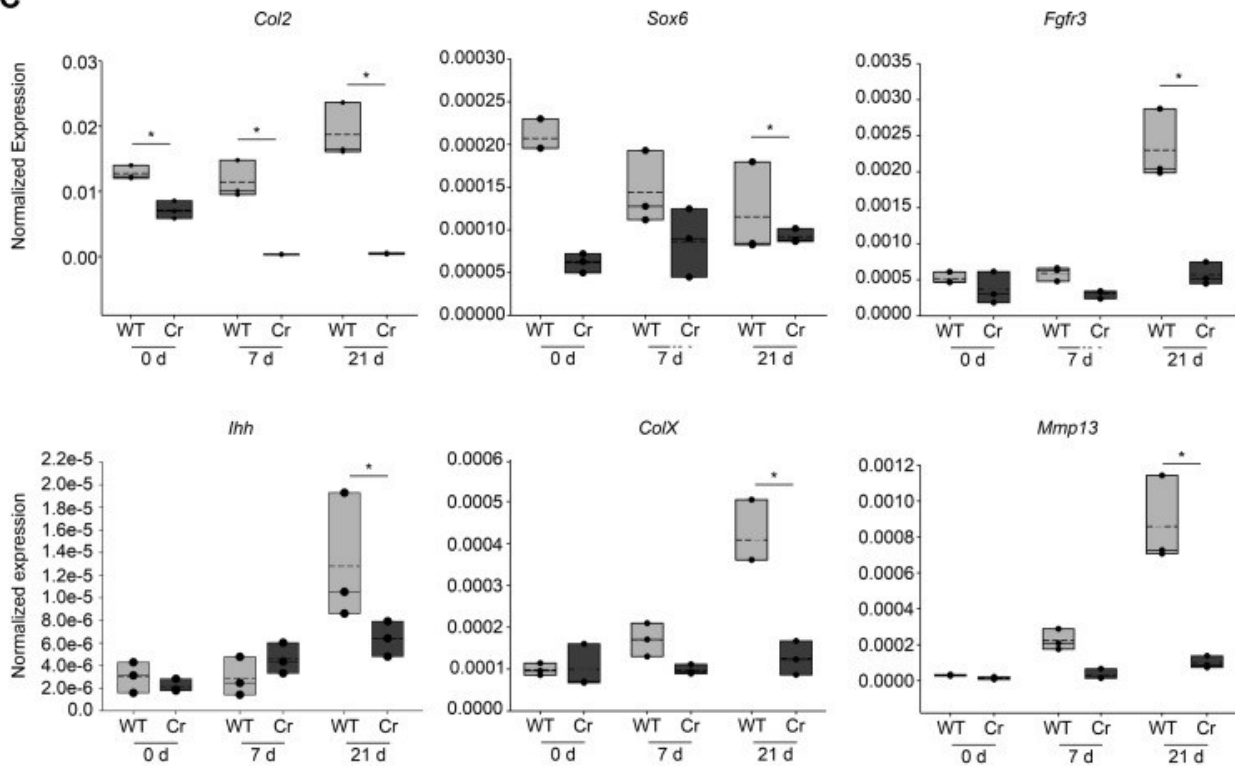
**A****B****C**

Figure 2.3. Loss of *Foxc1* expression in ATDC5 cells alters chondrocyte differentiation. A, deletion of *Foxc1* expression was achieved through Crispr mutagenesis. Reduced protein levels observed in *Foxc1* mutant cells (crFOXC1). B, WT and crFOXC1 cells were differentiated for 21 days and chondrogenesis measured by Alcian Blue staining. The number of chondrogenic nodules was counted in WT and mutant cells (n = 5). The scale bar represents 1 mm. C, levels of chondrocyte-expressed genes are affected in *Foxc1* mutant ATDC5 cells after 21 days of differentiation. The qRT-PCR data were collected from three biological replicates and normalized to the expression of housekeeping genes. The bottom and top boundaries of each box represent the 25th and 75th percentiles, respectively. The solid bar inside the box represents the median value, whereas the dashed line represents the mean. Dots indicate each data point. Statistical analysis was performed using one-way ANOVA with Holm–Sidak pairwise multiple comparisons. \*p-value < 0.05. crFOXC1, crisprmutated *Foxc1*; qRT-PCR, quantitative reverse transcriptase PCR.

### 2.3.3 *Foxc1* and *Foxc2* are expressed in the perichondrium and the resting zone of the growth plate

Next, we examined the localization of *Foxc1* and *Foxc2* expression in the developing skeleton. We focused on both *Foxc1* and *Foxc2* as each gene has a documented function for the proper formation of the skeleton (Kume et al., 1998; Winnier et al., 1997; Yoshida et al., 2015). More importantly, a direct comparison of gene expression patterns of *Foxc1* and *Foxc2* mRNA in the developing skeleton has yet to be performed. We used dual-labeling in situ hybridization to simultaneously localize *Foxc1* and *Foxc2* mRNAs in the growth plate of the mouse hind limb. We observed both overlapping and distinct expression patterns for *Foxc1* and *Foxc2* mRNAs. Both *Foxc1* and *Foxc2* are expressed in the condensing mesenchyme and anlage in the developing hind limb bud at 12 days post coitum (dpc), although *Foxc1* expression is more widely distributed than that of *Foxc2* at this time point (Fig. 2.4A). At 13.5 dpc *Foxc1* and *Foxc2* expression becomes restricted to the peripheral region of the proximal skeletal elements (Fig. 2.4B). In the less-mature distal skeletal elements, *Foxc1* expression is widely expressed throughout the newly forming bone, whereas *Foxc2* retains a more restricted expression pattern at this stage. In the tibia at 14.5 dpc, *Foxc1* mRNA was strongly detected in the perichondrium, resting zone chondrocytes, and late hypertrophic chondrocytes/primary ossification center and lower expression detected in the proliferating and prehypertrophic chondrocytes (Fig. 2.4C). We also observed strong *Foxc1* expression in the cells lying between the tibia and femur. *Foxc2* mRNA expression was restricted to the perichondrium and newly emerging primary ossification center at this time point (Fig. 2.4C). A distinct expression pattern for *Foxc2* mRNA was detected in the outer cell layer of perichondrium. Expression of *Foxc1* and *Foxc2* mRNAs in the proximal tibia at 16.5 dpc continued to be enriched in the surrounding perichondrium (Fig. 2.4, D–I). *Foxc1*- and *Foxc2*-

expressing cells were also detected in the resting zone chondrocytes (Fig. 4G) and in putative borderline chondrocytes cells found between the proliferating zone chondrocytes and the perichondrium (Fig. 2.4H). Very little *Foxc1* or *Foxc2* mRNA was detected in proliferating chondrocyte or hypertrophic chondrocyte cells (Fig. 2.4I). Together, these results indicate that *Foxc1* and *Foxc2* have restricted expression patterns in the developing bones: expression of both *Foxc1* and *Foxc2* is abundant in early stages of endochondral ossification (12–14.5 dpc) and becomes restricted to the perichondrium and resting chondrocytes at later stages (16.5 dpc).

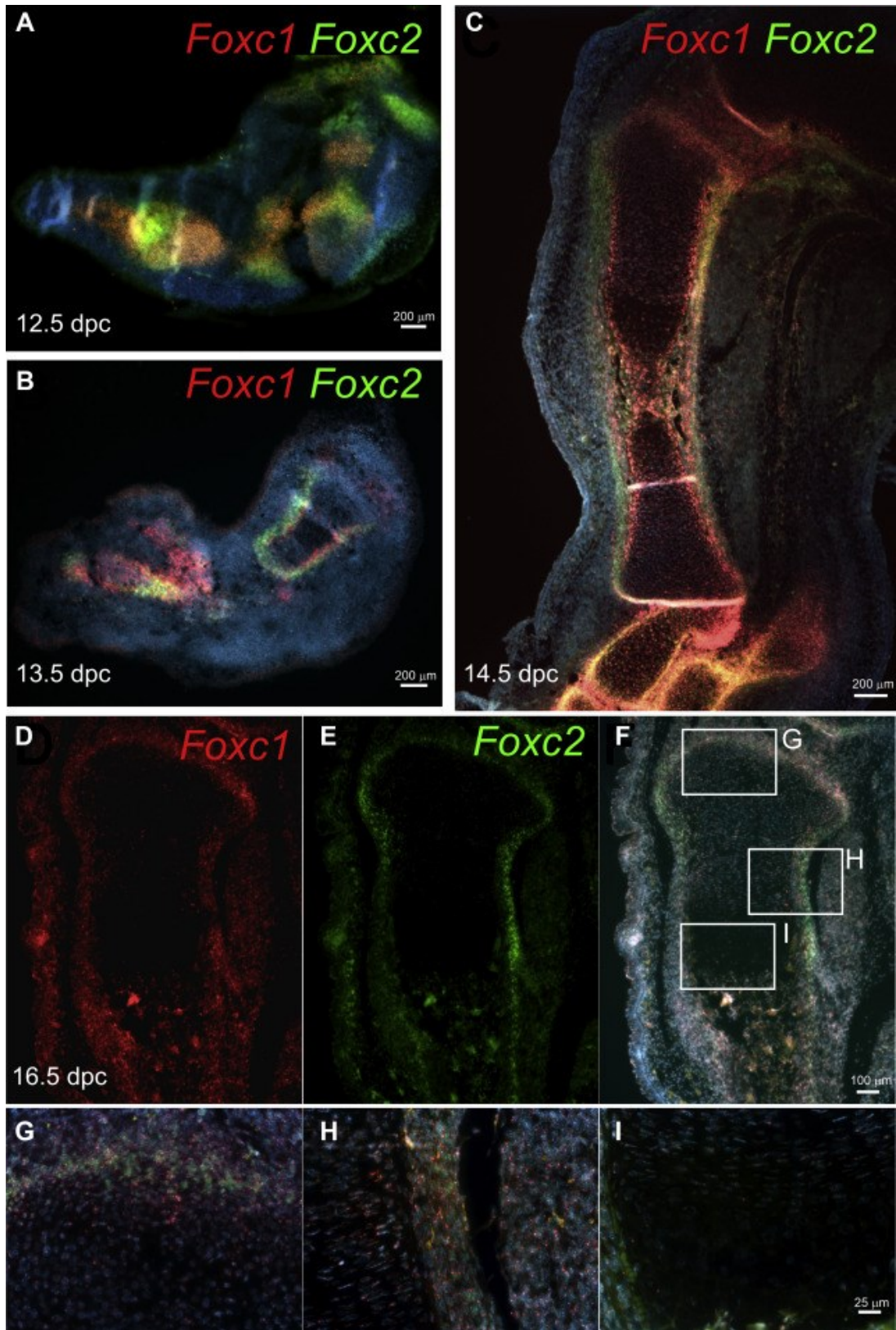


Figure 2.4. *Foxc1* and *Foxc2* are expressed in the perichondrium and resting zone of the growth plate. Localization of *Foxc1* and *Foxc2* mRNA expression was determined in the hind limb by in situ hybridization at (A) 12.5 dpc, (B) 13.5 dpc, and (C) 14.5 dpc. The scale bar (A–C) represents 200  $\mu\text{m}$ . D, *Foxc1* and (E) *Foxc2* mRNA expression in the proximal tibia at 16.5 dpc was abundant in the perichondrium. F, *Foxc1* and *Foxc2* mRNA displayed both overlapping and distinct expression patterns in the developing limb. The scale bar (D–F) represents 100  $\mu\text{m}$ . G, *Foxc1* transcripts (red) were detected in the perichondrium and resting zone, whereas *Foxc2* (green) was mainly expressed in the perichondrium. Low levels of *Foxc1* and *Foxc2* expression were detected in the proliferative zone (H) and hypertrophic zone (I). The scale bar (G and H) represents 25  $\mu\text{m}$ . dpc, days post coitum.

#### 2.3.4 Deletion of *Foxc1* and *Foxc2* in chondrocyte progenitors causes skeletal dysplasia

To understand the roles of *Foxc1* and *Foxc2* in the formation of the endochondral skeleton, we generated conditional, compound *Foxc1* and *Foxc2* mutant mice using the *Col2-cre* driver strain (Terpstra et al., 2003). We chose to delete both *Foxc1* and *Foxc2* genes to eliminate any potential genetic compensation that may occur when one *Foxc* paralog was deleted. First, we assessed the cre activity of this strain by crossing *Col2-cre* mice with ROSA26mTmG mice that expresses enhanced GFP (EGFP) when *cre* recombinase is present. At 14.5 dpc, EGFP was detected throughout the developing skeleton. In the hind limb, *cre* activity was detected in the growth plate chondrocytes, perichondrium, and primary ossification center (Fig. 2.5, A and B). This expression pattern indicates that the *Col-cre* strain is active in cells of the developing skeleton and cell layers that express *Foxc1* and *Foxc2*. Next, we crossed the *Col2-cre* mice to homozygous floxed (fl) *Foxc1;Foxc2* mice (Sasman et al., 2012) to generate *Col2-cre;Foxc1<sup>+/-</sup>;Foxc2<sup>+/-</sup>* heterozygotes. These mice were viable and displayed no overt health issues. To delete both copies of *Foxc1* and *Foxc2* in chondrocyte progenitors, we crossed male *Col2-cre;Foxc1<sup>+/-</sup>;Foxc2<sup>+/-</sup>* mice with *Foxc1<sup>fl/fl</sup>;Foxc2<sup>fl/fl</sup>* females. We confirmed by in situ hybridization that *Foxc1* and *Foxc2* mRNA expression was lost in the hind limbs of 16.5 dpc *Col2-cre;Foxc1<sup>Δ/Δ</sup>;Foxc2<sup>Δ/Δ</sup>* embryos (Fig. 2.5, C and D). No viable *Col2-cre;Foxc1<sup>Δ/Δ</sup>;Foxc2<sup>Δ/Δ</sup>*, *Col2-cre;Foxc1<sup>Δ/Δ</sup>;Foxc2<sup>+/-</sup>*, *Col2-cre;Foxc1<sup>+/-</sup>;Foxc2<sup>Δ/Δ</sup>* pups were found at birth. We then isolated embryos at 18.5 dpc for Alizarin red and Alcian blue skeletal staining and found all genotypes were present at expected Mendelian ratios. We detected a skeletal hypoplasia that worsened when *Foxc* gene dosage was lost (Fig. 2.6A). The skeletons of *Col2-cre;Foxc1<sup>+/-</sup>;Foxc2<sup>+/-</sup>* embryos at 18.5 dpc formed correctly and displayed no overt phenotypes compared with control (cre negative) embryos. *Col2-cre;Foxc1<sup>+/-</sup>;Foxc2<sup>Δ/Δ</sup>* displayed skeletal anomalies including underdeveloped occipital bones and vertebrae. In

the cervical vertebrae, the atlas and axis bones were markedly reduced in size compared with control embryos and compound *Col2-cre;Foxc1<sup>+/-Δ</sup>;Foxc2<sup>+/-Δ</sup>* mice.

The skeletons of *Col2-cre;Foxc1<sup>Δ/Δ</sup>;Foxc2<sup>Δ/Δ</sup>* displayed a smaller, misshapen rib cage, with malformed cervical vertebrae and occipital bones (Fig. 2.6A). The most severe phenotype was observed in the *Col2-cre;Foxc1<sup>Δ/Δ</sup>;Foxc2<sup>Δ/Δ</sup>* embryos and will be the remaining focus of this article. These embryos displayed a markedly underdeveloped skeleton. The occipital bones were missing, giving the skull a domed appearance (6/6 embryos). The cervical vertebrae were absent in *Col2-cre;Foxc1<sup>Δ/Δ</sup>;Foxc2<sup>Δ/Δ</sup>* embryos, and ossification of the remaining bones in the vertebral column was impaired (6/6 embryos; Fig. 2.6B). The rib cage was misshapen but patterned correctly as no missing or fused ribs were detected in the *Col2-cre;Foxc1<sup>Δ/Δ</sup>;Foxc2<sup>Δ/Δ</sup>* embryos (Fig. 2.6B). Likewise, the overall patterning of the limbs appeared normal although ossification was reduced or delayed (Fig. 2.6, B and C). Ossification of the proximal and middle phalanges bones was absent in the *Col2-cre;Foxc1<sup>Δ/Δ</sup>;Foxc2<sup>Δ/Δ</sup>* (6/6 embryos). Ossification of the distal phalange bones was variable, with ossification detected in four of six embryos examined.

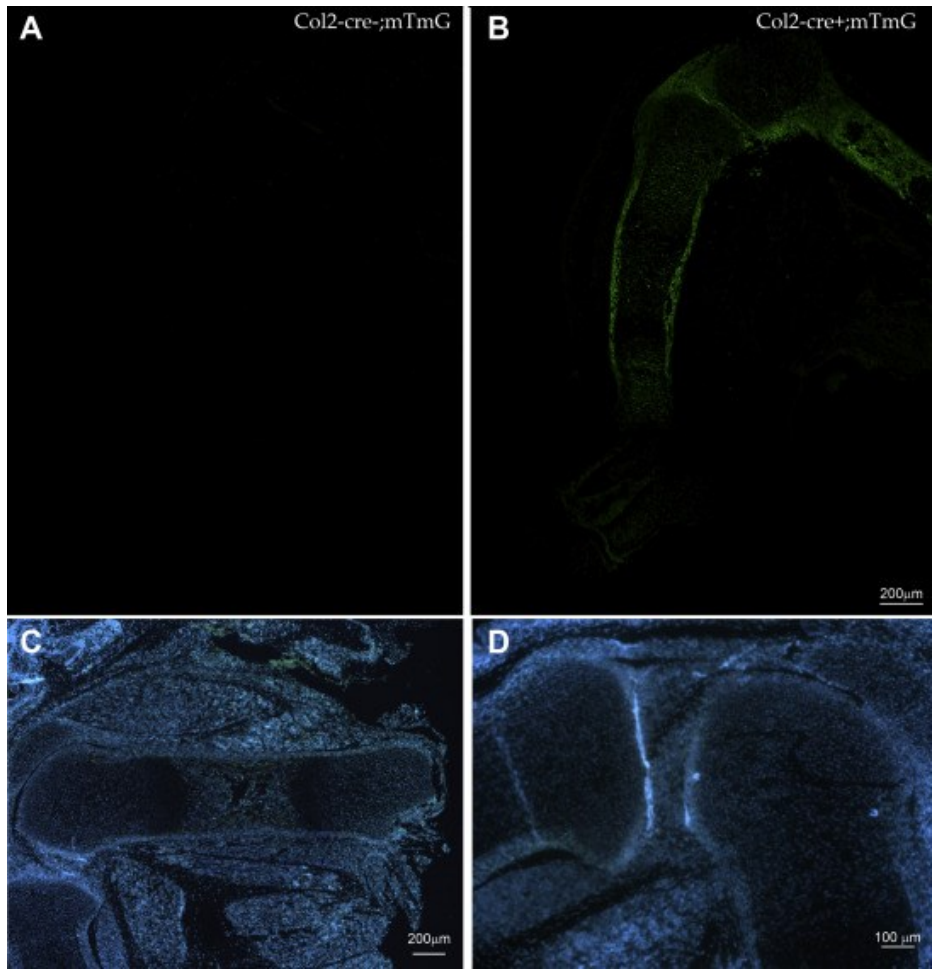


Figure 2.5. *Col2-cre* ablation of *Foxc1* and *Foxc2* expression in the developing limb. A and B, ROSA26<sup>tm4</sup>(ACTB-tdTomato,-EGFP)(mTmG) mice were crossed to *Col2-cre* mice to monitor *Cre* activity in the developing limb at 14.5 dpc. EGFP was only detected in the limbs of mice containing the *Col2-cre* transgene. C and D, to create chondrocyte-specific *Foxc1* and *Foxc2* mutant mice, *Col2-cre* mice were crossed with homozygous “floxed” *Foxc1* and *Foxc2* mice. No expression of *Foxc1* and *Foxc2* mRNA was detected by in situ hybridization in the developing humerus or proximal tibia in *Col2-cre;Foxc1<sup>Δ/Δ</sup>;Foxc2<sup>Δ/Δ</sup>* mice at 16.5 dpc. The scale bar represents (A–C) 200 μm and 100 μm (D). dpc, days post coitum; EGFP, enhanced GFP.

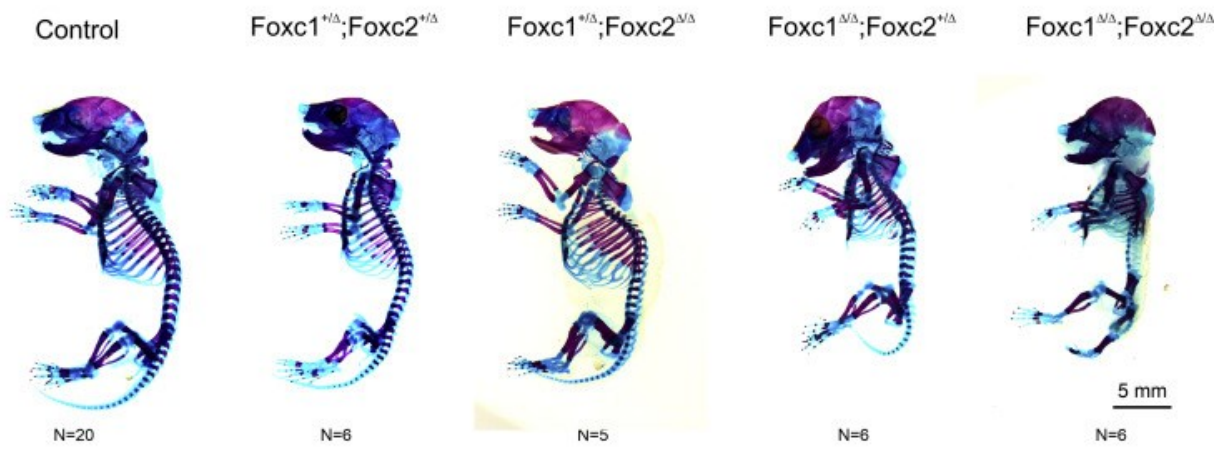
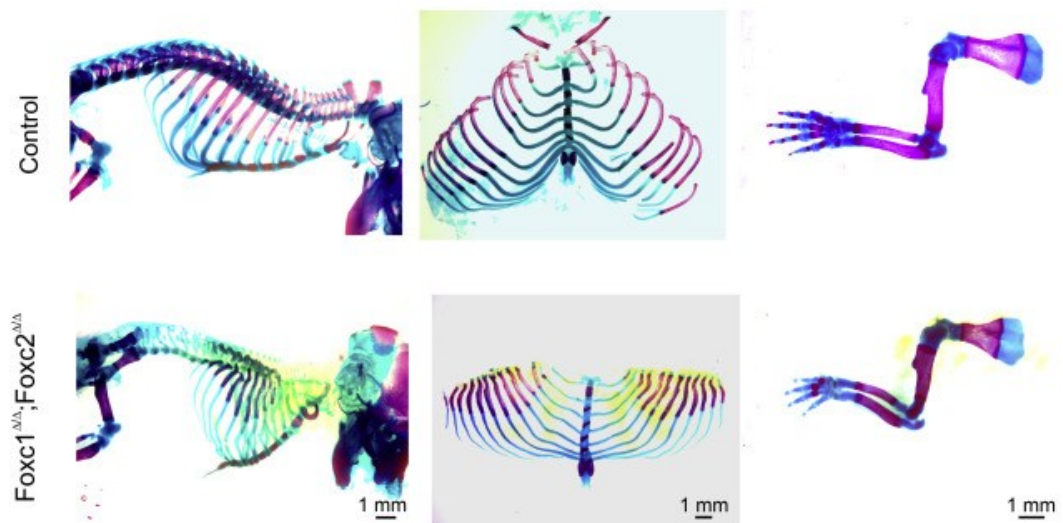
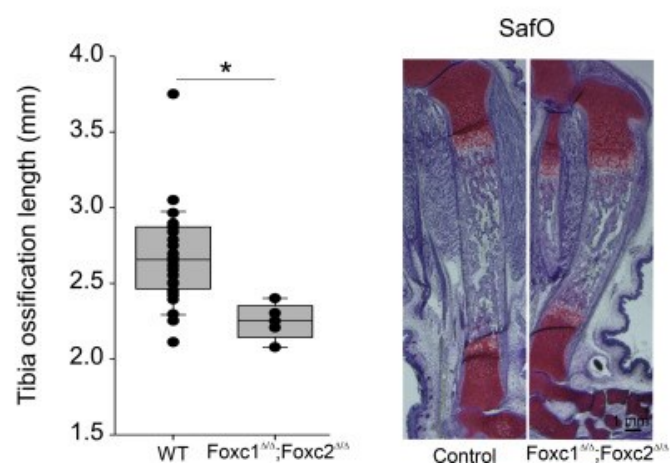
**A****B****C**

Figure 2.6. *Col2-cre* deletion of *Foxc1* and *Foxc2* causes skeletal hypoplasia. A, Alizarin red and Alcian blue skeleton preps from 18.5 dpc embryos. Control embryos lack the *Col2-cre* transgene. The scale bar represents 5 mm. B, disrupted endochondral ossification can be observed in the axial and appendicular skeleton of *Col2-cre;Foxc1<sup>Δ/Δ</sup>;Foxc2<sup>Δ/Δ</sup>* embryos. The scale bar represents 1 mm. C, length of ossification is reduced in the tibia at 18.5 dpc of *Col2-cre;Foxc1<sup>Δ/Δ</sup>;Foxc2<sup>Δ/Δ</sup>* mice. The lengths of ossification zones were measured from 20 control and five mutant embryos. Data were analyzed by Student's t test. \*p-value < 0.05. The scale bar represents 1 mm. dpc, days post coitum.

### 2.3.5 *Foxc1* and *Foxc2* are required for the formation of the growth plate

The limbs of *Col2-cre;Foxc1<sup>Δ/Δ</sup>;Foxc2<sup>Δ/Δ</sup>* embryos displayed reduced mineralization and reduction in length (Fig. 2.6C). We therefore decided to investigate the formation of the growth plate of these mutants to identify the contribution of *Foxc1* and *Foxc2* to the function of this structure. Sections through the 16.5 dpc proximal tibia revealed growth plate anomalies in the *Col2-cre;Foxc1<sup>Δ/Δ</sup>;Foxc2<sup>Δ/Δ</sup>* embryos (Fig. 2.7A). In particular, the characteristic stacked organization of the proliferative zone chondrocytes was not as prevalent in the *Col2-cre;Foxc1<sup>Δ/Δ</sup>;Foxc2<sup>Δ/Δ</sup>* embryos. The length of the resting zone chondrocytes layer was expanded, whereas the proliferating zone layer was reduced in the *Col2-cre;Foxc1<sup>Δ/Δ</sup>;Foxc2<sup>Δ/Δ</sup>* embryos (Fig. 2.7B). We next assessed whether this reduction in size of the proliferating zone chondrocytes corresponded to a reduction in cell proliferation. As observed in Figure 7C, we did detect a reduction in the number of KI67-positive cells in the growth plate of *Col2-cre;Foxc1<sup>Δ/Δ</sup>;Foxc2<sup>Δ/Δ</sup>* embryos. We also examined whether cell death was affected in *Col2-cre;Foxc1<sup>Δ/Δ</sup>;Foxc2<sup>Δ/Δ</sup>* embryos and found no changes in the number of apoptotic cells in the growth plates between control and *Col2-cre;Foxc1<sup>Δ/Δ</sup>;Foxc2<sup>Δ/Δ</sup>* embryos (data not shown).

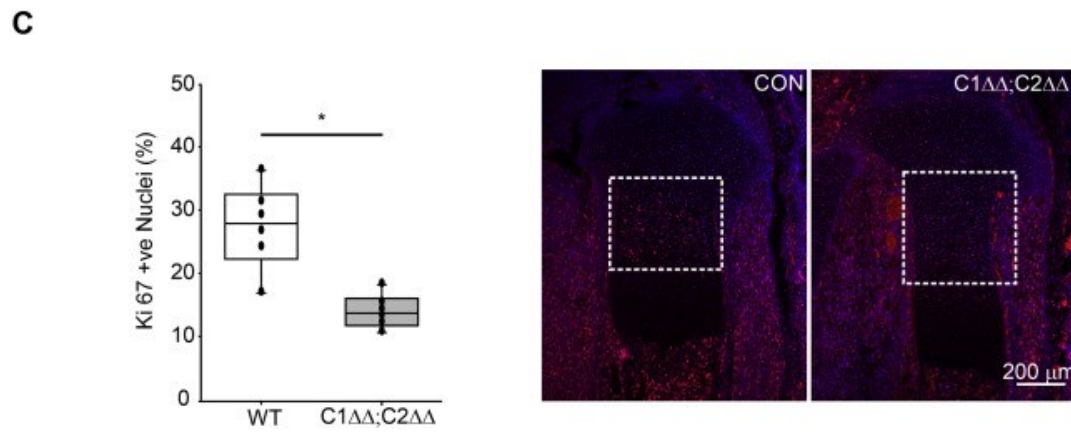
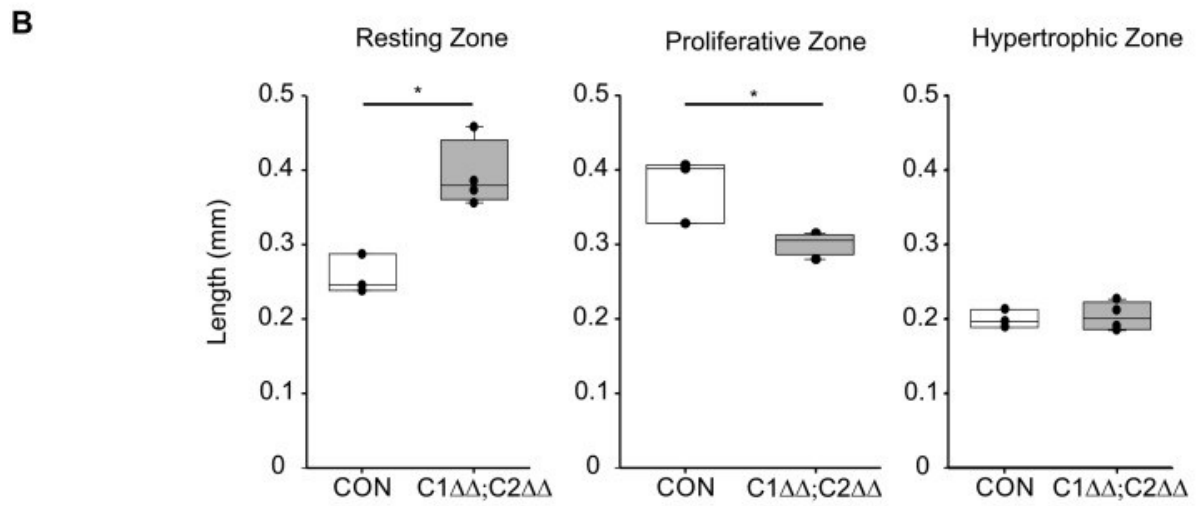
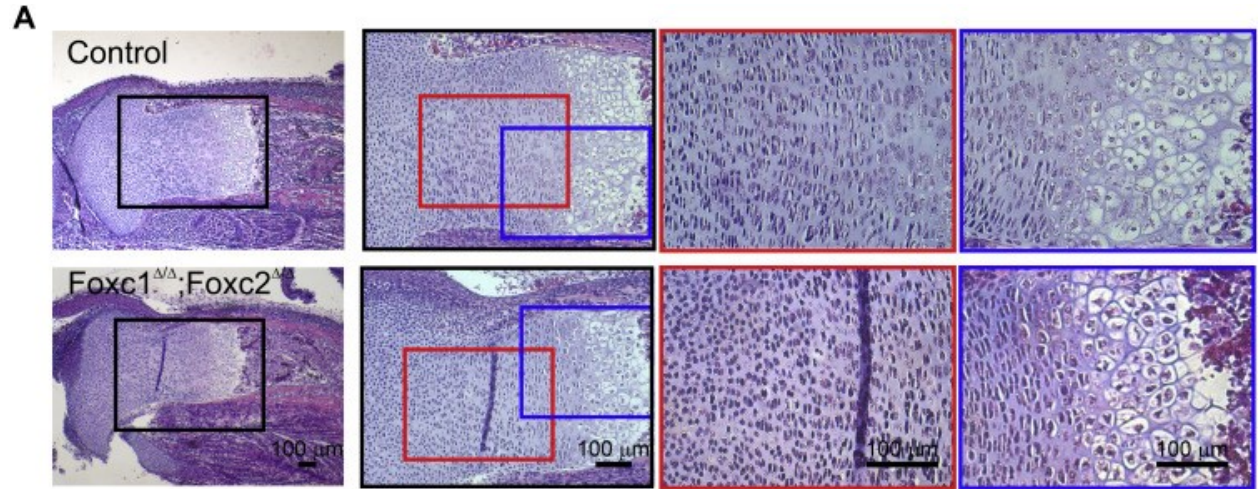


Figure 2.7. Disrupted growth plate organization in *Col2-cre;Foxc1<sup>Δ/Δ</sup>;Foxc2<sup>Δ/Δ</sup>* mutants. A, hematoxylin–eosin staining of the 16.5 dpc proximal tibia growth plate. Enlarged sections are depicted with colored boxes. The scale bar represents 100 μm. B, lengths of the resting, proliferative, and hypertrophic zone were measured in control (CON) or *Col2-cre;Foxc1<sup>Δ/Δ</sup>;Foxc2<sup>Δ/Δ</sup>* (*C1<sup>Δ/Δ</sup>;C2<sup>Δ/Δ</sup>*) growth plate (N = 4). Data were analyzed by Student's t test. \*p-value < 0.05. C, chondrocyte proliferation in control of *Col2-cre;Foxc1<sup>Δ/Δ</sup>;Foxc2<sup>Δ/Δ</sup>* was measured by KI67 immunofluorescence. The percentage of KI67-positive nuclei was determined from six mutant and six control tibia sections. Data were analyzed by Student's t test. \*p-value < 0.05. The scale bar represents 200 μm. dpc, days post coitum.

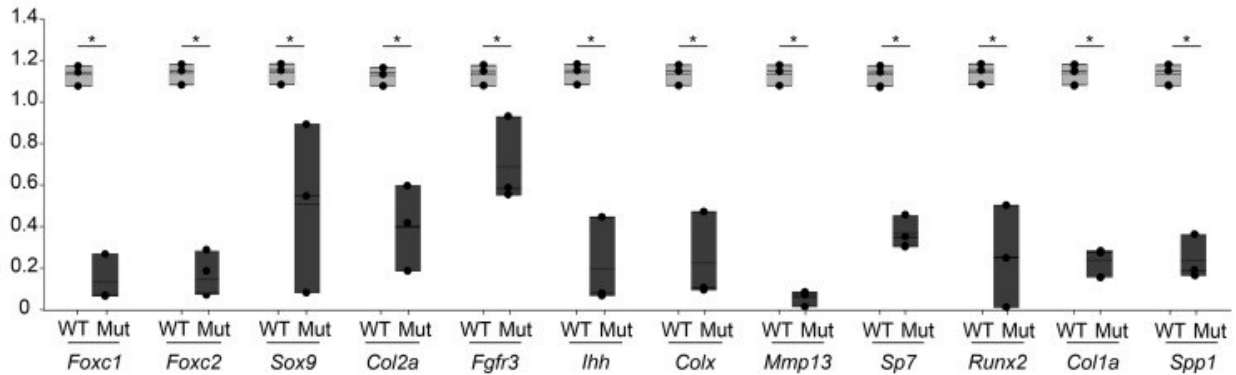
### 2.3.6 Endochondral ossification gene expression is reduced in *Col2-cre;Foxc1<sup>Δ/Δ</sup>;Foxc2<sup>Δ/Δ</sup>* embryos

Given that *Foxc1* and *Foxc2* are transcription factors, it is expected that these genes exert their effects through regulation of gene expression. To further understand how *Foxc1* and *Foxc2* contribute to the formation of the skeleton, we analyzed gene expression of endochondral genes in *Col2-cre;Foxc1<sup>Δ/Δ</sup>;Foxc2<sup>Δ/Δ</sup>* embryos. We isolated RNA from the rib cage of 16.5 dpc embryos and monitored gene expression by quantitative reverse transcriptase PCR (qRT-PCR). We chose the rib cage as a tissue source as nonskeletal tissues could be efficiently dissected away from the skeletal elements. Expression of *Foxc1* and *Foxc2* was reduced in rib cage RNA from *Col2-cre;Foxc1<sup>Δ/Δ</sup>;Foxc2<sup>Δ/Δ</sup>* embryos (Fig. 2.8A). We assayed expression of genes that act throughout all stages of endochondral ossification and found that all genes assessed had decreased expression levels when *Foxc1* and *Foxc2* were absent. For example, genes expressed early in the formation of chondrocytes (*Sox9*, *Sox6*, and *Col2a*) were reduced, and genes expressed in later chondrocyte differentiation stages such as *Ihh*, *Fgfr3*, and *ColX*, as well as genes expressed during osteoblast formation and mineralization (*Sp7*, *Runx2*, *Colla*, and *Spp1*) were also reduced in *Col2-cre;Foxc1<sup>Δ/Δ</sup>;Foxc2<sup>Δ/Δ</sup>* rib cage RNA (Fig. 2.8A).

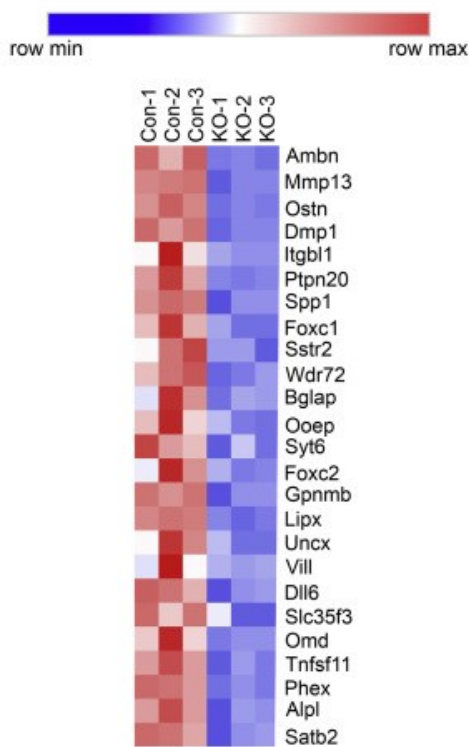
To gain a complete picture of gene expression changes in response to deletion of *Foxc1* and *Foxc2* in chondrocyte progenitors, we performed RNA-Seq from three additional samples of 16.5 rib cage RNA isolated from control and *Col2-cre;Foxc1<sup>Δ/Δ</sup>;Foxc2<sup>Δ/Δ</sup>* embryos. In total, we found 83 genes downregulated and 232 genes upregulated in rib cage RNA isolated from mutant embryos compared with controls ( $\log_2^{\text{foldchange}} \pm 1$ ;  $p$  value  $<0.05$ ; false discovery rate  $<0.01$ ; Tables 2.S1 and 2.S2). The 25 genes with the greatest reduction in expression in *Col2-cre;Foxc1<sup>Δ/Δ</sup>*

; *Foxc2*<sup>Δ/Δ</sup> embryos (Fig. 2.8B) included many of the genes involved in endochondral ossification. Gene ontology analysis revealed that the majority of biological functions affected in our downregulated gene set were involved in endochondral ossification, including cartilage development, osteoblast differentiation, and ossification (Fig. 2.8C). Functional classification of the genes present in the upregulated dataset were enriched with those involved in lipid metabolic processes, fatty acid metabolism, and epidermis development (Table 2.S3). Together, data from these gene expression analyses suggest that loss of *Foxc1* and *Foxc2* function in *Col2-cre*-expressing cells affected many stages of chondrocyte and osteoblast differentiation during the endochondral ossification processes.

**A**



**B**



**C**

Down Regulated Genes- Biological Process	P Value
Ossification <i>Bmp8, Dmp1, Ostn, Sost, Spp1</i>	2.10E-09
Osteoblast Differentiation <i>Rspo2, Sp7, Alpl, Bmp8a, Runx2, Spp1</i>	3.50E-06
Biomineral Tissue Development <i>Ambn, Bglap, Dmp1, Phex, Spp1</i>	3.60E-06
Bone Mineralization <i>Rspo2, Gpnmb, Ifitm5, Mmp13, Satb2, Omd</i>	7.80E-06
Skeletal System Development <i>Mmp13, Sp7, Alpl, Runx2, Spp1</i>	6.30E-04
Multicellular Organism Development <i>Uncx, Bmp8a, Dlx6, Ifitm5, Mlx, Pax9</i>	3.10E-03
Positive Regulation of Transcription <i>Sp7, Mlx, Pax9, Satb, Runx2</i>	3.30E-03
Cartilage Development <i>Smad9, Bmp8a, Mmp13, Satb2</i>	5.30E-03
Endochondral Ossification <i>Alpl, Mmp13, Runx2, Sp7</i>	7.20E-03
Cellular Response to BMP Stimulus <i>Bglap, Runx2, Tnmd</i>	7.4 E-03

Figure 2.8. Loss of *Foxc1* and *Foxc2* function in chondrocytes results in a general reduction of mRNA levels of genes expressed throughout endochondral ossification. A, RNA from the rib cage from three control and three *Col2-cre;Foxc1<sup>Δ/Δ</sup>;Foxc2<sup>Δ/Δ</sup>* embryos at 16.5 dpc was isolated and gene expression monitored by qRT-PCR. Data presented are relative expression normalized to control samples. The bottom and top boundaries of each box represent the 25th and 75th percentiles, respectively. The solid bar inside the box represents the median value, whereas the dashed line represents the mean. Dots indicate each data point. Statistical analysis was performed using one-way ANOVA with Holm–Sidak pairwise multiple comparisons. \*p-value < 0.05. B, heat map of the top-25 genes downregulated in 16.5 dpc *Col2-cre;Foxc1<sup>Δ/Δ</sup>;Foxc2<sup>Δ/Δ</sup>* rib cage RNA as determined by RNA-Seq analysis. C, functional annotation genes downregulated *Col2-cre;Foxc1<sup>Δ/Δ</sup>;Foxc2<sup>Δ/Δ</sup>* mutants. dpc, days post coitum; qRT-PCR, quantitative reverse transcriptase PCR.

Next, we examined the expression of chondrocyte differentiation genes in formation of the growth plate of *Col2-cre;Foxc1<sup>Δ/Δ</sup>;Foxc2<sup>Δ/Δ</sup>* embryos in more detail. We found that the localization of SOX9 and SOX6 protein was unaffected in the tibia growth plate. These proteins were found throughout the resting zone and proliferative zone in the proximal tibia at 16.5 dpc (Fig. 2.9, A and B). Expression of *Fgfr3* was detected in the proliferative zone of *Col2-cre;Foxc1<sup>Δ/Δ</sup>;Foxc2<sup>Δ/Δ</sup>* embryos (Fig. 2.9C) The extent of this expression domain appeared reduced in the *Col2-cre;Foxc1<sup>Δ/Δ</sup>;Foxc2<sup>Δ/Δ</sup>* embryos, likely because of the reduced size of the proliferating zone (Fig. 2.7). RUNX2 protein localized to the prehypertrophic chondrocytes of *Col2-cre;Foxc1<sup>Δ/Δ</sup>;Foxc2<sup>Δ/Δ</sup>* embryos (Fig. 2.9D), and *Ihh* mRNA was also expressed in this region, but expression intensity was reduced (Fig 2.9E). Localization of COLX protein in hypertrophic chondrocytes was also altered in the tibia growth plate of *Col2-cre;Foxc1<sup>Δ/Δ</sup>;Foxc2<sup>Δ/Δ</sup>* embryos at 16.5 dpc. Although the protein was present, its localization zone was expanded into the primary ossification in *Col2-cre;Foxc1<sup>Δ/Δ</sup>;Foxc2<sup>Δ/Δ</sup>* embryos (Fig. 2.9, F and H). MMP13 protein was also localized correctly to the hypertrophic chondrocytes at the osteochondral interface. Together, these expression patterns suggest that in *Col2-cre;Foxc1<sup>Δ/Δ</sup>;Foxc2<sup>Δ/Δ</sup>* embryos, chondrocytes are able to correctly form and progress through their differentiation processes; however, this progression is altered as evidenced by expanded COLX protein.

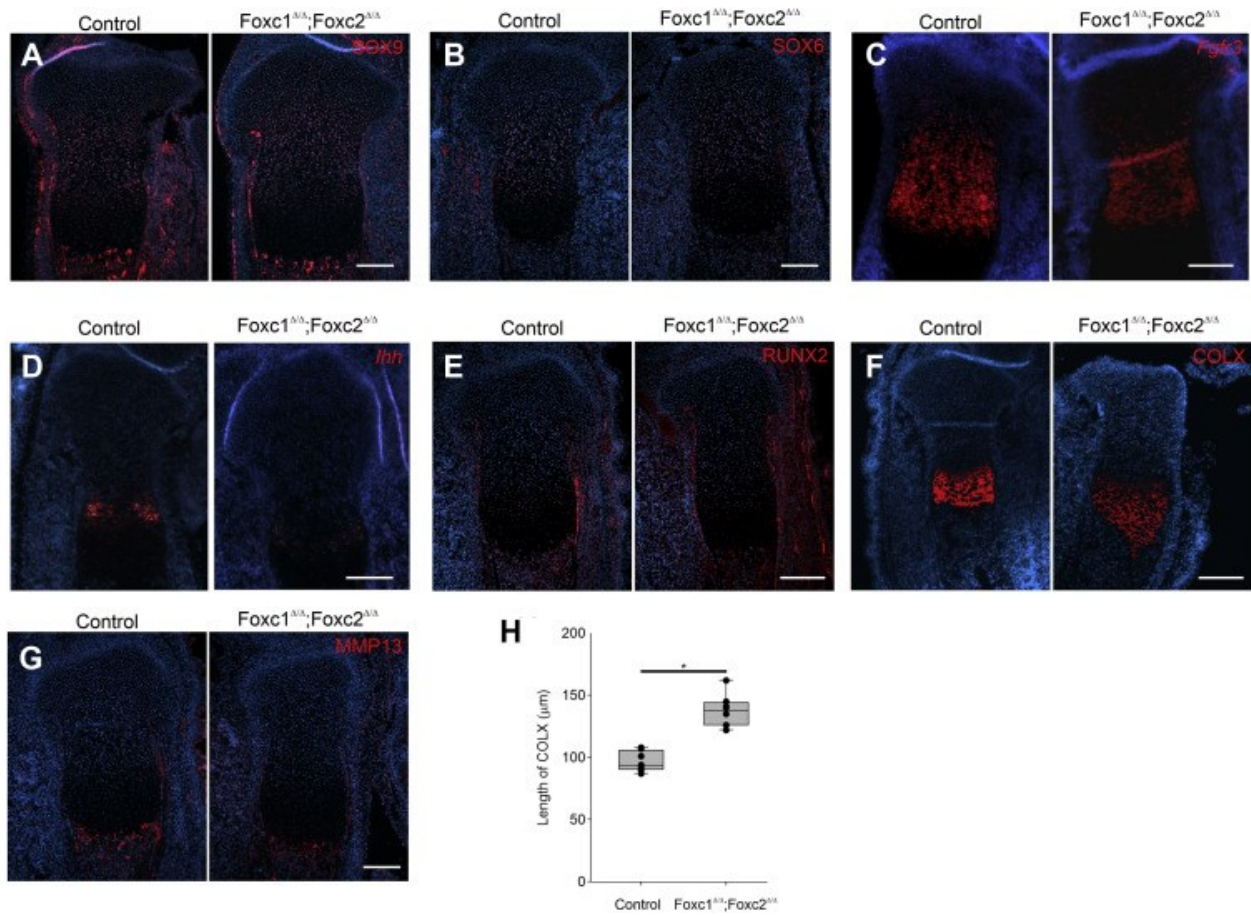


Figure 2.9. Altered chondrocyte differentiation in *Col2-cre;Foxc1<sup>Δ/Δ</sup>;Foxc2<sup>Δ/Δ</sup>* embryos. Gene expression pattern markers of chondrocyte differentiation were monitored in the proximal tibia growth plate at 16.5 dpc in control or *Col2-cre;Foxc1<sup>Δ/Δ</sup>;Foxc2<sup>Δ/Δ</sup>* embryos. A, SOX9 immunofluorescence (IF), (B) SOX6 IF, (C) *Fgfr3* in situ hybridization, (D) *Ihh* ISH, (E) runt related transcription factor 2 IF, (F) COLX IF, and (G) MMP13 IF. The scale bar represents 200 μm. H, length of COLX positive cells in control versus *Col2-cre;Foxc1<sup>Δ/Δ</sup>;Foxc2<sup>Δ/Δ</sup>* growth plates. The length of COLX expression regions was determined from six mutant and six control tibia sections. Data were analyzed by Student's t test. \*p-value < 0.05. ColX, collagen, type X, alpha 1; dpc, days post coitum; IHH, Indian hedgehog; *Mmp13*, matrix metalloproteinase 13; *Sox6*, SRY (sex-determining region Y)-box 6; SOX9, SRY (sex-determining region Y)-box 9.

Finally, we assessed the effect of loss of *Foxc1* and *Foxc2* function in the *Col2-cre*-expressing cells on the ossification process. Von Kossa staining in the 16.5 dpc tibia indicated that ossification occurred in the periosteum and osteochondral interface; however, large areas of the bone marrow space were unmineralized (Fig. 2.10, A, A0, B, and B0). We next examined whether osteoblast formation occurred correctly in the *Col2-cre;Foxc1<sup>Δ/Δ</sup>;Foxc2<sup>Δ/Δ</sup>* embryos by monitoring osterix (OSX) and osteopontin (OPN) protein localization. In 16.5 dpc tibias, OSX- and OPN-positive cells were found in the osteochondral interface and in the primary ossification center (Fig. 2.10, C and D), indicating that osteoblasts formed in the *Col2-cre;Foxc1<sup>Δ/Δ</sup>;Foxc2<sup>Δ/Δ</sup>*. Osteoblasts containing COL1a protein were detected at the osteochondral interface, the primary ossification center, the periosteum, and groove of Ranvier in both control and *Col2-cre;Foxc1<sup>Δ/Δ</sup>;Foxc2<sup>Δ/Δ</sup>* embryos, which further indicated that osteoblast could form in the mutant bones (Fig. 2.10, E and F). Vascular endothelial growth factor A (VEGFA) protein localization was present but reduced in the hypertrophic chondrocytes in *Col2-cre;Foxc1<sup>Δ/Δ</sup>;Foxc2<sup>Δ/Δ</sup>* embryos (Fig. 2.10, G and H). Together, these findings indicate that although endochondral bone formation and mineralization is abnormal in *Col2-cre;Foxc1<sup>Δ/Δ</sup>;Foxc2<sup>Δ/Δ</sup>* embryos, the molecular processes that regulate this bone formation do occur in *Col2-cre;Foxc1<sup>Δ/Δ</sup>;Foxc2<sup>Δ/Δ</sup>* embryos albeit in a disrupted manner.

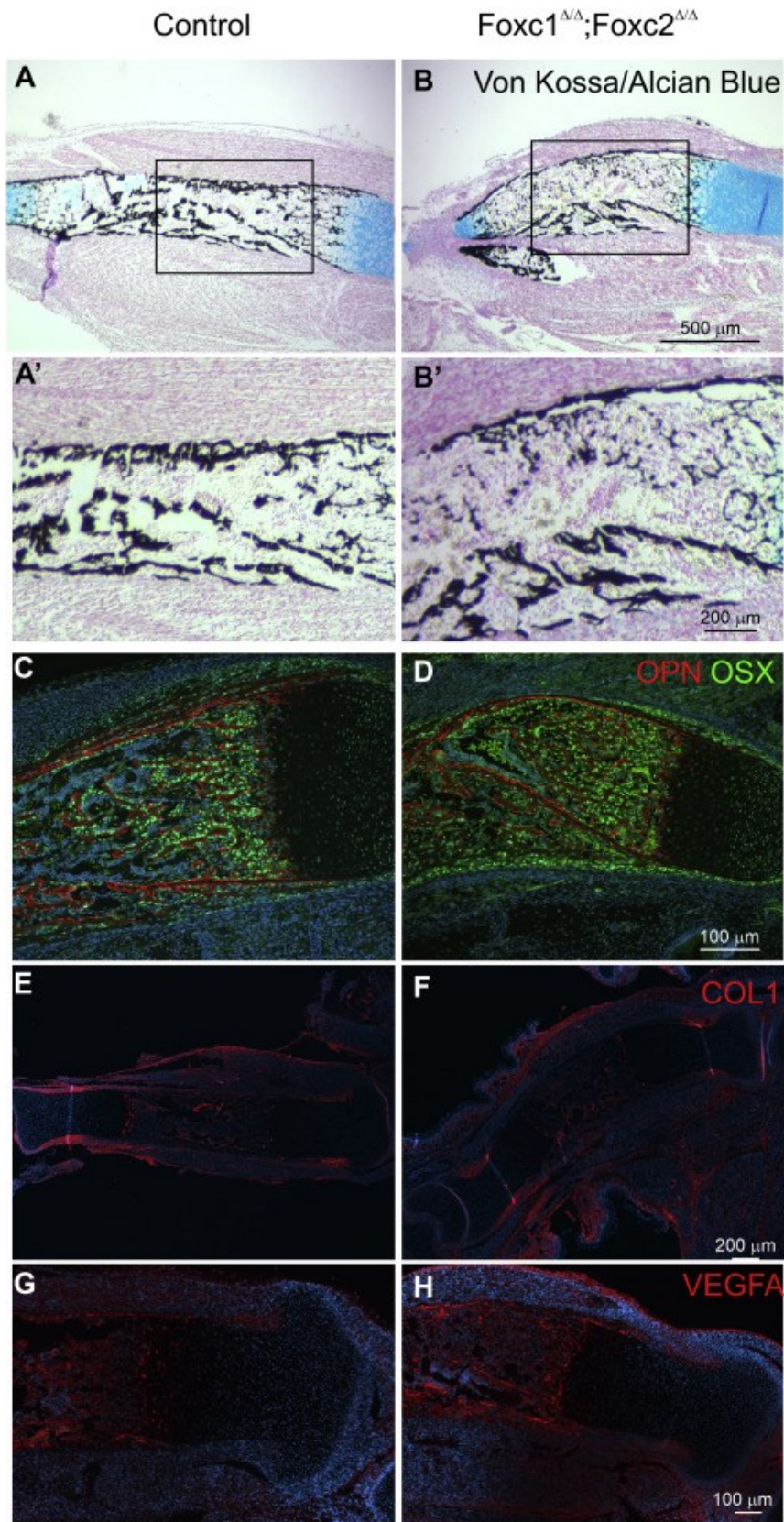


Figure 2.10. Impaired mineralization in *Col2-cre;Foxc1<sup>Δ/Δ</sup>;Foxc2<sup>Δ/Δ</sup>* mutants. A, A0 , B, and B0 , mineralization in the primary ossification center of control and *Col2-cre;Foxc1<sup>Δ/Δ</sup>;Foxc2<sup>Δ/Δ</sup>* embryos determined by Von Kossa staining. C and D, levels of osteopontin (red) and osterix protein (E and F), collagen I and MMP13 localization, and (G and H) VEGFA localization. Mmp13, matrix metalloproteinase 13.

## 2.4 Discussion:

*Foxc1* and *Foxc2* are required for normal skeletal development. We demonstrate that *Foxc1* and *Foxc2* are important regulators of chondrocyte formation and function required during endochondral ossification. *Foxc1* expression, but not *Foxc2*, is directly regulated by SOX9 activity. Enforced expression of *Foxc1* promoted the chondrocytic differentiation of mouse ES cells. Together, these results indicate that *Foxc1* acts early in the formation of chondrogenic cells. This idea is further illustrated given that expression of *Foxc1* in the developing growth plate was enriched in the resting zone chondrocytes, with less mRNA detected in more differentiated cells. Loss of both *Foxc1* and *Foxc2* function in early *Col2*-expressing chondrocytes resulted in a disruption of endochondral ossification, leading to severe skeletal hypoplasia levels promoted cells to the chondrocyte fate.

Little is known about the mechanisms that regulate *Foxc1* and *Foxc2* gene expression in the developing endochondral skeleton. We provide evidence that SOX9 can directly regulate expression of *Foxc1* in chondrocyte cells. Overexpression of *Sox9* in mES cells was sufficient to induce *Foxc1* mRNA. SOX9 binding to four distal regulatory regions in the *Foxc1* gene had been suggested from ChIP-seq studies (Ohba et al., 2015). We confirmed SOX9 association with regulatory elements in the *Foxc1* gene and ascribed functional activity to these regions. Although SOX9 was able to bind to all four elements, only one element (distal C) elicited a transcription response to SOX9 in ATDC5 chondrocyte cells. A second region (distal B) did confer increased reporter activity in ATDC5, suggesting it contains regulatory information to activate *Foxc1* expression in chondrocyte cells; however, its activity is likely independent of SOX9 as its activity was unaffected by SOX9 levels. Recently, expression of FOXC1 mRNA in human breast cancer cells was controlled by SOX9 (34). Regulation of *Foxc1* by SOX9 is further supported by the

reduction of *Foxc1* expression levels in the limbs of *Sox9*-deficient embryos (Liu et al., 2018). This study also reported a decrease in *Foxc2* mRNA in *Sox9* mutant mice, although we did not detect any induction of *Foxc2* expression using *Sox9*-inducible mES cells. It should be noted that these cells were not differentiated toward the chondrocyte lineage, and therefore, it is possible that SOX9 might regulate *Foxc2* expression in a tissue-specific context. *Foxc1* activation by SOX9 suggests a role for *Foxc1* function in the early stages of chondrocyte differentiation. We observed that *Foxc1* expression is spatially enriched in resting zone chondrocytes compared with proliferating and hypertrophic zone chondrocytes that represent later differentiation stages. In addition, overexpression of *Foxc1* in mES cells led to an increased chondrocyte differentiation capacity, suggesting this early increase in *Foxc1* levels promoted cells to the chondrocyte fate.

We also demonstrate the comparative expression patterns of *Foxc1* and *Foxc2* in the developing mouse limb. We determined that *Foxc1* and *Foxc2* have some overlapping as well as distinct expression patterns in the growing limb. Expression of *Foxc1* and *Foxc2* was readily detected in early condensing mesenchyme in the limb bud, and expression became restricted to the perichondrium surrounding the growth plate and in the resting zone chondrocytes later in as endochondral ossification proceeded. Together, these findings indicate a role for *Foxc1* and *Foxc2* in the initial formation of chondrocytes in the nascent skeletal element. These findings are consistent with our observation in Figure 1B, whereby activation of *Foxc1* expression enhances chondrogenic gene expression in mES cells. Although much of the overall expression pattern in these regions for *Foxc1* and *Foxc2* was similar, there were areas where only *Foxc1* or *Foxc2* expression could be detected, suggesting these factors may not have completely overlapping functions. Very few *Foxc1*- or *Foxc2*-expressing cells could be observed in the proliferating zone,

prehypertrophic and hypertrophic chondrocytes at 16.5 dpc. This expression pattern suggests that the chondrodysplasia that we observed in the *Col2-cre;Foxc1<sup>Δ/Δ</sup>;Foxc2<sup>Δ/Δ</sup>* mutants arose from either an indirect effect of *Foxc1* and *Foxc2* acting in the perichondrium to regulate chondrogenesis or as a consequence of loss of *Foxc1* and *Foxc2* function at an early stage of chondrocyte differentiation that disrupts cell function throughout later stages of development. We did detect *Foxc1* expression in a subset of cells lying between the perichondrium and the proliferating chondrocytes, suggesting that *Foxc1* may be expressed in borderline chondrocytes that supply skeletal stem cells later in life (Mizuhashi et al., 2019). Spatially, we observed increased *Foxc1* and *Foxc2* hybridization signals in distal skeletal elements compared with proximal ones. This expression pattern may reflect a role for *Foxc1* and *Foxc2* in the proximal–distal patterning of the limb. In addition, as endochondral ossification in the limb proceeds in a proximal to distal manner, this expression pattern may reflect a role for *Foxc1* and *Foxc2* in the early stages in the formation of skeletal elements and expression decreases as the element matures.

Global KO of either *Foxc1* or *Foxc2* results in a number of skeletal phenotypes in mice (Hong et al., 1999; Kume et al., 1998; Winnier et al., 1997). These mutations predominantly affect the axial skeleton, although the bones of the appendicular skeleton do display a modest reduction in size. Loss of both *Foxc1* and *Foxc2* in *Col2-cre*-expressing cells results in a more severe disruption to the endochondral skeleton than loss of either *Foxc1* or *Foxc2* alone. We observe a general disorganization of the growth plate that affects endochondral ossification processes as indicated by the broad reduction in gene expression of regulators of these events. We reported a reduction in gene expression affecting all stages of chondrocyte differentiation and function as well as genes involved in osteoblast formation and mineralization. The growth plate of the tibia

was disorganized in the *Col2-cre;Foxc1<sup>Δ/Δ</sup>;Foxc2<sup>Δ/Δ</sup>* mutants, and the columnar arrangement of the proliferative chondrocytes did not form, resulting in decreased cell proliferation that likely accounts for the reduced bone size. We did observe a reduction in *Ihh* mRNA levels, which likely accounts for the impaired proliferation observed in *Col2-cre;Foxc1<sup>Δ/Δ</sup>;Foxc2<sup>Δ/Δ</sup>* mutants. Chondroprogenitor cells lacking *Sox9* display a reduction in the length of the columnar chondrocyte zone and a reduced cell proliferation (Akiyama et al., 2002). Moreover, *Sox6* function is required to maintain columnar organization of proliferative zone chondrocytes (Lefebvre et al., 2001). We observe similar phenotypes in *Col2-cre;Foxc1<sup>Δ/Δ</sup>;Foxc2<sup>Δ/Δ</sup>* embryos although SOX9 and SOX6 protein levels were unaffected, suggesting that *Foxc1* and *Foxc2* may function in common aspects of *Sox9/Sox6*-dependent chondrogenic processes.

We did observe some differences in the *Col2-cre;Foxc1<sup>Δ/Δ</sup>;Foxc2<sup>Δ/Δ</sup>* mutants compared with global *Foxc1* or *Foxc2* gene mutations. Germline deletion of *Foxc2* results in fused ribs (Winnier et al., 1997). The number and positioning of the ribs was not affected in our mutants, suggesting a role for *Foxc2* in rib patterning and specification that occurs before rib chondrocyte formation. The sternum does not fully mineralize in *Foxc1<sup>-/-</sup>* mice and completely lacks ossification of the xiphoid process (Kume et al., 1998). In the *Col2-cre;Foxc1<sup>Δ/Δ</sup>;Foxc2<sup>Δ/Δ</sup>* mutants, the rib cage is reduced in size, but mineralization along the sternum appears unaffected. This difference in phenotype may arise from a less efficient *Cre* activity in cells that form the sternum, or a portion of these cells that make up this structure arise from cells that do not express *Col2a*. COLX and MMP13 protein levels were also markedly reduced in germline *Foxc1<sup>-/-</sup>* mutants (Yoshida et al., 2015a), whereas COLX expression was expanded in the *Col2-cre;Foxc1<sup>Δ/Δ</sup>;Foxc2<sup>Δ/Δ</sup>* mutants and MMP13 levels were not affected. These observed phenotype

differences may reflect a function for *Foxc1* and *Foxc2* in progenitor cells before the onset of *Col2a* expression or in cells that do not express *Col2a* and thus did not delete *Foxc1* and *Foxc2*.

The combined loss of both *Foxc1* and *Foxc2* in *Col2a* expressing cells resulted in delayed endochondral ossification events in both the appendicular and axial skeleton. These disruptions were more pronounced in the axial skeleton. There are a number of reasons to account for such observations. First, *Col2-cre* is detected in the sclerotome of the somites before these cells migrating to and condensing at sites of future vertebral bone formation (Ovchinnikov et al., 2000). In contrast, *Col2-cre* activity is not detected in the limbs until mesenchyme cells have migrated and condensed where the future bones will develop. This suggests that *Foxc1* and *Foxc2* are deleted at an earlier stage of vertebral bone formation that may prevent formation of adequate numbers of sclerotome cells needed to form the axial skeleton. Second, this disruption may reflect a difference in the chondrogenesis process occurring in the axial skeleton compared with the appendicular skeleton. In the sclerotome, cells must first receive Sonic Hedgehog signal from the notochord to initiate chondrogenesis, whereas such a signaling is not required in the limb skeleton (Karamboulas et al., 2010; Murtaugh et al., 1999). It is possible that *Foxc1* and *Foxc2* may function in processing this Sonic Hedgehog signal needed for chondrogenesis in the sclerotome. Third, additional transcription factors present in the limb skeleton may compensate for loss of *Foxc1* and *Foxc2*, and such compensation does not occur in the axial skeleton. Experiments to address such mechanisms are being pursued in our laboratory.

In conclusion, *Foxc1* and *Foxc2* functions in chondrocytes are required for correct endochondral ossification events to occur. Loss of *Foxc1* and *Foxc2* function in *Col2-cre*–

expressing cells results in skeletal dysplasia and disrupts skeletal mineralization. The expression patterns for these factors in the growth plate suggest they act at early stages of chondrogenesis and their loss of function impacts later chondrogenic differentiation stages. Chondrocytes do form in the absence of *Foxc1* and *Foxc2*, but they are unable to correctly differentiate, resulting in a disorganized growth plate, reduced chondrocyte proliferation, and delays in chondrocyte hypertrophy. Such disruptions have the overall effect of preventing correct ossification of the endochondral skeleton.

## 2.5 Experimental procedures:

### 2.5.1 Cell culture and in vitro differentiation:

mES cells containing an inducible *Sox9* or *Foxc1* expression cassette (Correa-Cerro et al., 2011; Nishiyama et al., 2009) were obtained from either the Coriell Institute (*Sox9*) or Dr Minoru Ko (*Foxc1*). mES cells were cultured in Dulbecco's modified Eagle's medium (DMEM) (MilliporeSigma) containing 15% fetal bovine serum (FBS; Gibco), 1% L-glutamine (Life Technologies), 1 mM  $\beta$ -mercaptoethanol (MilliporeSigma), 0.1 mM nonessential amino acids (Life Technologies), 1000 units/ml leukemia inhibitory factor (MilliporeSigma), 1% Penicillin/Streptomycin (Life Technologies), and 1  $\mu$ g/ml DOX. To induce gene expression, cells were repeatedly washed with PBS before replacement with DOXfree media. ATDC5 cells were purchased from European Collection of Authenticated Cell Cultures and cultured in DMEM:F12 containing 5% FBS. Mutagenesis of the *Foxc1* gene was achieved by using Alt-R CRISPR-Cas9 system (Integrated DNA Technologies [IDT]) using a predesigned gRNA (50 - CAACATCATGACGTCGCTGC-30) that targeted the second helix of the FOXC1 FOX DNA-binding domain. Ribonucleoprotein complexes were transfected into ATDC5 cells using RNAiMAX. Two days after transfection, cells were then plated as a single cell per well in a 96-well plate by diluting cells to approximately 80 cells/ml, and 100  $\mu$ l cell solution was added to each well. Single cells were then expanded to larger culture volumes and were screened for a reduction in *Foxc1* protein levels by immunoblotting with anti *Foxc1* antibodies (OriGene), followed by sequencing of the *Foxc1* ORF. Two cell lines were selected (crFOXC1-1 and crFOXC1-8) and used for subsequent functional studies. Both lines displayed similar properties in chondrocyte differentiation experiments, but results from a single line (crFOXC1-1) are reported here.

### 2.5.2 RNA isolation and qRT-PCR:

RNA was isolated from cell cultures and tissues using the RNeasy mini kit (Qiagen) following the manufacturer's protocol. All lysates were homogenized using QIAshredder (Qiagen). Tissue lysates were first disrupted with a microcentrifuge pestle before passing through a QIAshredder. RNA (500 ng) was then reverse-transcribed to cDNAs using the QuantiTect reverse transcription kit (Qiagen). qRT-PCR analysis was performed as described previously (Caddy et al., 2020; Hopkins et al., 2017). All qRT-PCR experiments were performed with at least three biological replicates, and each contained three technical replicates. Primers used for analysis were obtained as predesigned PrimeTime qPCR Primer Assays (IDT).

### 2.5.3 ChIP assays:

ChIP assays were performed as described previously (Hopkins et al., 2016) with the following modifications. Chromatin from ATDC5 cells sheared in ice using Branson Sonifier (ten cycles at 30% amplitude for 30 s with a 60-s rest). Cross-linked chromatin extracts were incubated overnight with 2- $\mu$ g anti-SOX9 antibody (Millipore), acetylated histone H3 (Millipore), or rabbit IgG. Amplification of recovered chromatin was performed by PCR using the following primers. Col2a intron 1 forward primer (5' -TGA AAC CCT GCC CGT ATT TAT T -3') and reverse primer (5' -GCC TTG CCT CTC ATG AAT GG-3'). *Foxc1* distal A forward primer (5' -GCC CTG AAT CCA GAA ACT TG -3') and reverse primer (5' -GCG AAT TCA TAT GGT TTT TCC -3'). *Foxc1* distal B forward primer (5' - GGCCATCATGTCTAGGGGAA -3') and reverse primer (5' - GTTGCTCTGAACTTGGGGTG -3'). *Foxc1* distal C forward primer (5' -TGT GAA ATC GCC TGT GAG AG-3') and reverse primer (5' -CCC CAT ATC CTC TTT GAG AGC-3').

*Foxc1* distal D forward primer (50 TGT CAG GAG AAC TGC TGT AAG AA-30 ) and reverse primer (50 -CTC TAG GCT GAC CAC GCT GT-30 ).

#### 2.5.4 Reporter cloning and luciferase assays:

DNA fragments corresponding to mouse *Foxc1* regulatory regions distal A (mm10 chr13:31,764,541-31,764,717), distal B (mm10 chr13:31,765,465-31,765,623), distal C (mm10 chr13:31,779,560-31,779,803), and distal D (mm10 chr13:31,820,626-31,820,791) were synthesized as gBlock fragments (IDT) and cloned into the EcoRV site of pGL4.23- luc2/minP vector (Promega) using Gibson Assembly. Plasmids containing the correct regulatory sequence were confirmed by sequencing. Dual luciferase reporter assays (Promega) were performed as described previously (Caddy et al., 2020).

#### 2.5.5 Chondrocyte-differentiation procedures:

For chondrocyte-differentiation experiments, mES cells were grown in DOX-free media for 2 days before induction of a chondrocyte differentiation protocol as described in ref ( (Kawaguchi et al., 2005)). Briefly, mES cells were grown as hanging drops (2500 cells/drop) to form embryoid bodies (EBs). After 2 days, EBs were pooled (24 EBs per 60-mm bacterial grade Petri dish) and grown in suspension culture containing 0.1  $\mu$ M transretinoic acid. Media were replaced after 3 days with retinoic acid-free media and cultured for an additional 3 days. EBs were then transferred to gelatin-coated, tissue culture-grade, 60-mm plates containing low serum media (1% FBS) and transforming growth factor beta 3 (10 ng/ml) until differentiation was complete (21 days). RNA was isolated from 24 hanging drops/EB, and experiments were performed three times. Chondrocyte differentiation of ATDC5 cells was initiated by supplementing cell culture media

with 1x insulin, transferrin, and selenium supplement (Cellgro). Differentiation media were replenished every 2 to 3 days.

#### 2.5.6 Mouse models:

All research using mouse models was approved by the University of Alberta Animal Care and Use Committee (AUP804). Col2-cre mice (Terpstra et al., 2003) were kindly provided by Dr René St-Arnaud (Shriners Hospital for Children, Montreal). The ROSA26mTmG mice (B6.129(Cg)-Gt(ROSA)26Sortm4(ACTBtdTomato,-EGFP)Luo/J) were purchased from the Jackson Laboratory. *Foxc1<sup>fl/fl</sup>*; *Foxc2<sup>fl/fl</sup>* mice (Sasman et al., 2012) were crossed with *Col2-cre<sup>+/-</sup>* mice to generate *Col2-cre<sup>+/-</sup>*; *Foxc1<sup>+/-</sup>*; *Foxc2<sup>+/-</sup>* offspring. Timed pregnancies were conducted by crossing male *Col2-cre<sup>+/-</sup>*; *Foxc1<sup>+/-</sup>*; *Foxc2<sup>+/-</sup>* mice to female *Foxc1<sup>fl/fl</sup>*; *Foxc2<sup>fl/fl</sup>* mice. Mice were maintained on mixed background C57B6 (*Col2-cre*), and Black Swiss (*Foxc1<sup>fl/fl</sup>*; *Foxc2<sup>fl/fl</sup>*) crosses were set up in the afternoons, and vaginal plugs were monitored in the morning, with noon of the day that a positive plug was detected, designated as 0.5 dpc. All comparisons were made between littermates. Weaned mice were genotyped using ear notch biopsies, while embryos were genotyped using skin DNA. Genotyping was performed using the KAPA mouse genotyping kit (MilliporeSigma). The following primer pairs were used: *Foxc1* (forward 50 - ATTTTTTTTCCCCCTACAGCG-30 ; reverse 50 -ATCTGTTA GTATCTCCGGGTA-30 ), *Foxc2* (forward 50 -CTCCTTTGCGTTTCCAGTGA-30 ; reverse 50 -ATTGGTCCTTCGTCT TCGCT-30 ), and *Col2-cre* (forward 50 -GCCTGCATTACCGGTCGATGCAACGA-30 ; reverse 50 -GTGGCAGATGGCGCGGCAACACCATT-30 ).

### 2.5.7 Skeletal preps and analysis:

Skeletons from embryos collected at 18.5 dpc were stained with Alizarin Red and Alcian Blue as described in (Rigueur and Lyons, 2014) (42). Images were captured with an Olympus E520 digital camera.

### 2.5.8 *In situ* hybridization:

Embryos were collected at the desired stage and fixed in 4% paraformaldehyde overnight at 4 C. Tissues were washed in PBS overnight before embedding in paraffin. Sections (7  $\mu$ m). were collected onto Superfrost slides (Fisher Scientific). In situ hybridization was performed using the RNAscope multiplex in situ hybridization kit (Advanced Cell Diagnostics). The following RNAscope (Advanced Cell Diagnostic) probes were used: *Foxc1* (412851-C2, lot 19155B), *Foxc2* (406011, lot 18289A), *Fgfr3* (440771, lot 18289A), and negative control probe (310043; lot 18197A). In situ hybridization experiments were performed using four different littermate pairs (mutant and control).

### 2.5.9 Immunofluorescence:

The following antibodies were used for immunofluorescence microscopy: COL IIa (Abcam, ab185430, lot GR3320839, 1:100); COLX (Abcam, ab5832, lot GR3210868-2, 1:50); COL I (Abcam, ab88147; GR3225500-1, 1:100); MMP13 (Abcam, ab39012, lot GR157414-15 1:100); RUNX2 (Abcam, ab76956, lot, 1:200) SOX6 (Abcam, ab30455, lot GR3174880- 1, 1:1000); VEGFA (Abcam, ab1316, lot GR3200812. 1:100), SOX9 (MilliporeSigma, AB55535, lot 3282152, 1:200); OPN (SCBT, sc22536-R, lot C2307, 1:100); OSX (SCBT, sc21742, lot D2908,

1:100); Ki67 (Bethyl, IHC00075, 1:100). Antibodies against GFP were a generous gift from Dr Luc Berthiaume (University of Alberta) and were used at a dilution of 1:500.

Paraffin sections were collected as described for in situ hybridization procedures. Slides were baked at 70 C for 1 h followed by rehydration through xylene and graded ethanol series. For SOX9, SOX6, OSX, OPN, KI67, RUNX2, and GFP antibodies, antigen retrieval was conducted by boiling slides in citrate buffer (10 mM trisodium citrate, pH 6.0; 0.05% Tween 20) for 20 min. For COL1, COL2a, COLX, MMP13, and VEGFA antibodies, sections were incubated in hyaluronidase. After antigen retrieval, slides were blocked in 5% donkey serum in PBS with 0.05% Triton X-100 for 1 h followed by incubation with the primary antibody overnight at 4 C. Slides were washed in PBS with 0.05% Triton X-100 before incubation in secondary antibodies for 1 h at room temperature, followed by staining with DAPI and mounted with coverslips using ProLong Gold. Immunofluorescence experiments were performed using six different littermate pairs (mutant and control).

#### 2.5.10 RNA-Seq:

RNA was isolated from the ribs of three control and three *Col2-cre;Foxc1<sup>Δ/Δ</sup>;Foxc2<sup>Δ/Δ</sup>* 16.5 dpc embryos as described above. RNA sample quality control was performed using the Agilent 2100 Bioanalyzer. Samples with RNA integrity number >8 were used for library preparation following the standard protocol for the NEBNext Ultra II Stranded mRNA (New England Biolabs). Library construction and sequencing was carried out at the Biomedical Research Centre Sequencing Facility (University of British Columbia, Canada). Sequencing was performed on the Illumina NextSeq 500 with Paired End 42 bp × 42 bp reads. Demultiplexed read sequences were then aligned to the

reference sequence using STAR (<https://www.ncbi.nlm.nih.gov/pubmed/23104886>) aligners. Two different pipelines, HISAT2-featureCountsDESeq2 and STAR-RSEM-DESeq2, were used for the downstream analysis through an inhouse script. For both the pipelines, mouse reference genome GRCm38 was downloaded from the NCBI ([https://www.ncbi.nlm.nih.gov/assembly/GCF\\_000001635.20/](https://www.ncbi.nlm.nih.gov/assembly/GCF_000001635.20/)) while gene annotation was downloaded from GENCODE (<https://www.gencodegenes.org/mouse/>). Briefly, read alignment was performed using both HISAT2 (<https://pubmed.ncbi.nlm.nih.gov/25751142/>) and STAR (<https://www.ncbi.nlm.nih.gov/pubmed/23104886>). Quantification using featureCounts (<https://pubmed.ncbi.nlm.nih.gov/24227677/>) and RSEM (<https://pubmed.ncbi.nlm.nih.gov/21816040/>) while differential expression analysis was performed using DESeq2 (<https://pubmed.ncbi.nlm.nih.gov/25516281/>) for both. The final output was a list of genes with significant p-value ( $<0.05$ ) after correction for multiple testing with a false discovery rate of less than 0.1. A combined list was obtained by averaging the genes with a filtered log<sub>2</sub> fold change  $\pm 1$ . Only common genes with consistent differential expression log<sub>2</sub> fold change values between both the pipelines were included in the list, whereas the inconsistent ones were excluded. Correlation for each sample between the pipelines was calculated using linear regression. RNA-Seq data are available on NCBI Gene Expression Omnibus under accession GSE165951.

#### 2.5.11 Statistical analysis:

Data were analyzed via Student's t test or one-way ANOVA with Holm–Sidak multiple pairwise comparisons using SigmaPlot 13.0 (build 13.0.0.83). Data availability RNA-Seq results are

available on NCBI Gene Expression Omnibus under accession GSE165951. All original data pertaining to this study will be made available upon request.

## **Chapter 3:**

# **Examination of *Foxc1* and *Foxc2* function in formation of the axial skeleton**

### **Contribution to manuscript:**

*Col2-cre; Foxc1<sup>Δ/Δ</sup>; Foxc2<sup>Δ/Δ</sup>* mouse model was previously established (Almubarak et al., 2021). Asra carried out the implementation of all the experiments in this chapter including slide preparation, histology staining, Immunofluorescence, *In situ* hybridization, Image preparation, and analysis. This chapter was written by Asra Almubarak and supervised by Fred B Berry.

# **Examination of *Foxc1* and *Foxc2* function in formation of the axial skeleton**

Asra Almubarak<sup>1</sup>, Tsutomu Kume<sup>2</sup>, and Fred B. Berry<sup>1,3</sup>

<sup>1</sup> Department of Medical Genetics, University of Alberta, Edmonton, Alberta, Canada

<sup>2</sup> Feinberg Cardiovascular and Renal Research Institute, Feinberg School of Medicine,  
Department of Medicine, Northwestern University, Chicago, IL, USA

<sup>3</sup>Department of Surgery, University of Alberta, Edmonton, Alberta, Canada

### **3.1 Introduction:**

The vertebral column provides physical support to the body parts and protect the spinal cord, allowing flexible movement and sensation(DeSai et al., 2022). In Human, the spine forms through synchronous development of both the paraxial mesoderm and the neural tube during early fetal development. The neural tube will form the central nervous system, while the paraxial mesoderm will form 42 pairs of somites localized along both sides of the neural tube in a craniocaudal direction(Kalamchi and Valle, 2022; Kaplan et al., 2005). The somites will then differentiate into dermomyotome, and sclerotome cell types. The dermomyotome will develop into the muscles and the skin, while the sclerotome clusters form the vertebral column and ribs. An intervertebral disc will form between each two clusters surrounding the notochord, where the central part of each intervertebral disc is called the nucleus pulposus and it is created by the notochord, and the outer loop of cells is the annulus fibrosus and it is developed from the migrated sclerotome cells(Ward et al., 2018; Williams et al., 2019). The vertebral body develops when the cranial side of a sclerotome combines with the adjacent caudal sclerotome group. Sclerotome cells also migrate around the neural tube and merge from the dorsal side forming the vertebral arches that protect the spinal cord(DeSai et al., 2022; Kalamchi and Valle, 2022; Kaplan et al., 2005). The sclerotome will differentiate into chondrocytes that mature and form hypertrophic chondrocytes that will eventually ossify (Harrison et al., 2013; Kalamchi and Valle, 2022; Prakash et al., 2007; Skórzewska et al., 2013). Each vertebra has five ossification centers where chondrocytes convert into osteoblasts that will maintain the formation of strong vertebrae (Cloete et al., 2013), while the intervertebral discs act as a flexible cushion between the vertebrae. In humans, the vertebral column contains 33 vertebrae consisting of: 7 cervical, 12 thoracic, 5 lumbar, 5 sacral, and 4 coccygeal (DeSai et al., 2022). However, the mouse vertebral column comprises 7 cervical, 13

thoracic, 6 lumbar, 4 sacral and 28 caudal vertebrae (Harrison et al., 2013). All together, the vertebrae with the skull, ribs, and the sternum form the axial skeleton (Docherty, 2007; Williams et al., 2019). Less is known about the axial skeleton endochondral ossification, its complex regulatory mechanisms, and the genes involve in this developmental process compared to the long bones. Additional molecular and genetic studies need to be conducted to enrich our understanding about the complex molecular pathways and the genes involved in the embryonic development process of the vertebral column. The normal regulatory function of transcription factors is one important aspect that will establish functional axial skeletal elements including the vertebral column. Two important transcription factors that have an upstream regulatory effect on embryonic skeletal development including the axial skeleton are FOXC1 and FOXC2 transcription factors.

FOXC1 and FOXC2 are two members of the fork-head box transcription factors that shown an overlapping function in various tissues during early embryonic tissue development such as the paraxial mesoderm, somites, cephalic mesoderm, cardiovascular tissues (Hiemisch et al., 1998; Iida et al., 1997; Kume et al., 1998; Winnier et al., 1999). *Foxc1* and *Foxc2* were also reported to have a key regulatory effect in the formation of paraxial versus intermediate mesoderm cell fates during early embryonic development (Wilm et al., 2004). *Foxc1* null mice developed axial skeleton phenotypes affecting the formation of the cranial vault of the skull and the sternum as well as the vertebral bodies and rib cage (Kume et al., 1998). Moreover, *Fox2* homozygous null deletion causes a similar phenotype to the *Foxc1* null mice, with aberrant patterning of the paraxial mesoderm, dramatic reduced sclerotome derived cells proliferation, development of craniofacial defects, several rib fusions and abnormal vertebral column development with lack or split vertebral bodies with minor appendicular skeletal phenotypes(Winnier et al., 1997). Interestingly,

compound *Foxc1* and *Foxc2* null homozygous mutation in mice affected the development of the somite and lead to early death around Embryonic (E) day 9 before any skeletal development due to failure in cardiovascular development (Kume et al., 2001). In order to understand how *Foxc1* and *Foxc2* regulate endochondral development our lab generated a conditional double knock out (KO) of *Foxc1* and *Foxc2* in mice using the *Col2-cre* driver (Almubarak et al., 2021). *Col2-cre; Foxc1<sup>Δ/Δ</sup>;Foxc2<sup>Δ/Δ</sup>* mice developed multiple skeletal abnormalities with more severe axial skeleton phenotype than the appendicular skeleton (Almubarak et al., 2021). Therefore, we hypothesize that *Foxc1* and *Foxc2* are essential for initiation of chondrogenesis in the vertebral column.

In this study, we focused our work on understanding the importance of *Foxc1* and *Foxc2* in endochondral ossification of the axial skeleton, and specifically the vertebral column, through assessing the phenotypes observed in the *Col2-cre; Foxc1<sup>Δ/Δ</sup>;Foxc2<sup>Δ/Δ</sup>* mouse model. In this investigation we assessed different stages of endochondral ossification in *Col2-cre; Foxc1<sup>Δ/Δ</sup>;Foxc2<sup>Δ/Δ</sup>* mice to examine the role of *Foxc1* and *Foxc2* in the formation of the vertebral column.

## 3.2 Materials and Methods:

### 3.2.1 Mouse models:

All mouse models that were used for research were approved by the University of Alberta Animal Care and Use Committee (AUP804). *Col2-cre* mice were generously provided by Dr René St-Arnaud (Shriners Hospital for Children, Montreal). Control and *Col2-cre*; *Foxc1<sup>fl/fl</sup>*; *Foxc2<sup>fl/fl</sup>* mice were generated, collected, and genotyped as it was described in (Almubarak et al., 2021). E14.5 and E16.5 whole mice embryos were collected, processed and molded in paraffin wax. Followed by sagittal cutting (5-7microns) of the whole embryo to obtain a sagittal vertebral column section.

### 3.2.2 *In situ* hybridization:

RNA scope multiplex *in situ* hybridization was performed using *Foxc1* (412851-C2, lot 19155B), *Foxc2* (406011, lot 18289A) probes as described previously in chapter two of this thesis and in (Almubarak et al., 2021).

### 3.2.3 Immunofluorescence:

Paraffin section were prepare as described in the *in situ* hybridization section, and (IF) of SOX9, SOX6, COL1, COL2, COL10 and KI67 were performed as described in chapter two of this thesis and in (Almubarak et al., 2021)

### 3.2.4 Safranin O staining:

Sagittal vertebral column sections were collected as described previously and stained with Safranin O staining to visualize cartage formation as in chapter two or (Almubarak et al., 2021).

### 3.3 Results:

#### 3.3.1 *Foxc1* and *Foxc2* expression varies spatially and temporally during embryonic vertebral development

The expression pattern of *Foxc1* and *Foxc2* in the developing vertebral column has not been thoroughly examined. Therefore, we first identified *Foxc1* and *Foxc2* mRNA localization via RNA scope multiplex *in situ* hybridization. *Foxc1* and *Foxc2* expression in the thoracic vertebrae revealed broader localization of both *Foxc1* and *Foxc2* at E14.5 than E16.5. At E14.5, we identified localization of both mRNAs in the periphery of the thoracic vertebrae, the endplate and the chondrocytes that surrounds the vertebral body and the annulus fibrosus ring (Fig 3.1A-D). Additionally, *Foxc2* mRNA were distinctively localized within the columnar chondrocytes of the vertebral body. At E16.5, the growth plate becomes more developed (Prakash et al., 2007; Takimoto et al., 2019), and *Foxc1* and *Foxc2* becomes more distinctively localized within the periphery, the end plate and the annulus fibrosus, while *Foxc2* localized only in the columnar chondrocytes. However, none of the two *Foxc* genes expressed in the hypertrophic chondrocytes zone at the center of the vertebral body or the nucleus pulposus (Fig 3.1B-H).

Control

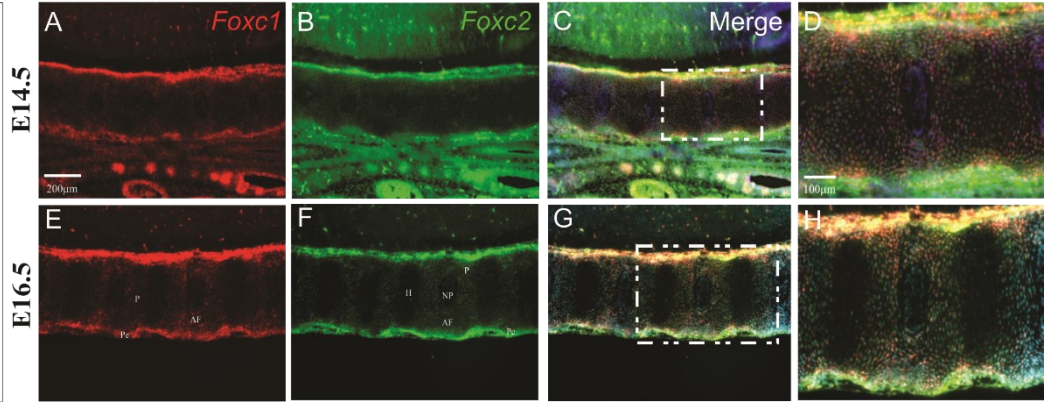
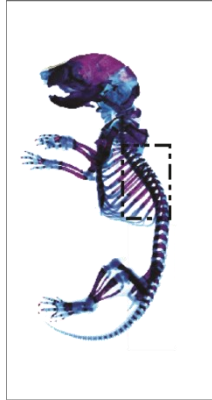


Figure 3.1. *Foxc1* and *Foxc2* have a similar expression pattern that undergo temporal changes in the vertebrae.

*Foxc1* and *Foxc2* co-express in the periphery (Pe), proliferative chondrocytes (P) of the vertebral bodies and in the annulus fibrosus of the intervertebral discs. Dual fluorescence *in situ* hybridization of E14.5 (A-D) and E16.5 (E-H) thoracic vertebrae showing vertebral development changes. However, we detected similar expression pattern of both *Foxc1* and *Foxc2* in the vertebrae. At E14.5 *Foxc1* and *Foxc2* express at the periphery, the end plate and the chondrocytes that fill out the whole vertebral body. However, at E16.5, expression of *Foxc1* and *Foxc2* were specified in the periphery, end plate and its adjacent chondrocytes, in addition to the annulus fibrosus of the intervertebral discs, but not in the newly formed hypertrophic chondrocytes at that stage (n=2).

### 3.3.2 Conditional *Foxc1* and *Foxc2* deletion in the sclerotome blocked initiation of chondrogenesis in the cervical vertebrae.

We next wanted to assess cartilage formation of both control and *Col2-cre; Foxc1<sup>Δ/Δ</sup>; Foxc2<sup>Δ/Δ</sup>* mice at E16.5. Therefore, we performed safranin O staining, which binds proteoglycans in cartilage. We have observed normal formation of the cervical vertebrae in control embryos, where the atlas vertebral body showed formation of the immature chondrocytes and the hypertrophic chondrocytes (Fig 3.2A). However, we only observed formation of small, irregular condensations in the cervical region of the *Col2-cre; Foxc1<sup>Δ/Δ</sup>; Foxc2<sup>Δ/Δ</sup>* embryo sections, that was not marked with the safranin O red staining (Fig 3.2B). In comparison to the normally developed thoracic vertebra and intervertebral discs in E16.5 control embryos (Fig 3.2C), *Col2-cre; Foxc1<sup>Δ/Δ</sup>; Foxc2<sup>Δ/Δ</sup>* thoracic vertebrae exhibited some underdeveloped cartilage formation. The thoracic vertebrae were small, fused and acquired abnormal shapes compared to the control (Fig 3.2D). Moreover, the intervertebral discs were underdeveloped. This indicates that *Foxc1* and *Foxc2* deletion has severely disrupted cartilage formation in the vertebral column.

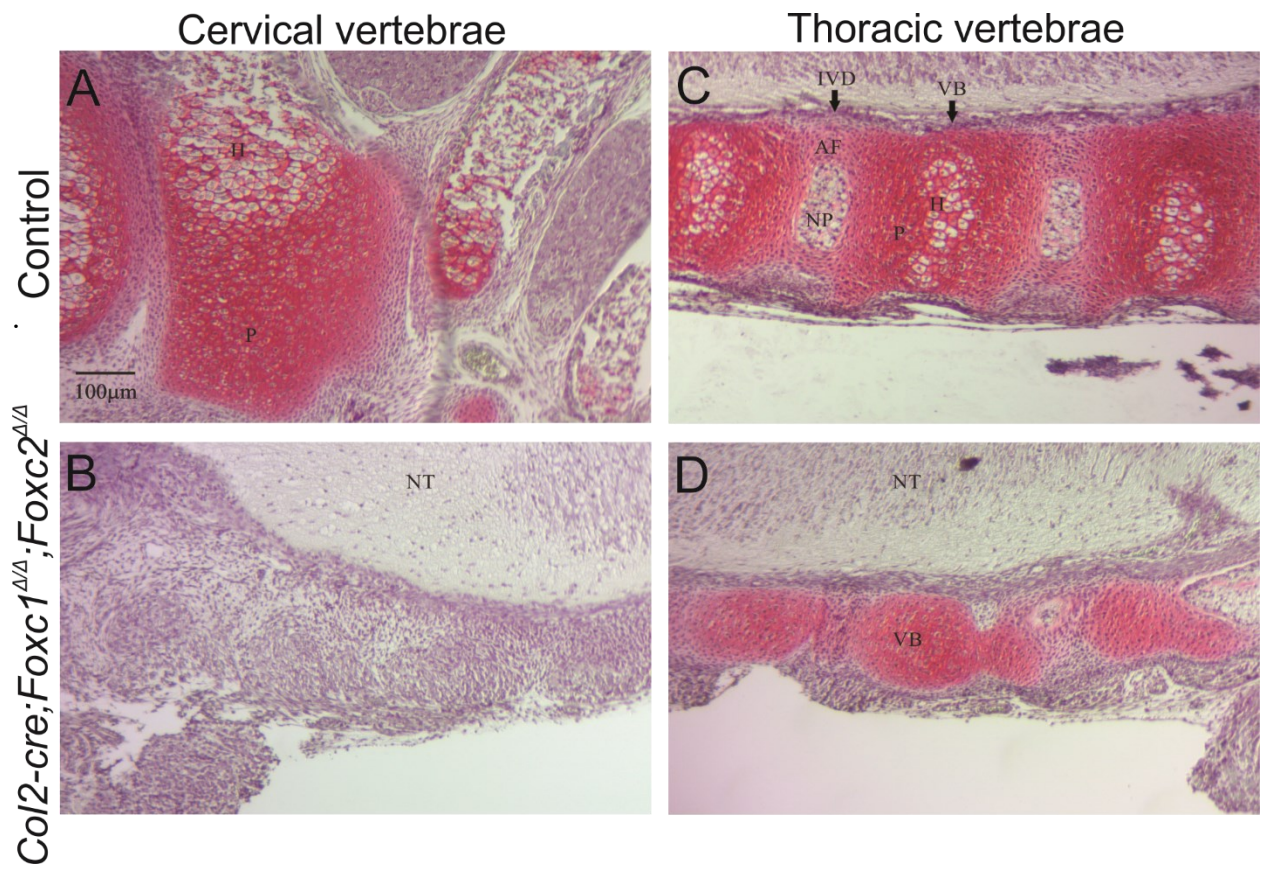


Figure 3.2. Less cartilage formed in the vertebral column in the absence of *Foxc1* and *Foxc2* genes. E16.5 Control and *Col2-cre; Foxc1<sup>Δ/Δ</sup>;Foxc2<sup>Δ/Δ</sup>* spine sections were stained with Safranin O to visualize cartilage formation in the cervical and thoracic vertebrae. (A) Control mice showed normal cartilage development in the cervical vertebrae with proliferative columnar chondrocytes (P) and hypertrophic chondrocytes formation (H). (B) *Col2-cre; Foxc1<sup>Δ/Δ</sup>;Foxc2<sup>Δ/Δ</sup>* exhibited a lack of safranin O staining. (C) control thoracic vertebrae had a normal development of the cartilage in the thoracic vertebrae and the IVD. (D) *Col2-cre; Foxc1<sup>Δ/Δ</sup>;Foxc2<sup>Δ/Δ</sup>* embryos developed aberrant morphology of the thoracic vertebrae. (n=3).

### 3.3.3 Delayed endochondral ossification process in the vertebral column by early deletion of *Foxc1* and *Foxc2*

Then, we wanted to assess chondrocyte differentiation through monitoring endochondral ossification markers in the vertebral column at E16.5 via immunofluorescence (IF). IF detection of SOX9 in the E16.5 cervical vertebrae identified chondrocytes throughout the vertebral bodies of control embryos (Fig 3.3A). However, we could not detect any SOX9 signal in the *Col2-cre; Foxc1<sup>Δ/Δ</sup>;Foxc2<sup>Δ/Δ</sup>* cervical region (Fig 3.3B). We also detected SOX6 localization within the early chondrocytes in the controls (Fig 3.3C). But, no SOX6 signal was shown in the cervical area of *Col2-cre; Foxc1<sup>Δ/Δ</sup>;Foxc2<sup>Δ/Δ</sup>* embryos (Fig 3.3D). Moreover, we detected COL2a1 staining within the control cervical vertebrae (Fig 3.3E). However, No COL2a1 was localized within the cervical region of the *Col2-cre; Foxc1<sup>Δ/Δ</sup>;Foxc2<sup>Δ/Δ</sup>* embryos (Fig 3.3F). COLX, a marker of the extra cellular collagen matrix secreted by hypertrophic chondrocytes was also detected within the mature chondrocytes of the cervical vertebrae (Fig 3.3E), but not in the *Col2-cre; Foxc1<sup>Δ/Δ</sup>;Foxc2<sup>Δ/Δ</sup>* cervical vertebrae (Fig 3.3F). COL1 localization was tested to assess initiation of bone formation and it was detected within the periphery of the control cervical vertebrae at E16.5 (Fig 3.3G), but not in the *Col2-cre; Foxc1<sup>Δ/Δ</sup>;Foxc2<sup>Δ/Δ</sup>* embryos (Fig 3.3H). Thus, these findings indicate that the loss of *Foxc1* and *Foxc2* blocked chondrogenesis in the cervical region of the vertebral column. In the thoracic vertebrae SOX9 was localized in chondrocytes of the vertebral body of both control and *Col2-cre; Foxc1<sup>Δ/Δ</sup>;Foxc2<sup>Δ/Δ</sup>* embryos (Fig 3.3I) However, SOX9 localization was reduced due to formation of small thoracic vertebra in *Col2-cre Foxc1<sup>Δ/Δ</sup>;Foxc2<sup>Δ/Δ</sup>* embryo (Fig 3.3J). SOX6 was also localized within the immature chondrocytes and within the nucleus pulposus of the intervertebral discs (Fig 3.3K). But, its localization was less intense within the *Col2-cre; Foxc1<sup>Δ/Δ</sup>;Foxc2<sup>Δ/Δ</sup>* small thoracic vertebrae. In addition, we couldn't detect any nucleus pulposus

formation in the mutants, as we could not visualize SOX6 between the vertebral bodies (Fig 3.3L). We also identified COL2a1 staining within the immature chondrocytes of the control and *Col2-cre* mutant thoracic vertebral bodies, but with less COL2a1 signal in the *Col2-cre; Foxc1<sup>Δ/Δ</sup>; Foxc2<sup>Δ/Δ</sup>* compared to the control ((Fig 3.3M, N). Moreover, we observed localization of COLX in the hypertrophic chondrocytes of control thoracic vertebrae (Fig 3.3M), which indicate a normal chondrocytes maturation process. However, COLX localization was less intense in the *Col2-cre; Foxc1<sup>Δ/Δ</sup>; Foxc2<sup>Δ/Δ</sup>* thoracic vertebral bodies. COL1 was detected in the periphery of the vertebrae and within the annulus fibrosus ring (Fig 3.3O), but the COL1 signal was reduced within the small malformed thoracic vertebrae found in *Col2-cre; Foxc1<sup>Δ/Δ</sup>; Foxc2<sup>Δ/Δ</sup>* mutants. Moreover, we could not detect COL1 localization within the annulus fibrosus region. These findings indicate that early deletion of *Foxc1* and *Foxc2* in the somatic mesoderm caused a general delay in endochondral ossification process through out the vertebral column, that impacted the formation of the vertebrae and the development of the intervertebral discs.

### Cervical vertebrae

### Thoracic Vertebrae

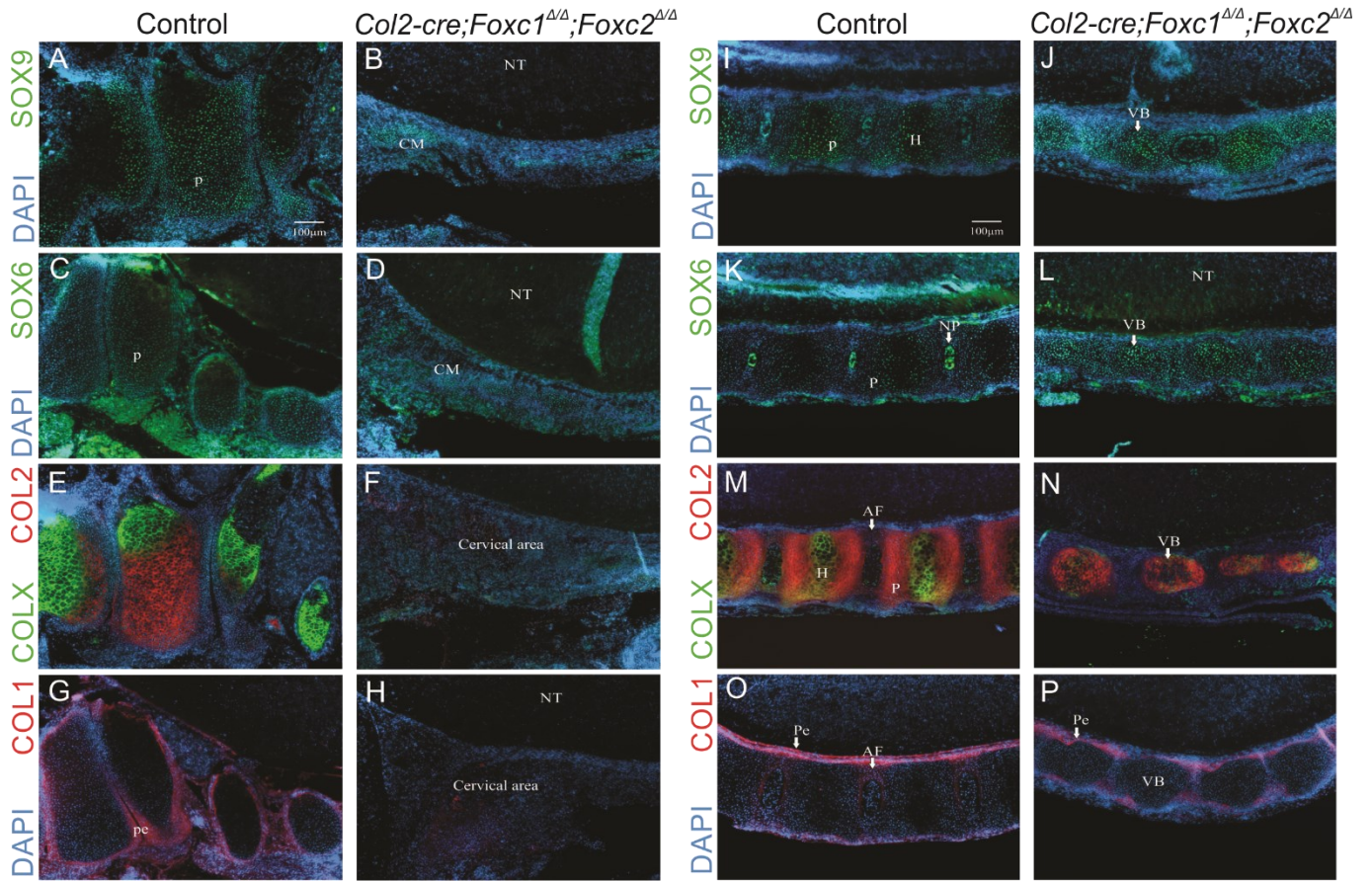


Figure 3.3. Deletion of *Foxc1* and *Foxc2* block endochondral ossification in the cervical vertebrae. IF staining was done on E16.5 control and *Col2-cre; Foxc1<sup>Δ/Δ</sup>; Foxc2<sup>Δ/Δ</sup>* spine to monitor endochondral ossification in the cervical (A-H) and the thoracic vertebrae (1-P). We used chondrocyte differentiation markers antibodies (SOX9, SOX6, COL2a1 to mark proliferative chondrocytes, COLX to identify the hypertrophic chondrocytes and COL1 to assess bone formation. condensing mesenchyme (CM), Neural tube (NT), Proliferative chondrocytes (P/PC), Hypertrophic chondrocytes (H), Annulus fibrosus (AF), Nucleus pulposus (NP). (n=2).

### 3.3.4 Deletion of *Foxc1* and *Foxc2* compromised vertebral chondrocyte proliferation.

Formation of the vertebral column in *Col2-cre; Foxc1<sup>Δ/Δ</sup>;Foxc2<sup>Δ/Δ</sup>* embryos was impaired, as the cervical vertebrae were absent, and the thoracic vertebrae were small and misshapen. We wanted to assess chondrogenic proliferation in the developing vertebrae through testing the nuclear protein KI67 (KI67) localization, a marker of cellular proliferation (Gerdes et al., 1984; Gerdes et al., 1984; Schonk et al., 1989). We observed KI67 positive chondrocytes in the control cervical vertebrae (Fig 3.4A). However, we could not detect any KI67 positive cells in the cervical region of the *Col2-cre; Foxc1<sup>Δ/Δ</sup>;Foxc2<sup>Δ/Δ</sup>* embryos (Fig 3.4B, E). KI67 was identified in both control and *Col2-cre; Foxc1<sup>Δ/Δ</sup>;Foxc2<sup>Δ/Δ</sup>* vertebrae (Fig 3.4C, D). Control thoracic vertebral showed a localization of KI67 throughout the columnar chondrocytes of the vertebral bodies and in both the annulus fibrosus and nucleus pulposus of the intervertebral discs (Fig 3.4C). But KI67 localization was slightly reduced in *Col2-cre; Foxc1<sup>Δ/Δ</sup>;Foxc2<sup>Δ/Δ</sup>* thoracic vertebrae with arbitrary distribution (Fig 3.4D, E), owing to the disrupted endochondral ossification developmental process of the thoracic vertebrae by the *Foxc1* and *Foxc2* deletion. These data suggest that *Foxc1* and *Foxc2* knockout (KO) had compromised chondrocytes proliferation activity in the vertebral column.

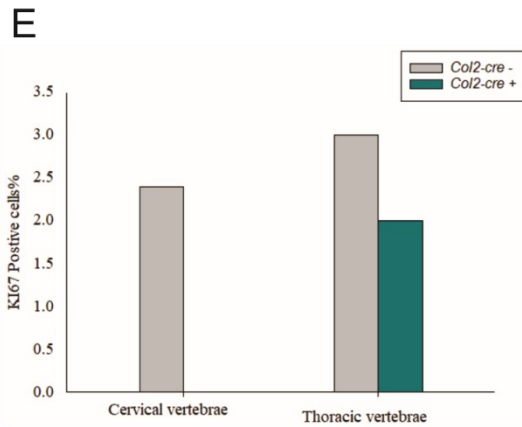
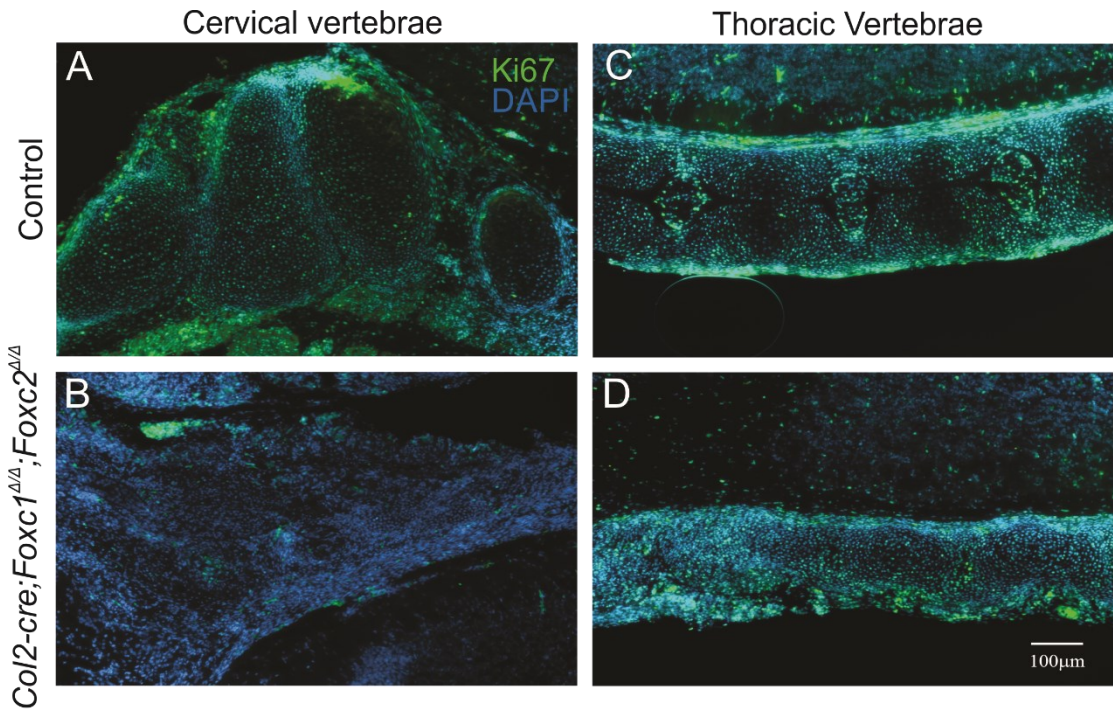


Figure 3.4. Thoracic vertebrae have fewer proliferating cells in the absence of *Foxc1* and *Foxc2* function. A. KI67 IF was conducted on E16.5 control and *Col2-cre; Foxc1<sup>Δ/Δ</sup>; Foxc2<sup>Δ/Δ</sup>* sagittal cervical (A, B) and thoracic (C, D) vertebrae sections to monitor cellular proliferation. (E) Quantification of KI67 positive cells in the cervical and thoracic vertebrae of control and mutant mice (n=2).

### 3. 4 Discussion:

*Col2-cre; Foxc1<sup>Δ/Δ</sup>; Foxc2<sup>Δ/Δ</sup>* embryos showed a number of malformations in the vertebral column. Deletion of *Foxc1* and *Foxc2* in *Col2-cre* positive cells blocked initiation of chondrogenesis in the cervical region leading to impaired formation of the cervical vertebrae. In addition, *Col2-cre; Foxc1<sup>Δ/Δ</sup>; Foxc2<sup>Δ/Δ</sup>* mice developed smaller, thoracic vertebrae with malformed intervertebral discs compared to the control. We were able to identify localization of endochondral ossification proteins associated with early chondrocytes formation such as SOX9, SOX6 and COL2a1; chondrocytes hypertrophy such as COLX, and bone formation like COL1 in E16.5 control vertebral column. We could not detect expression of any of these genes within the cervical region of *Col2-cre; Foxc1<sup>Δ/Δ</sup>; Foxc2<sup>Δ/Δ</sup>* embryos. However, the small malformed thoracic vertebrae exhibited reduced expression of chondrocytes formation and mineralization markers. We could not identify KI67 positive chondrocytes in the *Col2-cre; Foxc1<sup>Δ/Δ</sup>; Foxc2<sup>Δ/Δ</sup>* cervical vertebrae. However, we observed reduced KI67 levels in the thoracic vertebrae chondrocytes. These findings suggest that conditional deletion of *Foxc1* and *Foxc2* in *Col2-cre* positive cells has blocked initiation of chondrogenesis in the cervical region of the spinal column and caused a delay in endochondral ossification process in the thoracic vertebrae.

Proliferation activity indicated by KI67 in the thoracic vertebrae was also compromised by *Foxc1* and *Foxc2* deletion. One possibility is that deletion of *Foxc1* has affected IHH signaling required for chondrocytes proliferation, as one group identified FOXC1 as an important co-transcription factor that induce GLI2 transcriptional activity in stimulating IHH signaling downstream targets. (Yoshida et al., 2015a).

The cervical vertebrae were more affected than the thoracic vertebrae in the *Col2-cre; Foxc1<sup>Δ/Δ</sup>;Foxc2<sup>Δ/Δ</sup>* embryos. We observed a complete absence of the cervical vertebrae and intervertebral discs formation in the region where the cervical vertebrae should form. The thoracic vertebrae were small, malformed and fused in *Col2-cre; Foxc1<sup>Δ/Δ</sup>;Foxc2<sup>Δ/Δ</sup>* embryos. This difference might be due to spatial variation of *Foxc1* and *Foxc2* expression throughout the vertebral column, where they probably express in more cells in the cervical region and less in the thoracic and lumbar vertebrae. This likelihood can be examined by assessing *Foxc1* and *Foxc2* expression level throughout the vertebral column during different time points of embryonic development, as temporal variation of *Foxc1* and *Foxc2* expression might also be another factor that contributed to the difference in phenotypic severity between the cervical and the thoracic vertebrae. Another likelihood is that the thoracic vertebrae formed before the cervical vertebrae, and that vertebral endochondral development was delayed by the deletion of *Foxc1* and *Foxc2* in the sclerotome(Almubarak et al., 2021), as scientists have shown that in human, some cervical vertebrae ossify after the thoracic vertebrae and the lumbar vertebrae (Skórzewska et al., 2013). Little is known about the vertebral column developmental process during prenatal growth. We can test the vertebral column development through assessing endochondral ossification markers in the spinal column during different time points of embryonic growth. Another possibility is that deletion of *Foxc1* and *Foxc2* in the sclerotome-derived chondrocytes (Almubarak et al., 2021)prevented sclerotome cells migration to the future vertebrae. Another explanation is that deletion of *Foxc1* and *Foxc2* in *Col2* positive cells has affected formation of sclerotome prior to the onset of chondrogenesis.

Conditional deletion of *Foxc1* and *Foxc2* in *Col2-cre* positive cells in mice resulted in multiple skeletal abnormalities preferentially affecting the axial skeleton over the appendicular skeleton (Almubarak et al., 2021). Mesenchymal progenitor cells that form the axial skeleton are derived from the sclerotome of somites (Mallo, 2016) whereas the progenitors that form the limb skeleton originate from the lateral plate mesoderm. Thus, there may be differences in the endochondral development of these distinct populations of cells. One notable example is that *Col2-cre* activity occurs at an earlier developmental time point before the onset of chondrogenesis in the axial skeleton (Ovchinnikov et al., 2000). There are several possible explanations to account for these phenotypic differences. One likelihood is that *Col2-cre* is active at an earlier stage in the progenitors of the vertebral column compared to the limb and fewer chondrogenic cells are formed. And so, we wanted to know if early *Foxc1* and *Foxc2* KO in the limb will also lead to worse phenotype. In chapter 4 of this thesis, early deletion of *Foxc1* and *Foxc2* in the lateral plate mesoderm resulted in impaired development of some bones such as the ulna and the fibula, and general delay in endochondral ossification of other bones such as the tibia with massive reduction of cartilage formation in the distal bone elements and reduction of bone mineralization. Yet, most phenotypes get normalized at late time points when *Foxc1* and *Foxc2* are deleted. This means that in axial and limb endochondral ossification there is a wave when *Foxc1* and *Foxc2* are needed to stimulate chondrogenesis and regulate normal endochondral development. However, this might not be the case in the axial skeleton, and that *Foxc1* and *Foxc2* are needed throughout the endochondral developmental process. To test this idea a conditional *Foxc1* and *Foxc2* deletion in the chondrocytes using the tamoxifen inducible aggrecan-CreERT2 driver (Henry et al., 2009) can be performed to assess if the deletion at later time point will result in a milder phenotype is observed. Another possibility is that *Foxc1* and *Foxc2* may have a different functions in sclerotome

derived vs lateral plate mesoderm, as the sclerotome and lateral plate mesoderm contribute to the formation of different cartilaginous and bone structural elements. In addition, it is possible that there are distinctive molecular and genetic pathways that participate in regulating endochondral development of the axial skeleton than the limb.

Our data suggest that both *Foxc1* and *Foxc2* regulates endochondral ossification in the appendicular and the axial skeleton distinctively. *Foxc1* and *Foxc2* genes involved in regulating terminal endochondral events such as hypertrophic formation and differentiation, mineralization, in addition to bone formation and remodelling in limbs. However, these genes played a different role in the axial skeleton through controlling early stages of chondrogenesis. These findings will add a great insight to the understanding of the *Foxc1* and *Foxc2* complex role in endochondral ossification, which will enhance the development of effective skeletal dysplasia treatments.

## Chapter 4:

### ***Foxc1* and *Foxc2* function in osteochondral progenitors for the progression through chondrocyte hypertrophy and mineralization of the primary ossification center.**

This chapter is under supervisory revision to be submitted for publication in Development journal in Fall 2022 under the title “***Foxc1* and *Foxc2* function in osteochondral progenitors for the progression through chondrocyte hypertrophy and mineralization of the primary ossification center**”.

#### **Contribution to the manuscript:**

*Prx1-cre;Foxc1<sup>Δ/Δ</sup>;Foxc2<sup>Δ/Δ</sup>* model was established previously in Berry Lab and Lassar Lab independently. This Manuscript was mainly performed, analyzed, and written by Asra Almubarak. Qiuwan Zhang was responsible for the performing, imaging and analyzing *Prx1-cre* skeletal prep work, Cheng-Hai Zhang crossed and generated the *Sox9-Cre* mice and *Prx1-Cre* mice used for preparing the skeletal prep. Andrew B. Lassar is a supervisory author, and he supervised the *Sox9-Cre* and the *Prx1-cre* skeletal prep work. Fred B Berry is a supervisory author, and who dissected some of the *Prx1-cre* mice used in this chapter.

***Foxc1* and *Foxc2* function in osteochondral progenitors for the progression through chondrocyte hypertrophy and mineralization of the primary ossification center.**

Asra Almubarak<sup>1</sup>, Qiuwan Zhang<sup>2</sup>, Cheng-Hai Zhang<sup>2</sup>, Andrew B. Lassar<sup>2</sup>, and Fred B Berry<sup>1,3</sup>

<sup>1</sup>Department of Medical Genetics, University of Alberta, Edmonton AB Canada

<sup>2</sup>Department of Biological Chemistry and Molecular Pharmacology

Blavatnik Institute at Harvard Medical School, 240 Longwood Ave, Boston, MA. 02115

<sup>3</sup>Department of Surgery, University of Alberta, Edmonton AB, Canada

Key words: *Foxc1*, *Foxc2*, *Phex*, endochondral ossification, long bone, chondrocytes, mineralization

#### 4.1 Abstract:

Endochondral ossification is a skeletal development process where mesenchymal progenitors first differentiate into chondrocytes before their replacement by bone-forming osteoblasts. *Foxc1* and *Foxc2* are two forkhead box family transcription factors that express at early stages of endochondral ossification. Compound *Foxc1* and *Foxc2* mutant mice die before any skeletal elements are formed. To study the role of *Foxc1* and *Foxc2* genes in endochondral ossification, we generated a conditional mutant that deletes *Foxc1* and *Foxc2* early in the limb bud mesoderm using the *Prx1-cre* transgene. Loss of *Foxc1* and *Foxc2* function in these early endochondral progenitors resulted in mice with shorter, bowed limbs that exhibited reduced mineralization, thinner digits, and smaller bone eminences. In the growth plate, absence of both *Foxc* genes affected the formation of *Ihh* expressing cells which compromised proliferation and lead to a delayed entry into hypertrophy E14.5. At E16.5, two discrete COLX expressing hypertrophic chondrocyte regions at either end of the bone were formed in control limbs, and instead, COLX expression was expanded into the primary ossification center of the mutant limb. Mutant limbs at E16.5 also displayed ectopic mineralization throughout the hypertrophic chondrocytes and asymmetric mineralization of the primary ossification center. *Foxc1* and *Foxc2* KO affected *Phex* expression in the primary ossification center enhanced OPN localization and decreased mineralization. These data indicate the importance of FOXC1 and FOXC2 proteins in regulating progression through chondrocyte hypertrophy and formation the primary ossification center of endochondral limb development

## 4.2 Introduction:

In mammals, the long bones, vertebrae, ribs and the pelvis are formed through a mechanism known as endochondral ossification. In this process, mesenchymal progenitor cells differentiate to chondrocytes that will go through a stepwise series of developmental events to eventually form a layered organized structure known as the growth plate. The longitudinal growth of a developing bone is driven by the growth plate, where chondrocytes in the distal end of the growth plate transition to a highly proliferative state before differentiating into hypertrophic chondrocytes. Hypertrophic chondrocytes will either differentiate into osteoblasts, or they will undergo apoptosis and be replaced with osteoblasts that form the bone (Sun and Beier, 2014; Yeung Tsang et al., 2014).

Endochondral ossification of the limbs initiates when the lateral plate mesoderm differentiates into mesenchymal progenitor cells where they express genes such as SRY-Box Transcription Factor 9 (*Sox9*), Forkhead box protein C1 (*Foxc1*), and Forkhead box protein C2 (*Foxc2*) (Bi et al., 1999; Holger Hiemisch et al., 1998). *Sox9* is a master regulatory gene that regulates chondrogenesis (Akiyama et al., 2002; Dy et al., 2012; Lefebvre et al., 2001). Mesenchymal cells will then condense and form chondrocytes progenitor cells in the resting zone where they start to express early chondrocytes genes such as *Fgfr1*, *Sox9*, *Sox6* and *Col2* (Dy et al., 2012; Hajihosseini et al., 2004; Lefebvre et al., 2001; Ovchinnikov et al., 2000). The resting zone cells will turn into more flattened, actively proliferating columnar chondrocytes marked by genes like Fibroblast growth factor receptor3 (*Fgfr3*), *Sox9* and Collagen 2 (*Col2*) (Lee et al., 2017; Zhou et al., 2015). These columnar chondrocytes will then differentiate into pre-hypertrophic chondrocytes that starts expressing RUNX Family Transcription Factor 2 (*Runx2*), a master

regulatory transcription factor responsible for regulating chondrocytes maturation, and Indian hedgehog (*Ihh*) a key regulator of chondrocytes proliferation (Koziel, 2005; Yoshida et al., 2004). In this mechanism, IHH is secreted by the pre-Hypertrophic chondrocytes to stimulates chondrogenic proliferation through binding to PTCH1 and PTCH2 receptors in columnar chondrocytes and signal the GLI proteins (GLI1, GLI2 and GLI3) to stimulate proliferation (Ikram et al., 2004; Miao et al., 2004; Mo et al., 1997; Yoshida et al., 2015). Moreover, IHH ligand will also stimulates PTHrP (*Pthlh*) activity located in the resting zone to enhance chondrocytes proliferation. As part of the regulatory process, The PTHrP will also reach the pre-hypertrophic chondrocytes through binding to the PTHR1 and negatively regulate IHH activity (Brown et al., 2003; Kobayashi et al., 2002; Yan et al., 2016).

During the terminal endochondral ossification process, the pre-hypertrophic chondrocytes exit from the cell cycle, enlarge, and mature to form hypertrophic chondrocytes. Hypertrophic chondrocytes are large chondrocyte cells with a 10–20mm diameter and have a role in cartilage calcification, remodelling and stimulating vascular invasion for bone formation. Hypertrophic chondrocytes express several genes such as Type X collagen (*Coll10a1*), which is a marker that supports endochondral ossification through compartmentalizing matrix elements and manipulating matrix mineralization (Lefebvre and Smits, 2005; Shen, 2005), In addition to the matrix metalloproteinase 13 (*Mmp13*) that degrades extracellular matrix to facilitate mineralization (Inada et al., 2004), and vascular endothelial growth factor (*Vegf*) that diffuses through the limbs to attract and signal endothelial cells to form vessels that facilitate building the bone (Gerber et al., 1999; Zelzer et al., 2004). Notably, the fate of hypertrophic chondrocytes during bone formation has been a topic of debate (Shapiro et al., 2005). While some hypertrophic chondrocytes undergo apoptosis (Aizawa et al., 1997; Farnum and Wilsman, 1987; Gibson, 1998), most of these cells

were observed to dedifferentiate to form osteoblasts, that synthesize bone matrix and coordinate the mineralization of the skeleton (Hu et al., 2017; Park et al., 2015). Osteoblasts express important genes such as Collagen Type 1 (*Coll1*), and Osterix (*Osx* or *Sp7*) that are required for osteoblasts differentiation and establishment of bone (Enishi et al., 2014; Zhou et al., 2010). Additionally, osteoblasts stimulate and activate Monocytes brought by the blood vessels into osteoclasts, that are responsible for dissolution and absorption of bone, through the receptor activator NF- $\kappa$ B ligand (RANKL), a regulating signal coded by the gene *Tnfsf11* (Boyce et al., 2009). *Fgfr1* gene was also found to regulate bone remodeling through its localization in both osteoblasts and osteoclasts, in addition to its role in regulating osteoclasts differentiation and activation (Lu et al., 2009; Su et al., 2014). Both osteoblasts and osteoclasts work together to form the primary ossification center (POC), maintain bone remodeling, and formation of bone marrow space needed for erythropoiesis (Boyce et al., 2009; Lademann et al., 2020). Any disruption in this embryonic developmental pathway will result in a range of growth disorders collectively known as skeletal dysplasia common causes of embryonic skeletal anomalies are abnormal chondrocyte differentiation, where transcription factors have a significant contribution. Transcription factors regulate the expression of genes that control the progression through endochondral ossification events and are thus an important feature to study in order to understand the developmental pathway (Civelek et al., 2014).

The transcription factors forkhead Box C1 and C2 (FOXC1 and FOXC2) are important regulators of skeletal development. These factors are expressed in various types of tissues including skeletal progenitors of the limb and the vertebrae (Hiemisch et al., 1998). Mice with homozygous null mutations in either *Foxc1* and *Foxc2* display severe anomalies in the axial

skeleton (the skull, vertebral column, and rib cage). In contrast, the bones in the limbs or appendicular skeleton are less affected with only thinner digits observed (Hong et al., 1999; Kume et al., 1998; Winnier et al., 1997). Compound *Foxc1*<sup>-/-</sup>; *Foxc2*<sup>-/-</sup> mice die around Embryonic (E) day 9 due to failure in cardiovascular development (Kume et al., 2001) and before any skeletal structures are formed, preventing any analysis of the possible association between the two transcription factors in endochondral ossification to be studied. Our lab demonstrated that deletion of *Foxc1* and *Foxc2* in the chondrocyte lineage impaired chondrocyte differentiation and led to a general skeletal hypoplasia without affecting vital organ systems (Almubarak et al., 2021). The rib cage and vertebral column was more affected in these compound homozygous mice compared to the bones in the limb. Given that *Foxc1* and *Foxc2* are abundantly expressed in the condensing limb bud mesenchyme (Almubarak et al., 2021; Hiemisch et al., 1998), such phenotypic differences between the axial and appendicular skeleton were surprising. The mesenchyme that forms the axial skeleton is derived from somatic mesoderm called sclerotome. Since the *Col2-cre* transgene is active in sclerotome cells prior to the onset of chondrogenesis (Ovchinnikov et al., 2000) we thought that this earlier timing of the deletion of *Foxc1* and *Foxc2* might explain the phenotypic differences we observe in the axial vs appendicular skeleton. To address these issues, we deleted *Foxc1* and *Foxc2* at an earlier development stage than when *Col2-cre* is active.

To further refine the roles for *Foxc1* and *Foxc2* in endochondral ossification we deleted these factors at the onset of chondrogenesis using *Sox9-cre* and in condensing limb bud mesenchyme using *Prx1-cre*

## 4.3 Materials and Methods:

### 4.3.1 Mouse models

All experiments using mouse models was approved by the University of Alberta Animal Care and Use Committee (AUP804). *Prx1-cre;Foxc1<sup>Δ/Δ</sup>;Foxc2<sup>Δ/Δ</sup>* were generated through crossing *Foxc1<sup>fl/fl</sup>;Foxc2<sup>fl/fl</sup>* (Sasman et al., 2012) with *Prx1-cre<sup>+/-</sup>* mice (Logan et al 2002; Jackson Laboratory). Timed pregnancies were performed by crossing male *Prx1-cre<sup>+/-</sup>;Foxc1<sup>+fl</sup>;Foxc2<sup>+fl</sup>* mice to female *Foxc1<sup>fl/fl</sup>;Foxc2<sup>fl/fl</sup>* mice. The day of the detection of a vaginal plug was denoted as E0.5. All experimental comparisons were made between littermates. We genotyped weaned mice using ear notch biopsies and collected embryos using skin DNA. The genotyping process was conducted using the KAPA mouse genotyping kit (Millipore Sigma) using the following primer pairs:

*Foxc1* (forward 5'-ATTTTTTTTCCCCCTACAGCG-3'; reverse 5'-ATCTGTTA  
GTATCTCCGGGTA-3'), *Foxc2* (forward 5' CTCCTTTGCGTTTCCAGTGA -3'; reverse 5'-  
ATTGGTCCTTCGTCT TCGCT -3') and

*Prx1-cre* (forward 50 -GCCTGCATTACCGGTCGATGCAACGA-30; reverse 50 -  
GTGGCAGATGGCGCGGCAACACCATT-30).

### 4.3.2 Tissue preparation

Tissues were dissected at specific stages and fixed in 4% paraformaldehyde at 4°C overnight before embedding in paraffin. Sections were cut at 5 μm thickness and collected on Superfrost-plus slides (Fisher Scientific). E17.5 limbs were decalcified with EDTA at 4°C overnight before paraffin embedding.

#### 4.3.3 Safranin O staining

Tibia sections were first dewaxed with xylene and rehydrated with graded ethanol and water. Then, samples were stained with hematoxylin for eight minutes and rinsed with running tap water for 10 minutes. Next, sections were stained with 0.001% Fast green for five minutes, followed with 1% Acetic acid wash for 10-15 seconds to stabilize the staining. Slides were then stained with 0.1% Safranin O for five minutes, rehydrated with 100% ethanol and xylene, and mounted with coverslips.

#### 4.3.4 Alcian blue Von-kossa staining

First, tibia sections were deparaffinized and rehydrated with graded ethanol and water. Second, sections were incubated with 1% silver nitrate solution under ultraviolet (UV) light for 20 minutes. Slides were then rinsed with two water changes followed by five minutes incubation with 5% sodium thiosulfate to remove the un-reacted silver. Third, sections were stained with Alcian blue for 30 minutes and counterstained with nuclear fast red for five minutes, washed and dehydrated through graded alcohol, and cleared with xylene. Slides were finally mounted with a Permount mounting medium and covered with a coverslip.

#### 4.3.5 TRAP staining:

Sections were deparaffinized and rehydrated through graded ethanol and water. Slides were then incubated in a pre-warmed TRAP Staining solution Mix at 37°C for 30 minutes. Next, slides were

rinsed with water and counterstained with 0.02% Fast green for 30 seconds and rinse quickly with water. Lastly, slides were dehydrated with graded alcohol and cleared in xylene and mounted.

#### 4.3.6 TUNEL (terminal deoxynucleotidyl transferase dUTP nick end labeling) assay

Apoptosis was detected using the *In situ* Cell Death Detection Kit, TMR red (Roche). Tibia sections were obtained and processed as described above. Next, slides were permeabilized with proteinase K working solution (10µg/ml in 10mM Tris/HCL, PH 7.4-8) for 30 minutes at 37°C and washed twice with 1xPBS. Then, sections were treated with the TUNEL reaction mixture for 60 minutes in a humidified atmosphere at 37°C. Slides were then washed three times with 1xPBS and stained with DAPI for 5 minutes and mounted with Prolong Gold anti-fade reagent (Invitrogen).

#### 4.3.7 *In situ* hybridization

Fluorescent ISH for multiplex was performed using RNA scope Multiplex Fluorescent kit (Advanced Cell Diagnostics). Paraffin-embedded tibia sections were collected and processed for ISH as described above. Sections were baked at 60°C for one hour, followed by rehydration through xylene, graded ethanol and water. Next, sections were incubated in hydrogen peroxide for 10 minutes at room temperature, rinsed in two water changes, and treated with antigen retrieval for 15 minutes at 95-100°C. Then, sections were rinsed in water for 15 seconds, followed with 100% ethanol for three minutes, circled with the hydrophobic pen, and let dry overnight. On the next day, sections were treated with protease plus reagent for 30 minutes at 40°C and washed with two changes of water. Slides were treated with probes for two hours at 40°C and washed twice

with the washing buffer. Slides were then treated with three detection reagents at 40°C for 30, 30, and 15 minutes respectively, followed by 2X2 washes with wash buffer after each step. Upon completion of the signal detection step, slides were treated with the Multiplex HRP blocker for 15 minutes and rinsed in 2X2 in the wash buffer. Signal detection was performed by treating the slides with channel one (C1) opal dye diluted in the Tyramide Signal Amplification (TSA) buffer (1:500) for 30 minutes at 40°C and 2X2 washes in the washing buffer, followed by incubating the slides in HRP-blocker buffer for 15 minutes at 40°C. C2 opal dye was added in samples that had two probes, following the same steps for signal detection. Otherwise, slides were counterstained with DAPI for 30 seconds at room temperature, washed off with 2X5 1XPBS, and mounted with Prolong Gold anti-fade reagent from Invitrogen (REF: P36930). The following probes were used. Negative control (REF: 310043); *Foxc1* (REF: 412851); *Foxc2* (REF: 406011); *Fgfr3* (REF: 440771); *Fgfr1*(REF: 454941); *Ihh* (REF: 413091); *Gli1*(REF:311001) ; *Gli2* (FEF: 405771-C2); *Gli3* (REF:445511); *Pthlh* (REF: 456521); *Pth1r* (REF: 426191) ; *Ptch1* (REF: 402811); *Ptch2* (REF: 435131); *Colx* (REF:433491); *Tnfsf11*(REF: 410921); *Vegf*(REF: 436961); and *Phex* (REF: 426201)

#### 4.3.8 Immunofluorescence

Paraffin sections were collected as described above. Tibia slides were dewaxed and rehydrated through xylene and graded ethanol series. For SOX9, OSX, OPN, KI67, and RUNX2 antibodies, antigen retrieval was performed through boiling the slides in citrate buffer (10 mM trisodium citrate, pH 6.0; 0.05% Tween20) for 20 minutes. For COL1, COL2a, COLX, MMP13, VEGFA antibodies, samples were incubated in hyaluronidase for 30 minutes at 37°C. Next, slides were blocked in 5% donkey serum in PBS with 0.05% Triton X-100 (PBSX) for one hour. Slides were

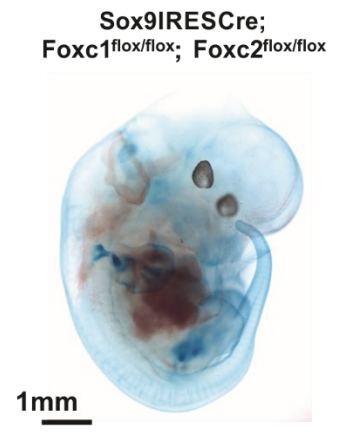
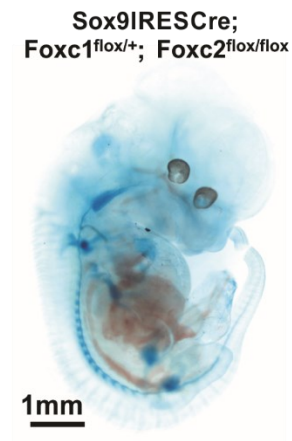
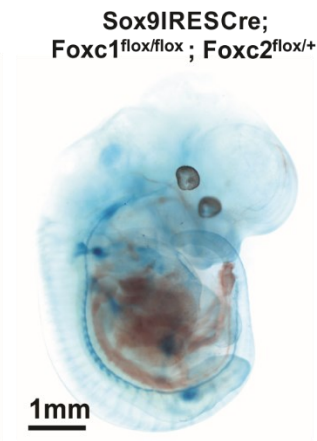
then incubated with the desired primary antibody overnight at 4°C. Slides were washed with PBSX followed by a two hour incubation with secondary antibody at room temperature. Finally, slides were stained with DAPI for 5 minutes and mounted with coverslip using Prolong Gold.

The following antibodies were used for immunofluorescence microscopy: COL IIa (Abcam, ab185430, 1:100); COLX (Abcam, ab5832, 1:50); COL I (Abcam, ab88147; GR3225500-1, 1:100); MMP13 (Abcam, ab39012, 1:100); RUNX2 (Abcam, ab76956, 1:200), IB4 (Thermo Fisher Scientific cat: VECTB1205, 1:500), SOX9 (MilliporeSigma, AB55535, 1:200); OPN (SCBT, sc22536-R, 1:100); OSX (SCBT, sc21742, 1:100); KI67 (Bethyl, IHC00075, 1:100).

## 4.4 Results:

### 4.4.1 Impaired formation of cartilaginous elements in early deletion of *Foxc1* and *Foxc2* in *Sox9*-*cre* expressing cells

*Foxc1* and *Foxc2* genes are expressed in condensing mesenchyme cells prior to the onset of chondrogenesis in the limb skeleton (Almubarak et al., 2021; Hiemisch et al., 1998). We examined chondrocyte differentiation (by alcian blue staining) in embryos engineered to contain floxed alleles of both these transcription factors plus a *Cre* recombinase that had been knocked in to the 3' UTR of the *Sox9* locus (*Sox9<sup>ires-Cre</sup>*) (Akiyama et al., 2005; Sasman et al., 2012). E12.5 embryos that lacked the *Cre* driver displayed alcian blue staining of both their paraxial mesoderm-derived and appendicular skeletal structures. In contrast, *Sox9<sup>ires-Cre/+</sup>;Foxc1<sup>flox/flox</sup>;Foxc2<sup>flox/flox</sup>* littermates displayed a dramatic loss of alcian blue staining in their paraxial mesoderm, but maintained that in their developing limb buds ( Fig 4S.1). *Sox9<sup>ires-Cre/+</sup>;Foxc1<sup>flox/flox</sup>;Foxc2<sup>flox/+</sup>* and *Sox9<sup>ires-Cre/+</sup>;Foxc1<sup>flox/+</sup>;Foxc2<sup>flox/flox</sup>* embryos displayed intermediate levels of alcian blue staining in their paraxial mesoderm. These results indicate that *Foxc1* and *Foxc2* share overlapping roles in promoting chondrogenesis of the paraxial-derived mesoderm. In addition, it suggests that other factors may work in parallel with *Foxc1* and *Foxc2* to promote the initiation of chondrogenesis in the appendicular skeleton.



Supplementary Figure 4.S1. *Foxc1* and *Foxc2* share redundant roles to promote axial chondrogenesis.

E12.5 littermate embryos of the indicated genotypes were stained with alcian blue to detect chondrogenic differentiation. Similar results have been obtained with embryos from 2 litters, containing 3 embryos of the least frequently occurring genotype (i.e., *Sox9<sup>ires-</sup>*

*Cre/+;Foxc1<sup>flox/flox</sup>;Foxc2<sup>flox/flox</sup>*).

*Sox9<sup>ires-Cre/+</sup>;Foxc1<sup>flox/flox</sup>;Foxc2<sup>flox/flox</sup>* mice embryos were not viable, as they stop developing after E12.5, preventing further analysis of skeletal development. Therefore, *Prx1-Cre* was used to delete these genes in limb bud mesenchyme. *Prx1-Cre* has been shown to drive efficient recombination in the developing limb buds, sternum, and calvarial precursors (Logan et al., 2002). *Prx1-cre;Foxc1<sup>Δ/Δ</sup>;Foxc2<sup>Δ/Δ</sup>* embryos die shortly after birth. These embryos exhibited smaller limbs and feet with abnormal forelimb positioning that resembled decerebrate posture (white arrow) and exencephaly (yellow arrow) (Fig. 4.1A, B) (Kume et al., 1998). We sought to confirm deletion of *Foxc1* and *Foxc2* in *Prx1-cre;Foxc1<sup>Δ/Δ</sup>;Foxc2<sup>Δ/Δ</sup>* limbs through multiplex RNA scope *in situ* hybridization (ISH). We observed a distinct overlapping between *Foxc1* and *Foxc2* expression in the perichondrium, resting zone chondrocytes, the osteochondral junction, and the primary ossification center of E16.5 control tibia (Fig 4.1C, D) similar to what we previously reported (Almubarak et al., 2021). Both *Foxc1* and *Foxc2* gene expression was not detected in *Prx1-cre;Foxc1<sup>Δ/Δ</sup>;Foxc2<sup>Δ/Δ</sup>* mutant limbs, which indicates a successful deletion of *Foxc1* and *Foxc2* (Fig. 4.1E, F).

We then wanted to assess cartilage formation by performing Safranin O staining of the E16.5 limbs. Staining showed the development of the growth plate in both control and *Prx1-cre;Foxc1<sup>Δ/Δ</sup>;Foxc2<sup>Δ/Δ</sup>* mice (Fig 4.1G, H). Far from what we expected, early deletion of *Foxc1* and *Foxc2* in limb chondrocyte progenitors did not block initiation of chondrogenesis. However, the hypertrophic chondrocyte zone was expanded (Fig 4.1G, H). Next, we examined the presence of any structural phenotypes in the fore- and hindlimbs. We isolated E15.5 and E18.5 limbs of control and *Prx1-cre;Foxc1<sup>Δ/Δ</sup>;Foxc2<sup>Δ/Δ</sup>* embryos for whole mount Alizarin red and Alcian blue skeletal staining. Loss of *Foxc1* and *Foxc2* in the developing limb bud drastically affected zeugopod and autopod formation; severely decreasing both the length and thickness of the ulna

and fibula in the zeugopod and causing a loss of both wrist and ankle cartilage rudiments and an extreme thinning of the more distal autopod cartilage elements in both the developing fore- and hindlimbs (Fig. 4.1I). The *Prx1-Cre* mutant limbs showed a severe stunting of skeletal elements in the zeugopod and a thinning or loss of autopod cartilage elements, we also noted that in both the fore- and hindlimbs of *Prx1-cre;Foxc1<sup>Δ/Δ</sup>;Foxc2<sup>Δ/Δ</sup>* embryos, regions of attachment of the skeletal elements to tendons were smaller than in control littermates. In addition, the deltoid tuberosity (black arrow) was initially formed at E15.5 but fails to grow by E18.5. Similar to the deltoid tuberosity (black arrow), the olecranon (red arrow) in the forelimb, and the calcaneal tuberosity (green arrow) and the patella (blue arrow) in the hindlimb, also fail to significantly grow in *Prx1-cre;Foxc1<sup>Δ/Δ</sup>;Foxc2<sup>Δ/Δ</sup>* embryos (Fig. 4.1I). These findings signify the importance of *Foxc1* and *Foxc2* in proper formation of the zeugopod and autopod elements and development of the bone eminences in the fore- and hindlimbs.

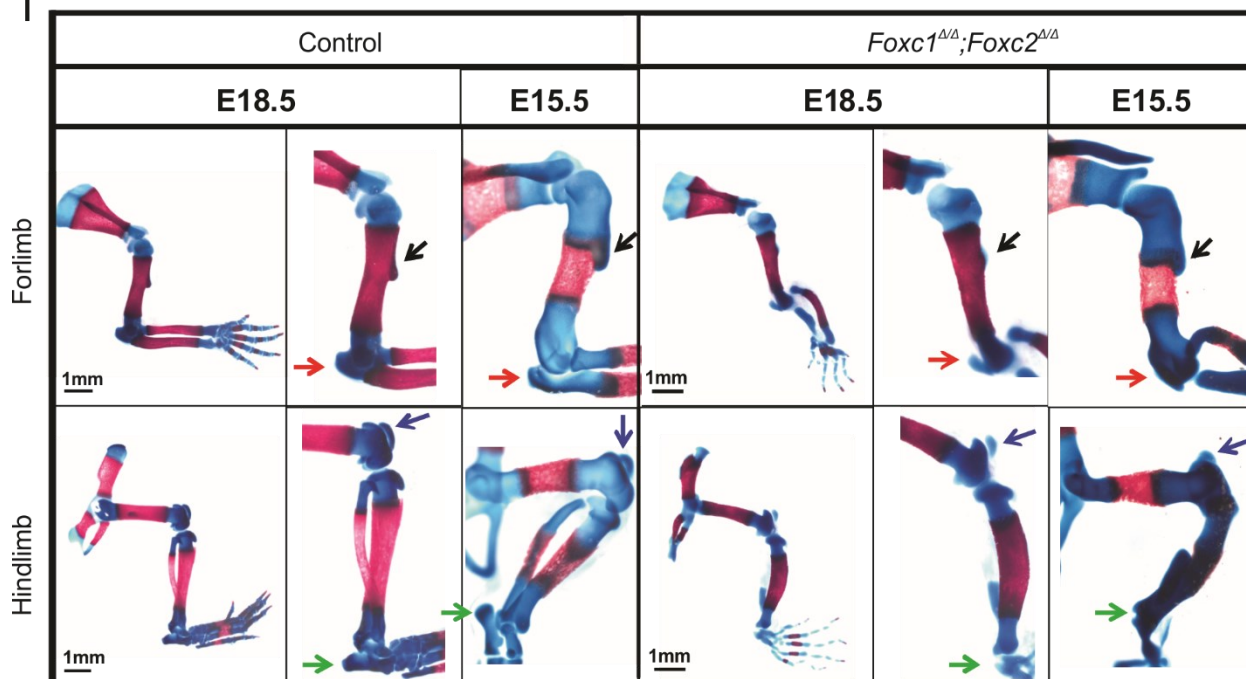
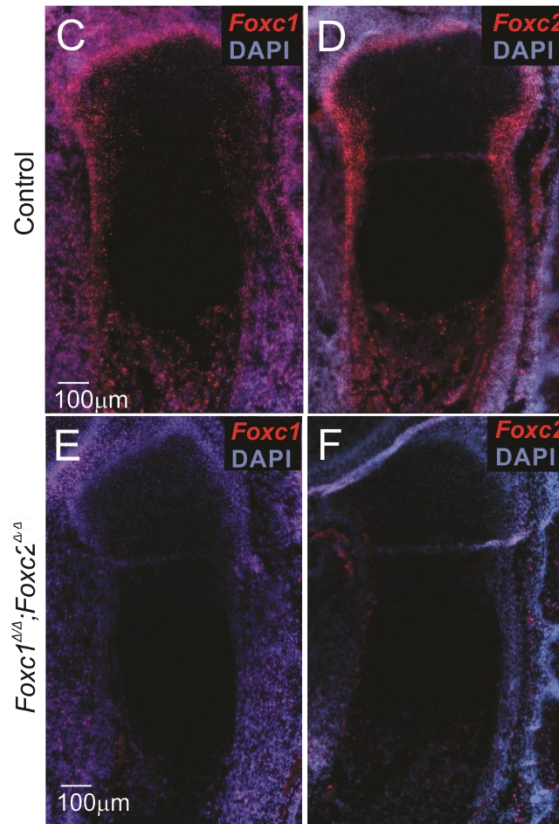
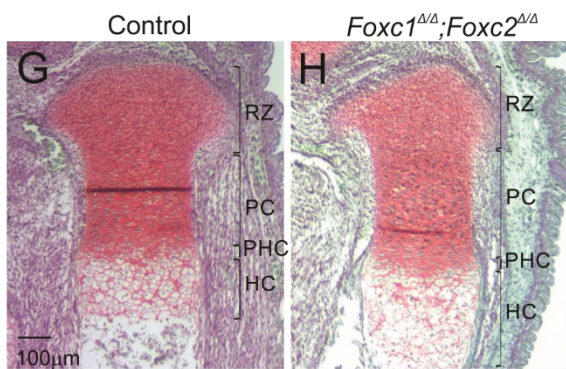
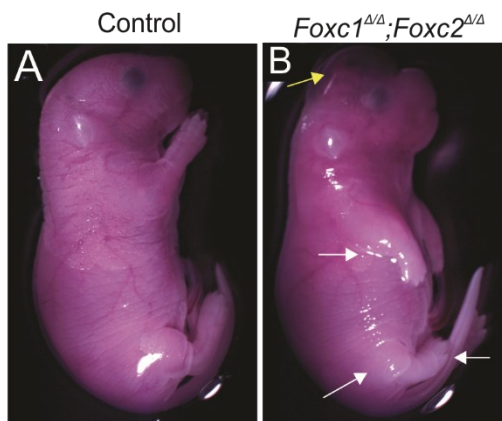


Figure 4.1. *Foxc1* and *Foxc2* play critical roles in the formation of the distal regions of the appendicular skeleton and support the growth of the bone eminences.

E16.5 control (A) and *Prx1-cre;Foxc1<sup>Δ/Δ</sup>;Foxc2<sup>Δ/Δ</sup>* (B) Embryos. The *Prx1-cre* mutant mice shows the development of hydrocephalus (yellow arrow) and reduction of forelimbs and hindlimbs size (white arrow). E16.5 control tibia stained with RNA scope ISH of *Foxc1* (C) and *Foxc2* (D). In the control, *Foxc1* and *Foxc2* RNAs localized in the growth plate periphery resting zone, groove of ranvier and the primary ossification center. No expression was detected for *Foxc1* nor *Foxc2* within the *Prx1-cre* limb (E, F). Safranin O staining of E16.5 control (G) and *Prx1-cre;Foxc1<sup>Δ/Δ</sup>;Foxc2<sup>Δ/Δ</sup>* tibia (H) shows the formation of all developmental stages of the growth plate in both limbs with expansion of the hypertrophic chondrocytes in the absence of both *Foxc1* and *Foxc2*. Resting zone (RZ), Columnar chondrocytes (CC), Pre-hypertrophic chondrocytes (PHC) and hypertrophic chondrocytes (HC). E15.5 or E18.5 littermate embryos of the indicated genotypes were stained with alcian blue (to detect chondrogenesis) and alizarin red (to detect mineralization) (I). Staining revealed disrupted appendicular skeleton formation and bone eminences. Arrows indicate the deltoid tuberosity (black arrow) and olecranon (red arrow) in the forelimb, and the calcaneal tuberosity (green arrow) and the patella (blue arrow) in the hindlimb. Similar results have been obtained with embryos from 9 litters, containing a total of 12 embryos of the least frequently occurring genotype (i.e., *Prx1-Cre; Foxc1<sup>Δ/Δ</sup>;Foxc2<sup>Δ/Δ</sup>*).

#### 4.4.2 *Foxc1* and *Foxc2* regulation of endochondral ossification varies spatially and temporally during endochondral bone development

Loss of *Foxc1* and *Foxc2* in the developing limb bud caused more severe bone phenotype in the distal elements (zeugopod; autopod) compared to the proximal parts (stylopod). Thus, we wanted to investigate whether *Foxc1* and *Foxc2* expression varies spatially or temporally during embryonic bone development. Safranin O staining of E16.5 hindlimbs showed robust red staining that marked normal chondrocytes formation in the control limb (Fig. 4.2A). However, the *Prx1-cre;Foxc1<sup>Δ/Δ</sup>;Foxc2<sup>Δ/Δ</sup>* limbs displayed reduced staining in the autopod compared to the proximal bone elements (Fig. 4.2B). One possibility is that *Foxc1* and *Foxc2* expression levels vary spatially in the limb. Alternatively, as the limb develops in a distal to proximal manner, skeletal elements in the autopod represent an earlier developmental point than the stylopod. We conducted ISH of *Foxc1* and *Foxc2* in E16.5 hindlimbs and the staining revealed more intense RNA signal of both genes in the foot compared to the tibia and the femur. (Fig. 4.2C, D). At E14.5, we detected increase expression of expression *Foxc1* and *Foxc2* at early time points of E12.5, E13.5, and E14.5 (Fig. 4.2E, F) than later stage of E16.6, which highlight a temporal variation in their expression during limb development (Almubarak et al., 2021). At E14.5, both *Foxc1* and *Foxc2* RNA signals were prominent in the perichondrium and the growth plate including the hypertrophic chondrocytes (Fig. 4.2G, H) compared to the more restricted expression of *Foxc1* and *Foxc2* in the periphery and the POC in the E16.5 limbs (Fig. 4.2C, D). Yet, like the E16.5, the E14.5 limbs also displayed more *Foxc1* and *Foxc2* expressing chondrocytes in the autopod than the other proximal bone elements, these data indicate that *Foxc1* and *Foxc2* expression pattern go through both spatial and temporal changes during embryonic limb development.

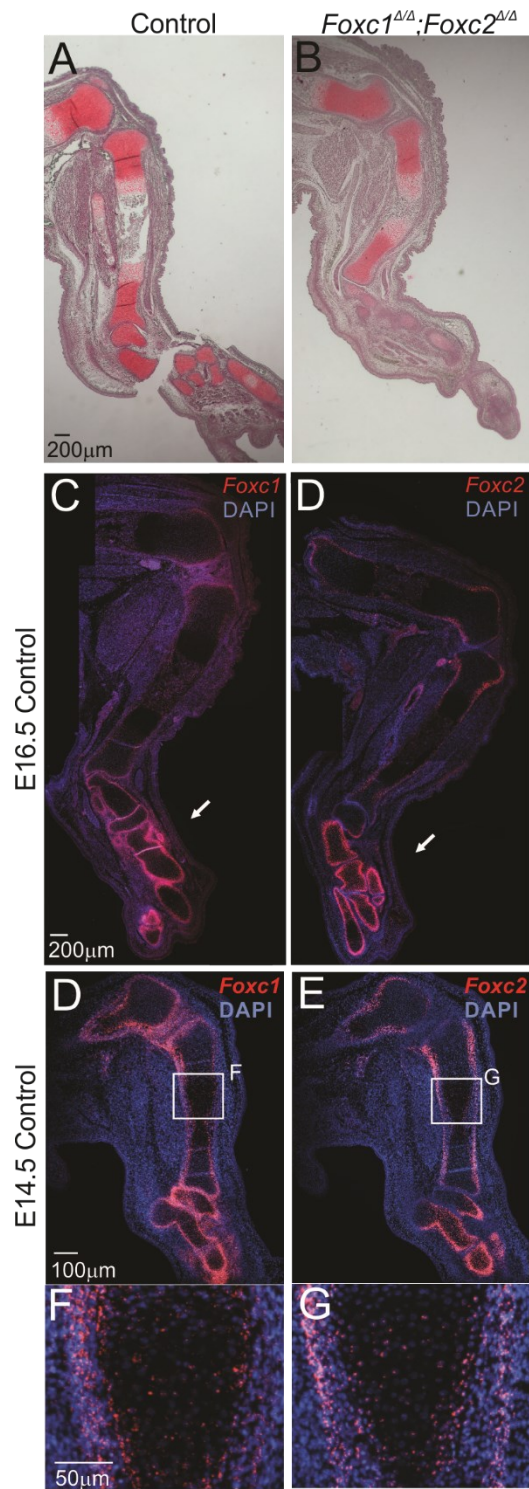


Figure 4.2. *Foxc1* and *Foxc2* expression varies spatially and temporally during embryonic bone development.

Safranin O staining of E16.5 Control (A) and *Prx1-cre;Foxc1<sup>Δ/Δ</sup>;Foxc2<sup>Δ/Δ</sup>* hindlimb (B). The *Prx1-cre* limb displayed less cartilage formation in the distal bone elements compared to the proximal parts. RNA scope ISH of *Foxc1* (C) and *Foxc2* (D) in control E16.5 and E14.5 hindlimb showed higher expression level of both genes in the distal end of the limb where the severe skeletal phenotype appears upon the deletion of both genes. E14.5 control limbs displayed more *Foxc1* and *Foxc2* expressing chondrocytes (E, F), including the hypertrophic chondrocytes (F, G) (n=3).

#### 4.4.3 Loss of *Foxc1* and *Foxc2* reduced proliferation activity during early growth plate development

The proliferative zone has a role in maintaining longitudinal bone growth (Sun and Beier, 2014; Tsang et al., 2014). We tested whether reduced chondrocyte proliferation accounted for the reduced size of the mutant limbs. We examined proliferation activity in both control and *Prx1-cre;Foxc1<sup>Δ/Δ</sup>;Foxc2<sup>Δ/Δ</sup>* growth plates using IF to observe KI67 positive cells. KI67 is a protein localized only in actively dividing cells (Gerdes et al., 1984). Analysis of control limbs revealed the highest number of KI67-positive cells in the growth plate at E14.5 in comparison to later time points (Fig. 4.3A-C). This finding indicates that the proliferative chondrocytes were more abundant at E14.5 than later time points. Interestingly, the *Prx1-cre;Foxc1<sup>Δ/Δ</sup>;Foxc2<sup>Δ/Δ</sup>* E14.5 growth plate exhibited around 50% reduction in the number of KI67-positive chondrocytes compared to its analogous area in control limbs (Fig. 4.3C). However, proliferation activity appeared similarly lower in both control and mutant limbs at E15.5 and E16.5. This result suggests the importance of *Foxc1* and *Foxc2* in chondrocytes proliferation.

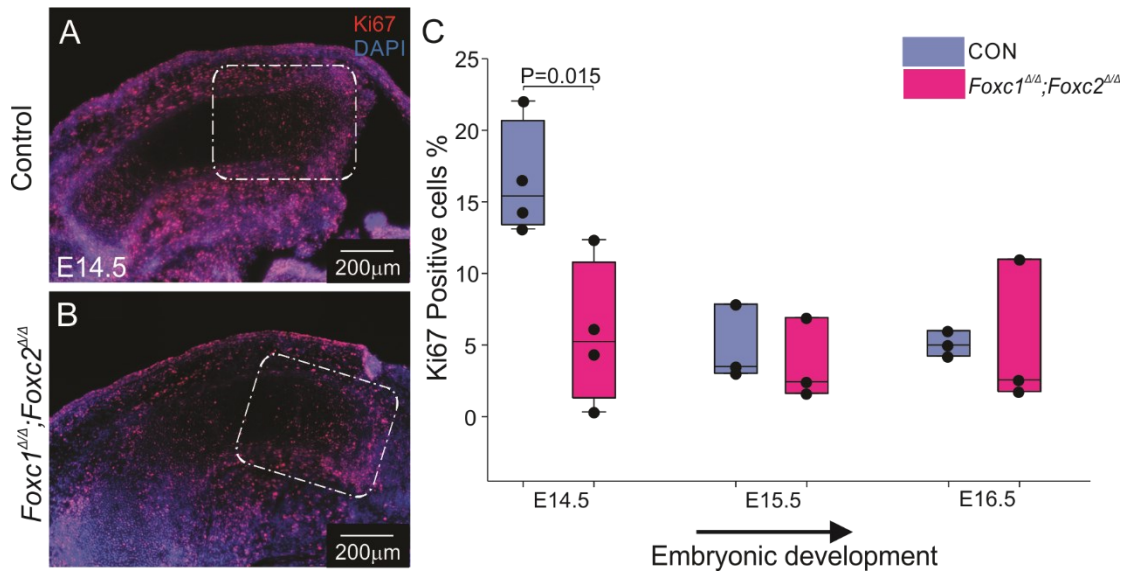


Figure 4.3. *Foxc1* and *Foxc2* KO cause decreased chondrocytes proliferation at E14.5.

KI67 IF of E14.5 control (A) and *Prx1-cre;Foxc1<sup>Δ/Δ</sup>;Foxc2<sup>Δ/Δ</sup>* tibia (B). KI67 IF signal was counted in E14.5, E15.5 and E16.5 control and *Prx1-cre;Foxc1<sup>Δ/Δ</sup>;Foxc2<sup>Δ/Δ</sup>* tibia and plotted in a box and scattered plots (C). 14.5 *Prx1-cre;Foxc1<sup>Δ/Δ</sup>;Foxc2<sup>Δ/Δ</sup>* growth plate showed reduction in the number of KI67 positive cells. But was normalized at later time points. (n=3-4). Statistic was done using student t-test via Sigma Plot 13.

To explain the reduction in proliferation activity in *Foxc1* and *Foxc2* deficient chondrocytes, we assessed the signaling pathways associated with chondrocyte proliferation in the growth plate. We examined the expression of IHH and PTHRP signaling molecules at E14.5. We detected a prominent expression of *Ihh* in the pre- and early hypertrophic chondrocytes of the control limb (Fig. 4.4A, B). In contrast, the *Prx1-cre;Foxc1<sup>Δ/Δ</sup>;Foxc2<sup>Δ/Δ</sup>* tibia displayed a reduction in the size of the *Ihh* expression domain (Fig. 4.4C). Both mRNAs for IHH receptors, *Ptch1* and *Ptch2*, were expressed in the control and our mutant limbs (Fig. 4.4D-G). *Gli1*, *Gli2* and *Gli3* mRNA localization were unaffected in *Prx1-cre;Foxc1<sup>Δ/Δ</sup>;Foxc2<sup>Δ/Δ</sup>* embryos compared to control (Fig. 4.4H-M). Further, *Pthlh* showed a comparable expression in the control growth plate and in the *Prx1-cre;Foxc1<sup>Δ/Δ</sup>;Foxc2<sup>Δ/Δ</sup>* (Fig. 4.4N, O). *Pthlh* has a negative feedback loop through binding to its receptor PTH1R. The Parathyroid hormone receptor (*Pth1r*) was shown to be expressed in a smaller domain within the *Prx1-cre;Foxc1<sup>Δ/Δ</sup>;Foxc2<sup>Δ/Δ</sup>* tibia compared to the control (Fig. 4.4p-R). Collectively, these data indicate that the absence of *Foxc1* and *Foxc2* compromises the formation of *Ihh*-expressing pre-hypertrophic chondrocytes but does not affect *Ihh* and *Pthlh*-mediated signalling pathways at E14.5.

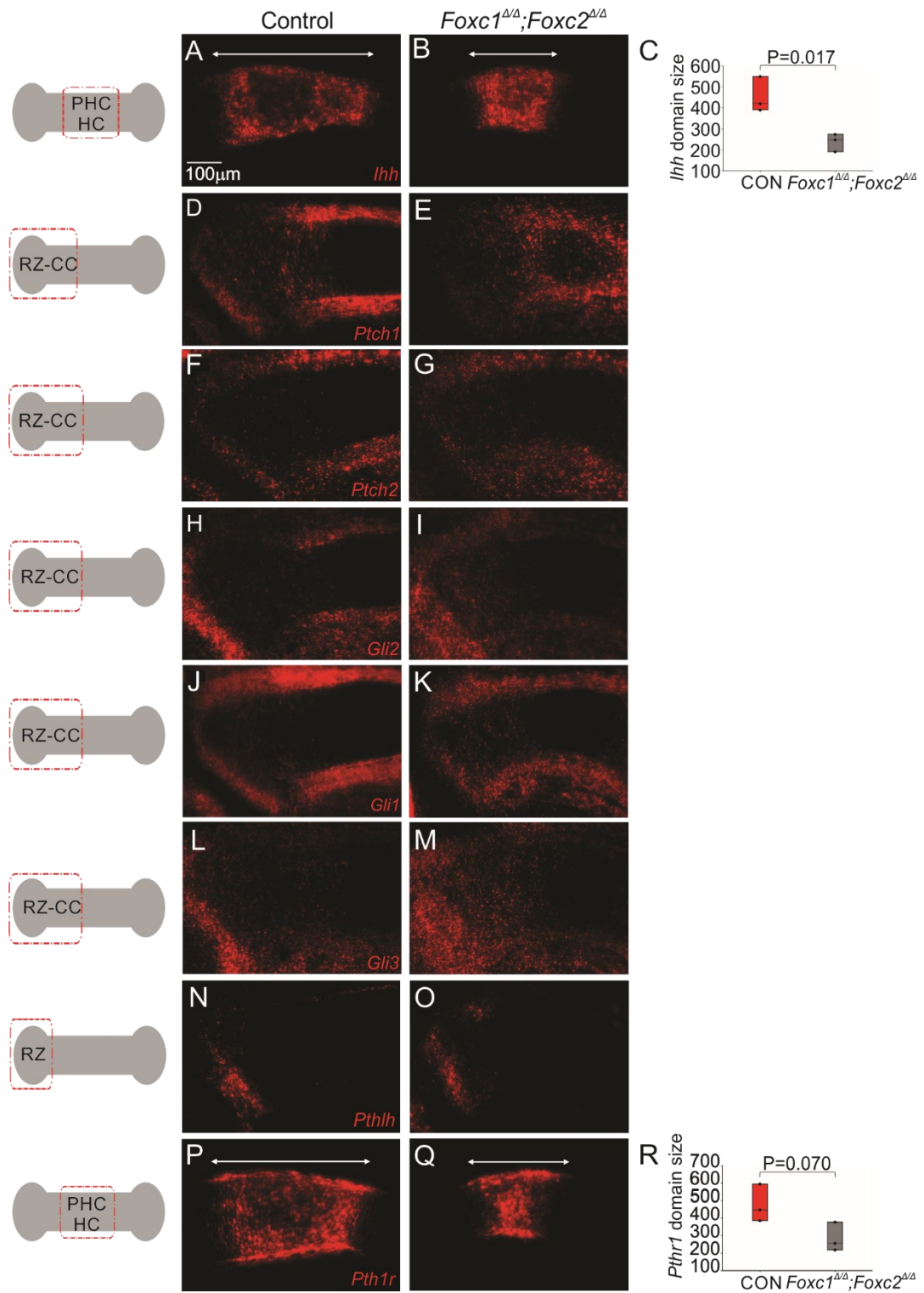
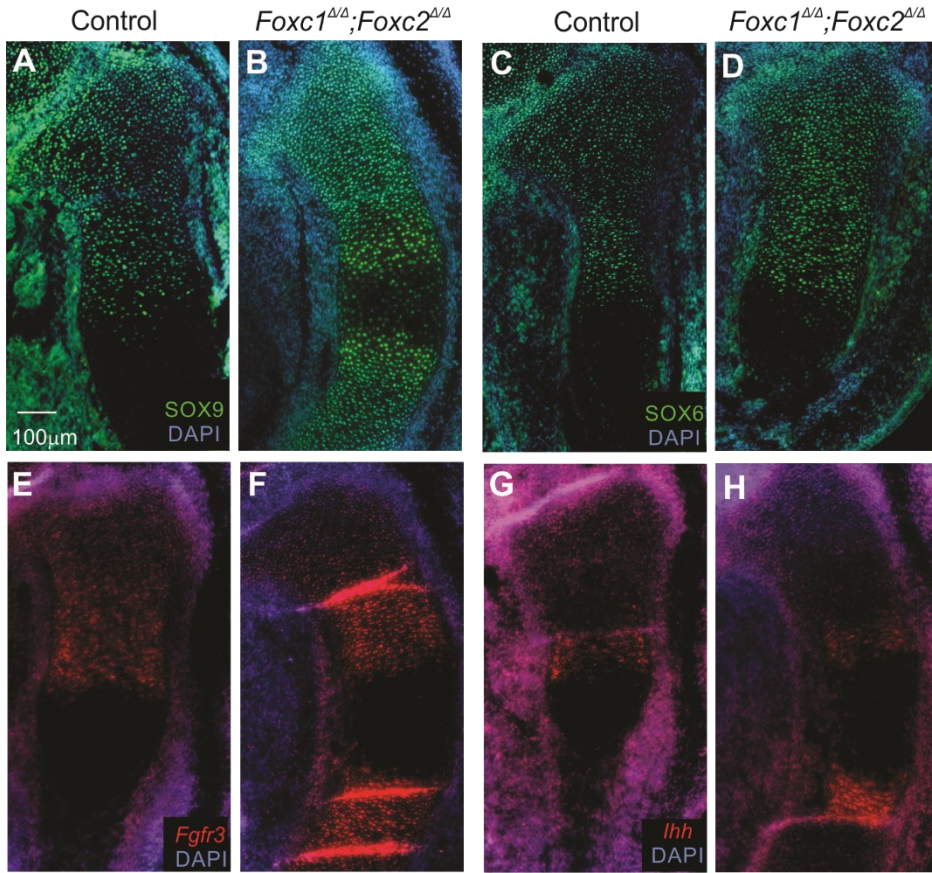


Figure 4.4. Deletion of *Foxc1* and *Foxc2* affected the formation of *Ihh* expression chondrocytes. Expression of *Ihh* (A, B), *Ptch1* (D, E), *Ptch2* (F,G), *Gli2*(H,I), *Gli1*(J,K), *Gli3* (L,M), *Pthlh* (N,O), *Pth1r* (P,Q). Expression localization of each gene was indicated in schematic diagram on the left. box blot of *Ihh* expression domain (C), and *Pth1r* expression domain (R). Staining showed comparable expression of *Ihh* receptors (*Ptch1*, *Ptch2*) and down stream targets (*Gli1*,*Gli2*,*Gli3*,*Pthlh*) in both control and *Prx1-cre* mutant growth plates. But exhibited reduction in *Ihh* and *Pth1r* localization region in the absence of *Foxc1*and *Foxc2*. Statistic was done using student t-test via Sigma Plot 13. (n=3).

#### 4.4.4 Loss of *Foxc1* and *Foxc2* function expands hypertrophic chondrocyte zone.

Next, we assessed chondrogenic differentiation and growth plate organization in the *Prx1-cre;Foxc1<sup>Δ/Δ</sup>;Foxc2<sup>Δ/Δ</sup>* embryos. The tibias from E15.5 and E16.5 embryos isolated, and gene expression monitored by ISH and protein localization through immunofluorescence (IF). Both control and *Prx1-cre;Foxc1<sup>Δ/Δ</sup>;Foxc2<sup>Δ/Δ</sup>* E15.5 growth plates showed localization of SOX9 (Fig. 4.S2A, B), and SOX6 (Fig. 4.S2C, D) transcription factors throughout the resting zone and the columnar chondrocytes. SOX9 was also detected in the pre-hypertrophic chondrocytes of E15.5 *Prx1-cre;Foxc1<sup>Δ/Δ</sup>;Foxc2<sup>Δ/Δ</sup>* growth plate (Fig. 4.S2B). Moreover, localization of *Fgfr3* RNA confirmed the formation of the columnar chondrocytes (Fig. 4.S2E, F), and pre-hypertrophic chondrocytes labeled by *Ihh* RNA staining was also unaffected in both control and mutant limbs (Fig. 4.S2G, H).



Supplementary Figure 4.S2. Deletion of *Foxc1* and *Foxc2* did not block chondrogenesis.

Endochondral ossification was examined on E15.5 through IF of SOX9 (A, B), SOX6 (C, D) that label the resting zone and columnar chondrocytes respectively and RNA scope ISH of *Fgfr3* (E, F) that mark the columnar chondrocytes and *Ihh* (G, H) in the pre-hypertrophic chondrocytes. Staining indicates the formation of all growth plate chondrocytes in both control and *Prx1-cre;Foxc1<sup>Δ/Δ</sup>;Foxc2<sup>Δ/Δ</sup>* limbs at E15.5.(n=3)

The organization of the growth plate was restored in the *Prx1-cre;Foxc1<sup>Δ/Δ</sup>;Foxc2<sup>Δ/Δ</sup>* mice by E16.5 . *Fgfr1* and *Fgfr3* mRNAs were detected in similar pattern in the resting zone and columnar chondrocytes, respectively in both control and mutant growth plates (Fig. 4.5A-D). *Ihh* mRNA and RUNX2 protein were similarly localized to the pre-hypertrophic chondrocyte zone in both control and mutant limbs (Fig. 4.5E-H). However, some RUNX2 signal was detected in the hypertrophic chondrocytes in the E16.5 *Prx1-cre;Foxc1<sup>Δ/Δ</sup>;Foxc2<sup>Δ/Δ</sup>* growth plate but not in the controls (Fig. 4.5E, F). COLX IF revealed an expanded hypertrophic chondrocyte zone in the absence of *Foxc1* and *Foxc2* (Fig. 4.5I, J). However this expansion was not a result of increased expression as *Colx* mRNA levels were similar in both the control and the *Prx1-cre;Foxc1<sup>Δ/Δ</sup>;Foxc2<sup>Δ/Δ</sup>* hypertrophic zone (Fig. 4.5K, L). Rather, these findings suggest that COLX protein level were persistent in *Prx1-cre;Foxc1<sup>Δ/Δ</sup>;Foxc2<sup>Δ/Δ</sup>* likely from impaired hypertrophic chondrocyte turn over.

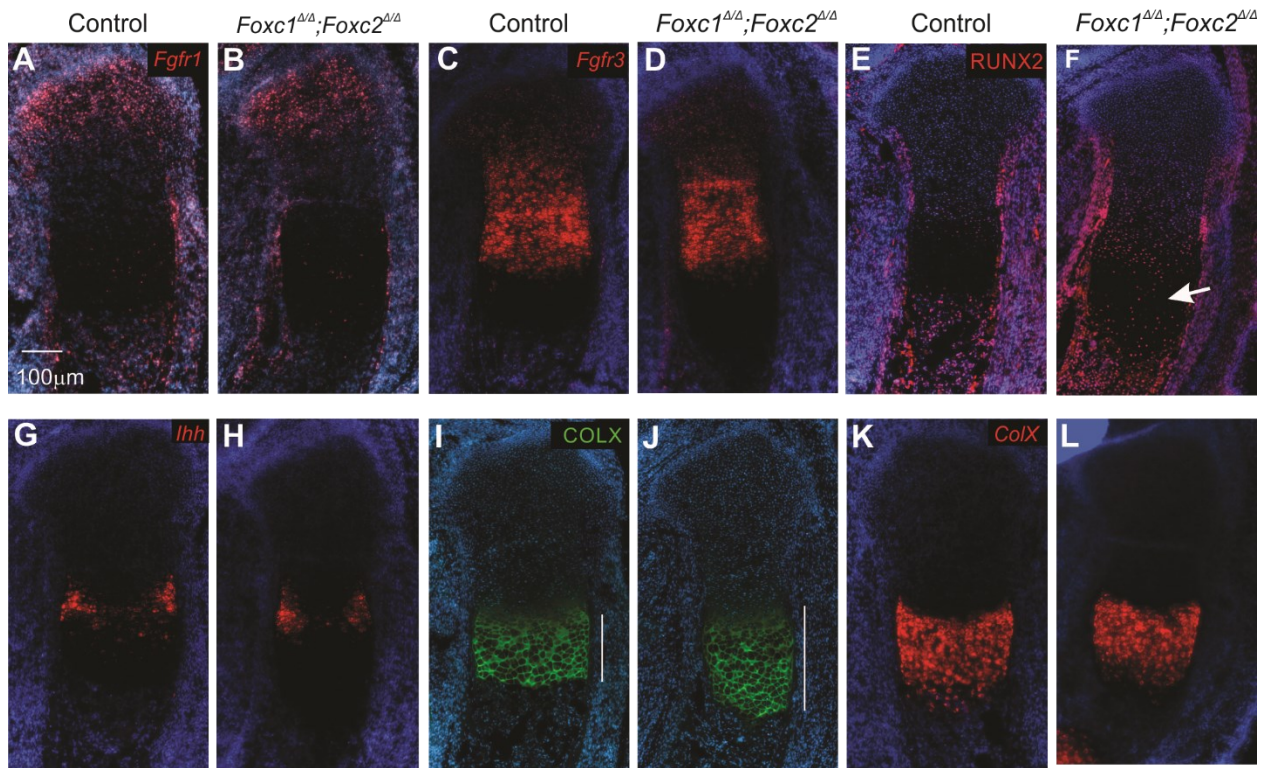


Figure 4.5. Early deletion of *Foxc1* and *Foxc2* disrupted terminal endochondral ossification process.

Endochondral ossification was examined on E16.5 using IF or RNA scope ISH of specific markers of each stage of chondrocyte proliferation in the growth plate. RNA scope ISH of *Fgfr1* (Resting zone) (A, B), *Fgfr3* (columnar chondrocytes) (C, D). RNA scope ISH of *Ihh* plus IF of RUNX2 (pre-hypertrophic chondrocytes) (E-H), COLX (hypertrophic chondrocytes) (I, J) and RNA scope ISH of *Colx* (K, L) was conducted on control and *Prx1-cre;Foxc1<sup>Δ/Δ</sup>;Foxc2<sup>Δ/Δ</sup>* E16.5 tibia. (n=3)

#### 4.4.5 Entry and exit from chondrocyte hypertrophy is delayed in *Prx1-cre;Foxc1<sup>Δ/Δ</sup>;Foxc2<sup>Δ/Δ</sup>* mice.

In the *Prx1-cre;Foxc1<sup>Δ/Δ</sup>;Foxc2<sup>Δ/Δ</sup>* tibia, we saw a reduction in proliferation of columnar chondrocytes, the formation of smaller *Ihh*-expressing pre-hypertrophic chondrocyte zone at E14.5, and the expansion of the hypertrophic chondrocytes zone at E16.5. These findings suggested that the pace (or the flow) of the embryonic endochondral ossification process was altered in *Prx1-cre;Foxc1<sup>Δ/Δ</sup>;Foxc2<sup>Δ/Δ</sup>* mice. Specifically, these results point to a primary defect in terminal differentiation and ossification. Thus, we decided to track the chondrogenic differentiation progression in the growth plate by labeling the growth plate with COL2 and COLX via IF at early, middle, and late stages of the endochondral ossification process. COL2 localization indicated no differences in the resting and proliferative chondrocyte zone lengths between the control and *Prx1-cre;Foxc1<sup>Δ/Δ</sup>;Foxc2<sup>Δ/Δ</sup>* growth plates (Fig. 4.S3A-P). However, COLX localization showed a reduction in the hypertrophic chondrocyte zone at E14.5 and E15.5 in *Prx1-cre;Foxc1<sup>Δ/Δ</sup>;Foxc2<sup>Δ/Δ</sup>* tibia (Fig. 4.6A-F). At later ages we observed an expansion of the proximal and distal hypertrophic chondrocyte domains at E16.5 and E17.5 compared to the control limbs (Fig. 4.6G-O). Further, the primary ossification center (POC), located between the two extended hypertrophic chondrocyte domains, at E16.5 and E17.5 was much smaller in *Prx1-cre;Foxc1<sup>Δ/Δ</sup>;Foxc2<sup>Δ/Δ</sup>* limbs compared to the widely formed POC in control limbs (Fig. 4.6G-P). These data suggest that absence of *Foxc1* and *Foxc2* in chondrocytes caused a delayed entry into hypertrophy followed by a delayed exit, which led to the formation of a smaller primary ossification center.



Supplementary Figure 4.S3. Absence of *Foxc1* and *Foxc2* did not alter the developmental rate of COL2 Positive chondrocytes in the growth plate.

IF of COL2 (red) and COLX (green) were conducted on control and *Prx1-cre;Foxc1<sup>Δ/Δ</sup>;Foxc2<sup>Δ/Δ</sup>* tibia at different time points. COL2 area (red) was measured and plotted. E14.5 (A-D), E15.5 (E-H), E16.5 (I-L) and E17.5 (M-P). length of COL2 positive area of the growth plate did not significantly changed between the control and *Prx1-cre;Foxc1<sup>Δ/Δ</sup>;Foxc2<sup>Δ/Δ</sup>* growth plates. 1-COL2-positive immature chondrocytes proximal domain (1-COL2-PD), 2-COL2-positive immature chondrocytes distal domain (2-COL2-DD). Statistic was done using student t-test via Sigma Plot 13. (n=4).

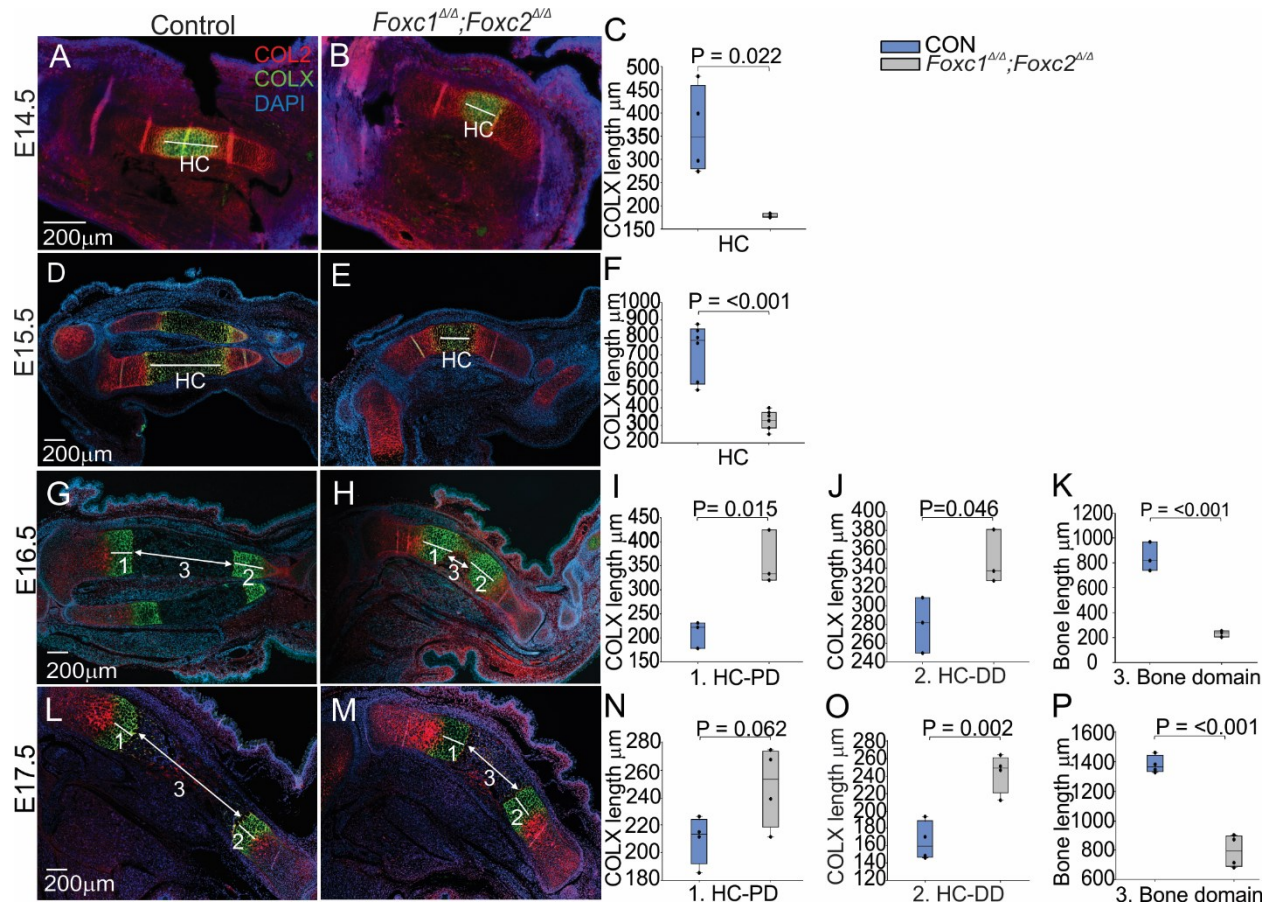


Figure 4.6. Early *Foxc1* and *Foxc2* deletion caused a delay in entry and exit from hypertrophy, causing formation of a small primary ossification center at later time points. Developmental rate of the proliferative and the hypertrophic chondrocytes was measured through IF staining of COL2 (red) to mark the resting and the proliferative chondrocytes and with COLX (green) to mark the hypertrophic chondrocytes at different time points. the length of COLX positive regions and bone sizes were measured and plotted at E14.5 (A-C), E15.5 (D-F), E16.5 (G-K) and E17.5 (L-P). Measurements showed reduced size of hypertrophy at E14.5 and E15.5 *Prx1-cre;Foxc1<sup>Δ/Δ</sup>;Foxc2<sup>Δ/Δ</sup>* tibia that followed by a sudden expansion of COLX positive hypertrophic domain at E16.5 and E17.5. 1-Hypertrophic chondrocytes proximal domain (1-HC-PD), 2-COLX-positive Hypertrophic chondrocytes distal domain (2-HC-DD). 3- Bone domain/primary ossification center. Statistic was done using student t-test via Sigma Plot 13. (n=4).

To test whether the expansion of the hypertrophic chondrocytes in *Prx1-cre;Foxc1<sup>Δ/Δ</sup>;Foxc2<sup>Δ/Δ</sup>* mice was due to changes in cellular death, we performed terminal deoxynucleotidyl transferase dUTP nick end labeling (TUNEL) *in situ hybridization* (TUNEL) at E15.5 and E16.5. At E15.5, Apoptosis was detected in a population of cells adjacent to the perichondrium bordering the hypertrophic chondrocytes in both control and mutant limbs (white arrow) (Fig. 4.7A, B). But, cell death was not detected within the growth plate chondrocytes (yellow asterisk) (Fig. 4.7A, B). This finding indicates that the delay in entry into hypertrophy was as a result of reduced chondrocytes proliferation and not increased apoptosis. At a later stage, apoptosis activity was found among the perichondrium, osteochondral junction and POC cell population (green asterisk) (Fig. 4.7C). However, in *Prx1-Cre* mutant limbs, cell death was only detected in the perichondrium and the small POC projecting from the perichondrium and periosteum cell population, with no staining identified within the expanded hypertrophic chondrocyte (green asterisk) (Fig. 4.7D), which suggests that hypertrophic chondrocytes remodeling was compromised by the absence of *Foxc1* and *Foxc2*.

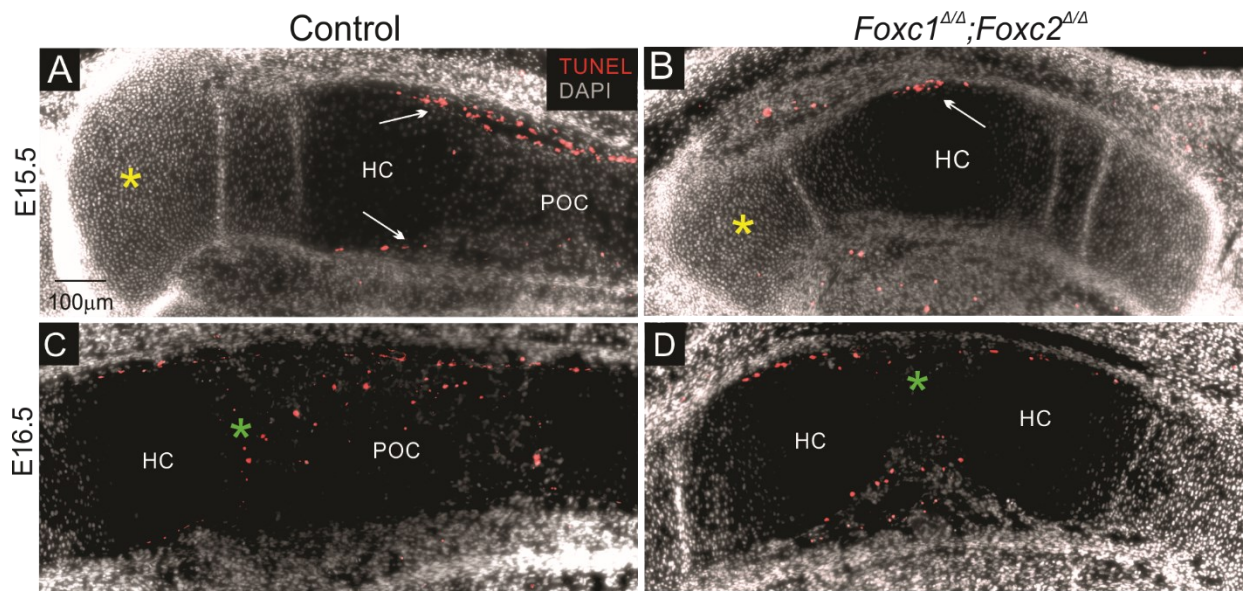


Figure 4.7. *Foxc1* and *Foxc2* KO did not promote cellular apoptosis within the growth plate chondrocytes.

TUNEL ISH was performed in E15.5 and E16.5 control and *Prx1-cre;Foxc1<sup>Δ/Δ</sup>;Foxc2<sup>Δ/Δ</sup>* tibia.

E15.5 limbs showed distinctive apoptosis activity in a cell population adjacent to the perichondrium and the periosteum (white arrows). However, no cell death was detected in the growth plate chondrocytes in both control and *Prx1-cre* mutant limbs (yellow asterisk) (A, B).

E16.5 control limbs displayed cellular apoptosis within the osteochondral junction and the developed POC (green asterisk) (C). But no cellular death was detected within the expanded hypertrophic zone in our mutants (green asterisk) (D). (n=3)

#### 4.4.6 *Foxc1* and *Foxc2* are required for proper mineralization and bone formation

We wanted to know if absence of *Foxc1* and *Foxc2* have an effect on bone mineralization or formation. Thus, we assess mineralization in tibia limb through Alcian blue-Von Kossa staining and IF of mineralization markers COL1, MMP13 and osteoblasts formation markers via OSX IF at E15.5, E16.5 and E17.5. E15.5 tibia showed a distinctive mineralization marked by MMP13 in the center of the limb, and COL1 lining the bone collar (Fig. 4.8A), in addition to the black Von Kossa staining lines (Fig. 4.8C). Moreover, OSX labeled osteoblasts were also detected in the pre-hypertrophic chondrocytes and the newly formed POC, indicating bone formation in the center of the control limb (Fig. 4.8B). In contrast, mutant limbs showed reduced COL1 staining, absence of MMP13 and OSX localization (Fig. 4.8D, E). In addition, black Von Kossa staining was not detected in E15.5 *Prx1-cre;Foxc1<sup>Δ/Δ</sup>;Foxc2<sup>Δ/Δ</sup>* (Fig. 4.8F). At E16.5 control limbs exhibited mineralization and bone formation localization as evidenced by MMP13, COL1 and Von Kossa staining within the periosteum and the osteochondral junction (Fig 4.8G-I). Moreover, OSX evenly marked the pre-hypertrophic chondrocytes and osteoblast in the POC and the periosteum (Fig. 4.8H). However, mineralization and bone formation was disrupted in *Prx1-cre;Foxc1<sup>Δ/Δ</sup>;Foxc2<sup>Δ/Δ</sup>* limbs, that was indicated by the disrupted localization of COL1, MMP13, the reduction of OSX staining in the center of the growth plate (yellow asterisk), with OSX positive osteoblasts located only in the periosteum (white arrows) (Fig. 4.8J, K). In addition, Von Kossa staining revealed mineralized hypertrophic chondrocyte and asymmetrical black staining within the bone collar (black arrow), in addition to reduced mineralization in the POC. (Fig. 4.8L). At E17.5 the control limbs showed an overlapping distribution of MMP13 and COL1 proteins in the POC (Fig. 4.8M). Moreover, Von Kossa staining marked regular mineralization within osteochondral junction, periosteum, and POC (Fig. 4.8O). We also detected osteoblast formation through OSX localization

in the POC of the E17.5 control limbs. (Fig. 4.8N) Mineralization continued to be reduced in *Prx1-cre;Foxc1<sup>Δ/Δ</sup>;Foxc2<sup>Δ/Δ</sup>* limbs at late stage of E17.5, where MMP13, COL1 and Von Kossa staining were reduced (Fig. 4.8P, R). Furthermore, POC marked by OSX was smaller than the control (Fig. 4.8Q). Interestingly, OSX staining of control E17.5 POC showed formation of the marrow space in the control POC (Fig. 4.8N). The small *Prx1-cre;Foxc1<sup>Δ/Δ</sup>;Foxc2<sup>Δ/Δ</sup>* bone area on the other hand exhibited more compacted osteoblasts cells marked by OSX with less marrow space in the POC (Fig. 4.8Q). Collectively, these data revealed that *Foxc1* and *Foxc2* are essential for proper mineralization and formation of osteoblasts in the trabecular bone.

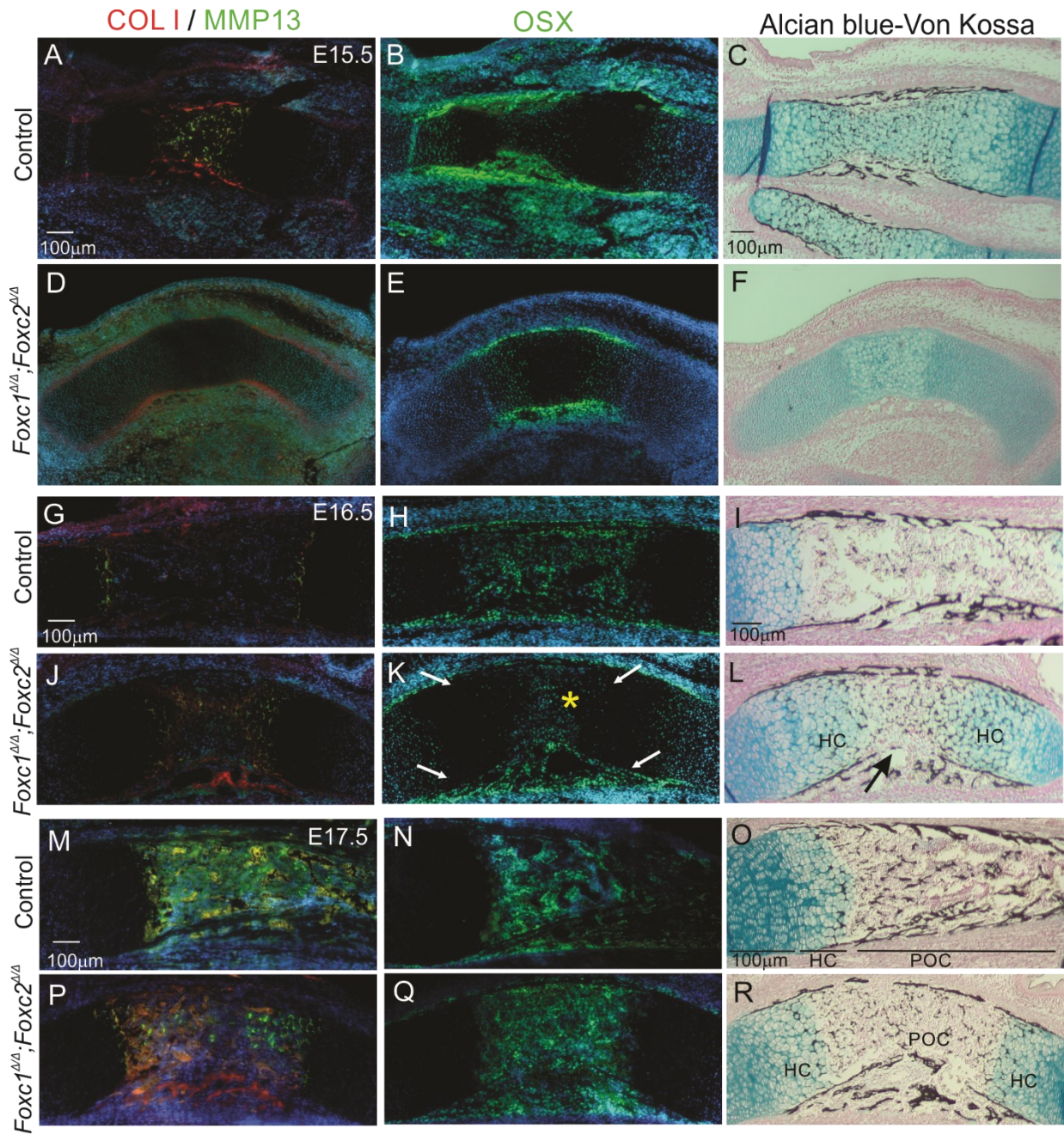


Figure 4.8. Lack of *Foxc1* and *Foxc2* affected endochondral mineralization and bone formation. Mineralization and bone formation were tested via Alcian blue Von Kossa staining and IF of mineralization (MMP13) and bone formation markers (COL1, and OSX) at E15.5, E16.5 and E17.5. E15.5 control tibia showed normal mineralization and localization of bone formation markers (A-C). However, we did not detect any sign of mineralization or bone formation in the *Prx1-cre;Foxc1<sup>Δ/Δ</sup>;Foxc2<sup>Δ/Δ</sup>* at the same time point (D-F). E16.5 control tibia exhibited normal localization of MMP13 within the mature hypertrophic chondrocytes, COL1 in the periosteum and the POC that hosted OSX positive osteoblasts as well. Alcian blue Von Kossa staining revealed red mineralized hypertrophic chondrocytes with reduced and asymmetric mineralization in the POC (black arrow). Additionally, weaker COL1 and OSX signal was detected in the center of the POC (yellow asterisk), and strong signal in the perichondrium (white arrows) of the E16.5 *Prx1-cre;Foxc1<sup>Δ/Δ</sup>;Foxc2<sup>Δ/Δ</sup>* limb (J-L). E17.5 control limb exhibited a characteristic localization of MMP13, COL1, OSX and black mineralization staining in the POC (M-O). Yet, *Prx1-cre;Foxc1<sup>Δ/Δ</sup>;Foxc2<sup>Δ/Δ</sup>* limbs continues to show less mineralization staining, with reduced COL1 MMP13 and OSX staining within the small POC (P-R).(N=3)

#### 4.4.7 Bone remodeling was compromised by the absence of *Foxc1* and *Foxc2* in long bones

Since the formation of the POC was disrupted in *Prx1-cre;Foxc1<sup>Δ/Δ</sup>;Foxc2<sup>Δ/Δ</sup>* mutants, we examined whether impaired bone remodeling or vascularization was responsible for the disrupted bone phenotype in the *Prx1-cre;Foxc1<sup>Δ/Δ</sup>;Foxc2<sup>Δ/Δ</sup>* limbs. We performed Tartrate-Resistant Acid Phosphatase (TRAP) staining to visualize osteoclasts in the POC of E16.5 and E17.5 control and *Prx1-cre;Foxc1<sup>Δ/Δ</sup>;Foxc2<sup>Δ/Δ</sup>* limbs. Both control and mutant limbs showed osteoclasts localization in the perichondrium, periosteum, and the osteochondral junction. However, there were fewer osteoclast cells in the *Prx1-Cre* mutants compared to the control limb at both time points (Fig. 4.9A-E). The low number of osteoclasts may cause slower bone resorption activity leading to reduced bone remodeling and formation of shorter limbs in our mutants (Lademann et al., 2020). We then tested the expression of *Tnfsf11* mRNA (RANKL) using RNA scope ISH. Expression of *Tnfsf11* was detected in both control and *Prx1-Cre* mutant limbs, But, its expression region was much smaller in the *Prx1-cre;Foxc1<sup>Δ/Δ</sup>;Foxc2<sup>Δ/Δ</sup>*, owing to the reduction of osteoblast formation in E16.5 mutant limb compared to the control (Fig. 4.9F, G). E16.5 control tibia showed normal localization of *Fgfr1* RNA signal in the POC (Fig. 4.9 H, I). But, *Prx1-cre;Foxc1<sup>Δ/Δ</sup>;Foxc2<sup>Δ/Δ</sup>* POC displayed a reduced *Fgfr1* expression, which might be another reason behind the low number of osteoclasts, since *Fgfr1* was reported to play a role in osteoclasts differentiation and activation (Lu et al., 2009).

Angiogenesis and blood vessel invasion of the POC are necessary for bone formation (Sivaraj and Adams, 2016). Thus, we next assessed vascularization by monitoring expression of *Vegfa* mRNA and localization of the vascular endothelial marker isolectin-B4 (IB4) (Gerber et al.,

1999; Weinman et al., 2014; Zelzer et al., 2004). *Vegfa* mRNA localized in the hypertrophic chondrocytes in both control and the *Prx1-cre* mutant limbs, with more *Vegfa* signal marking the extended hypertrophic chondrocytes zone in the *Prx1-cre;Foxc1<sup>Δ/Δ</sup>;Foxc2<sup>Δ/Δ</sup>* E16.5 tibia (Fig. 4.9J, K). Moreover, IB4 localization confirmed the presence of blood vessels in both E17.5 control and mutant bones (Fig. 4.9L, M). Collectively, these results showed that deletion of *Foxc1* and *Foxc2* did not block bone vascularization. However, both *Foxc* genes have an essential role in facilitating osteoclasts differentiation and activation for proper bone formation and resorption.

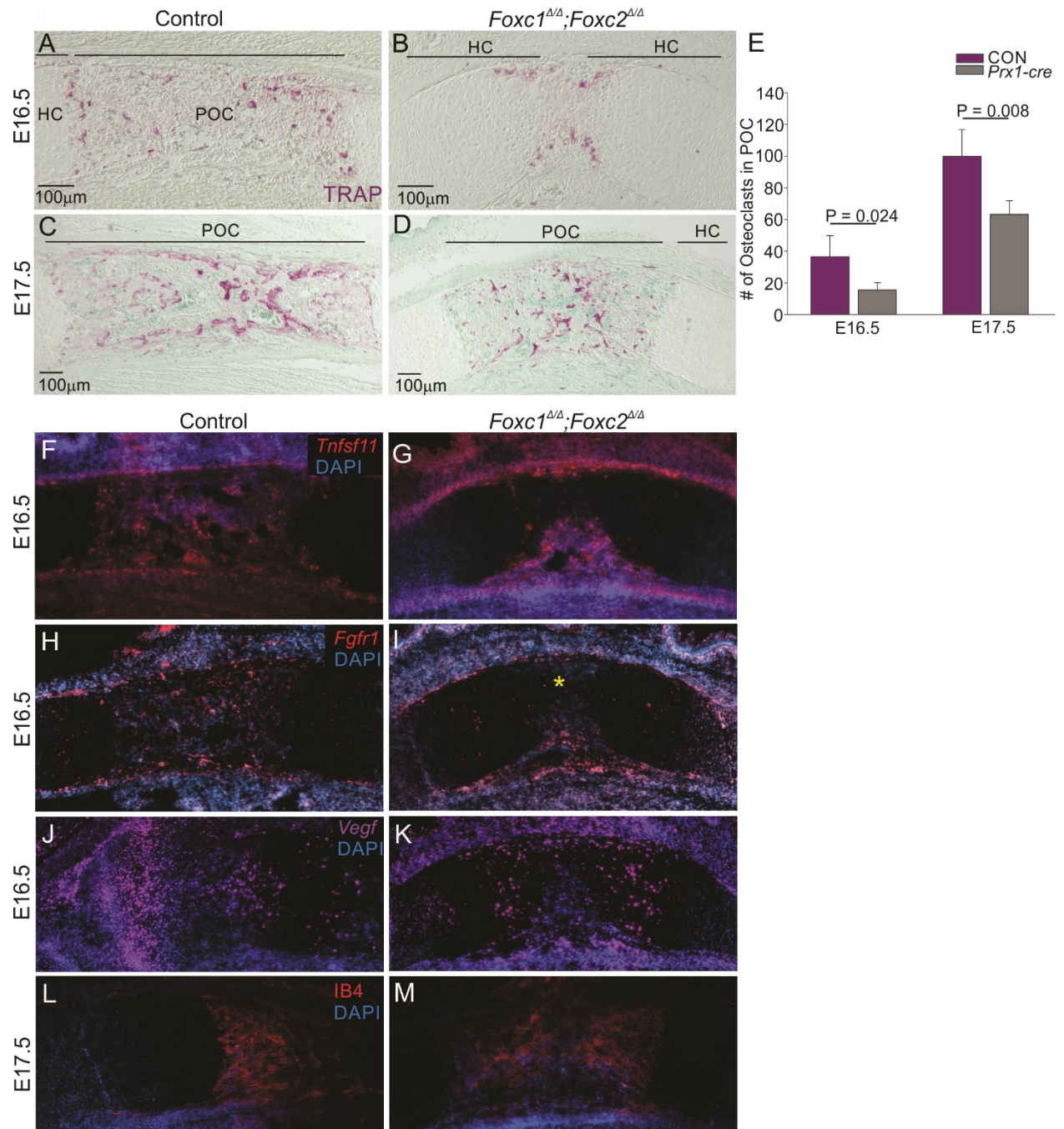


Figure 4.9. Absence of *Foxc1* and *Foxc2* in the lateral plate mesoderm had a detrimental effect on bone remodeling process.

TRAP staining was performed on E16.5 (A, B) and E17.5 (C, D) control and *Prx1-cre;Foxc1<sup>Δ/Δ</sup>;Foxc2<sup>Δ/Δ</sup>* tibia to assess osteoclast localization in the primary ossification center. Staining showed a widespread distributed multinucleated cell in the control POC(A). In contrast, our mutant limbs showed disrupted localization of osteoclasts in E16.5 mutant bone where they mainly localized at the bone collar (B). At E17.5, osteoclasts had a comparable distribution pattern throughout the POC in both control and mutant limbs (C, D). Statistical analysis showed fewer multinucleated cells in the *Prx1-cre;Foxc1<sup>Δ/Δ</sup>;Foxc2<sup>Δ/Δ</sup>* limb at E16.5 and E17.5 in comparison to their controls (E). RNA scope ISH showed localization of *Tnfsf11* in the control POC and within the small POC developed in the *Prx1-cre;Foxc1<sup>Δ/Δ</sup>;Foxc2<sup>Δ/Δ</sup>* limb. (F, G). *Fgfr1* RNA signal showed a comparable localization of both E16.5 control and *Prx1-cre* limbs. But with much less RNA signal within the mutant POC (yellow star) (H, I). Both control and mutant limbs exhibited comparable localization of *Vegfa* (J, K). IB4 was detected in both E17.5 control and *Prx1-cre;Foxc1<sup>Δ/Δ</sup>;Foxc2<sup>Δ/Δ</sup>* POC (L, M). Statistic was done using student t-test via Sigma Plot 13. (n=3).

#### 4.4.8 *Foxc1* is required for *Phex* expression to maintain bone mineralization

We then wanted to further investigate the reason behind the reduction in mineralization and osteogenic differentiation in our mutants. OPN is a glycoprotein that marks osteoblasts, osteocytes, and osteoclasts in bone, and is encoded by the *SPP1* gene (Q. Chen et al., 2014). This protein is rich with negatively charged cell binding arginine-glycine-aspartic acid (RGD) amino acid sequence (Zurick et al., 2013). We detected OPN localization in the bone collar and the primary ossification center in both control and *Prx1-cre;Foxc1<sup>Δ/Δ</sup>;Foxc2<sup>Δ/Δ</sup>* limbs (Fig. 4.10A-D). However, there were more intense OPN signal located within the small POC in our mutant limbs at E16.5 and E17.5 (Fig. 4.10B, D). OPN is a substrate for different enzymes such as the Phosphate regulating endopeptidase homolog X-linked (PHEX). PHEX is an enzyme that binds to OPN with high affinity and stimulate it for degradation to regulate bone mineralization (Addison et al., 2010). We identified *Phex* mRNA signal within the control POC in both time points (Fig. 4.10E-G). On the other hand, *Prx1-cre;Foxc1<sup>Δ/Δ</sup>;Foxc2<sup>Δ/Δ</sup>* bones showed a reduction in *Phex* expression (Fig. 4.10F, H), which explained the increase in OPN intensity (Fig. 4.10B, D). We then wanted to test if *Foxc1* co-expressed with *Phex* in the same cells. ISH demonstrated overlapping expression for both *Foxc1* and *Phex* in the POC at E16.5 and E17.5 in control limbs (Fig. 4.10M, O). On the other hand, no expression of either *Foxc1* or *Phex* mRNA was detected in the *Prx1-cre;Foxc1<sup>Δ/Δ</sup>;Foxc2<sup>Δ/Δ</sup>* bone (Fig. 4.10N, P). These results indicate that *Foxc1* and *Foxc2* are required for the expression of *Phex* in the POC, and that reduced *Phex* expression may lead to improper processing of OPN and inhibition of mineralization in *Prx1-cre;Foxc1<sup>Δ/Δ</sup>;Foxc2<sup>Δ/Δ</sup>* mutants.

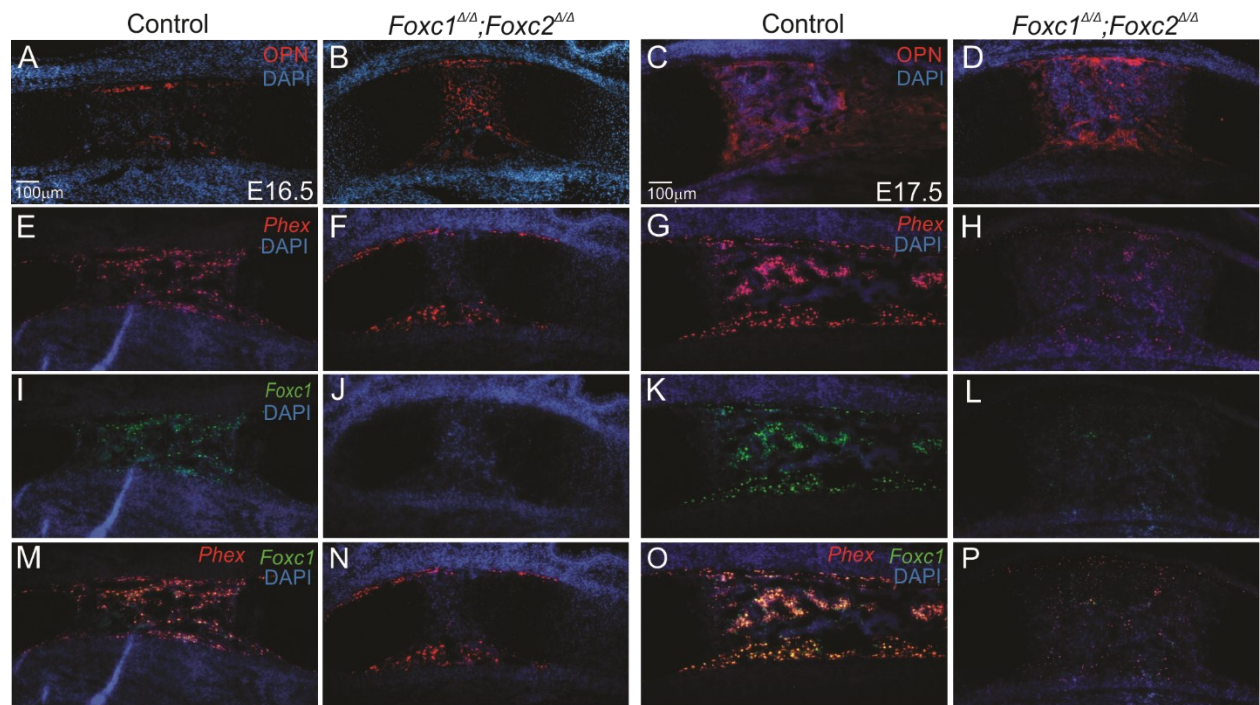


Figure 4.10. *Phex* expression was compromised by the absence of *Foxc1* and *Foxc2*.

Reduction of mineralization was investigated via IF of OPN and RNA scope ISH of *Phex* in E16.5 and E17.5 control and *Prx1-cre;Foxc1<sup>Δ/Δ</sup>;Foxc2<sup>Δ/Δ</sup>* tibia. E16.5 and E16.6 control limbs showed a regular OPN localization within the POC (A, C). However, mutant limbs exhibited a more intense OPN signal at both time points (B, D). E16.5 and E17.5 control limbs exhibited normal *Phex* expression within the POC (E, G). But, less *Phex* RNA signal was detected within the POC at both time points of the *Prx1-cre;Foxc1<sup>Δ/Δ</sup>;Foxc2<sup>Δ/Δ</sup>* tibia (F, H). Co-expression of *Foxc1* and *Phex* was tested via RNA scope ISH. E16.5 and E17.5 Control limbs showed localization of *Foxc1* RNA within the POC (I, K). In contrast, *Foxc1* expression was absent at E16.5 (J) and reduced at E17.5 in our mutant limbs (L). Both control and *Prx1-cre;Foxc1<sup>Δ/Δ</sup>;Foxc2<sup>Δ/Δ</sup>* bone exhibited co-expression of both *Foxc1* and *Phex* mRNAs (M, O). Yet, both *Foxc1* and *Phex* mRNA signals were reduced in our *Prx1-Cre* mutant limbs at E16.5 and E17.5 (N, P). (n=3).

## 4.5 Discussion:

To understand how *Foxc1* and *Foxc2* control early steps of endochondral ossification, we generated a number of conditional *Foxc1* and *Foxc2* double homozygous mutants. First using *Sox9ires-Cre* to delete *Foxc1* and *Foxc2* in prechondrogenic progenitor cells, and then using *Prx1-cre* to delete *Foxc1* and *Foxc2* in limb bud Osteochondral progenitors. We demonstrated that *Foxc1* and *Foxc2* genes regulate different stages of long bone development. Although deletion of both genes in these lineages did not prevent chondrogenesis, it did lead to delayed or reduced chondrocyte differentiation. *Prx1-cre;Foxc1<sup>Δ/Δ</sup>;Foxc2<sup>Δ/Δ</sup>* embryos displayed short, bent limbs with smaller bone eminences. Our data showed that absence of both *Foxc* genes can reduce chondrocytes proliferation at E14.5 leading to a delayed entry into hypertrophy. At later ages, the *Prx1-cre;Foxc1<sup>Δ/Δ</sup>;Foxc2<sup>Δ/Δ</sup>* model showed impaired hypertrophic chondrocytes remodeling and disrupted mineralization. Finally, our work revealed that expression of *Phex* in the POC was dependent on *Foxc1* and *Foxc2* function, and that reduced *Phex* expression altered OPN processing and impair bone mineralization. Collectively, this study indicates that *Foxc1* and *Foxc2* are required for long bone endochondral ossification.

### 4.5.1 *Foxc1* compensate for the deletion of *Foxc2* and vice versa in skeletal development.

*Foxc1* and *Foxc2* mRNAs are co-expressed in the condensing mesenchyme and growth plate chondrocytes in embryonic limbs with distinctive expression of *Foxc1* or *Foxc2* in some regions of the growth plate (Almubarak et al., 2021). Deletion of either *Foxc1* or *Foxc2* in mice lead to skeletal phenotypes that mainly affect the axial skeleton compared to that seen in the appendicular skeleton (Hong et al., 1999; Kume et al., 1998; Winnier et al., 1997). Conditional

deletion of both *Foxc* genes in *Col2-cre*-expressing chondrocytes disrupted endochondral ossification events but again preferentially affected the axial skeleton (Almubarak et al 2021). Here we showed that conditional deletion of *Foxc1* and *Foxc2* from the condensing mesenchyme using the *Sox9-cre* derive resulted in impaired formation of cartilaginous elements in the mouse skeleton at E12.5 in a dose dependent manner. These findings indicate a compensation between *Foxc1* and *Foxc2* in endochondral bone development.

#### 4.5.2 *Foxc1* and *Foxc2* function in the limb skeleton preferentially in the distal vs proximal elements

*Prx1-cre;Foxc1<sup>Δ/Δ</sup>;Foxc2<sup>Δ/Δ</sup>* forelimbs and hindlimbs exhibited an increase in phenotype severity in the distal skeletal elements compared to the proximal ones of the long bones. We observed a pronounced reduction in the thickness of autopod bone elements compared to the control (Fig. 4.1D). Moreover, Safranin O staining indicated a reduction in chondrocytes formation in autopod compared to the zeugopod and stylopod. *Foxc1* and *Foxc2* expression varied spatially throughout the limb, with elevated *Foxc1* and *Foxc2* expression levels detected in the autopod compared to the stylopod and the zeugopod (Fig. 4.2C-F) (Almubarak et al., 2021). These results indicate that both *Foxc1* and *Foxc2* are required for chondrogenesis with preferential function within the distal bone elements than the proximal.

#### 4.5.3 *Foxc1* and *Foxc2* are required at different stages of endochondral ossification

We showed that *Foxc1* and *Foxc2* expression patterns change over time during the process of endochondral ossification. *Foxc1* and *Foxc2* mRNAs localize in the pre-and early hypertrophic chondrocytes at E14.5. However, at E16.5 *Foxc1* and *Foxc2* expression is reduced in the growth plate and become concentrated in the perichondrium and POC (Almubarak et al 2021). At E14.5, *Prx1-cre;Foxc1<sup>Δ/Δ</sup>;Foxc2<sup>Δ/Δ</sup>* limb displayed a shorter *Ihh* expression domain that marked the pre-and early hypertrophic chondrocytes, which lead to limited IHH signaling to stimulate columnar chondrocyte proliferation (Joeng and Long, 2009; Yoshida et al., 2015). As a result, the columnar chondrocytes showed a reduced number of Ki67 positive cells in the *Prx1-Cre* mutant compared to control at E14.5. This effect become less pronounced over time as *Ihh* expression pattern were normalized when *Foxc1* and *Foxc2* expression weakened within the hypertrophic chondrocytes at E15.5 E16.5, consistent with a stage specific role for *Foxc1* and *Foxc2* in limb endochondral ossification. These results suggest that *Foxc1* and *Foxc2* have stage specific functions during growth plate development. For example, they regulate chondrocyte differentiation towards the initial of hypertrophic chondrocytes population at E14.5, but is no longer required at subsequent stages as indicated by the restoration of growth plate chondrocyte expression patterns observed in *Prx1-cre;Foxc1<sup>Δ/Δ</sup>;Foxc2<sup>Δ/Δ</sup>* embryos at E15.5 and E16.5. This notion may also explain why *Foxc1* and *Foxc2* have profound effects on *in vitro* chondrocyte differentiation models as these systems may not recapitulate the waves of chondrogenic differentiation occurring in a tissue (Yoshida et al 2015; Almubarak et al., 2021).

As expression of *Foxc1* and *Foxc2* decline in the growth plate chondrocytes after E14.5, it is possible that other transcription factors, potentially FOXA factors, may drive subsequent

chondrocyte differentiation after this time (Ionescu et al., 2012b). It is also possible that some skeletal elements were more sensitive to *Foxc1* and *Foxc2* loss such as the autopod and vertebrae may not be able to compensate for this initial impairment in HC differentiation.

Interestingly, unlike control limbs, the *Prx1-cre;Foxc1<sup>Δ/Δ</sup>;Foxc2<sup>Δ/Δ</sup>* limbs showed a persistence of SOX9 positive cells in the pre-hypertrophic chondrocytes at E15.5 and RUNX2 positive hypertrophic chondrocytes at E16.5. This aberrant expression pattern may indicate a stalled progression of growth plate differentiation events leading to the persistence of immature chondrocytes in the hypertrophic chondrocytes zone.

Expression of *Pthlh* (PTHrP) within the resting zone was comparable in both control and *Prx1-cre;Foxc1<sup>Δ/Δ</sup>;Foxc2<sup>Δ/Δ</sup>* growth plate. This finding did not support another study that suggest that FOXC1 directly regulates PTHrP in chondrocytes (Yoshida et al., 2015). There were some differences between the two studies. We identified localization of *Pthlh* RNA within the resting zone in mice growth plate. But the other group findings were based on an *ex vivo* work. In their study, they identified a reduction in *Pthlh* expression level when *Foxc1* was deleted. Moreover, they detect FOXC1 binding to the *Pthlh* promoter through performing DNA-pull down and ChIP assays on primary chondrocytes. There are different explanations for having two contradictory findings. One thing is that reduction in *Pthlh* expression in *Foxc1<sup>ch/ch</sup>* chondrocytes does not imply a direct association between the two genes. It is possible that *Pthlh* RNA level was compromised by the disrupted IHH-GLI2 signaling pathway in the absence of FOXC1 from the growth plate. Moreover, presence of FOXC1 binding site in the *Pthlh* promoter does not necessarily mean that FOXC1 is directly binding to it during endochondral ossification. Another explanation is that

another FOX transcription factor/s can also bind and regulate the *Pthlh* promoter in the growth plate, and it compensates for the absence of FOXC1 in our *Prx1-cre;Foxc1<sup>Δ/Δ</sup>;Foxc2<sup>Δ/Δ</sup>* model. More investigation needs to be done to understand this complex association between the two genes. For example, *Foxc1* effect on *Pthlh* functional activity can be tested using Dual luciferase assay in chondrocytes. FOXC1 direct binding to the *Pthlh* promoter can be verified via electrophoresis mobility shift assay (EMSA). Other FOX transcription factors that are believed to be involved in chondrogenesis can also be tested to assess their compensation when *Foxc1* is deleted.

Our analysis of *Prx1-cre;Foxc1<sup>Δ/Δ</sup>;Foxc2<sup>Δ/Δ</sup>* indicates an important role for *Foxc1* and *Foxc2* in coordinating the progression through chondrocyte hypertrophy and formation of the POC. *Prx1-cre;Foxc1<sup>Δ/Δ</sup>;Foxc2<sup>Δ/Δ</sup>* tibia revealed an expansion of mineralized hypertrophic chondrocytes at later time points marked by Alcian blue Von-kossa staining, MMP13 and *Vegfa*, that were validated by the COLX measurements. This phenotype could be due to either increase in *Colx* expression, acceleration into chondrocytes hypertrophy or delay in exiting hypertrophy. RNA scope ISH showed unaffected *Colx* mRNA signal in *Prx1-cre;Foxc1<sup>Δ/Δ</sup>;Foxc2<sup>Δ/Δ</sup>* E16.5 growth plate, which made us exclude the first possibility. When we moved forward to tested chondrocytes proliferation at E16.5, we did not detect any increase in chondrocyte proliferation activity within the *Prx1-cre;Foxc1<sup>Δ/Δ</sup>;Foxc2<sup>Δ/Δ</sup>* growth plate compared to the control at E14.5. Moreover, COL2 positive cell measurements showed comparable COL2 domains size, that mark the resting zone and the columnar chondrocytes, between the control and *Prx1-Cre* mutant limbs at later time points. This analysis rules out the likelihood that the expansion of the hypertrophic chondrocytes in our mutant limbs was due to acceleration of hypertrophy. However, measurement of COLX positive chondrocytes at later time points of E16.5 and E17.5 displayed expanded hypertrophic chondrocytes domains with the formation of a very short primary ossification center

that was indicated by the reduction in the size of bone formation markers COL1, OSX and OPN in limbs during embryonic development. Interestingly, the TUNEL assay showed apoptosis activity within osteochondral junction of control limbs at E16.5. But, we did not detect any signal of cellular apoptosis within the expanded hypertrophic chondrocytes in the *Prx1-cre;Foxc1<sup>Δ/Δ</sup>;Foxc2<sup>Δ/Δ</sup>*. These results suggest that the change in *Foxc1* and *Foxc2* expression pattern over time, that started with broad localization at early time points to more restricted localization at later time points, is a key in controlling the entry and the exit of chondrocyte hypertrophy; and that early KO of *Foxc1* and *Foxc2* in the condensing mesenchyme may promoted hypertrophic maturation and disrupted hypertrophic chondrocytes remodeling, preventing their transitioning into osteoblasts during embryonic limb development.

In comparison to the well-developed POC in control limbs, *Prx1-cre;Foxc1<sup>Δ/Δ</sup>;Foxc2<sup>Δ/Δ</sup>* limbs exhibited a shorter POC, that highlighted the importance of *Foxc1* and *Foxc2* in bone formation. Localization of OSX, OPN and COL1 revealed a smaller POC in the absence of *Foxc1* and *Foxc2*. There are many factors that can contribute to this reduction in bone size. One possibility is the absence of angiogenesis; however, we were able to visualize vascularization markers such as *Vegfa* mRNA and IB4, a marker of vascular endothelial cells in both control and *Prx1-cre;Foxc1<sup>Δ/Δ</sup>;Foxc2<sup>Δ/Δ</sup>* limbs. Another possible reason is the terminal delay in endochondral ossification process and transitioning of hypertrophic chondrocytes into osteoblasts. Measurements of the COLX positive hypertrophic chondrocytes zones and the POC between the hypertrophic domains showed a delay in exit into hypertrophy, that highlighted the role of *Foxc1* and *Foxc2* in hypertrophic chondrocytes remodeling and formation of osteoblasts that was verified by OSX, OPN and COL1 IF staining of the *Prx1-cre;Foxc1<sup>Δ/Δ</sup>;Foxc2<sup>Δ/Δ</sup>* limbs. Unlike the abundant OSX signal that was distributed evenly throughout the control POC at E16.5, *Prx1-*

*cre;Foxc1<sup>Δ/Δ</sup>;Foxc2<sup>Δ/Δ</sup>* tibias exhibited restricted localization of OSX to a small population of cells arising from the bone collar. Such impaired in the development of the osteoblasts can compromise the availability of many important factors that are expressed by these cells and play a significant role in bone formation and remodeling. For instance, studies have shown that RANKL and FGFR1 are required to promote osteoclasts differentiation and activation that will maintain bone formation and remodeling (Boyce et al., 2009; Lu et al., 2009; Su et al., 2014). In comparison to the control limbs that showed evenly distributed *Tnfsf11*(RANKL) and *Fgfr1* mRNA within the POC, *Prx1-cre;Foxc1<sup>Δ/Δ</sup>;Foxc2<sup>Δ/Δ</sup>* limbs showed reduced expression of these genes. As a result, fewer osteoclasts were found within the poorly developed POC of *Prx1-cre;Foxc1<sup>Δ/Δ</sup>;Foxc2<sup>Δ/Δ</sup>* limbs compared to its E16.5 and E17.5 controls. Such irregularity in the osteoblasts and osteoclasts may affect bone formation and remodeling process. Consequently, long bones will fail to heal bone fractures or form enough marrow space to sustain vital erythropoietic activity.

#### 4.5.4 *Phex* expression is reduced in *Prx1-cre;Foxc1<sup>Δ/Δ</sup>;Foxc2<sup>Δ/Δ</sup>* limbs

Mineralization of the POC was disrupted in the *Prx1-cre;Foxc1<sup>Δ/Δ</sup>;Foxc2<sup>Δ/Δ</sup>* despite the formation of osteoblasts. We observed elevated levels of OPN in the POC at E16.5 and E17.5. Although OPN is produced in osteoblasts, this glycoprotein is proteolytically processed and degraded in order for mineralization to occur. OPN is a substrate for the PHEX which OPN and allows mineralization to proceed. *Phex* mutation was shown to cause the most common form of inherited hypophosphatemic rickets, A type of Rickets that does not respond to vitamin D treatment (Barros et al., 2013). Absence of such important enzyme leads to reduced reabsorption of phosphate in kidney in addition to its inability to cleave other mineral inhibitory proteins such

as OPN, causing its massive accumulation within the bone extracellular matrix (Addison et al., 2010; Barros et al., 2013; Zurick et al., 2013). We observed a reduced expression level of *Phex* in the POC of *Prx1-cre;Foxc1<sup>Δ/Δ</sup>;Foxc2<sup>Δ/Δ</sup>* mice. *Phex* mRNA levels were also reduced in the ribs from *Col2-cre;Foxc1<sup>Δ/Δ</sup>;Foxc2<sup>Δ/Δ</sup>* mice (Almubarak et al., 2021). *Phex* and *Foxc1* mRNA expression overlapped in the primary ossification center. Thus, the reduced mineralization we observed in these mutants may be the result of FOXC1 and FOXC2 regulating (directly or indirectly) *Phex* expression.

In this study, we deleted *Foxc1* and *Foxc2* in the condensing limb bud mesenchyme using the *Prx1-cre* transgene (Logan et al., 2002). *Prx1-cre;Foxc1<sup>Δ/Δ</sup>;Foxc2<sup>Δ/Δ</sup>* embryos did display a more pronounced limb phenotype compared with *Col2-cre;Foxc1<sup>Δ/Δ</sup>;Foxc2<sup>Δ/Δ</sup>* mutants. Deletion of *Foxc1* and *Foxc2* in *Col2-cre* expressing chondrocytes resulted in a more pronounced effect on the formation of the axial skeleton compared to the appendicular skeleton. The cervical vertebrae were absent, and mineralization of the thoracic and lumbar vertebrae were limited to rudimentary ossification centers (Almubarak et al., 2021). The limbs displayed a milder phenotype consisting of a smaller, disorganized growth plate and reduced mineralization. These milder limb phenotypes were surprising given the abundant expression of *Foxc1* and *Foxc2* in limb bud mesenchyme and chondrocytes (Almubarak et al., 2021; Yoshida et al., 2015). *Foxc1* and *Foxc2* were shown to regulate different stages of limb development. At early stages where they found to regulate *Ihh*-mediated proliferation and causes an overall delay in endochondral ossification process. This finding raises the question: could the effect we see in the spine be the result of *Foxc1* and *Foxc2* acting on the *Ihh* pathway and not being able to recover like the limb bones do? This

can be investigated through testing proliferation and apoptosis activity in control and mutant *Col2-cre;Foxc1<sup>Δ/Δ</sup>;Foxc2<sup>Δ/Δ</sup>* spine at early time points.

## **Chapter 5:**

### **Do *Foxc1* and $\beta$ -*Catenin* function together?**

#### **Contributions to the manuscript:**

This chapter is an original work performed by Asra Almubarak and Christi Li who contributed to the pulldown assay with Asra Almubarak. All experiments were supervised by Fred B Berry.

## **Do *Foxc1* and $\beta$ -*Catenin* function together?**

Asra Almubarak<sup>1</sup> and Christi Li<sup>1</sup>, Fred B Berry<sup>1,2</sup>

<sup>1</sup> Department of Medical Genetics, University of Alberta, Edmonton, Alberta, Canada

<sup>2</sup>Department of Surgery, University of Alberta, Edmonton, Alberta, Canada

## 5.1 Introduction:

In vertebrates, skeletal development proceeds through two essential mechanisms: endochondral or intramembranous ossification. Intramembranous ossification involves mesenchymal progenitors differentiating directly into osteoblasts to form bones such as the cranial bones of the skull, flat bones of the face and the clavicles (Franz-Odenaal, 2011). On the other hand, in endochondral ossification, mesenchymal progenitors first differentiate into chondrocytes to form a cartilaginous template. These chondrocytes then undergo several differentiation events to create four layers of an organized pattern of differentiating cells known as the growth plate. The first layer is called the resting zone, which is located at both ends of the bone and consists of chondrocyte progenitors that will differentiate into more flattened, highly organized proliferative chondrocytes. Columnar chondrocytes serve a role in maintaining longitudinal bone growth. Then, proliferative chondrocytes further differentiate into a third layer consisting of pre-hypertrophic cells, where they exit the cell cycle. Next, pre-hypertrophic chondrocytes will enlarge and mature to form hypertrophic chondrocytes. These hypertrophic chondrocytes secrete a mineralized matrix that helps establish the final bone properties. Finally, hypertrophic chondrocytes have been observed to either convert into osteoblasts or undergo apoptosis and be replaced with osteoblasts that form bone (Hu et al., 2017; Sun and Beier, 2014; Yang et al., 2014; Yeung Tsang et al., 2014).

Every stage of the endochondral ossification process occurs under a complex regulatory network by many signaling factors that involve specific transcription factors and signaling molecules. Maturation of any of these regulatory factors may negatively affect other downstream genes associated with endochondral limb development.

One transcription factor that has appeared as being an essential upstream regulator of endochondral skeletal development is FOXC1 transcription factor (Almubarak et al., 2021; Kume et al., 1998). *Foxc1* is a phosphoprotein transcription factor from the Forkhead family of genes, that contains a conserved 110 amino acid DNA binding domain called the Forkhead domain (Weigel and Jäckle, 1990). This domain consists of a helix-turn-helix core of four  $\alpha$ -helices, two anti-parallel  $\beta$ -sheets with the last one flanked by two loops that can bind and bend DNA (80–90°) to obtain stable DNA-protein binding (Berry et al., 2005; Saleem et al., 2004). Most Fox transcription factors including FOXC1 were reported to act as transcriptional activators. However, a few FOX factors showed a negative regulatory effect on their downstream target genes such as FOXD2, FOXD3 and XBF1(FOXG1) (Bourguignon et al., 1998; Freyaldenhoven et al., 1997; Sutton et al., 1996) .

$\beta$ -CATENIN, a transcription factor encoded by the *CTTNB1* gene, and a main central factor in the canonical Wnt/  $\beta$ -CATENIN signaling pathway, translocates to the nucleus after its activation to stimulate the expression of Wnt downstream target genes (Clevers, 2006; Dao et al., 2012; Maupin et al., 2013). This signaling mechanism activates when a WNT ligand binds to any associated transmembrane receptors Frizzled (Fzd), and receptors lipoprotein-related protein 5 and 6 (LRP-5 and LRP6). When WNT ligands are absent, a destruction complex forms that includes glycogen synthase kinase 3 $\beta$  (GSK3 $\beta$ ), adenomatosis polyposis coli (APC) and axin which binds to cytoplasmic  $\beta$ -CATENIN. This binding will contribute to  $\beta$ -CATENIN phosphorylation by GSK3 $\beta$  that will then trigger  $\beta$ -CATENIN ubiquitination and degradation (Clevers, 2006; MacDonald et al., 2009). However, when WNT ligand binds to its receptor, the destruction complex will not form, which allows the accumulation  $\beta$ -CATENIN and its translocation to the

nucleus to act as a co-activator of TCF/LEF transcription factors to stimulate the expression of WNT downstream target genes. WNT signaling can be negatively regulated by members of the Dickkopf (DKK) family, Wnt inhibitory factor 1 (WIF-1), and secreted Frizzled-related proteins (sFRP) (Kawano and Kypta, 2003).

Previous studies reported the involvement of WNT signaling in regulating skeletal development including formation of the growth plate, development of the apical ectodermal ridge (AER), maintaining the dorsal–ventral axis of the limbs, and formation of bone and synovial joints (Guo et al., 2004; Houben et al., 2016; Rodda and McMahon, 2006; Soshnikova et al., 2003). During early growth plate development,  $\beta$ -CATENIN and SOX9 factors antagonize each other to regulate proper chondrocyte differentiation pattern (Dao et al., 2012). Moreover, controlled  $\beta$ -CATENIN activity is required for normal limb growth plate development that involves chondrocyte differentiation, hypertrophic chondrocyte maturation, bone formation and remodelling (Houben et al., 2016). Deletion of  *$\beta$ -Catenin* from various tissue types such as the neural crest or limb bud mesenchymal cells, chondrocytes, and osteoblasts caused different developmental abnormalities. For instance, conditional deletion of  *$\beta$ -Catenin* in chondrocyte progenitors impaired skeletal development, leading to the formation of domed skulls, short limbs and underdeveloped tarsal synovial joints (Guo et al., 2004). Moreover, conditional KO of  *$\beta$ -Catenin* from the limb ectoderm disrupted the development of hindlimbs that were missing of some bone elements (Soshnikova et al., 2003). Prenatal deletion of  *$\beta$ -Catenin* in osteoblasts precursors in the *Osx1-GFP::Cre; $\beta$ -catenin<sup>cn</sup>* mouse model affected bone mineralization and bone formation owing to incomplete osteoblasts differentiation (Rodda and McMahon, 2006).

Expression of a stabilized  $\beta$ -CATENIN variant in the hypertrophic chondrocytes in E16.5 *tnnb<sup>GOFHTC</sup>* mutant limbs leads to expanded mineralized hypertrophic chondrocytes, and reduced bone formation and remodeling (Houben et al., 2016). This phenotype is similar to what we observe in *Prx1-cre;Foxc1<sup>Δ/Δ</sup>;Foxc2<sup>Δ/Δ</sup>* mutants at E16.5. Houben and colleagues (2016) identified relevant roles of  $\beta$ -CATENIN in regulating osteoclastogenesis and participating in hypertrophic chondrocytes trans-differentiation into osteoblasts that form the trabecular bone. Moreover, another study has found that  $\beta$ -CATENIN non- autonomously regulates hypertrophic chondrocytes maturation independently from PTHrP through distinctive mechanism (Guo et al., 2009). Given the similar phenotypes observed when  $\beta$ -CATENIN is stabilized in hypertrophic chondrocytes of E16.5 *tnnb<sup>GOFHTC</sup>* mutant limbs with the E16.5 *Prx1-cre;Foxc1<sup>Δ/Δ</sup>;Foxc2<sup>Δ/Δ</sup>* limbs suggest that these two factors may participate in common processes during endochondral limb development.

## 5.2 Materials and Methods:

### 5.2.1 Cell culture:

ATDC5 and U2OS cells were acquired from European Collection of Authenticated Cell Cultures and American Type Culture Collections (ATCC), respectively. Wild type (WT) and *CrFoxc1* ATDC5 (*Foxc1* mutation was achieved using the Alt-R CRISPR–Cas9 system (Almubarak et al., 2021)) cells were cultured in DMEM /Ham's F-12 (50/50 Mix) media with L-glutamine & 15 mM HEPES (CORNING) and 5%FBS. U2OS cells were culture in DMEM containing 10% FBS.

### 5.2.2 Cell transfection and luciferase assays:

Cells were plated into 24 well tissue culture plates at a concentration of  $4 \times 10^4$  cells per well. The following day, cells were transfected with expression vectors for Foxc1 or  $\beta$ -Catenin along with either TOPFlash or 6xFoxc1 BS-luc and pGL4.74[hRluc/TK] (Renilla vector) using Mirus Transit LT1 reagent at a 3:1 (ml Mirus: mg DNA) ratio. Where necessary, CHIR99021 (CHIR;  $3 \mu\text{M}$ ) was added 24 hours later (Lian et al., 2012). Cells were collected and processed for dual luciferase assays 48 hours post transfection following the manufacture's protocol (Promega). Each transfection was performed in triplicate and each experiment was performed three or four times. The following vectors were used: pCI HA-Empty vector, pCI-HA-FOXC1, pCDNA4-Xpress-Empty vector, pCDNA Xpress-FOXC1, and pCDNA4 Xpress-S131L expression vectors, 6X-FOXC1 binding site-luciferase reporter described in (Berry et al., 2006; Saleem et al., 2001; Saleem et al., 2004). pCDNA FLAG- $\beta$ -CATENIN plasmid # 44750, PCDNA FLAG-S33Y Plasmid # 13371 and the TOPFlash-luciferase reporter vector # 12456 were obtained from Addgene (Veeman et al., 2003) .

### 5.2.3 Transfections and protein extractions.

U2OS Cells were plated in 10cm plates and transfected with FOXC1 or  $\beta$ -CATENIN expression plasmids as described above. Proteins were harvested 48 hours post transfections. Cells were washed twice with 1X PBS, collected in a 1.5 ml microcentrifuge tubes then lysed in cell lysis buffer.

### 5.2.4 Western Blot (Licor Protocol):

Protein samples (50 $\mu$ g) were treated with 2X SDS buffer (125mM Tris hydrochloride (Tris-HCl) PH.8, 4%SDS, 20%glycerol, 0.02%(v/v)  $\beta$ -Mercaptoethanol 0.005% bromophenol blue) for 5 min at 95°C. and loaded into SDS-PAGE gel. The gel was transferred into a nitrocellulose membrane in transfer buffer (20% Methanol, 25mM Tris, 192mM glycine, 0.1% SDS) at 350 mA for 1 h at 4°C or at 30V overnight at RT. Next, the membrane was incubated in a 50% blocking buffer in 1XPBS 0.05% Tween20 (1XPBST) for 1 h at RT on a rocking platform. Then, Primary antibodies ( anti-AH rabbit:ab9110 abcam; anti-FLAG mouse: F1804-50UG SIGMA, anti-FOXC1 goat:Y212890 abm; anti non-phosphorylated (Active)  $\beta$ -CATENIN rabbit: 05-665-25UG Millipore; anti-TOTAL- $\beta$ -CATENIN rabbit: ab32572 abcam; anti  $\beta$ -TUBULIN mouse: G098 abm ;anti- $\beta$ -ACTIN mouse:G043 abm anti-Xpress: P/N 46-0528 Invitrogen) were diluted in 1XPBST and blocking buffer (1:1) according to the manufacturer recommendation, added into the nitrocellulose membrane and incubated overnight at 4°C on a rocking platform. The next day, membrane was washed with PBST (6x5 min washes). Following this step, secondary antibody diluted 1XPBST (1:1000-1:10000) was added to the membrane and incubated for 2 hours at RT

on a rocking platform. The membrane was washed again and visualized using the LI-COR Odyssey Scanner.

#### 5.2.5 Pulldown assay:

Nickel Agarose Pulldown assay was performed in U2OS cell extracts treated with or without CHIR (GSK3 inhibitor). U2OS cell lysate (300 µg) was incubated with nickel magnetic beads, to eliminate any nonspecific binding, followed by overnight incubation with 2.4µg recombinant His-tagged FOXC1 at 4°C. The next day, samples were washed 4 times with wash buffer and digested in 2X SDS PAGE loading buffer and boiled for 5 min at 95°C and loaded onto 10% SDS PAGE gel. Input samples (50 µg of U2OS and U2OS+CHIR protein extract), and purified FOXC1 protein sample were also induced as controls.

#### 5.2.6 RNA Scope *in situ* hybridization:

Single-plex RNA scope ISH was performed using *Lef1* probe REF: 441861 as described in (Almubarak et al., 2021), and chapter two in this thesis (page 76).

## 5.3 Results:

### 5.3.1 *Foxc1* inhibited $\beta$ -CATENIN activity in U2OS cells

First, we tested whether FOXC1 could alter  $\beta$ -CATENIN activity using the  $\beta$ -CATENIN-responsive TOPFlash-luciferase reporter vector (Veeman et al., 2003). U2OS osteosarcoma cells were transfected with TOPFlash-luciferase along with *Foxc1*- or empty expression vectors and were treated with or without GSK3 inhibitor (CHIR) (Lian et al., 2012). Treatment with CHIR resulted in a robust activation in luciferase activity in the absence of FOXC1 (Fig 5.1). When cells were transfected with FOXC1, TOPFlash-luciferase activity was not induced by CHIR suggesting that FOXC1 could inhibit  $\beta$ -CATENIN activity (Fig 5.1).

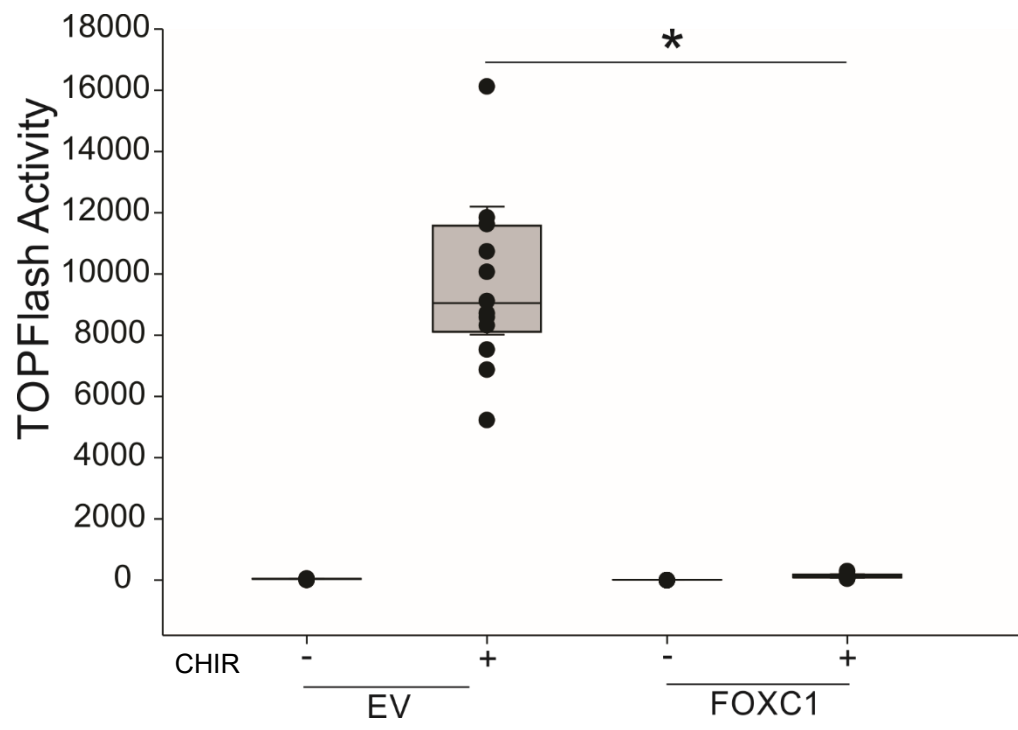


Figure 5.1. Transfection of FOXC1 expression vector inhibited TOPFlash luciferase activity.

U2OS were transfected with TOPFlash luciferase reporter vectors, along with either PCI HA-Empty vector (EV) or PCI HA-FOXC1, with (+) or without (-) CHIR 99021 followed by performing TOPFlash luciferase assay (n=4). The box plot indicates the median with 95% and 95% confidence interval of TOPFlash activity ratios and each dot in the scattered plot represent the values of the TOPFlash activity ratio. Statistics were done using two-way ANOVA analysis with post hoc analysis (all pairwise multiple comparison (Holm-Sidak method)) via Sigmaplot-13. \*P<0.05.

### 5.3.2 HA-FOXC1 vector activated 6X FOXC1 binding site-luciferase reporter:

We sought to examine if the HA-FOXC1 expressing vector was functioning, and if treating cells with CHIR could negatively interfere with its activity in U2OS cells. FOXC1 function was first tested using 6X FOXC1 binding site-luciferase reporter, in the absence and presence of CHIR. Transfection of HA-FOXC1 vector stimulated 6X FOXC1 binding site-luciferase activity in CHIR treated and untreated cells, compared to HA-FOXC1 non-transfected control reactions (Fig 5.2). These results indicate that HA-FOXC1 expressing vector was functional and that CHIR did not impair its activity.

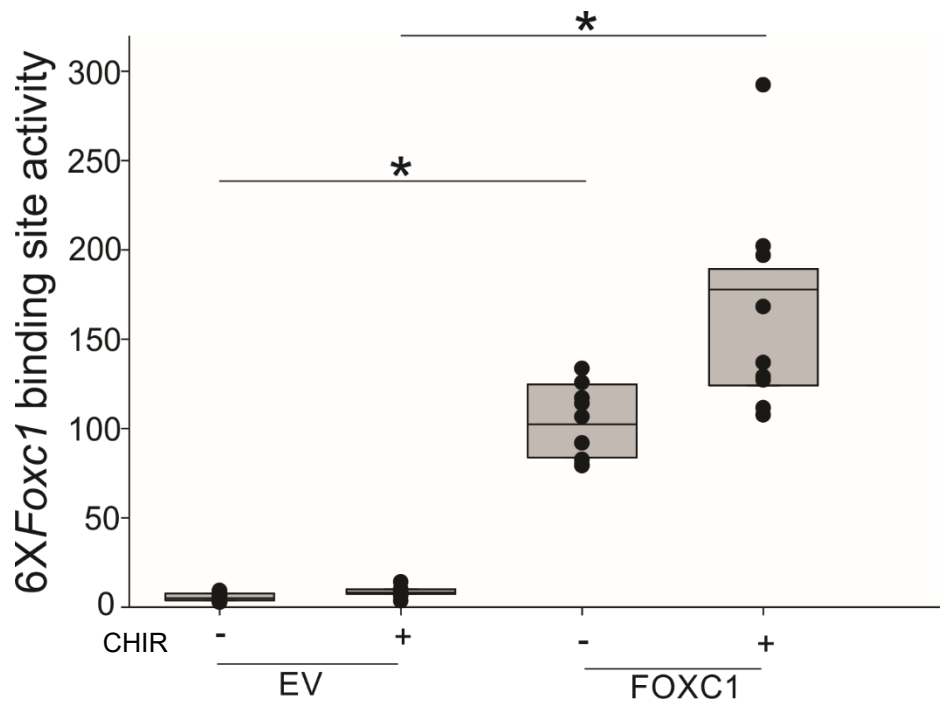


Figure 5.2. HA-FOXC1 vector activated the 6X FOXC1 binding site-luciferase reporter in U2OS cells.

6X FOXC1 binding site dual luciferase assay was performed using PCI HA-EV or PCI HA-FOXC1 vector with (+) or without (-) CHIR. The Box plots represent the median and 95% and 95% confidence interval of the activity, and each dot in the scattered plot represent the values of the luciferase activity ratio. Statistics were done using Two-way ANOVA analysis with Post hoc analysis (all Pairwise multiple comparison (Holm-Sidak method)) via Sigmaplot-13. (n=3).

\*P<0.05.

We then wanted to verify HA-FOXC1 transfection in U2OS cells and assess  $\beta$ -CATENIN protein level through western blot. HA-FOXC1 bands were clearly localized in cells transfected with HA-FOXC1 vectors only. Non-phosphorylated (active)  $\beta$ -CATENIN was also detected in all reactions. However, its levels were reduced in HA-FOXC1 transfected U2OS cells.  $\beta$ -CATENIN protein was restored in CHIR treated cells (Fig 5.3). These data verified a successful transfection of our HA-FOXC1 vector in U2OS cells, and that FOXC1 may negatively affect active  $\beta$ -CATENIN.

HA-FOXC1	-	-	+	+
HA-EV	+	+	-	-
CHIR	-	+	-	+

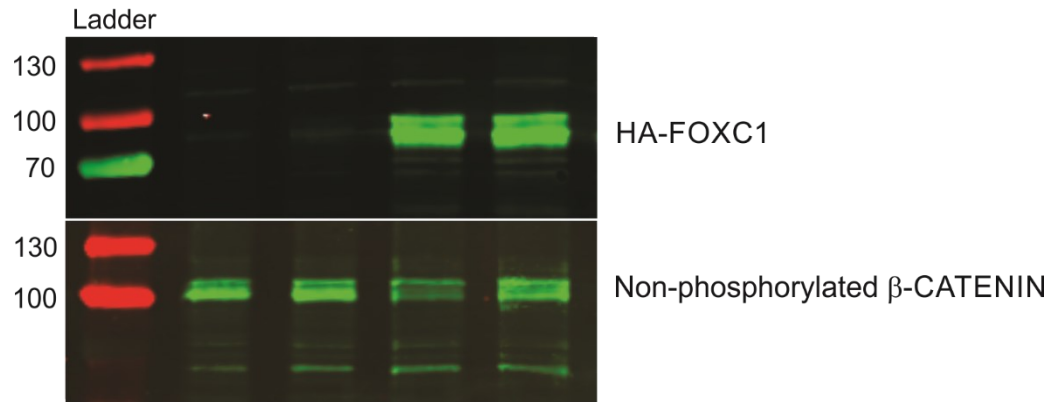


Figure 5.3. Transfected HA-FOXC1 vector was functional in U2OS cells.

Western blot was performed in 5 $\mu$ g PCI HA-EV or PCI HA-FOXC1 transfected U2OS, with or without CHIR. WB was performed using anti-HA (rabbit) to detect transfected FOXC1 protein and anti non-phosphorylated (active)  $\beta$ -CATENIN (rabbit), (n=3).

### 5.3.3 FOXC1 inhibited the activity of active (non-phosphorylated) $\beta$ -CATENIN in U2OS cells

We then wanted to verify if FOXC1 interfered with the activity of  $\beta$ -CATENIN. In this experiment, we set up different conditions to run the TOPFlash luciferase assay, where we employed S33Y, which is a mutant form of  $\beta$ -CATENIN that is always active and resist GSK inhibitory effect (Takahashi and Yamanaka, 2006). Here, we transfected U2OS cells with either FLAG- $\beta$ -CATENIN or FLAG-S33Y expressing vectors along with TOPFlash-luciferase reporter and HA-FOXC1 expressing vector, followed by CHIR after 24 hours. The dual luciferase assay revealed an increase in TOPFlash activity in WT  $\beta$ -CATENIN and S33Y transfected cells with CHIR, but with slightly less TOPFlash activity in the S33Y transfected cells (Fig 5.4). Apparently, saturating the cells with so much  $\beta$ -CATENIN had a slight negative effect on the TOPFlash activity. When FOXC1 was co-expressed with either WT  $\beta$ -CATENIN or S33Y, TOPFlash activity was diminished (Fig 5.4). Since FOXC1 inhibited both WT  $\beta$ -CATENIN and S33Y activity, this indicates that FOXC1 is not preventing the activation and stabilization of  $\beta$ -CATENIN. Thus, the effect we observed with FOXC1 is likely occurring in the nucleus.

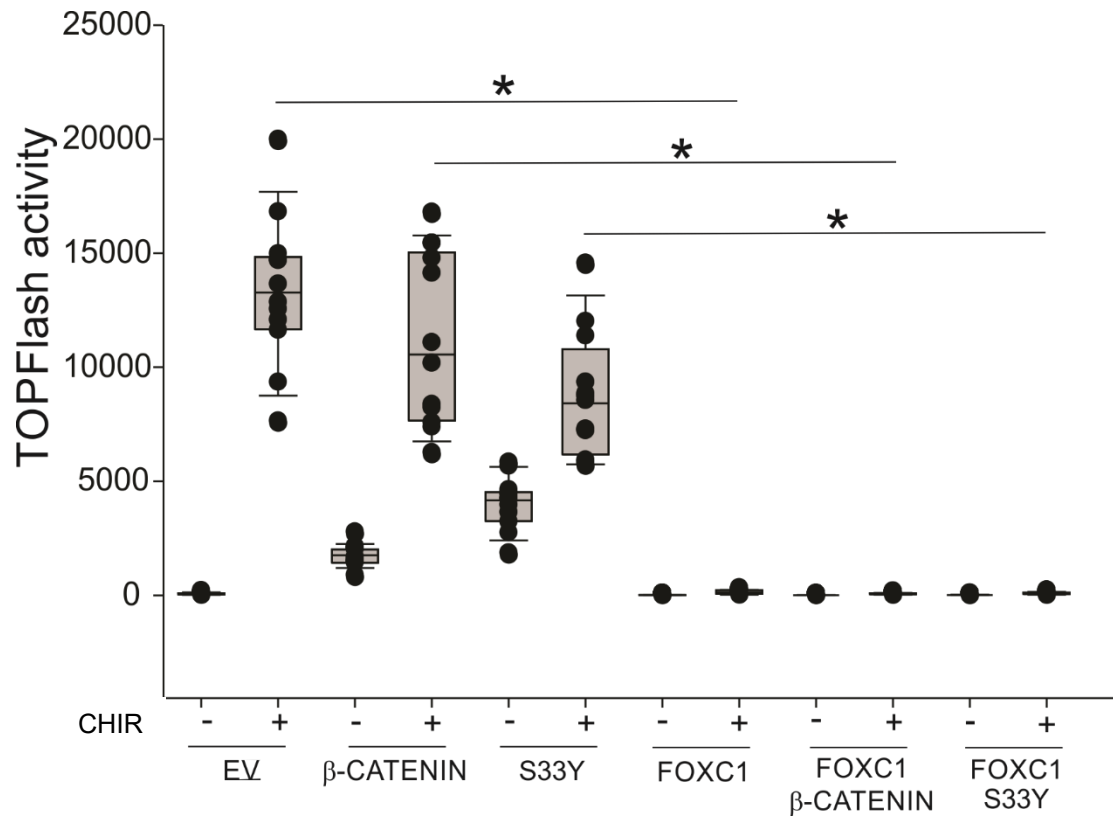


Figure 5.4. Transfected FOXC1 expressing vector inhibited TOPFlash activity in WT  $\beta$ -CATENIN and S33Y transfected U2OS cells.

U2OS cells were transfected with either HA-EV, FLAG- $\beta$ -CATENIN, FLAG-S33Y, with or without FOXC1 expressing vector. After 24 hours of transfection, cells were either treated (+) or untreated (-) with CHIR. Box plots represent the median with 95% and 5% confidence interval of the TOPFlash luciferase activity, and each dot in the scattered plot represent TOPFlash activity values. Statistics were done using Two-way ANOVA analysis with Post hoc analysis (all Pairwise multiple comparison (Holm-Sidak method)) via Sigmaplot-13. (n=4).

\* P<0.05.

Next, we wanted to verify the transfection of expression vectors and examine if FOXC1 has a negative effect on the transfected  $\beta$ -CATENIN protein level. We detected bands within all HA-FOXC1 transfected samples, which indicate that FOXC1 was expressed in these cells (Fig 5.5). We identified FLAG bands in WT  $\beta$ -CATENIN and S33Y transfected cells that did not have FOXC1. However, FLAG  $\beta$ -CATENIN and S33Y bands were reduced in FOXC1 transfected cells, indicating that the presence of FOXC1 negatively affected transfected  $\beta$ -CATENIN and S33Y protein levels (Fig 5.5). Interestingly, CHIR treated U2OS cells had more FOXC1 than the CHIR untreated samples. This result suggested that the high 6XFoxc1 binding site-luciferase activity that was previously identified in FOXC1+CHIR reactions was probably due to increased FOXC1 protein levels (Fig 5.2).

HA-FOXC1	-	-	-	-	+	+	+	-	-	-	-	+	+	+
FLAG-S33Y	-	-	-	+	-	-	+	-	-	-	+	-	-	+
FLAG-β-CATENIN	-	-	+	-	-	+	-	-	-	+	-	-	+	-
HA-EV	-	+	+	+	+	-	-	-	+	+	+	+	-	-
CHIR	-	-	-	-	-	-	-	+	+	+	+	+	+	+

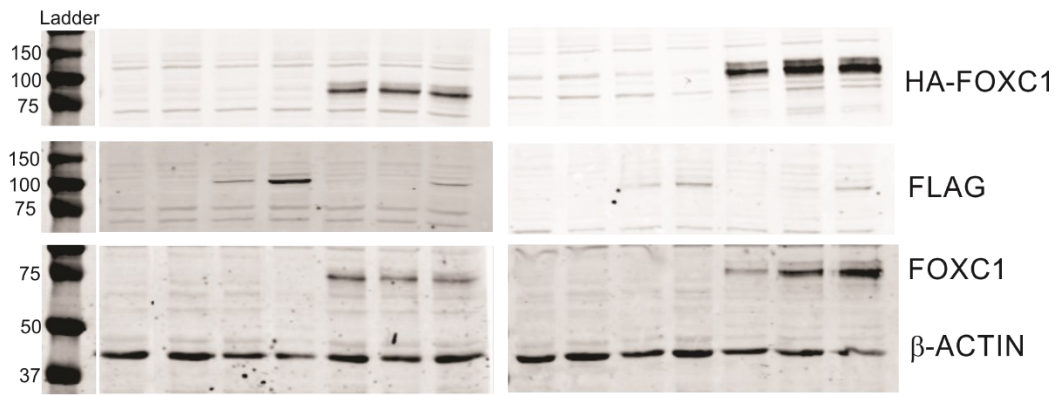


Figure 5.5. Transfection of FOXC1 vector had a negative effect on FLAG- $\beta$ -CATENIN and FLAG-S33Y protein levels in U2OS cells.

U2OS cells were transfected with PCI HA-EV with either PCDNA FLAG- $\beta$ -CATENIN or PCDNA FLAG-S33Y expression vectors along with or without PCI HA-FOXC1 expressing vectors. 24 hours after transfections cells were either treated or untreated 3mM CHIR. Total protein lysate was isolated for WB using anti-FLAG (mouse) to detect FLAG- $\beta$ -CATENIN, and FLAG-S33Y bands and with anti-HA (rabbit) to identify HA-FOXC1 bands. Anti-FOXC1 (goat) was used to detect FOXC1 protein bands, and anti- $\beta$ -ACTIN (mouse) was used as a control. (n=3).

#### 5.3.4 FOXC1 inhibit $\beta$ -CATENIN activity through different means in U2OS cells

Our data indicates that FOXC1 had a negative effect on  $\beta$ -CATENIN activity. One possibility is that FOXC1 could regulate  $\beta$ -CATENIN from the transcription level, where FOXC1 transcription factor binds and stimulates another gene to inhibit  $\beta$ -CATENIN function. The other likelihood is that FOXC1 could regulate  $\beta$ -CATENIN activity from the protein level to stimulate its degradation or binds to it and interfere with its transcriptional activity. To test the first possibility and see if FOXC1 needs to bind DNA to inhibit  $\beta$ -CATENIN function, we performed TOPFlash dual luciferase assay in U2OS cells transfected with a FOXC1 that contains S131L point mutation in the forkhead domain, that prevents it from binding DNA, but does not affect its nuclear localization (Saleem et al., 2001). Similar to our previous results, the TOPFlash reporter revealed high activity in FOXC1 non-transfected cells when treated with CHIR, while the luciferase activity decreased when FOXC1 was co-transfected into the U2OS cells (Fig 5.6). Although transfection of S131L inhibited the TOPFlash activity as well, its inhibitory effect was not as potent as the WT FOXC1, as some of the TOPFlash activity appeared upon the transfection of the S131L plasmid (Fig 5.6). These findings indicate that FOXC1 DNA-binding activity is not sufficient to completely inhibit  $\beta$ -CATENIN activity, and that FOXC1 is possibly inhibiting  $\beta$ -CATENIN function through different means.

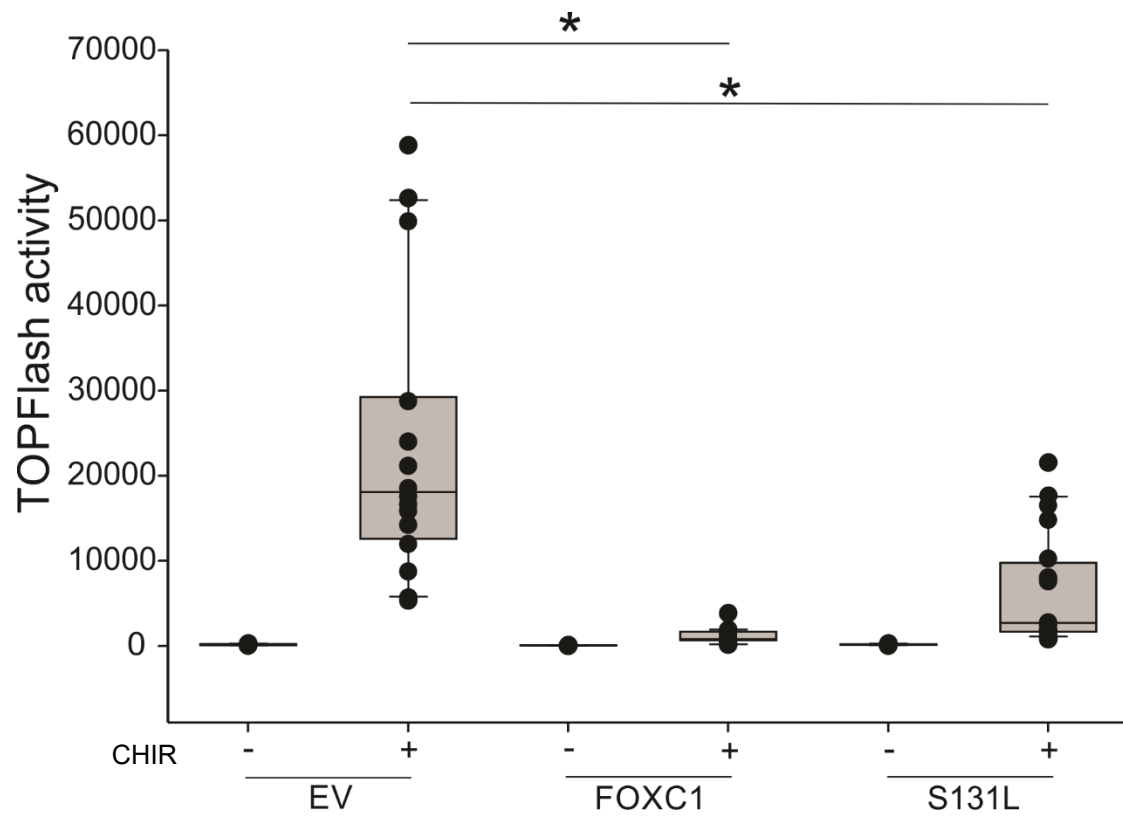


Figure 5.6. FOXC1 needs to bind DNA to block  $\beta$ -CATENIN activity.

U2OS cells were transfected with TOPFlash dual luciferase reporter along with either PCDNA4 Xpress-EV or PCDNA4 Xpress-FOXC1 or PCDNA4- Xpress-S131L expression vectors. After 24 hours, cells were either treated or untreated with CHIR. Next day, dual luciferase assay was performed to assess TOPFlash-luciferase activity under these conditions. The boxplot indicates the median with 95% and 95% confidence interval of TOPFlash activity ratios, and each dot in the scattered plot represent the individual value of TOPFlash activity ratio, with few outliers. Statistics were done using Two-way ANOVA analysis with Post hoc analysis (all Pairwise multiple comparison (Holm-Sidak method)) via Sigmaplot-13. \*P<0.05. (n=4)

### 5.3.5 GSK inhibition enhanced FOXC1 formation in U2OS cells

Next, we sought to verify the presence of transfected FOXC1 and S131L proteins in our U2OS cells through identifying Xpress protein in WB. Xpress-FOXC1 and Xpress-S131L were detected in the transfected samples (Fig 5.7). In addition, more intense FOXC1 bands were shown when GSK kinase was inhibited by the addition of CHIR (Fig. 5.7). This data verified the transfection of FOXC1 and S131L expression vectors into U2OS cells and indicated that inhibiting GSK3 by adding CHIR has a positive effect on FOXC1 protein.

Xpress-S131L	-	-	-	+	-	-	+
Xpress-FOXC1	-	-	+	-	-	+	-
Xpress-EV	-	+	-	-	+	-	-
CHIR	-	-	-	-	+	+	+

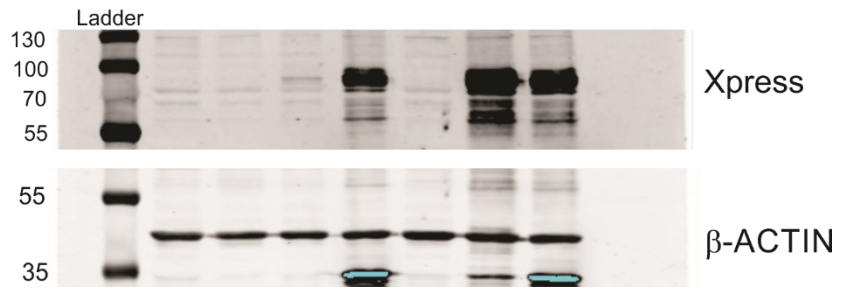


Figure 5.7. More FOXC1 was made when GSK was inhibited by CHIR.

U2OS cells were transfected with either 5 $\mu$ g PCDNA4 Xpress tagged EV or WT-FOXC1 or S131L expression vectors. Next day, cells were either treated or untreated with CHIR. WB was conducted using anti-Xpress (mouse) to detect transfected FOXC1 and S131L proteins, and anti- $\beta$ -ACTIN (mouse) was used as a control. (n=3).

### 5.3.6 FOXC1 did not bind physically to $\beta$ -CATENIN in U2OS cells

We then wanted to test if FOXC1 transcription factor can physically bind  $\beta$ -CATENIN protein. Therefore, we performed Nickel Agarose Pulldown assay, with and without recombinant His-tagged FOXC1, in CHIR treated and untreated U2OS cells. Input samples and purified, recombinant FOXC1 protein sample were also included as controls.  $\beta$ -CATENIN was identified in both input samples, and FOXC1 band was also detected in the pure recombinant His-tagged FOXC1 control reaction. However, the pulldown didn't detect any clear localization of  $\beta$ -CATENIN in the FOXC1 positive samples, which rules out the likelihood of FOXC1 binding physically to  $\beta$ -CATENIN (Fig. 5.8).

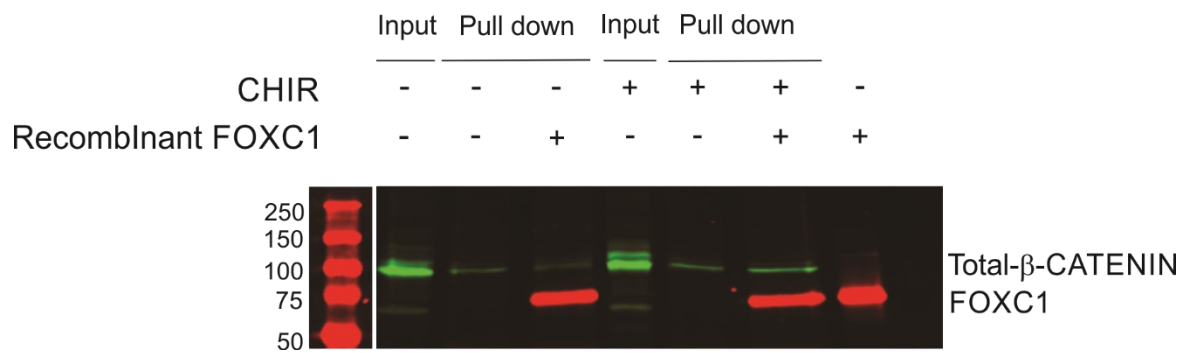


Figure 5.8. No physical binding between FOXC1 and  $\beta$ -CATENIN protein in U2OS cells.

Pulldown assay of recombinant FOXC1 was performed in CHIR treated and untreated U2OS.

Total protein lysate was used to assess possible binding of  $\beta$ -CATENIN to FOXC1 recombinant protein. (n=2).

### 5.3.7 Loss of FOXC1 function stabilized $\beta$ -CATENIN in ATDC5 cells

We then sought to test the effect of FOXC1 loss of function on  $\beta$ -CATENIN protein using WT and *crFoxc1* ATDC5 pre-chondrocytes with or without CHIR (Almubarak et al., 2021). Untreated CHIR cells showed very weak  $\beta$ -CATENIN bands, probably due to GSK inhibitory effect on  $\beta$ -CATENIN. *Foxc1* crisper deletion in ATDC5 resulted in a more  $\beta$ -CATENIN stable band compared to the weaker band in WT ATDC5 in CHIR treated cells (Fig 5.9). This result supported our previous findings of FOXC1 inhibitory effect on  $\beta$ -CATENIN in U2OS cells.

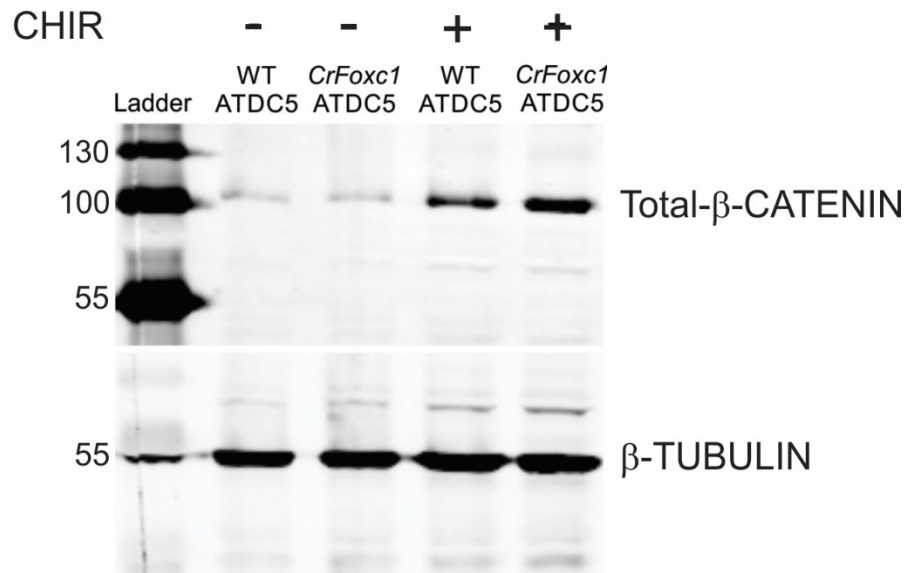


Figure 5.9. Crisper *Foxc1* deletion stabilized  $\beta$ -CATENIN in ATDC5 pre-chondrocytes treated with CHIR

WB assay was performed to assess total  $\beta$ -CATENIN protein in WT and *cFoxc1* ATDC5 cells, in the presence or absence of CHIR. For total  $\beta$ -CATENIN detection, we used anti-total  $\beta$ -CATENIN rabbit along with anti- $\beta$ -TUBULIN mouse as a control.

### 5.3.8 *Lefl* enhanced activity was identified in E16.5 *Prx1-cre;Foxc1<sup>Δ/Δ</sup>;Foxc2<sup>Δ/Δ</sup>* growth plate

Our previous experiments indicated that FOXC1 has a negative effect on  $\beta$ -CATENIN activity. We wanted to assess whether  $\beta$ -CATENIN activity in the growth plate was affected when FOXC1 is absent in *Prx1-cre;Foxc1<sup>Δ/Δ</sup>;Foxc2<sup>Δ/Δ</sup>* skeletal tissues. We examined whether expression of the  $\beta$ -CATENIN target gene, Lymphoid Enhancer Binding Factor 1 (*Lefl*) (Clevers, 2006) was altered in *Prx1-cre;Foxc1<sup>Δ/Δ</sup>;Foxc2<sup>Δ/Δ</sup>* growth plate. Comparable *Lefl* expression in the resting zone and the columnar chondrocytes at E14.5 was observed in the tibia control and *Prx1-cre;Foxc1<sup>Δ/Δ</sup>;Foxc2<sup>Δ/Δ</sup>* embryos (Fig 5.10A, B). By E16.5, control limbs displayed restricted localization of *Lefl* mRNAs within the resting zone (yellow asterisk) and the Groove of Ranvier (white arrows) (Fig 5.10C). In contrast, the *Prx1-cre;Foxc1<sup>Δ/Δ</sup>;Foxc2<sup>Δ/Δ</sup>* growth plate exhibited more *Lefl* expressed columnar chondrocytes (yellow arrow) (Fig 5.10 D). This preliminary finding supports the idea that *Foxc1* may act to inhibit  $\beta$ -CATENIN transcriptional regulatory activity.

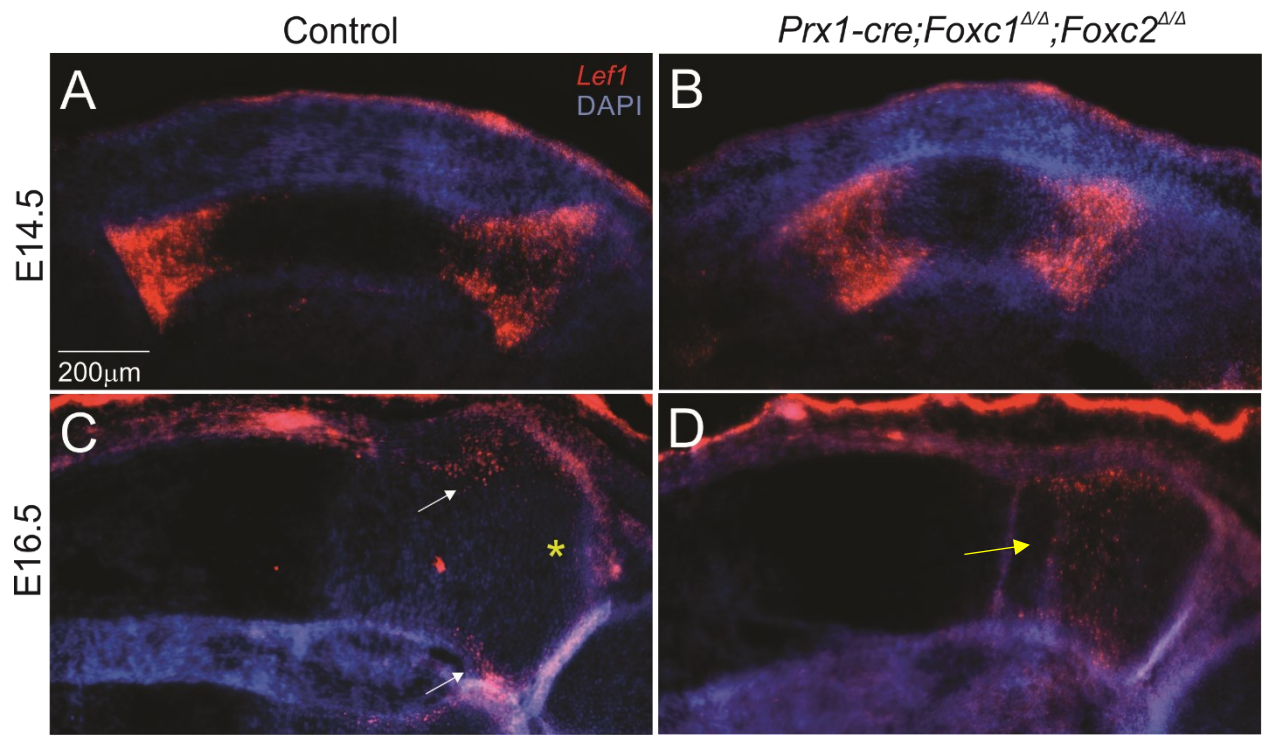


Figure 5.10. Absence of FOXC1 enhanced *Lef1* localization in E16.5 *Prx1-cre;Foxc1<sup>Δ/Δ</sup>;Foxc2<sup>Δ/Δ</sup>* growth plate compared to the control.

RNA scope ISH of *Lef1* was performed in E14.5 and E16.5 tibia. No change in *Lef1* expression was observed between E14.5 control and *Prx1-cre;Foxc1<sup>Δ/Δ</sup>;Foxc2<sup>Δ/Δ</sup>* tibia (A, B). *Lef1* expression was restrictedly localized within the Groove of Ranvier of E16.5 control limbs (C). Dominant expression of *Lef1* was identified in E16.5 *Prx1-cre;Foxc1<sup>Δ/Δ</sup>;Foxc2<sup>Δ/Δ</sup>* columnar chondrocytes (D). (n=3).

## 5.4 Discussion:

Expression of a stabilized variant of  $\beta$ -CATENIN in the limb hypertrophic chondrocytes (Houben et al., 2016) resulted in similar growth plate abnormalities to the *Prx1-cre;Foxc1<sup>Δ/Δ</sup>;Foxc2<sup>Δ/Δ</sup>* limbs such as expanded hypertrophic chondrocyte zone, reduction of mineralization, bone formation and bone remodeling (Houben et al., 2016). Given these similar phenotypes, we tested whether FOXC1 and  $\beta$ -CATENIN are working in similar pathways during endochondral ossification. In this study, we investigated FOXC1 loss of function and gain of function on  $\beta$ -CATENIN activity in ATDC5 pre-chondrocytes and U2OS cells. We identified increased  $\beta$ -CATENIN protein in *CrFoxc1* cells compared to the WT-ATDC5 pre-chondrocytes. Moreover, TOPFlash reporter activity revealed high activity in the absence of *Foxc1*, and substantial inhibition of the TOPFlash when *Foxc1* was transfected to the U2OS cells treated with CHIR. Interestingly, the TOPFlash luciferase showed that transfection of *Foxc1* had a similar inhibitory effect on both WT- $\beta$ -CATENIN and its active form S33Y, which indicates that *Foxc1* can inhibit active  $\beta$ -CATENIN. Moreover, the assessment of the TOPFlash activity with transfected FOXC1 and S131L expression vectors in U2OS cells, revealed a slightly weaker inhibitory effect of S131L compared to the strong WT-FOXC1 inhibition on the TOPFlash reporter activity. This indicates that FOXC1 is interfering with active  $\beta$ -CATENIN through different ways. However, pulldown assay of recombinant FOXC1 in U2OS cells did not detect any physical binding between FOXC1 and  $\beta$ -CATENIN. The FOXC1 inhibitory effect was also shown in the E16.5 tibia growth plate. Expression of *Lef1*, a  $\beta$ -CATENIN target gene, revealed broader localization of *Lef1* positive chondrocytes in E16.5 *Prx1-cre;Foxc1<sup>Δ/Δ</sup>;Foxc2<sup>Δ/Δ</sup>* growth plate compared to the more restricted *Lef1* expression within the Groove of Ranvier cell population (Usami et al., 2019). These findings supported our hypothesis that FOXC1 has an inhibitory effect

on  $\beta$ -CATENIN activity. FOXC1 transcriptional regulatory activity was stimulated by the addition of CHIR in U2OS cells. Treating cells with CHIR that inhibits GSK3 phosphorylation activity also increased levels of transfected FOXC1 protein. These results suggest that inhibiting GSK3 via CHIR enhanced FOXC1 activity, possibly by protein stabilizing.

Our data showed that FOXC1 requires DNA binding activity to efficiently inhibit  $\beta$ -CATENIN activity. We could not detect physical binding between FOXC1 and  $\beta$ -CATENIN. This does not rule out that FOXC1 can interfere with  $\beta$ -CATENIN through different means in the protein level. Although the S131L FOXC1 mutant reduced TOPFlash activity, this effect was not as pronounced as WT FOXC1. There are a number of possible ways where FOXC1 can inhibit  $\beta$ -CATENIN activity. For instance, FOXC1 can bind and stimulate the expression of  $\beta$ -CATENIN inhibitors that will either interfere with  $\beta$ -CATENIN expression or stimulates its degradation or interfere with its DNA binding activity (Almubarak et al., 2021; Choi et al., 2012). RNA-seq analysis of ribs tissue isolated from the *Col2-cre;Foxc1<sup>Δ/Δ</sup>;Foxc2<sup>Δ/Δ</sup>* mice displayed reduced Dickkopf-related protein 1 (DKK1) expression level, a potent extracellular Wnt antagonist (Choi et al., 2012; Glinka et al., 1998). DKK1 binds Wnt coreceptor LRP5/6 and prevents it from forming a ternary receptor complex and block  $\beta$ -CATENIN signaling (Mao et al., 2001). In addition to LRP5/6, DKK1 also attaches to the membrane receptors Kremen (Krm)- 1/2 that can stimulate LRP5/6 endocytosis and inhibit  $\beta$ -CATENIN signaling (Mao et al., 2002). Another possibility is that FOXC1 can interfere with  $\beta$ -CATENIN DNA binding through blocking its binding site or impede with the formation of its transcription complex in the nucleus (MacDonald et al., 2009).

Expression of stabilized  $\beta$ -CATENIN in the growth plate hypertrophic chondrocytes showed similar limb phenotype to the *Col2-cre;Foxc1<sup>Δ/Δ</sup>;Foxc2<sup>Δ/Δ</sup>* limb with decreased mineralization and expansion of the hypertrophic chondrocytes and impaired bone formation and remodeling (Houben et al., 2016). Gue et al. (2009) showed that active  $\beta$ -CATENIN signaling acts cell-autonomously to control chondrocyte identity during embryonic growth plate development. As a result, overexpression of active  $\beta$ -catenin inhibits chondrocyte cell fate determination and maintenance. Moreover, Wnt/ $\beta$ -CATENIN signaling also regulates hypertrophic chondrocytes final maturation (Guo et al., 2009). Wnt/ $\beta$ -CATENIN signaling is required for proper extracellular matrix remodeling and regulating hypertrophic chondrocytes trans-differentiation into osteoblasts(Houben et al., 2016). Stabilization of  $\beta$ -CATENIN in *Coll10a1-Cre* mice caused impaired ECM remodeling process and form expanded mineralized HC, leading to delay trabecular bone formation (Houben et al., 2016). These similarities suggested a possible association between FOXC1 and  $\beta$ -CATENIN in the growth plate. Our results showed that FOXC1 inhibited  $\beta$ -CATENIN activity *in vitro*. Interestingly, we observed expanded expression of *Lef1* mRNA in the columnar chondrocytes of E16.5 *Col2-cre;Foxc1<sup>Δ/Δ</sup>;Foxc2<sup>Δ/Δ</sup>* growth plate compared to its distinctive localization in the groove of Ranvier in the control growth plate(Usami et al., 2019). Although, this was one  *$\beta$ -Catenin* target gene that was tested, it supports that idea that  $\beta$ -CATENIN activity can be regulated by *Foxc1* in the growth plate, and that in *Prx1-cre;Foxc1<sup>Δ/Δ</sup>;Foxc2<sup>Δ/Δ</sup>*,  $\beta$ -CATENIN activity might be stimulated by the absence of *Foxc1* and promoted other genes in the growth plate that contributed to a similar endochondral phenotypes to the ones identified in the (Houben et al., 2016) mice model. Together, these findings spot the light on a possible important and a complex association between the canonical Wnt/ $\beta$ -CATENIN

signaling and FOXC1 activity that may contribute to the regulation of different aspects in endochondral skeletal development.

## Chapter 6:

### 6.1 Discussion and conclusion:

In this study, we investigated the molecular and biological roles of *Foxc1* and *Foxc2* in embryonic endochondral ossification. SOX9, a pioneer transcription factor in endochondral ossification, binds to and activates *Foxc1* through a distal enhancer. We show that *Foxc1* gain of function in mouse embryonic stem cells, stimulate chondrocyte differentiation, whereas *Foxc1* loss of function in ATDC5 cells constrained chondrocytes differentiation. These findings indicate an important role for *Foxc1* in regulating chondrogenesis (Almubarak et al., 2021).

*Foxc1* and *Foxc2* displayed both overlapping and distinct expression patterns at different time points in limb and vertebral column development. Conditional deletion of *Foxc1* and *Foxc2* in mouse chondrocytes using the *Col2-Cre* driver caused skeletal abnormalities with increasing levels of severity when *Foxc1* gene dosage was reduced, with *Col2-cre;Foxc1<sup>Δ/Δ</sup>;Foxc2<sup>Δ/Δ</sup>* mice show the strongest phenotypes than single mutants. Skeletal prep of E18.5 *Col2-cre;Foxc1<sup>Δ/Δ</sup>;Foxc2<sup>Δ/Δ</sup>* embryos demonstrated a general skeletal dysplasia with more severe axial skeleton phenotypes than the appendicular skeleton. The occipital bones failed to develop, affecting the normal shape of the skull. The cervical vertebrae were also missing with impaired formation of and ossification of the thoracic vertebrae. The rib cage was small, but with normal patterning. On the other hand, *Col2-cre;Foxc1<sup>Δ/Δ</sup>;Foxc2<sup>Δ/Δ</sup>* limbs exhibited less severe phenotypes compared to the axial skeleton with small limbs owing in part to the low proliferation rate in columnar chondrocytes. Moreover, histological staining of *Col2-cre;Foxc1<sup>Δ/Δ</sup>;Foxc2<sup>Δ/Δ</sup>* limbs showed reduced mineralization and disrupted growth plate patterning. IF and ISH in E16.5 tibia demonstrated reduction in endochondral ossification markers. These results were verified by qRT-

PCR, and RNA sequencing analysis of control and *Col2-cre;Foxc1<sup>Δ/Δ</sup>;Foxc2<sup>Δ/Δ</sup>* ribs that demonstrated reduction in gene expression associated with various aspects of skeletal development such as cartilage endochondral ossification, mineralization, and osteoblasts differentiation. The phenotypic variation between the axial skeleton and the limbs in *Col2-cre;Foxc1<sup>Δ/Δ</sup>;Foxc2<sup>Δ/Δ</sup>* embryos is probably due to the difference in *Col2a1* expression time between the two skeletal elements. *Col2a1* is expressed at early time point in the sclerotome before it starts expressing in the resting zone of the limb growth plate (Monsoro-Burq, 2005; Ovchinnikov et al., 2000). It is possible that early loss of *Foxc1* and *Foxc2* in the mesenchymal cells can result in a more severe endochondral developmental abnormality in comparison to their deletion at a later time point in the chondrocytes progenitors (Ovchinnikov et al., 2000). Another possibility is that *Foxc1* and *Foxc2* are expressed at higher levels the axial skeletal elements than the limb. A third possibility is that *Foxc1* and *Foxc2* function differently in the axial than the appendicular skeleton.

Our study was then extended to the axial skeleton and particularly the vertebral column that showed variation in its developmental phenotype. In this aim, we identified comparable broad *Foxc1* and *Foxc2* expression within the periphery and immature chondrocytes at early time point of E14.5. Interestingly, their expression become more restricted and were no longer detected in the hypertrophic chondrocytes at E16.5. Safranin O staining of E16.5 control and *Col2-cre;Foxc1<sup>Δ/Δ</sup>;Foxc2<sup>Δ/Δ</sup>* vertebral column detected normal cartilage formation of the cervical vertebrae in the control mice. But the staining didn't detect any cartilage development in the cervical vertebrae of the *Col2-cre;Foxc1<sup>Δ/Δ</sup>;Foxc2<sup>Δ/Δ</sup>* mice. As expected, staining also showed normal development of the thoracic vertebrae in control mice, where the chondrocytes differentiated and formed large hypertrophic chondrocytes at the center of the vertebral bodies.

Additionally, control thoracic vertebrae showed normal formation of the intervertebral discs including the anulus fibrosus ring and normal development of the nucleus pulposus in between each two vertebrae (Almubarak et al., 2021; Kalamchi and Valle, 2022). Safranin O staining also revealed formation of cartilage in the *Col2-cre;Foxc1<sup>Δ/Δ</sup>;Foxc2<sup>Δ/Δ</sup>* thoracic vertebrae, but the vertebrae were small, fused and misshaped, with underdeveloped intervertebral discs. IF staining of functional proteins and cartilage associated with endochondral ossification process in the vertebral column identified localization of chondrocytes formation, differentiation and ossification factors in the control cervical vertebrae, indicating proper chondrocytes differentiation, maturation into hypertrophy and ossification process in the control cervical vertebrae. However, we couldn't identify any proteins or collagens in the cervical area of the vertebral column of *Col2-cre;Foxc1<sup>Δ/Δ</sup>;Foxc2<sup>Δ/Δ</sup>* embryos. This verified that loss of *Foxc1* and *Foxc2* function has blocked chondrogenesis in the cervical vertebrae. Similar to the control cervical vertebrae results, the thoracic vertebrae IF exhibited normal endochondral ossification process, where chondrocytes formation and differentiation functional proteins and collagens localized normally in the control thoracic vertebrae and the developed intervertebral disc. Although were able to detect endochondral ossification markers within the *Col2-cre;Foxc1<sup>Δ/Δ</sup>;Foxc2<sup>Δ/Δ</sup>* small, malformed thoracic vertebrae, all protein localization were reduced (Almubarak et al., 2021). These results suggest that deletion of *Foxc1* and *Foxc2* resulted in a delayed endochondral development of the thoracic vertebrae and consequently, impaired formation of intervertebral discs.

There are many possibilities that can explain the variation in phenotype severity between the cervical and the thoracic vertebrae. One possibility is that *Foxc1* and *Foxc2* function in more cells in the cervical vertebrae than the thoracic vertebrae, and other likelihood is that the in normal

vertebral column development, thoracic vertebrae form before the cervical vertebrae and that loss of *Foxc1* and *Foxc2* led to a general delay in endochondral ossification process throughout the vertebral column, as a previous study reported ossification of the thoracic vertebral bodies before the cervical vertebrae (Kalamchi and Valle, 2022; Skórzewska et al., 2013).

Our third aim focused on investigating *Foxc1* and *Foxc2* function in the limbs and assess early conditional deletion of *Foxc1* and *Foxc2* in osteochondroprogenitor cells using the *Prx1-cre* driver. RNA scope ISH of *Foxc1* and *Foxc2* revealed similar expression patterns of *Foxc1* and *Foxc2* mRNAs. Interestingly, both genes expressed more intensely in the autopod than in the zeugopod and the stylopod. Moreover, we detected more *Foxc1* and *Foxc2* positive cells along the growth plate at E14.5 including early hypertrophic chondrocytes. At E16.5 expression becomes more restricted to the perichondrium and the resting zone, with reduced expression in the columnar chondrocytes and hypertrophic chondrocytes. This data suggests that *Foxc1* and *Foxc2* expression differs spatially and temporally during the limb development. Skeletal prep analysis of both control and *Prx1-cre;Foxc1<sup>Δ/Δ</sup>;Foxc2<sup>Δ/Δ</sup>* embryos demonstrated preferentially more severe distal skeletal abnormalities than the proximal bone parts. Fore-and hindlimbs were formed with some underdeveloped bone elements, bone eminences and severely thin digits. Less cartilage formation was observed through safranin O staining in the autopod compared to the proximal bone elements, which is probably due to having more *Foxc1* and *Foxc2* expression in the distal than the proximal bone components. Loss of *Foxc1* and *Foxc2* in limbs caused a general delay in endochondral ossification process including pre-hypertrophic chondrocyte formation that was identified by the short region of *Ihh* mRNA localization in the *Prx1-cre;Foxc1<sup>Δ/Δ</sup>;Foxc2<sup>Δ/Δ</sup>* growth plate (Yoshida et al., 2015). This developmental delay has affected *Ihh* signaling proliferation marked by the

reduced KI67 positive cells in the growth plate and subsequently delay entry into hypertrophy. However, development of the *Ihh* signaling region was normalized by the reduce expression of *Foxc1* and *Foxc2* mRNAs in the hypertrophic chondrocytes at E16.5. Interestingly, Loss of *Foxc1* function did not impact PTHrP expression that was identified by *Pthlh* mRNA ISH staining within the resting zone of the limb growth plate. This result did not support a previous study that identified *Pthlh* (PTHrP) as a direct downstream target for *Foxc1* through *in vitro* testing (Yoshida et al., 2015). Still, our finding does not rule out the possibility of FOXC1 regulating PTHrP in a different type of cells, since their study was performed in *in vitro* system(Yoshida et al., 2015b). E16.5 *Prx1-cre;Foxc1<sup>Δ/Δ</sup>;Foxc2<sup>Δ/Δ</sup>* growth plate exhibited expanded and mineralize hypertrophic chondrocytes domains, that did not show any sign of cellular apoptosis within the expanded region. By E16.5 and E17.5 *Prx1-cre;Foxc1<sup>Δ/Δ</sup>;Foxc2<sup>Δ/Δ</sup>* tibia showed formation of a very small POC compared to the widely formed POC in control limbs. These findings suggest that deletion of *Foxc1* and *Foxc2* in the limbs lead to a delay in entry followed by a delay in exit from hypertrophy that compromises bone formation. Analysis of the control and *Prx1-cre;Foxc1<sup>Δ/Δ</sup>;Foxc2<sup>Δ/Δ</sup>* tibia demonstrated normal bone mineralization and localization of the osteoblasts and osteoclasts in the control POC, However, *Prx1-cre;Foxc1<sup>Δ/Δ</sup>;Foxc2<sup>Δ/Δ</sup>* limbs showed reduced mineralization with a small POC, with osteoblast originating from the bone collar but few in the trabecular bone. Vascularization was detected in the *Prx1-cre;Foxc1<sup>Δ/Δ</sup>;Foxc2<sup>Δ/Δ</sup>* tibia, suggesting that impairment of this process was not responsible for the observed phenotypes. However, expression of osteoclast differentiation and activation factors such as *Fgfr1* and *Tnfsf11* expressed by osteoblasts were reduced likely due to impaired osteoblast formation (Boyce et al., 2009; Lu et al., 2009) (Figure 6.1).

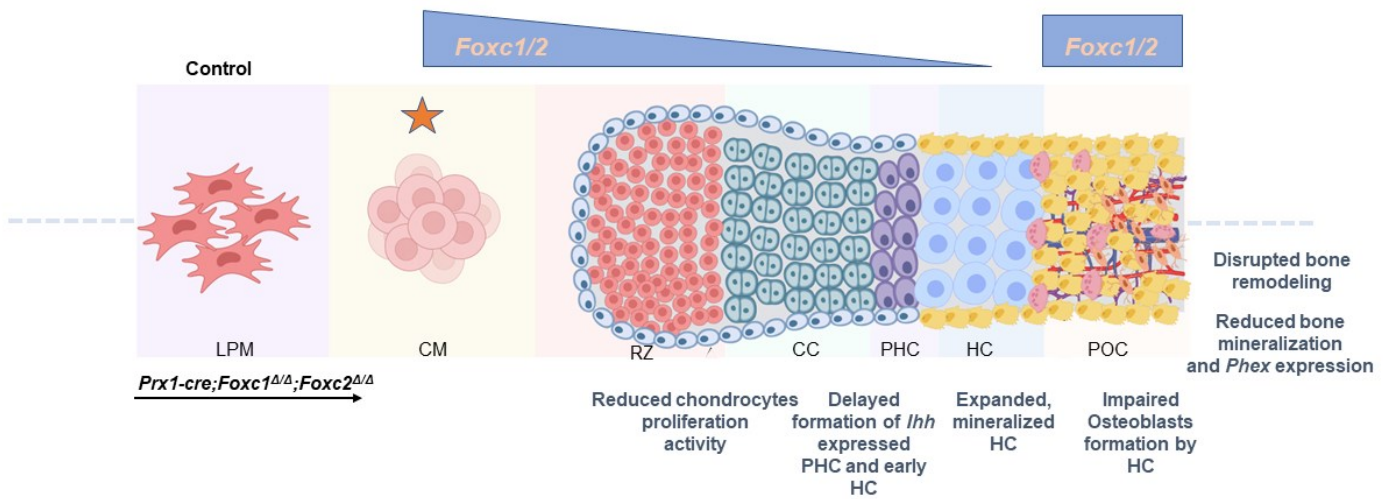


Figure 6.1 Summary of *Prx1-cre;Foxc1<sup>Δ/Δ</sup>;Foxc2<sup>Δ/Δ</sup>* growth plate phenotype.

*Foxc1* and *Foxc2* are expressed at higher levels in condensing mesenchyme cells (orange star) and immature chondrocytes. Expression was reduced in hypertrophic chondrocytes and reactivated in the osteochondral junction and POC. Deletion of *Foxc1* and *Foxc2* in limb bud mesenchyme (*Prx1-cre;Foxc1<sup>Δ/Δ</sup>;Foxc2<sup>Δ/Δ</sup>*) resulted in different phenotypic abnormalities during growth plate development including reduced chondrocyte proliferation, delay in *Ihh* expression in hypertrophic chondrocytes at E14.5. At later stages, impaired hypertrophic chondrocytes remodeling and osteoblasts formation, reduced bone mineralization and remodeling were observed. (LPM) Lateral plate mesoderm; (CM) condensing mesenchyme; (RZ) Resting zone; (CC) Columnar chondrocytes; (PHC) Pre-hypertrophic chondrocytes; (HC) Hypertrophic chondrocytes; (POC) Primary ossification center.

Loss of *Foxc1* and *Foxc2* in the limb progenitors reduced *Phex* expression in the POC, causing an accumulation of OPN and consequently, reduced bone mineralization (Addison et al., 2010; David et al., 2011). *Foxc1* and *Phex* were co-expressed in the POC. This data provides a putative mechanism of how *Foxc1* and *Foxc2* may regulate mineralization.

The fourth aim focused on whether FOXC1 and  $\beta$ -CATENIN could function together in the regulation of endochondral ossification. Overexpression of *Foxc1* can negatively regulate  $\beta$ -CATENIN transcriptional coregulatory activity in U2OS cells. We also demonstrate that FOXC1 inhibits  $\beta$ -CATENIN transcriptional regulatory activity through different ways, as S131L incompletely inhibited the TOPFlash activity without binding to DNA. Finally, we show that CHIR treatment enhanced FOXC1 transcriptional activity and increased levels of FOXC1 transfected proteins, indicating that either GSK3 inhibition or activation of  $\beta$ -CATENIN can enhance FOXC1 transactivation (Savage et al., 2010).

Deletion of *Foxc1* and *Foxc2* in the *Prx1-cre;Foxc1<sup>Δ/Δ</sup>;Foxc2<sup>Δ/Δ</sup>* mouse model led to a more severe skeletal limb phenotypes compared to the *Col2-cre;Foxc1<sup>Δ/Δ</sup>;Foxc2<sup>Δ/Δ</sup>* limbs (Almubarak et al., 2021). In *Prx1-cre;Foxc1<sup>Δ/Δ</sup>;Foxc2<sup>Δ/Δ</sup>* mice, *Foxc1* and *Foxc2* were deleted early in the lateral plate mesoderm prior to their initiation of expression in the condensing mesenchyme, whereas in the *Col2-cre;Foxc1<sup>Δ/Δ</sup>;Foxc2<sup>Δ/Δ</sup>*, both *Foxc* genes were deleted in chondrocytes when *Col2a* is expressed (Ovchinnikov et al., 2000). Looking at the difference in the phenotypic severity between limbs of the two mice models indicate that early *Foxc1* and *Foxc2* expression in the condensing mesenchyme, before chondrogenesis, is required for normal chondrocytes differentiation and patterning during growth plate development.

*Foxc1* and *Foxc2* were shown to have a stimulatory effect on chondrogenesis. For instance, in micromass cultures isolated from the sternal primordium of *Mfl<sup>-/-</sup>* (*Foxc1<sup>-/-</sup>*) embryos, fewer cartilaginous nodules were detected compared to wild type (Kume et al., 1998). Similar findings were observed with *Foxc2<sup>-/-</sup>* embryos (Winnier et al., 1997). In addition, frameshift deletion of *Foxc1* in ATDC5 cells impaired chondrogenesis, while *Foxc1* over expression in mESCs stimulated chondrogenesis. (Almubarak et al., 2021). These findings suggest that *Foxc1* and *Foxc2* function in the initiation of chondrogenesis, but their function is indispensable.

We have observed a change in *Foxc1* and *Foxc2* expression pattern over time during limb skeletal development. Expression of *Foxc1* and *Foxc2* is detected throughout the forming endochondral bone at E14.5. At later time points, expression of *Foxc1* and *Foxc2* becomes more restricted. For example, at E16.5 *Foxc1* and *Foxc2* mRNAs become restricted to the resting zone chondrocytes, the perichondrium and the POC. *Ihh* expression was affected by loss of *Foxc1* and *Foxc2* in limb bud progenitors in *Prx1-cre;Foxc1<sup>Δ/Δ</sup>;Foxc2<sup>Δ/Δ</sup>*. *Ihh* expressed region was reduced at E14.5 when *Foxc1* and *Foxc2* supposed to express on the same region (Almubarak et al., 2021; Yoshida et al., 2015). Interestingly, this effect becomes less pronounced overtime as *Ihh* expression started to normalize at E16.5 when expression of both *Foxc* genes reduced in hypertrophic chondrocytes. Early loss of FOXC1 and FOXC2 function in the limb impaired formation of *Ihh* expressed chondrocytes that compromised *Ihh* signaling proliferation marked by reduce KI67 positive cells in the growth plate chondrocytes at E14.5. This observation indicates that *Foxc1* and *Foxc2* have a stage specific function during limb endochondral development. In vertebrates, proximal bone parts (stylopod) start to develop first followed by the zeugopod and

distal bone elements in the autopod that develop at the end (Shubin et al., 1997). In this process, cells in the distal parts are less mature in comparison to the proximal bone elements. *Foxc1* and *Foxc2* expressed with higher intensity in the immature cells within the distal bone elements compared to the mature chondrocytes in the proximal parts at E16.5. This data highlights the importance of early *Foxc1* and *Foxc2* expression in regulating chondrocytes differentiation and transitioning into bone.

*Foxc1* and *Foxc2* have both overlapping and distinctive expression within the limb growth plate (Almubarak et al., 2021). For example, both *Foxc* genes expressed in the perichondrium, columnar chondrocytes, and the primary ossification center while *Foxc1* distinctively express within the chondrocyte progenitors in the resting zone (Almubarak et al., 2021). This suggest a definite function of *Foxc1* that can't be achieved by *Foxc2* in the resting zone of the growth plate. Although there were some similarities between skeletal abnormalities caused by single *Foxc1* or *Foxc2* deletion in mice, *Foxc1*<sup>-/-</sup> null mice also exhibited distinctive skeletal phenotypes. *Foxc1*<sup>-/-</sup> null mice showed absence of the cranial vault, severely underdeveloped sternum and rib cage, formation of very small vertebrae and disconnected vertebral arches (Kume et al., 1998). *Foxc2*<sup>-/-</sup> null mice develop craniofacial and vertebral column abnormalities with fused ribs. However, there were no missing cranial vault because *Foxc2* dose not express in the cranial vault mesenchyme (Winnier et al., 1999). Conditional deletion of either *Foxc1* or *Foxc2* in *Col2* positive cells also showed a similar range of skeletal abnormalities between *Foxc1* and *Foxc2* embryos at E18.5 (Almubarak et al., 2021). However, *Col2-cre;Foxc1*<sup>Δ/Δ</sup>;*Foxc2*<sup>+/Δ</sup> mutant mice developed a more severe skeletal hypoplasia with short limbs, much smaller and misshapen rib cage, underdeveloped cervical vertebrae and occipital bones. while *Col2-cre;Foxc1*<sup>+/Δ</sup>;*Foxc2*<sup>Δ/Δ</sup> embryos of similar age

displayed less severe skeletal anomalies (Almubarak et al., 2021). Yet, Compound deletion of *Foxc1* and *Foxc2* in *Col2* positive cells (*Col2-cre;Foxc1<sup>Δ/Δ</sup>;Foxc2<sup>Δ/Δ</sup>*) displayed a more severe skeletal anomalies than the single mutants (Almubarak et al., 2021). These data suggest that both *Foxc1* and *Foxc2* function together during embryonic skeletal development, and that both have overlapping and distinctive functions which indicate a compensation rather than a redundancy between the two transcription factors. We also showed that early *Foxc1* and *Foxc2* expression in endochondral progenitor cells is a key for normal transitioning from mesenchymal cells to chondrocytes and into bone. Yet, both transcription factors work at different stages during growth plate formation where they have a stage specific function throughout the growth plate. Moreover, *Foxc1* and *Foxc2* function differently in the appendicular than the axial skeleton, as the regulatory network seems to be different between these skeletal elements.

## 6.2 Limitations and future directions:

Conditional deletion of *Foxc1* and *Foxc2* in *Col2-Cre* expressing cells leads to axial skeletal phenotypes. How both *Foxc* genes function in the sclerotome and contribute to the formation of the vertebral column is not completely known. One possibility is that deletion of *Foxc1* and *Foxc2* may affected the sclerotome proliferation activity and led to the development of few cells at early time points of embryonic development. This possibility can be tested through assessing cellular proliferation within the sclerotome through KI67 or BrdU assays at E9.5 and E10.5 (Monsoro-Burq, 2005). Another likelihood is that *Foxc1* and *Foxc2* KO has impacted sclerotome migration to the notochord and around the neural tube, which prevented the vertebrae from forming normally (DeSai et al., 2022; Kalamchi and Valle, 2022; Monsoro-Burq, 2005). As mentioned earlier, this idea can be examined through performing lineage tracing of the *Col2-Cre* positive cells at early time points through crossing the *Col2-cre;Foxc1<sup>Δ/Δ</sup>;Foxc2<sup>Δ/Δ</sup>* mouse with the ROSA26<sup>tm4(ACTB-tdTomato,-EGFP)</sup>(mTmG) mouse to be able to trace GFP positive cells (Almubarak et al., 2021). Unfortunately, *Col2-cre;Foxc1<sup>Δ/Δ</sup>;Foxc2<sup>Δ/Δ</sup>*, *Col2-cre;Foxc1<sup>Δ/Δ</sup>;Foxc2<sup>+/<sup>Δ</sup></sup>*, and *Col2-cre;Foxc1<sup>+/<sup>Δ</sup></sup>;Foxc2<sup>Δ/Δ</sup>* pups die at birth, which did not allow us to assess their skeletal development postnatally (Almubarak et al., 2021). This is probably due to the formation of small, underdeveloped ribcage and absence of sternum that can impact lungs development and function, preventing the mice from surviving after birth (Almubarak et al., 2021; Kume et al., 1998). However, *Col2-cre;Foxc1<sup>+/+</sup>;Foxc2<sup>Δ/Δ</sup>* mice were viable, which gives a chance to investigate *Foxc2* role in axial and appendicular skeletal development during embryonic, and postnatal stages, and assess its relevance in bone fracture repair. Moreover, all *Prx1-cre* and *Col2-cre* mice embryos were viable during gestation, which can be employed to study the specific deletion of *Foxc1* or *Foxc2* independently using the heterozygous embryos.

We identified a distinctive *Foxc1* and *Foxc2* mRNA localization within the osteoblasts of the primary ossification center (Almubarak et al., 2021). However, how *Foxc1* and *Foxc2* function in osteoblasts and contribute to bone growth and fracture healing is not well understood. This can be achieved through using an inducible *Col2a-Cre/ERT* mouse to KO *Foxc* genes postnatally. This model can be used to assess *Foxc1* and *Foxc2* regulatory effect on both intramembranous endochondral bone formation. In addition, bone fracture testing can be also performed to test their possible contribution to bone fracture healing.

Our results demonstrated co-expression of both *Foxc1* and *Phex* within the control primary ossification center. Moreover, deletion of *Foxc1* and *Foxc2* reduced *Phex* mRNA level in the primary ossification center. This result indicates that either *Foxc1* or *Foxc2* or maybe both can regulate *Phex* expression in osteoblasts. Our lab identified FOXC1 binding to *Phex* gene via electrophoresis mobility shift assay and is currently exploring the regulation of *Phex* expression further.

Transfection of *Foxc1* had a negative effect on  $\beta$ -CATENIN activity in U2OS cells that was tested and verified using different luciferase systems. However, there is also a small possibility that overexpressing *Foxc1* in culture cells may force the cells to act differently, which might impact normal signaling pathways including  $\beta$ -CATENIN signaling activity. Moreover, we tried to assess FOXC1-  $\beta$ -CATENIN association in chondrocytes, but the osteosarcoma U2OS cells showed a much better transfection efficiency than the ATDC5 cells, which are not primary chondrocytes as well. This limitation can be overcome through verifying FOXC1 inhibitory effect on  $\beta$ -CATENIN

activity *in vivo*, using our *Prx1-cre;Foxc1<sup>Δ/Δ</sup>;Foxc2<sup>Δ/Δ</sup>* limbs that lacks *Foxc1* expression. This can be done through identifying  $\beta$ -CATENIN mRNA and protein localization and assessing the expression and localization of other  $\beta$ -CATENIN target genes in the growth plate.

## References:

- Addison, W.N., Masica, D.L., Gray, J.J., McKee, M.D., 2010. Phosphorylation-dependent inhibition of mineralization by osteopontin ASARM peptides is regulated by PHEX cleavage. *Journal of Bone and Mineral Research* 25, 695–705. <https://doi.org/10.1359/jbmr.090832>
- Aghajanian, P., Mohan, S., 2018. The art of building bone: emerging role of chondrocyte-to-osteoblast transdifferentiation in endochondral ossification. *Bone Res* 6, 19. <https://doi.org/10.1038/s41413-018-0021-z>
- Aizawa, T., Kokubun, S., Tanaka, Y., 1997. Apoptosis and proliferation of growth plate chondrocytes in rabbits. *J Bone Joint Surg Br* 79, 483–6. <https://doi.org/10.1302/0301-620x.79b3.7221>
- Akasaki, Y., Hasegawa, A., Saito, M., Asahara, H., Iwamoto, Y., Lotz, M.K., 2014. Dysregulated FOXO transcription factors in articular cartilage in aging and osteoarthritis. *Osteoarthritis Cartilage* 22, 162–70. <https://doi.org/10.1016/j.joca.2013.11.004>
- Akhurst, R.J., Padgett, R.W., 2015. Matters of context guide future research in TGF $\beta$  superfamily signaling. *Sci Signal* 8, re10. <https://doi.org/10.1126/scisignal.aad0416>
- Akiyama, H., Chaboissier, M.-C., Martin, J.F., Schedl, A., de Crombrughe, B., 2002. The transcription factor Sox9 has essential roles in successive steps of the chondrocyte differentiation pathway and is required for expression of Sox5 and Sox6. *Genes Dev* 16, 2813–28. <https://doi.org/10.1101/gad.1017802>
- Akiyama, H., Kim, J.-E., Nakashima, K., Balmes, G., Iwai, N., Min Deng, J., Zhang, Z., Martin, J.F., Behringer, R.R., Nakamura, T., de Crombrughe, B., 2005. Osteo-chondroprogenitor cells are derived from Sox9 expressing precursors.
- Alman, B.A., 2015. The role of hedgehog signalling in skeletal health and disease. *Nature Reviews Rheumatology* 11, 552–560. <https://doi.org/10.1038/nrrheum.2015.84>
- Almubarak, A., Lavy, R., Srnic, N., Hu, Y., Maripuri, D.P., Kume, T., Berry, F.B., 2021. Loss of Foxc1 and Foxc2 function in chondroprogenitor cells disrupts endochondral ossification. *Journal of Biological Chemistry* 101020. <https://doi.org/10.1016/j.jbc.2021.101020>
- Alvarez-Garcia, O., Matsuzaki, T., Olmer, M., Kohei Miyata, |, Mokuda, S., Sakai, D., Koichi Masuda, |, Asahara, H., Lotz, M.K., 2018. FOXO are required for intervertebral disk homeostasis during aging and their deficiency promotes disk degeneration. <https://doi.org/10.1111/accel.12800>
- Aoki, K., Kurashige, M., Ichii, M., Higaki, K., Sugiyama, T., Kaito, T., Ando, W., Sugano, N., Sakai, T., Shibayama, H., HANDAI Clinical Blood Club, Takaori-Kondo, A., Morii, E., Kanakura, Y., Nagasawa, T., 2021. Identification of CXCL12-abundant reticular cells in human adult bone marrow. *Br J Haematol* 193, 659–668. <https://doi.org/10.1111/bjh.17396>
- Arseni, L., Lombardi, A., Orioli, D., 2018. From Structure to Phenotype: Impact of Collagen Alterations on Human Health. *Int J Mol Sci* 19. <https://doi.org/10.3390/ijms19051407>
- Bandyopadhyay, A., Tsuji, K., Cox, K., Harfe, B.D., Rosen, V., Tabin, C.J., 2006. Genetic analysis of the roles of BMP2, BMP4, and BMP7 in limb patterning and skeletogenesis. *PLoS Genetics* 2, 2116–2130. <https://doi.org/10.1371/journal.pgen.0020216>

- Barone, C., Bartoloni, G., Baffico, A.M., Pappalardo, E., Mura, I., Ettore, G., Bianca, S., 2014. Novel c.358C>T mutation of SOX9 gene in prenatal diagnosis of campomelic dysplasia. *Congenit Anom (Kyoto)* 54, 193–4. <https://doi.org/10.1111/cga.12054>
- Barros, N.M.T., Hoac, B., Neves, R.L., Addison, W.N., Assis, D.M., Murshed, M., Carmona, A.K., McKee, M.D., 2013. Proteolytic processing of osteopontin by PHEX and accumulation of osteopontin fragments in Hyp mouse bone, the murine model of X-linked hypophosphatemia. *Journal of Bone and Mineral Research* 28, 688–699. <https://doi.org/10.1002/jbmr.1766>
- Bell, D.M., Leung, K.K., Wheatley, S.C., Ng, L.J., Zhou, S., Ling, K.W., Sham, M.H., Koopman, P., Tam, P.P., Cheah, K.S., 1997. SOX9 directly regulates the type-II collagen gene. *Nat Genet* 16, 174–8. <https://doi.org/10.1038/ng0697-174>
- Berendsen, A.D., Olsen, B.R., 2015. Bone development. *Bone* 80, 14–18. <https://doi.org/10.1016/j.bone.2015.04.035>
- Berry, F.B., Mirzayans, F., Walter, M.A., 2006. Regulation of FOXC1 stability and transcriptional activity by an epidermal growth factor-activated mitogen-activated protein kinase signaling cascade. *J Biol Chem* 281, 10098–104. <https://doi.org/10.1074/jbc.M513629200>
- Berry, F.B., Saleem, R.A., Walter, M.A., 2002. FOXC1 transcriptional regulation is mediated by N- and C-terminal activation domains and contains a phosphorylated transcriptional inhibitory domain. *J Biol Chem* 277, 10292–7. <https://doi.org/10.1074/jbc.M110266200>
- Berry, F.B., Tamimi, Y., Carle, M. v, Lehmann, O.J., Walter, M.A., 2005. The establishment of a predictive mutational model of the forkhead domain through the analyses of FOXC2 missense mutations identified in patients with hereditary lymphedema with distichiasis. *Hum Mol Genet* 14, 2619–27. <https://doi.org/10.1093/hmg/ddi295>
- Bi, W., Deng, M., Zhang, Z., Behringer, R.R., Benoit De Crombrughe, &, 1999. Sox9 is required for cartilage formation.
- Bonafe, L., Cormier-Daire, V., Hall, C., Lachman, R., Mortier, G., Mundlos, S., Nishimura, G., Sangiorgi, L., Savarirayan, R., Sillence, D., Spranger, J., Superti-Furga, A., Warman, M., Unger, S., 2015. Nosology and classification of genetic skeletal disorders: 2015 revision. *Am J Med Genet A* 167A, 2869–92. <https://doi.org/10.1002/ajmg.a.37365>
- Bourguignon, C., Li, J., Papalopulu, N., 1998. XBF-1, a winged helix transcription factor with dual activity, has a role in positioning neurogenesis in *Xenopus* competent ectoderm. *Development* 125, 4889–900. <https://doi.org/10.1242/dev.125.24.4889>
- Boyce, B.F., Yao, Z., Xing, L., 2009. Osteoclasts have multiple roles in bone in addition to bone resorption. *Crit Rev Eukaryot Gene Expr* 19, 171–80. <https://doi.org/10.1615/critreveukargeneexpr.v19.i3.10>
- Brice, G., 2002. Analysis of the phenotypic abnormalities in lymphoedema-distichiasis syndrome in 74 patients with FOXC2 mutations or linkage to 16q24. *Journal of Medical Genetics* 39, 478–483. <https://doi.org/10.1136/jmg.39.7.478>
- Brown, G., Hughes, P.J., Michell, R.H., 2003. Cell differentiation and proliferation - Simultaneous but independent? *Experimental Cell Research*. [https://doi.org/10.1016/S0014-4827\(03\)00393-8](https://doi.org/10.1016/S0014-4827(03)00393-8)
- Brunet, A., Bonni, A., Zigmond, M.J., Lin, M.Z., Juo, P., Hu, L.S., Anderson, M.J., Arden, K.C., Blenis, J., Greenberg, M.E., 1999. Akt promotes cell survival by phosphorylating and

- inhibiting a Forkhead transcription factor. *Cell* 96, 857–68. [https://doi.org/10.1016/s0092-8674\(00\)80595-4](https://doi.org/10.1016/s0092-8674(00)80595-4)
- Byon, C.H., Sun, Y., Chen, J., Yuan, K., Mao, X., Heath, J.M., Anderson, P.G., Tintut, Y., Demer, L.L., Wang, D., Chen, Y., 2011. Runx2-upregulated receptor activator of nuclear factor  $\kappa$ B ligand in calcifying smooth muscle cells promotes migration and osteoclastic differentiation of macrophages. *Arterioscler Thromb Vasc Biol* 31, 1387–96. <https://doi.org/10.1161/ATVBAHA.110.222547>
- Caddy, J.C., Luoma, L.M., Berry, F.B., 2020. FOXC1 negatively regulates BMP-SMAD activity and Id1 expression during osteoblast differentiation. *Journal of Cellular Biochemistry* 121, 3266–3277. <https://doi.org/10.1002/jcb.29595>
- Chawla, B., Bhadange, Y., Dada, R., Kumar, M., Sharma, S., Bajaj, M.S., Pushker, N., Chandra, M., Ghose, S., 2013. Clinical, Radiologic, and Genetic Features in Blepharophimosis, Ptosis, and Epicanthus Inversus Syndrome in the Indian Population. *Investigative Ophthalmology & Visual Science* 54, 2985. <https://doi.org/10.1167/iovs.13-11794>
- Chen, J., Holguin, N., Shi, Y., Silva, M.J., Long, F., 2014. mTORC2 Signaling Promotes Skeletal Growth and Bone Formation in Mice. <https://doi.org/10.1002/jbmr.2348>
- Chen, Q., Shou, P., Zhang, L., Xu, C., Zheng, C., Han, Y., Li, W., Huang, Y., Zhang, X., Shao, C., Roberts, A.I., Rabson, A.B., Ren, G., Zhang, Y., Wang, Y., Denhardt, D.T., Shi, Y., 2014. An osteopontin-integrin interaction plays a critical role in directing adipogenesis and osteogenesis by mesenchymal stem cells. *Stem Cells* 32, 327–337. <https://doi.org/10.1002/stem.1567>
- Choi, H.J., Park, H., Lee, H.W., Kwon, Y.G., 2012. The Wnt pathway and the roles for its antagonists, DKKS, in angiogenesis. *IUBMB Life* 64, 724–731. <https://doi.org/10.1002/iub.1062>
- Civelek, M., Lusic, A.J., Genetics, M., Angeles, L., 2014. *HHS Public Access* 15, 34–48. <https://doi.org/10.1038/nrg3575>
- Clark, K.L., Halay, E.D., Lai, E., Burley, S.K., 1993. Co-crystal structure of the HNF-3/fork head DNA-recognition motif resembles histone H5. *Nature* 364, 412–420. <https://doi.org/10.1038/364412a0>
- Clevers, H., 2006. Wnt/beta-catenin signaling in development and disease. *Cell* 127, 469–80. <https://doi.org/10.1016/j.cell.2006.10.018>
- Cloete, E., Battin, M.R., Imam, F.B., Teele, R.L., 2013. Ossification of sacral vertebral bodies in neonates born 24 to 38 weeks' gestational age and its relevance to spinal ultrasonography. *Am J Perinatol* 30, 519–22. <https://doi.org/10.1055/s-0032-1329186>
- Colnot, C., Lu, C., Hu, D., Helms, J.A., 2004. Distinguishing the contributions of the perichondrium, cartilage, and vascular endothelium to skeletal development. *Dev Biol* 269, 55–69. <https://doi.org/10.1016/j.ydbio.2004.01.011>
- Correa-Cerro, L.S., Piao, Y., Sharov, A.A., Nishiyama, A., Cadet, J.S., Yu, H., Sharova, L. v, Xin, L., Hoang, H.G., Thomas, M., Qian, Y., Dudekula, D.B., Meyers, E., Binder, B.Y., Mowrer, G., Basse, U., Longo, D.L., Schlessinger, D., Ko, M.S.H., 2011. Generation of mouse ES cell lines engineered for the forced induction of transcription factors. *Sci Rep* 1, 167. <https://doi.org/10.1038/srep00167>

- Couly, G.F., Coltey, P.M., le Douarin, N.M., 1992. The developmental fate of the cephalic mesoderm in quail-chick chimeras. *Development* 114, 1–15.  
<https://doi.org/10.1242/dev.114.1.1>
- Cui, Y.-M., Jiao, H.-L., Ye, Y.-P., Chen, C.-M., Wang, J.-X., Tang, N., Li, T.-T., Lin, J., Qi, L., Wu, P., Wang, S.-Y., He, M.-R., Liang, L., Bian, X.-W., Liao, W.-T., Ding, Y.-Q., 2015. FOXC2 promotes colorectal cancer metastasis by directly targeting MET. *Oncogene* 34, 4379–90.  
<https://doi.org/10.1038/onc.2014.368>
- Czarny-Ratajczak, M., Lohiniva, J., Rogala, P., Kozłowski, K., Perälä, M., Carter, L., Spector, T.D., Kolodziej, L., Seppänen, U., Glazar, R., Królewski, J., Latos-Bielenska, A., Ala-Kokko, L., 2001. A mutation in COL9A1 causes multiple epiphyseal dysplasia: further evidence for locus heterogeneity. *Am J Hum Genet* 69, 969–80. <https://doi.org/10.1086/324023>
- Danciu, T.E., Chupreta, S., Cruz, O., Fox, J.E., Whitman, M., Iñiguez-Lluhí, J.A., 2012. Small ubiquitin-like modifier (SUMO) modification mediates function of the inhibitory domains of developmental regulators FOXC1 and FOXC2. *J Biol Chem* 287, 18318–29.  
<https://doi.org/10.1074/jbc.M112.339424>
- Dao, D.Y., Jonason, J.H., Zhang, Y., Hsu, W., Chen, D., Hilton, M.J., O’Keefe, R.J., 2012. Cartilage-specific  $\beta$ -catenin signaling regulates chondrocyte maturation, generation of ossification centers, and perichondrial bone formation during skeletal development. *J Bone Miner Res* 27, 1680–94. <https://doi.org/10.1002/jbmr.1639>
- David, V., Martin, A., Hedge, A.M., Drezner, M.K., Rowe, P.S.N., 2011. Asarm peptides: PHEX-dependent and -independent regulation of serum phosphate. *American Journal of Physiology - Renal Physiology* 300. <https://doi.org/10.1152/AJPRENAL.00304.2010>
- de Vos, I.J.H.M., Stegmann, A.P.A., Webers, C.A.B., Stumpel, C.T.R.M., 2017. The 6p25 deletion syndrome: An update on a rare neurocristopathy. *Ophthalmic Genetics* 38, 101–107.  
<https://doi.org/10.3109/13816810.2016.1164191>
- DeSai, C., Reddy, V., Agarwal, A., 2022. Anatomy, Back, Vertebral Column.
- Docherty, B., 2007. Skeletal system. Part Three--The axial skeleton. *Nurs Times* 103, 26–7.
- Dressler, S., Meyer-Marcotty, P., Weissschuh, N., Jablonski-Momeni, A., Pieper, K., Gramer, G., Gramer, E., 2010. Case Report Dental and Craniofacial Anomalies Associated with Axenfeld-Rieger Syndrome with PITX2 Mutation. *Case Reports in Medicine* 2010.  
<https://doi.org/10.1155/2010/621984>
- Dy, P., Wang, W., Bhattaram, P., Wang, Q., Wang, L., Ballock, R.T., Lefebvre, V., 2012. Sox9 Directs Hypertrophic Maturation and Blocks Osteoblast Differentiation of Growth Plate Chondrocytes. *Developmental Cell* 22, 597–609.  
<https://doi.org/10.1016/j.devcel.2011.12.024>
- Enishi, T., Yukata, K., Takahashi, M., Sato, R., Sairyō, K., Yasui, N., 2014. Hypertrophic chondrocytes in the rabbit growth plate can proliferate and differentiate into osteogenic cells when capillary invasion is interposed by a membrane filter. *PLoS ONE* 9.  
<https://doi.org/10.1371/journal.pone.0104638>
- FALLS, H.F., KERTESZ, E.D., 1964. A NEW SYNDROME COMBINING PTERYGIUM COLLI WITH DEVELOPMENTAL ANOMALIES OF THE EYELIDS AND LYMPHATICS OF THE LOWER EXTREMITIES. *Trans Am Ophthalmol Soc* 62, 248–75.

- Fang, J., Dagenais, S.L., Erickson, R.P., Arlt, M.F., Glynn, M.W., Gorski, J.L., Seaver, L.H., Glover, T.W., 2000a. Mutations in FOXC2 (MFH-1), a Forkhead Family Transcription Factor, Are Responsible for the Hereditary Lymphedema-Distichiasis Syndrome. *Am. J. Hum. Genet* 67, 1382–1388.
- Fang, J., Dagenais, S.L., Erickson, R.P., Arlt, M.F., Glynn, M.W., Gorski, J.L., Seaver, L.H., Glover, T.W., 2000b. Mutations in FOXC2 (MFH-1), a Forkhead Family Transcription Factor, Are Responsible for the Hereditary Lymphedema-Distichiasis Syndrome. *The American Journal of Human Genetics* 67, 1382–1388. <https://doi.org/10.1086/316915>
- Farnum, C.E., Wilsman, N.J., 1987. Morphologic stages of the terminal hypertrophic chondrocyte of growth plate cartilage. *The Anatomical Record* 219, 221–232. <https://doi.org/10.1002/ar.1092190303>
- Franz-Odenaal, T.A., 2011. Induction and patterning of intramembranous bone. *Front Biosci (Landmark Ed)* 16, 2734–46. <https://doi.org/10.2741/3882>
- Freyaldenhoven, B.S., Freyaldenhoven, M.P., Iacovoni, J.S., Vogt, P.K., 1997. Avian winged helix proteins CWH-1, CWH-2 and CWH-3 repress transcription from Qin binding sites. *Oncogene* 15, 483–8. <https://doi.org/10.1038/sj.onc.1201189>
- Geister, K.A., Camper, S.A., 2015. Advances in Skeletal Dysplasia Genetics. Downloaded from [www.annualreviews.org](http://www.annualreviews.org) Access 16, 199–227. <https://doi.org/10.1146/annurev-genom-090314-045904>
- Gerber, H.P., Vu, T.H., Ryan, A.M., Kowalski, J., Werb, Z., Ferrara, N., 1999. VEGF couples hypertrophic cartilage remodeling, ossification and angiogenesis during endochondral bone formation. *Nature Medicine* 5, 623–628. <https://doi.org/10.1038/9467>
- Gerdes, J., Lemke, H., Baisch, H., Wacker, H.H., Schwab, U., Stein, H., 1984. Cell cycle analysis of a cell proliferation-associated human nuclear antigen defined by the monoclonal antibody Ki-67. *J Immunol* 133, 1710–5.
- Gerdes, S.J., Lemke, H., Baisch, H., Wacker, H.H., Schwab, U., 1984. Ki-67. antigen defined by the monoclonal antibody proliferation-associated human nuclear Cell cycle analysis of a cell.
- Gibson, G., 1998. Active role of chondrocyte apoptosis in endochondral ossification. *Microscopy Research and Technique*. [https://doi.org/10.1002/\(SICI\)1097-0029\(19981015\)43:2<191::AID-JEMT10>3.0.CO;2-T](https://doi.org/10.1002/(SICI)1097-0029(19981015)43:2<191::AID-JEMT10>3.0.CO;2-T)
- Gkirginoudis, A., Tatsi, C., DeWard, S.J., Friedman, B., Faucz, F.R., Stratakis, C.A., 2020. A SOX5 gene variant as a possible contributor to short stature. *Endocrinol Diabetes Metab Case Rep* 2020. <https://doi.org/10.1530/EDM-20-0133>
- Glass, D.A., Bialek, P., Ahn, J.D., Starbuck, M., Patel, M.S., Clevers, H., Taketo, M.M., Long, F., McMahon, A.P., Lang, R.A., Karsenty, G., 2005. Canonical Wnt signaling in differentiated osteoblasts controls osteoclast differentiation. *Dev Cell* 8, 751–64. <https://doi.org/10.1016/j.devcel.2005.02.017>
- Glinka, A., Wu, W., Delius, H., Monaghan, A.P., Blumenstock, C., Niehrs, C., 1998. Dickkopf-1 is a member of a new family of secreted proteins and functions in head induction. *Nature* 391, 357–362. <https://doi.org/10.1038/34848>
- Green, A.C., Rudolph-Stringer, V., Straszowski, L., Tjin, G., Crimeen-Irwin, B., Walia, M., Martin, T.J., Sims, N.A., Purton, L.E., 2018. Retinoic Acid Receptor g Activity in Mesenchymal Stem

- Cells Regulates Endochondral Bone, Angiogenesis, and B Lymphopoiesis.  
<https://doi.org/10.1002/jbmr.3558>
- Guo, X., Day, T.F., Jiang, X., Garrett-Beal, L., Topol, L., Yang, Y., 2004. Wnt/beta-catenin signaling is sufficient and necessary for synovial joint formation. *Genes Dev* 18, 2404–17.  
<https://doi.org/10.1101/gad.1230704>
- Guo, X., Mak, K.K., Taketo, M.M., Yang, Y., 2009. The Wnt/ $\beta$ -catenin pathway interacts differentially with PTHrP signaling to control chondrocyte hypertrophy and final maturation. *PLoS ONE* 4. <https://doi.org/10.1371/journal.pone.0006067>
- Hajihosseini, M.K., Lalioti, M.D., Arthaud, S., Burgar, H.R., Brown, J.M., Twigg, S.R.F., Wilkie, A.O.M., Heath, J.K., 2004. Skeletal development is regulated by fibroblast growth factor receptor 1 signalling dynamics. *Development* 131, 325–335.  
<https://doi.org/10.1242/dev.00940>
- Hallett, S.A., Matsushita, Y., Ono, W., Sakagami, N., Mizuhashi, K., Tokavanich, N., Nagata, M., Zhou, A., Hirai, T., Kronenberg, H.M., Ono, N., 2021. Chondrocytes in the resting zone of the growth plate are maintained in a Wnt-inhibitory environment. *Elife* 10.  
<https://doi.org/10.7554/eLife.64513>
- Harrison, M., O'Brien, A., Adams, L., Cowin, G., Ruitenberg, M.J., Sengul, G., Watson, C., 2013. Vertebral landmarks for the identification of spinal cord segments in the mouse. *Neuroimage* 68, 22–29. <https://doi.org/10.1016/J.NEUROIMAGE.2012.11.048>
- Hayashi, H., Kume, T., 2008. Foxc transcription factors directly regulate Dll4 and Hey2 expression by interacting with the VEGF-Notch signaling pathways in endothelial cells. *PLoS One* 3, e2401. <https://doi.org/10.1371/journal.pone.0002401>
- Henry, S.P., Jang, C.-W., Deng, J.M., Zhang, Z., Behringer, R.R., de Crombrughe, B., 2009. Generation of aggrecan-CreERT2 knockin mice for inducible Cre activity in adult cartilage. *Genesis* 47, 805–14. <https://doi.org/10.1002/dvg.20564>
- Hiemisch, H., Monaghan, A.P., Schütz, G., Kaestner, K.H., 1998. Expression of the mouse Fkh1/Mf1 and Mfh1 genes in late gestation embryos is restricted to mesoderm derivatives. *Mech Dev* 73, 129–32. [https://doi.org/10.1016/s0925-4773\(98\)00039-2](https://doi.org/10.1016/s0925-4773(98)00039-2)
- Hill-Harfe, K.L., Kaplan, L., Stalker, H.J., Zori, R.T., Pop, R., Scherer, G., Wallace, M.R., 2005. Fine mapping of chromosome 17 translocation breakpoints  $\geq$  900 Kb upstream of SOX9 in acampomelic campomelic dysplasia and a mild, familial skeletal dysplasia. *Am J Hum Genet* 76, 663–71. <https://doi.org/10.1086/429254>
- Hjalt, T.A., Semina, E. v, 2005. Current molecular understanding of Axenfeld-Rieger syndrome. *Expert Rev Mol Med* 7, 1–17. <https://doi.org/10.1017/S1462399405010082>
- Hong, H.K., Lass, J.H., Chakravarti, A., 1999. Pleiotropic skeletal and ocular phenotypes of the mouse mutation congenital hydrocephalus (ch/Mf1) arise from a winged helix/forkhead transcription factor gene. *Hum Mol Genet* 8, 625–37.
- Hopkins, A., Coatham, M.L., Berry, F.B., 2017. FOXC1 Regulates FGFR1 Isoform Switching to Promote Invasion Following TGF $\beta$ -Induced EMT. *Molecular Cancer Research* 15, 1341–1353. <https://doi.org/10.1158/1541-7786.MCR-17-0185>
- Hopkins, A., Mirzayans, F., Berry, F., 2016. Foxc1 Expression in Early Osteogenic Differentiation Is Regulated by BMP4-SMAD Activity. *Journal of Cellular Biochemistry* 117, 1707–1717. <https://doi.org/10.1002/jcb.25464>

- Houben, A., Kostanova-Poliakova, D., Weissenböck, M., Graf, J., Teufel, S., von der Mark, K., Hartmann, C., 2016.  $\beta$ -catenin activity in late hypertrophic chondrocytes locally orchestrates osteoblastogenesis and osteoclastogenesis. *Development* 143, 3826–3838. <https://doi.org/10.1242/dev.137489>
- Hu, D.P., Ferro, F., Yang, F., Taylor, A.J., Chang, W., Miclau, T., Marcucio, R.S., Bahney, C.S., 2017. Cartilage to bone transformation during fracture healing is coordinated by the invading vasculature and induction of the core pluripotency genes. *Development (Cambridge)* 144, 221–234. <https://doi.org/10.1242/dev.130807>
- Hung, I.H., Schoenwolf, G.C., Lewandoski, M., Ornitz, D.M., 2016. A combined series of Fgf9 and Fgf18 mutant alleles identifies unique and redundant roles in skeletal development. *Dev Biol* 411, 72–84. <https://doi.org/10.1016/j.ydbio.2016.01.008>
- Iida, K., Koseki, H., Kakinuma, H., Kato, N., Mizutani-Koseki, Y., Ohuchi, H., Yoshioka, H., Noji, S., Kawamura, K., Kataoka, Y., Ueno, F., Taniguchi, M., Yoshida, N., Sugiyama, T., Miura, N., 1997. Essential roles of the winged helix transcription factor MFH-1 in aortic arch patterning and skeletogenesis. *Development* 124, 4627–4638. <https://doi.org/10.1242/dev.124.22.4627>
- Ikram, M.S., Neill, G.W., Regl, G., Eichberger, T., Frischauf, A.-M., Aberger, F., Quinn, A., Philpott, M., 2004. GLI2 Is Expressed in Normal Human Epidermis and BCC and Induces GLI1 Expression by Binding to its Promoter. *Journal of Investigative Dermatology* 122, 1503–1509. <https://doi.org/10.1111/j.0022-202X.2004.22612.x>
- Inada, M., Wang, Y., Byrne, M.H., Rahman, M.U., Miyaura, C., López-Otín, C., Krane, S.M., 2004. Critical roles for collagenase-3 (Mmp13) in development of growth plate cartilage and in endochondral ossification. *Proc Natl Acad Sci U S A* 101, 17192–17197. <https://doi.org/10.1073/pnas.0407788101>
- Ionescu, A., Kozhemyakina, E., Nicolae, C., Kaestner, K.H., Olsen, B.R., Lassar, A.B., 2012a. FoxA Family Members Are Crucial Regulators of the Hypertrophic Chondrocyte Differentiation Program. *Developmental Cell* 22, 927–939. <https://doi.org/10.1016/J.DEVCEL.2012.03.011>
- Ionescu, A., Kozhemyakina, E., Nicolae, C., Kaestner, K.H., Olsen, B.R., Lassar, A.B., 2012b. FoxA family members are crucial regulators of the hypertrophic chondrocyte differentiation program. <https://doi.org/10.1016/j.devcel.2012.03.011>
- Jackson, B.C., Carpenter, C., Nebert, D.W., Vasiliou, V., 2010. Update of human and mouse forkhead box (FOX) gene families. *Hum Genomics* 4, 345–52. <https://doi.org/10.1186/1479-7364-4-5-345>
- Joeng, K.S., Long, F., 2009. The Gli2 transcriptional activator is a crucial effector for Ihh signaling in osteoblast development and cartilage vascularization. *Development* 136, 4177–85. <https://doi.org/10.1242/dev.041624>
- Kalamchi, L., Valle, C., 2022. Embryology, Vertebral Column Development.
- Kannu, P., Bateman, J., Savarirayan, R., 2012. Clinical phenotypes associated with type II collagen mutations. *J Paediatr Child Health* 48, E38-43. <https://doi.org/10.1111/j.1440-1754.2010.01979.x>
- Kannu, P., Oei, P., Slater, H.R., Khammy, O., Aftimos, S., 2006. Epiphyseal dysplasia and other skeletal anomalies in a patient with the 6p25 microdeletion syndrome. *American Journal of Medical Genetics Part A* 140A, 1955–1959. <https://doi.org/10.1002/ajmg.a.31411>

- Kaplan, K.M., Spivak, J.M., Bendo, J.A., 2005. Embryology of the spine and associated congenital abnormalities. *The Spine Journal* 5, 564–576.  
<https://doi.org/10.1016/j.spinee.2004.10.044>
- Karamboulas, K., Dranse, H.J., Underhill, T.M., 2010. Regulation of BMP-dependent chondrogenesis in early limb mesenchyme by TGF $\beta$  signals. *Journal of Cell Science* 123, 2068–2076. <https://doi.org/10.1242/jcs.062901>
- Karp, S.J., Schipani, E., St-Jacques, B., Hunzelman, J., Kronenberg, H., McMahon, A.P., 2000. Indian hedgehog coordinates endochondral bone growth and morphogenesis via parathyroid hormone related-protein-dependent and -independent pathways. *Development* 127, 543–8. <https://doi.org/10.1242/dev.127.3.543>
- Kato, Masuko, Kato, Masaru, 2004. Human FOX gene family (Review). *Int J Oncol* 25, 1495–500.
- Kawaguchi, J., Mee, P.J., Smith, A.G., 2005. Osteogenic and chondrogenic differentiation of embryonic stem cells in response to specific growth factors. *Bone* 36, 758–769.  
<https://doi.org/10.1016/j.bone.2004.07.019>
- Kawano, Y., Kypta, R., 2003. Secreted antagonists of the Wnt signalling pathway. *J Cell Sci* 116, 2627–34. <https://doi.org/10.1242/jcs.00623>
- Kishimoto, H., Akagi, M., Zushi, S., Teramura, T., Onodera, Y., Sawamura, T., Hamanishi, C., 2010. Induction of hypertrophic chondrocyte-like phenotypes by oxidized LDL in cultured bovine articular chondrocytes through increase in oxidative stress. *Osteoarthritis Cartilage* 18, 1284–90. <https://doi.org/10.1016/j.joca.2010.05.021>
- Klenova, E.M., Chernukhin, I. v, El-Kady, A., Lee, R.E., Pugacheva, E.M., Loukinov, D.I., Goodwin, G.H., Delgado, D., Filippova, G.N., León, J., Morse, H.C., Neiman, P.E., Lobanenkova, V. v, 2001. Functional phosphorylation sites in the C-terminal region of the multivalent multifunctional transcriptional factor CTCF. *Mol Cell Biol* 21, 2221–34.  
<https://doi.org/10.1128/MCB.21.6.2221-2234.2001>
- Kobayashi, T., Chung, U. il, Schipani, E., Starbuck, M., Karsenty, G., Katagiri, T., Goad, D.L., Lanske, B., Kronenberg, H.M., 2002. PTHrP and Indian hedgehog control differentiation of growth plate chondrocytes at multiple steps. *Development* 129, 2977–2986.
- Kobayashi, T., Soegiarto, D.W., Yang, Y., Lanske, B., Schipani, E., McMahon, A.P., Kronenberg, H.M., 2005. Indian hedgehog stimulates periarticular chondrocyte differentiation to regulate growth plate length independently of PTHrP. *J Clin Invest* 115, 1734–42.  
<https://doi.org/10.1172/JCI24397>
- Koziel, L., 2005. Gli3 acts as a repressor downstream of Ihh in regulating two distinct steps of chondrocyte differentiation. *Development* 132, 5249–5260.  
<https://doi.org/10.1242/dev.02097>
- Krakov, D., 2015. Skeletal dysplasias. *Clin Perinatol* 42, 301–19, viii.  
<https://doi.org/10.1016/j.clp.2015.03.003>
- Kume, T., Deng, K.Y., Winfrey, V., Gould, D.B., Walter, M.A., Hogan, B.L., 1998. The forkhead/winged helix gene *Mf1* is disrupted in the pleiotropic mouse mutation congenital hydrocephalus. *Cell* 93, 985–96. [https://doi.org/10.1016/s0092-8674\(00\)81204-0](https://doi.org/10.1016/s0092-8674(00)81204-0)
- Kume, T., Jiang, H., Topczewska, J.M., Hogan, B.L.M., 2001. The murine winged helix transcription factors, *Foxc1* and *Foxc2*, are both required for cardiovascular development

- and somitogenesis. *Genes and Development* 15, 2470–2482.  
<https://doi.org/10.1101/gad.907301>
- Lademann, F., Hofbauer, L.C., Rauner, M., 2020. The Bone Morphogenetic Protein Pathway: The Osteoclastic Perspective. *Frontiers in Cell and Developmental Biology*.  
<https://doi.org/10.3389/fcell.2020.586031>
- Lam, E.W.-F., Brosens, J.J., Gomes, A.R., Koo, C.-Y., 2013. Forkhead box proteins: tuning forks for transcriptional harmony. *Nat Rev Cancer* 13, 482–95. <https://doi.org/10.1038/nrc3539>
- Laing, K.L., Cortes, M., Domowicz, M.S., Henry, J.G., Baria, A.T., Schwartz, N.B., 2014. Aggrecan is required for growth plate cytoarchitecture and differentiation. *Dev Biol* 396, 224–36.  
<https://doi.org/10.1016/j.ydbio.2014.10.005>
- Lee, Y.C., Song, I.W., Pai, Y.J., Chen, S. de, Chen, Y.T., 2017. Knock-in human FGFR3 achondroplasia mutation as a mouse model for human skeletal dysplasia. *Scientific Reports* 7. <https://doi.org/10.1038/SREP43220>
- Lefebvre, V., Behringer, R.R., de Crombrughe, B., 2001. L-Sox5, Sox6 and Sox9 control essential steps of the chondrocyte differentiation pathway. *Osteoarthritis Cartilage* 9 Suppl A, S69-75. <https://doi.org/10.1053/joca.2001.0447>
- Lefebvre, V., Smits, P., 2005. Transcriptional control of chondrocyte fate and differentiation. *Birth Defects Research Part C - Embryo Today: Reviews* 75, 200–212.  
<https://doi.org/10.1002/bdrc.20048>
- Lehmann, O.J., Ebenezer, N.D., Jordan, T., Fox, M., Ocala, L., Payne, A., Leroy, B.P., Clark, B.J., Hitchings, R.A., Povey, S., Khaw, P.T., Bhattacharya, S.S., 2000. Chromosomal Duplication Involving the Forkhead Transcription Factor Gene FOXC1 Causes Iris Hypoplasia and Glaucoma. *Am. J. Hum. Genet* 67, 1129–1135.
- Li, C., Ding, H., Tian, J., Wu, L., Wang, Y., Xing, Y., Chen, M., 2016. Forkhead Box Protein C2 (FOXC2) Promotes the Resistance of Human Ovarian Cancer Cells to Cisplatin In Vitro and In Vivo. *Cell Physiol Biochem* 39, 242–52. <https://doi.org/10.1159/000445620>
- Lian, X., Hsiao, C., Wilson, G., Zhu, K., Hazeltine, L.B., Azarin, S.M., Raval, K.K., Zhang, J., Kamp, T.J., Palecek, S.P., 2012. Robust cardiomyocyte differentiation from human pluripotent stem cells via temporal modulation of canonical Wnt signaling. *Proceedings of the National Academy of Sciences* 109. <https://doi.org/10.1073/pnas.1200250109>
- Liu, C.-F., Angelozzi, M., Haseeb, A., Lefebvre, V., 2018. SOX9 is dispensable for the initiation of epigenetic remodeling and the activation of marker genes at the onset of chondrogenesis. *Development* 145. <https://doi.org/10.1242/dev.164459>
- Logan, M., Martin, J.F., Nagy, A., Lobe, C., Olson, E.N., Tabin, C.J., 2002. Expression of Cre recombinase in the developing mouse limb bud driven by aPrxl enhancer. *genesis* 33, 77–80. <https://doi.org/10.1002/gene.10092>
- Lu, X., Su, N., Yang, J., Huang, W., Li, C., Zhao, L., He, Q., Du, X., Shen, Y., Chen, B., Chen, L., 2009. Fibroblast growth factor receptor 1 regulates the differentiation and activation of osteoclasts through Erk1/2 pathway. *Biochemical and Biophysical Research Communications* 390, 494–499. <https://doi.org/10.1016/j.bbrc.2009.09.123>
- MacDonald, B.T., Tamai, K., He, X., 2009. Wnt/beta-catenin signaling: components, mechanisms, and diseases. *Dev Cell* 17, 9–26.  
<https://doi.org/10.1016/j.devcel.2009.06.016>

- Machol, K., Mendoza-Londono, R., Lee, B., 1993. Cleidocranial Dysplasia Spectrum Disorder.
- Mallo, M., 2016. The Axial Musculoskeletal System. Kaufman's Atlas of Mouse Development Supplement 165–175. <https://doi.org/10.1016/b978-0-12-800043-4.00013-0>
- Mangiavini, L., Merceron, C., Schipani, E., 2016. Analysis of Mouse Growth Plate Development, Current protocols in mouse biology. <https://doi.org/10.1002/9780470942390.mo150094>
- Mansour, S., Brice, G.W., Jeffery, S., Mortimer, P., 1993. Lymphedema-Distichiasis Syndrome.
- Mao, B., Wu, W., Davidson, G., Marhold, J., Li, M., Mechler, B.M., Dellus, H., Hoppe, D., Stannek, P., Walter, C., Glinka, A., Niehrs, C., 2002. Kremen proteins are Dickkopf receptors that regulate Wnt/ $\beta$ -catenin signalling. *Nature* 417, 664–667. <https://doi.org/10.1038/nature756>
- Mao, B., Wu, W., Li, Y., Hoppe, D., Stannek, P., Glinka, A., Niehrs, C., 2001. LDL-receptor-related protein 6 is a receptor for Dickkopf proteins. *Nature* 411, 321–325. <https://doi.org/10.1038/35077108>
- Marini, J.C., Blissett, A.R., 2013. New genes in bone development: what's new in osteogenesis imperfecta. *J Clin Endocrinol Metab* 98, 3095–103. <https://doi.org/10.1210/jc.2013-1505>
- Matsushita, Y., Nagata, M., Kozloff, K.M., Welch, J.D., Mizuhashi, K., Tokavanich, N., Hallett, S.A., Link, D.C., Nagasawa, T., Ono, W., Ono, N., 2020. A Wnt-mediated transformation of the bone marrow stromal cell identity orchestrates skeletal regeneration. *Nature Communications* 11. <https://doi.org/10.1038/s41467-019-14029-w>
- Mattiske, D., Sommer, P., Kidson, S.H., Hogan, B.L.M., 2006. The role of the forkhead transcription factor, *Foxc1*, in the development of the mouse lacrimal gland. *Dev Dyn* 235, 1074–80. <https://doi.org/10.1002/dvdy.20702>
- Maupin, K.A., Droscha, C.J., Williams, B.O., 2013. A Comprehensive Overview of Skeletal Phenotypes Associated with Alterations in Wnt/ $\beta$ -catenin Signaling in Humans and Mice Overview of Wnt signal transduction. *Bone Research* 1, 27–71. <https://doi.org/10.4248/BR201301004>
- McBride-Gagyi, S.H., McKenzie, J.A., Buettmann, E.G., Gardner, M.J., Silva, M.J., 2015. *Bmp2* conditional knockout in osteoblasts and endothelial cells does not impair bone formation after injury or mechanical loading in adult mice. *Bone* 81, 533–543. <https://doi.org/10.1016/j.bone.2015.09.003>
- Mears, A.J., Jordan, T., Mirzayans, F., Dubois, S., Kume, T., Parlee, M., Ritch, R., Koop, B., Kuo, W.-L., Collins, C., Marshall, J., Gould, D.B., Pearce, W., Carlsson, P., Enerbäck, S., Morissette, J., Bhattacharya, S., Hogan, B., Raymond, V., Walter, M.A., 1998. Mutations of the Forkhead/Winged-Helix Gene, *FKHL7*, in Patients with Axenfeld-Rieger Anomaly. *The American Journal of Human Genetics* 63, 1316–1328. <https://doi.org/10.1086/302109>
- Méjécasse, C., Nigam, C., Moosajee, M., Bladen, J.C., 2021. The Genetic and Clinical Features of *FOXL2*-Related Blepharophimosis, Ptosis and Epicanthus Inversus Syndrome. <https://doi.org/10.3390/genes>
- Miao, D., Liu, H., Plut, P., Niu, M., Huo, R., Goltzman, D., Henderson, J.E., 2004. Impaired endochondral bone development and osteopenia in *Gli2*-deficient mice. *Exp Cell Res* 294, 210–22. <https://doi.org/10.1016/j.yexcr.2003.10.021>

- Mizuhashi, K., Nagata, M., Matsushita, Y., Ono, W., Ono, N., 2019. Growth Plate Borderline Chondrocytes Behave as Transient Mesenchymal Precursor Cells. *Journal of Bone and Mineral Research* 34, 1387–1392. <https://doi.org/10.1002/jbmr.3719>
- Mo, R., Freer, a M., Zinyk, D.L., Crackower, M. a, Michaud, J., Heng, H.H., Chik, K.W., Shi, X.M., Tsui, L.C., Cheng, S.H., Joyner, a L., Hui, C., 1997. Specific and redundant functions of Gli2 and Gli3 zinc finger genes in skeletal patterning and development. *Development* 124, 113–123.
- Monsoro-Burq, A.H., 2005. Sclerotome development and morphogenesis: When experimental embryology meets genetics. *International Journal of Developmental Biology* 49, 301–308. <https://doi.org/10.1387/ijdb.041953am>
- Murtaugh, L.C., Chyung, J.H., Lassar, A.B., 1999. Sonic hedgehog promotes somitic chondrogenesis by altering the cellular response to BMP signaling. *Genes & Development* 13, 225–237. <https://doi.org/10.1101/gad.13.2.225>
- Nishimura, D.Y., Searby, C.C., Alward, W.L., Walton, D., Craig, J.E., Mackey, D.A., Kawase, K., Kanis, A.B., Patil, S.R., Stone, E.M., Sheffield, V.C., 2001. A spectrum of FOXC1 mutations suggests gene dosage as a mechanism for developmental defects of the anterior chamber of the eye. *Am J Hum Genet* 68, 364–72. <https://doi.org/10.1086/318183>
- Nishimura, D.Y., Swiderski, R.E., Alward, W.L., Searby, C.C., Patil, S.R., Bennet, S.R., Kanis, A.B., Gastier, J.M., Stone, E.M., Sheffield, V.C., 1998. The forkhead transcription factor gene FKHL7 is responsible for glaucoma phenotypes which map to 6p25. *Nat Genet* 19, 140–7. <https://doi.org/10.1038/493>
- Nishiyama, A., Xin, L., Sharov, A.A., Thomas, M., Mowrer, G., Meyers, E., Piao, Y., Mehta, S., Yee, S., Nakatake, Y., Stagg, C., Sharova, L., Correa-Cerro, L.S., Basse, U., Hoang, H., Kim, E., Tapnio, R., Qian, Y., Dudekula, D., Zalzman, M., Li, M., Falco, G., Yang, H.-T., Lee, S.-L., Monti, M., Stanghellini, I., Islam, M.N., Nagaraja, R., Goldberg, I., Wang, W., Longo, D.L., Schlessinger, D., Ko, M.S.H., 2009. Uncovering early response of gene regulatory networks in ESCs by systematic induction of transcription factors. *Cell Stem Cell* 5, 420–33. <https://doi.org/10.1016/j.stem.2009.07.012>
- Ohba, S., 2016. Hedgehog Signaling in Endochondral Ossification. *Journal of Developmental Biology* 4, 20. <https://doi.org/10.3390/jdb4020020>
- Ohba, S., He, X., Hojo, H., McMahon, A.P., 2015. Distinct Transcriptional Programs Underlie Sox9 Regulation of the Mammalian Chondrocyte. *Cell Rep* 12, 229–43. <https://doi.org/10.1016/j.celrep.2015.06.013>
- Omatsu, Y., Seike, M., Sugiyama, T., Kume, T., Nagasawa, T., 2014. Foxc1 is a critical regulator of haematopoietic stem/progenitor cell niche formation. *Nature* 508, 536–40. <https://doi.org/10.1038/nature13071>
- Ono, N., Ono, W., Nagasawa, T., Kronenberg, H.M., 2014. A subset of chondrogenic cells provides early mesenchymal progenitors in growing bones. <https://doi.org/10.1038/ncb3067>
- Ornitz, D.M., Marie, P.J., 2015. Fibroblast growth factor signaling in skeletal development and disease. *Genes Dev* 29, 1463–86. <https://doi.org/10.1101/gad.266551.115>

- Ovchinnikov, D.A., Deng, J.M., Ogunrinu, G., Behringer, R.R., 2000. Col2a1-directed expression of Cre recombinase in differentiating chondrocytes in transgenic mice. *Genesis* 26, 145–146. [https://doi.org/10.1002/\(SICI\)1526-968X\(200002\)26:2<145::AID-GENE14>3.0.CO;2-C](https://doi.org/10.1002/(SICI)1526-968X(200002)26:2<145::AID-GENE14>3.0.CO;2-C)
- Pan, Q., Yu, Y., Chen, Q., Li, C., Wu, H., Wan, Y., Ma, J., Sun, F., 2008. Sox9, a key transcription factor of bone morphogenetic protein-2-induced chondrogenesis, is activated through BMP pathway and a CCAAT box in the proximal promoter. *J Cell Physiol* 217, 228–41. <https://doi.org/10.1002/jcp.21496>
- Park, J., Gebhardt, M., Golovchenko, S., Perez-Branguli, F., Hattori, T., Hartmann, C., Zhou, X., de Crombrughe, B., Stock, M., Schneider, H., von der Mark, K., 2015. Dual pathways to endochondral osteoblasts: A novel chondrocyte-derived osteoprogenitor cell identified in hypertrophic cartilage. *Biology Open* 4, 608–621. <https://doi.org/10.1242/bio.201411031>
- Pierrou, S., Hellqvist, M., Samuelsson, L., Enerbäck, S., Carlsson, P., 1994. Cloning and characterization of seven human forkhead proteins: binding site specificity and DNA bending. *EMBO J* 13, 5002–12.
- Prakash, Prabhu, L. v., Saralaya, V. v., Pai, M.M., Ranade, A. v., Singh, G., Madhyastha, S., 2007. Vertebral body integrity: a review of various anatomical factors involved in the lumbar region. *Osteoporosis International* 18, 891–903. <https://doi.org/10.1007/s00198-007-0373-5>
- Rigueur, D., Lyons, K.M., 2014. Whole-mount skeletal staining. *Methods Mol Biol* 1130, 113–121. [https://doi.org/10.1007/978-1-62703-989-5\\_9](https://doi.org/10.1007/978-1-62703-989-5_9)
- Robinow, M., Johnson, G.F., Verhagen, A.D., 1970. Distichiasis-lymphedema. A hereditary syndrome of multiple congenital defects. *Am J Dis Child* 119, 343–7.
- Rodda, S.J., McMahon, A.P., 2006. Distinct roles for Hedgehog and canonical Wnt signaling in specification, differentiation and maintenance of osteoblast progenitors. *Development* 133, 3231–44. <https://doi.org/10.1242/dev.02480>
- Ross, S.E., Erickson, R.L., Hemati, N., MacDougald, O.A., 1999. Glycogen synthase kinase 3 is an insulin-regulated C/EBPalpha kinase. *Mol Cell Biol* 19, 8433–41. <https://doi.org/10.1128/MCB.19.12.8433>
- Salazar, V.S., Gamer, L.W., Rosen, V., 2016. BMP signalling in skeletal development, disease and repair. *Nat Rev Endocrinol* 12, 203–21. <https://doi.org/10.1038/nrendo.2016.12>
- Saleem, R A, Banerjee-Basu, S., Berry, F.B., Baxevanis, A.D., Walter, M.A., 2001. Analyses of the effects that disease-causing missense mutations have on the structure and function of the winged-helix protein FOXC1. *Am J Hum Genet* 68, 627–41. <https://doi.org/10.1086/318792>
- Saleem, R.A., Banerjee-Basu, S., Murphy, T.C., Baxevanis, A., Walter, M.A., 2004. Essential structural and functional determinants within the forkhead domain of FOXC1. *Nucleic Acids Res* 32, 4182–93. <https://doi.org/10.1093/nar/gkh742>
- Sasman, A., Nassano-Miller, C., Shim, K.S., Koo, H.Y., Liu, T., Schultz, K.M., Millay, M., Nanano, A., Kang, M., Suzuki, T., Kume, T., 2012. Generation of conditional alleles for Foxc1 and Foxc2 in mice. *Genesis* 50, 766–74. <https://doi.org/10.1002/dvg.22036>
- Savage, J., Voronova, A., Mehta, V., Sendi-Mukasa, F., Skerjanc, I.S., 2010. Canonical Wnt signaling regulates Foxc1/2 expression in P19 cells. *Differentiation* 79, 31–40. <https://doi.org/10.1016/J.DIFF.2009.08.008>

- Schonk, D.M., Kuijpers, H.J.H., van Drunen, E., van Dalen, C.H., Geurts Van Kessel, A.H.M., Verheijen, R., Ramaekers, F.C.S., 1989. Assignment of the gene(s) involved in the expression of the proliferation-related Ki-67 antigen to human chromosome 10. *Hum Genet* 83, 297–299.
- Shapiro, I.M., Adams, C.S., Freeman, T., Srinivas, V., 2005. Fate of the hypertrophic chondrocyte: Microenvironmental perspectives on apoptosis and survival in the epiphyseal growth plate. *Birth Defects Research Part C - Embryo Today: Reviews* 75, 330–339. <https://doi.org/10.1002/bdrc.20057>
- Shaw-Smith, C., 2010. Genetic factors in esophageal atresia, tracheo-esophageal fistula and the VACTERL association: roles for FOXF1 and the 16q24.1 FOX transcription factor gene cluster, and review of the literature. *Eur J Med Genet* 53, 6–13. <https://doi.org/10.1016/j.ejmg.2009.10.001>
- Shen, G., 2005. The role of type X collagen in facilitating and regulating endochondral ossification of articular cartilage. *Orthodontics and Craniofacial Research* 8, 11–17. <https://doi.org/10.1111/j.1601-6343.2004.00308.x>
- Shiang, R., Thompson, L.M., Zhu, Y.Z., Church, D.M., Fielder, T.J., Bocian, M., Winokur, S.T., Wasmuth, J.J., 1994. Mutations in the transmembrane domain of FGFR3 cause the most common genetic form of dwarfism, achondroplasia. *Cell* 78, 335–342. [https://doi.org/10.1016/0092-8674\(94\)90302-6](https://doi.org/10.1016/0092-8674(94)90302-6)
- Shields, M.B., Buckley, E., Klintworth, G.K., Thresher, R., 1985. Axenfeld-Rieger syndrome. A spectrum of developmental disorders. *Survey of Ophthalmology* 29, 387–409. [https://doi.org/10.1016/0039-6257\(85\)90205-X](https://doi.org/10.1016/0039-6257(85)90205-X)
- Shih, H.P., Seymour, P.A., Patel, N.A., Xie, R., Wang, A., Liu, P.P., Yeo, G.W., Magnuson, M.A., Sander, M., 2015. A Gene Regulatory Network Cooperatively Controlled by Pdx1 and Sox9 Governs Lineage Allocation of Foregut Progenitor Cells. *Cell Reports* 13, 326–336. <https://doi.org/10.1016/j.celrep.2015.08.082>
- Shu, B., Zhang, M., Xie, R., Wang, M., Jin, H., Hou, W., Tang, D., Harris, S.E., Mishina, Y., O’Keefe, R.J., Hilton, M.J., Wang, Y., Chen, D., 2011. BMP2, but not BMP4, is crucial for chondrocyte proliferation and maturation during endochondral bone development. *Journal of Cell Science* 124, 3428–3440. <https://doi.org/10.1242/jcs.083659>
- Shubin, N., Tabin, C., Carroll, S., 1997. Fossils, genes and the evolution of animal limbs. *Nature* 388, 639–648. <https://doi.org/10.1038/41710>
- Sillence, D., 1981. Osteogenesis imperfecta: an expanding panorama of variants. *Clin Orthop Relat Res* 11–25.
- Sivaraj, K.K., Adams, R.H., 2016. Blood vessel formation and function in bone. *Development (Cambridge)* 143, 2706–2715. <https://doi.org/10.1242/dev.136861>
- Skórzewska, A., Grzymisławska, M., Bruska, M., Lupicka, J., Woźniak, W., 2013. Ossification of the vertebral column in human fetuses: histological and computed tomography studies. *Folia Morphol (Warsz)* 72, 230–8. <https://doi.org/10.5603/fm.2013.0038>
- Song, L., Liu, M., Ono, N., Bringhurst, F.R., Kronenberg, H.M., Guo, J., 2012. Loss of wnt/ $\beta$ -catenin signaling causes cell fate shift of preosteoblasts from osteoblasts to adipocytes. *J Bone Miner Res* 27, 2344–58. <https://doi.org/10.1002/jbmr.1694>

- Soshnikova, N., Zechner, D., Huelsken, J., Mishina, Y., Behringer, R.R., Taketo, M.M., Crenshaw, E.B., Birchmeier, W., 2003. Genetic interaction between Wnt/beta-catenin and BMP receptor signaling during formation of the AER and the dorsal-ventral axis in the limb. *Genes Dev* 17, 1963–8. <https://doi.org/10.1101/gad.263003>
- Stankiewicz, P., Sen, P., Bhatt, S.S., Storer, M., Xia, Z., Bejjani, B.A., Ou, Z., Wiszniewska, J., Driscoll, D.J., Bolivar, J., Bauer, M., Zackai, E.H., McDonald-McGinn, D., Nowaczyk, M.M.J., Murray, M., Shaikh, T.H., Martin, V., Tyreman, M., Simonic, I., Willatt, L., Paterson, J., Mehta, S., Rajan, D., Fitzgerald, T., Gribble, S., Prigmore, E., Patel, A., Shaffer, L.G., Carter, N.P., Cheung, S.W., Langston, C., Shaw-Smith, C., 2009. Genomic and Genic Deletions of the FOX Gene Cluster on 16q24.1 and Inactivating Mutations of FOXF1 Cause Alveolar Capillary Dysplasia and Other Malformations. *The American Journal of Human Genetics* 84, 780–791. <https://doi.org/10.1016/j.ajhg.2009.05.005>
- Su, N., Jin, M., Chen, L., 2014. Role of FGF/FGFR signaling in skeletal development and homeostasis: learning from mouse models. *Bone Research* 2. <https://doi.org/10.1038/boneres.2014.3>
- Su, N., Yang, J., Xie, Y., Du, X., Chen, H., Zhou, H., Chen, L., 2019. Bone function, dysfunction and its role in diseases including critical illness. *Int. J. Biol. Sci* 15, 776–787. <https://doi.org/10.7150/ijbs.27063>
- Sun, M.M.-G., Beier, F., 2014. Chondrocyte hypertrophy in skeletal development, growth, and disease. *Birth Defects Res C Embryo Today* 102, 74–82. <https://doi.org/10.1002/bdrc.21062>
- Sutton, J., Costa, R., Klug, M., Field, L., Xu, D., Largaespada, D.A., Fletcher, C.F., Jenkins, N.A., Copeland, N.G., Klemsz, M., Hromas, R., 1996. Genesis, a winged helix transcriptional repressor with expression restricted to embryonic stem cells. *J Biol Chem* 271, 23126–33. <https://doi.org/10.1074/jbc.271.38.23126>
- Takahashi, K., Yamanaka, S., 2006. Induction of pluripotent stem cells from mouse embryonic and adult fibroblast cultures by defined factors. *Cell* 126, 663–76. <https://doi.org/10.1016/j.cell.2006.07.024>
- Takimoto, A., Kokubu, C., Watanabe, H., Sakuma, T., Yamamoto, T., Kondoh, G., Hiraki, Y., Shukunami, C., 2019. Differential transactivation of the upstream aggrecan enhancer regulated by PAX1/9 depends on SOX9-driven transactivation. *Scientific Reports* 9, 4605. <https://doi.org/10.1038/s41598-019-40810-4>
- Tavian, D., Missaglia, S., Micheli, S., Maltese, P.E., Manara, E., Mordente, A., Bertelli, M., 2020. FOXC2 Disease Mutations Identified in Lymphedema Distichiasis Patients Impair Transcriptional Activity and Cell Proliferation. *International Journal of Molecular Sciences* 21, 5112. <https://doi.org/10.3390/ijms21145112>
- Terpstra, L., Prud'homme, J., Arabian, A., Takeda, S., Karsenty, G., Dedhar, S., St-Arnaud, R., 2003. Reduced chondrocyte proliferation and chondrodysplasia in mice lacking the integrin-linked kinase in chondrocytes. *J Cell Biol* 162, 139–48. <https://doi.org/10.1083/jcb.200302066>
- Tickle, C., Towers, M., 2017. Sonic Hedgehog Signaling in Limb Development. *Frontiers in Cell and Developmental Biology* 5. <https://doi.org/10.3389/fcell.2017.00014>
- Tolchin, D., Yeager, J.P., Prasad, P., Dorrani, N., Russi, A.S., Martinez-Agosto, J.A., Haseeb, A., Angelozzi, M., Santen, G.W.E., Ruivenkamp, C., Mercimek-Andrews, S., Depienne, C., Kuechler, A., Mikat, B., Ludecke, H.-J., Bilan, F., le Guyader, G., Gilbert-Dussardier, B., Keren, B., Heide, S., Haye, D., van Esch, H., Keldermans, L., Ortiz, D., Lancaster, E., Krantz, I.D., Krock, B.L., Pechter,

- K.B., Arkader, A., Medne, L., DeChene, E.T., Calpena, E., Melistaccio, G., Wilkie, A.O.M., Suri, M., Foulds, N., Genomics England Research Consortium, Begtrup, A., Henderson, L.B., Forster, C., Reed, P., McDonald, M.T., McConkie-Rosell, A., Thevenon, J., le Tanno, P., Coutton, C., Tsai, A.C.H., Stewart, S., Maver, A., Gorazd, R., Pichon, O., Nizon, M., Cogné, B., Isidor, B., Martin-Coignard, D., Stoeva, R., Lefebvre, V., le Caignec, C., 2020. De Novo SOX6 Variants Cause a Neurodevelopmental Syndrome Associated with ADHD, Craniosynostosis, and Osteochondromas. *Am J Hum Genet* 106, 830–845. <https://doi.org/10.1016/j.ajhg.2020.04.015>
- Topczewska, J.M., Topczewski, J., Solnica-Krezel, L., Hogan, B.L.M., 2001. Sequence and expression of zebrafish *foxc1a* and *foxc1b*, encoding conserved forkhead/winged helix transcription factors. *Mechanisms of Development* 100, 343–347. [https://doi.org/10.1016/S0925-4773\(00\)00534-7](https://doi.org/10.1016/S0925-4773(00)00534-7)
- Usami, Y., Gunawardena, A.T., Francois, N.B., Otsuru, S., Takano, H., Hirose, K., Matsuoka, M., Suzuki, A., Huang, J., Qin, L., Iwamoto, M., Yang, W., Toyosawa, S., Enomoto-Iwamoto, M., 2019. Possible Contribution of Wnt-Responsive Chondroprogenitors to the Postnatal Murine Growth Plate. <https://doi.org/10.1002/jbmr.3658>
- Vajo, Z., Francomano, C.A., Wilkin, D.J., 2000. The molecular and genetic basis of fibroblast growth factor receptor 3 disorders: the achondroplasia family of skeletal dysplasias, Muenke craniosynostosis, and Crouzon syndrome with acanthosis nigricans. *Endocr Rev* 21, 23–39. <https://doi.org/10.1210/edrv.21.1.0387>
- Veeman, M.T., Slusarski, D.C., Kaykas, A., Louie, S.H., Moon, R.T., 2003. Zebrafish Prickle, a Modulator of Noncanonical Wnt/Fz Signaling, Regulates Gastrulation Movements. *Current Biology* 13, 680–685. [https://doi.org/10.1016/S0960-9822\(03\)00240-9](https://doi.org/10.1016/S0960-9822(03)00240-9)
- Wagner, T., Wirth, J., Meyer, J., Zabel, B., Held, M., Zimmer, J., Pasantes, J., Bricarelli, F.D., Keutel, J., Hustert, E., Wolf, U., Tommerup, N., Schempp, W., Scherer, G., 1994. Autosomal sex reversal and campomelic dysplasia are caused by mutations in and around the SRY-related gene SOX9. *Cell* 79, 1111–1120. [https://doi.org/10.1016/0092-8674\(94\)90041-8](https://doi.org/10.1016/0092-8674(94)90041-8)
- Walzer, S.M., Cetin, E., Grübl-Barabas, R., Sulzbacher, I., Rueger, B., Girsch, W., Toegel, S., Windhager, R., Fischer, M.B., 2014. Vascularization of primary and secondary ossification centres in the human growth plate. *BMC Dev Biol* 14, 36. <https://doi.org/10.1186/s12861-014-0036-7>
- Ward, L., Pang, A.S.W., Evans, S.E., Stern, C.D., 2018. The role of the notochord in amniote vertebral column segmentation. *Dev Biol* 439, 3–18. <https://doi.org/10.1016/j.ydbio.2018.04.005>
- Warman, M.L., Cormier-Daire, V., Hall, C., Krakow, D., Lachman, R., LeMerrer, M., Mortier, G., Mundlos, S., Nishimura, G., Rimoin, D.L., Robertson, S., Savarirayan, R., Sillence, D., Spranger, J., Unger, S., Zabel, B., Superti-Furga, A., 2011. Nosology and classification of genetic skeletal disorders: 2010 revision. *Am J Med Genet A* 155A, 943–68. <https://doi.org/10.1002/ajmg.a.33909>
- Weigel, D., Jäckle, H., 1990. The fork head domain: a novel DNA binding motif of eukaryotic transcription factors? *Cell* 63, 455–6. [https://doi.org/10.1016/0092-8674\(90\)90439-I](https://doi.org/10.1016/0092-8674(90)90439-I)
- Weigel, D., Jürgens, G., Küttner, F., Seifert, E., Jäckle, H., 1989. The homeotic gene fork head encodes a nuclear protein and is expressed in the terminal regions of the *Drosophila* embryo. *Cell* 57, 645–58. [https://doi.org/10.1016/0092-8674\(89\)90133-5](https://doi.org/10.1016/0092-8674(89)90133-5)

- Weigelt, J., Climent, I., Dahlman-Wright, K., Wikström, M., 2001. Solution structure of the DNA binding domain of the human forkhead transcription factor AFX (FOXO4). *Biochemistry* 40, 5861–9. <https://doi.org/10.1021/bi001663w>
- Weinman, O., Babic, D., Regli, L., Hoerstrup, S.P., Gerhardt, H., Schwab, M.E., Vogel, J., 2014. Quantitative assessment of angiogenesis, perfused blood vessels and endothelial tip cells in the postnatal mouse brain. <https://doi.org/10.1038/nprot.2015.002>
- Williams, S., Alkhatib, B., Serra, R., 2019. Development of the axial skeleton and intervertebral disc. *Curr Top Dev Biol* 133, 49–90. <https://doi.org/10.1016/bs.ctdb.2018.11.018>
- Wilm, B., James, R.G., Schultheiss, T.M., Hogan, B.L.M., 2004. The forkhead genes, *Foxc1* and *Foxc2*, regulate paraxial versus intermediate mesoderm cell fate. *Developmental Biology* 271, 176–189. <https://doi.org/10.1016/J.YDBIO.2004.03.034>
- Winnier, G.E., Hargett, L., Hogan, B.L.M., 1997. The winged helix transcription factor MFH1 is required for proliferation and patterning of paraxial mesoderm in the mouse embryo. *Genes and Development* 11, 926–940. <https://doi.org/10.1101/gad.11.7.926>
- Winnier, G.E., Kume, T., Deng, K., Rogers, R., Bundy, J., Raines, C., Walter, M.A., Hogan, B.L., Conway, S.J., 1999. Roles for the winged helix transcription factors MF1 and MFH1 in cardiovascular development revealed by nonallelic noncomplementation of null alleles. *Dev Biol* 213, 418–31. <https://doi.org/10.1006/dbio.1999.9382>
- Xu, C., Dinh, V.V., Kruse, K., Jeong, H.-W., Watson, E.C., Adams, S., Berkenfeld, F., Stehling, M., Rasouli, S.J., Fan, R., Chen, R., Bedzhov, I., Chen, Q., Kato, K., Pitulescu, M.E., Adams, R.H., 2022. Induction of osteogenesis by bone-targeted Notch activation. *Elife* 11. <https://doi.org/10.7554/eLife.60183>
- Yan, B., Zhang, Z., Jin, D., Cai, C., Jia, C., Liu, W., Wang, T., Li, S., Zhang, H., Huang, B., Lai, P., Wang, H., Liu, A., Zeng, C., Cai, D., Jiang, Y., Bai, X., 2016. mTORC1 regulates PTHrP to coordinate chondrocyte growth, proliferation and differentiation. *Nature Communications* 7. <https://doi.org/10.1038/ncomms11151>
- Yang, J., Andre, P., Ye, L., Yang, Y.-Z., 2015. The Hedgehog signalling pathway in bone formation. *Int J Oral Sci* 7, 73–9. <https://doi.org/10.1038/ijos.2015.14>
- Yang, L., Tsang, K.Y., Tang, H.C., Chan, D., Cheah, K.S.E., 2014. Hypertrophic chondrocytes can become osteoblasts and osteocytes in endochondral bone formation. *Proc Natl Acad Sci U S A* 111, 12097–12102. <https://doi.org/10.1073/pnas.1302703111>
- Yeung Tsang, K., Wa Tsang, S., Chan, D., Cheah, K.S.E., 2014. The chondrocytic journey in endochondral bone growth and skeletal dysplasia. *Birth Defects Res C Embryo Today* 102, 52–73. <https://doi.org/10.1002/bdrc.21060>
- Yoshida, C.A., Yamamoto, H., Fujita, T., Furuichi, T., Ito, K., Inoue, K.I., Yamana, K., Zanma, A., Takada, K., Ito, Y., Komori, T., 2004. Runx2 and Runx3 are essential for chondrocyte maturation, and Runx2 regulates limb growth through induction of Indian hedgehog. *Genes and Development* 18, 952–963. <https://doi.org/10.1101/gad.1174704>
- Yoshida, M., Hata, K., Takashima, R., Ono, K., Nakamura, E., Takahata, Y., Murakami, T., Iseki, S., Takano-Yamamoto, T., Nishimura, R., Yoneda, T., 2015a. The transcription factor *Foxc1* is necessary for *Ihh*-*Gli2*-regulated endochondral ossification. *Nat Commun* 6, 6653. <https://doi.org/10.1038/ncomms7653>

- Yoshida, M., Hata, K., Takashima, R., Ono, K., Nakamura, E., Takahata, Y., Murakami, T., Iseki, S., Takano-Yamamoto, T., Nishimura, R., Yoneda, T., 2015b. The transcription factor Foxc1 is necessary for Ihh-Gli2-regulated endochondral ossification. *Nature Communications* 6, 1–15. <https://doi.org/10.1038/ncomms7653>
- Zelzer, E., Mamluk, R., Ferrara, N., Johnson, R.S., Schipani, E., Olsen, B.R., 2004. VEGFA is necessary for chondrocyte survival during bone development. *Development* 131, 2161–2171. <https://doi.org/10.1242/dev.01053>
- Zhou, X., Zhang, Z., Feng, J.Q., Dusevich, V.M., Sinha, K., Zhang, H., Darnay, B.G., de Crombrughea, B., 2010. Multiple functions of Osterix are required for bone growth and homeostasis in postnatal mice. *Proc Natl Acad Sci U S A* 107, 12919–12924. <https://doi.org/10.1073/pnas.0912855107>
- Zhou, Z.-Q., Ota, S., Deng, C., Akiyama, H., Hurlin, P.J., 2015. Mutant activated FGFR3 impairs endochondral bone growth by preventing SOX9 downregulation in differentiating chondrocytes. *Hum Mol Genet* 24, 1764–73. <https://doi.org/10.1093/hmg/ddu594>
- Zurick, K.M., Qin, C., Bernards, M.T., 2013. Mineralization induction effects of osteopontin, bone sialoprotein, and dentin phosphoprotein on a biomimetic collagen substrate. *Journal of Biomedical Materials Research - Part A* 101 A, 1571–1581. <https://doi.org/10.1002/jbm.a.34462>

## Appendices:

### Appendix 1:

**Table 2.S1 list of down regulated genes in rib cage RNA isolated from mutant embryos:**

Genes	Avg FC	log2FoldChange_fc	pvalue_fC	padj_fc	log2FoldChange_RSEM	pvalue_RSEM	padj_RSEM
1700030C10Rik	- 5.28616 41	-5.328479	0.00152 4415	0.05520 406	-5.2438492	0.002110 228	0.06855 226
Ambn	- 4.78206 715	-4.3826946	0.00000 121	0.00020 1618	-5.1814397	0.000319 883	0.01892 289
Mmp13	- 2.98382 355	-2.9883604	0.00028 0745	0.01633 382	-2.9792867	0.000256 195	0.01620 844
Gm48898	- 2.84190 885	-2.8407818	3.91E-10	0.00000 0183	-2.8430359	0.000002 54	0.00047 5947
Ostn	- 2.69839 765	-2.672557	7.97E-33	1.83E-28	-2.7242383	8.66E-32	1.57E-27
Gm18787	- 2.59260 885	-2.5030813	0.00016 4638	0.01105 444	-2.6821364	0.001434 171	0.05469 695
Dmp1	- 2.55450 07	-2.5037455	8.96E-14	9.78E-11	-2.6052559	9.3E-15	2.12E-11
Itgbl1	- 2.47692 265	-2.4628528	1.1E-10	5.87E-08	-2.4909925	4.55E-10	0.00000 0306
Ptpn20	- 2.40320 74	-2.3393426	0.00001 16	0.00131 6415	-2.4670722	0.000470 416	0.02546 969
Spp1	- 2.37018 235	-2.3727107	0.00014 2132	0.00999 4142	-2.367654	0.000144 868	0.01069 351
Foxc1	- 2.33621 935	-2.3317364	1.64E-09	0.00000 0658	-2.3407023	3.77E-09	0.00000 196
Sstr2	- 2.30778 6	-2.5041905	0.00000 232	0.00035 0367	-2.1113815	0.001844 424	0.06391 193

Wdr72	- 2.30693 11	-2.3150567	0.00000 0013	0.00000 402	-2.2988055	0.000003 43	0.00060 0119
Bglap	- 2.15764 695	-1.52384	0.00204 8248	0.06641 845	-2.7914539	0.000012 5	0.00163 6111
Ooep	- 2.12274 155	-2.1491524	0.00000 0976	0.00017 0843	-2.0963307	0.000032 2	0.00340 2241
Syt6	- 2.11538 01	-2.1161872	0.00000 0721	0.00013 4286	-2.114573	0.000297 647	0.01792 866
Foxc2	- 2.02649 115	-1.9879277	0.00000 12	0.00020 0646	-2.0650546	0.000022 3	0.00261 453
Gpnmb	- 2.02388 475	-2.051982	4.03E-10	0.00000 0185	-1.9957875	0.000000 717	0.00017 3961
Lipc	- 1.98920 945	-2.0457379	1.3E-13	1.36E-10	-1.932681	0.000028 4	0.00314 5052
Uncx	- 1.92956 42	-1.9342107	0.00005 75	0.00484 2078	-1.9249177	0.002054 037	0.06732 799
Vill	- 1.87869 52	-1.9408734	0.00001 49	0.00161 4593	-1.816517	0.000379 406	0.02156 925
Dlx6	- 1.82208 54	-1.8763857	0.00000 0227	0.00004 81	-1.7677851	0.000112 504	0.00886 0069
Slc35f3	- 1.81957 77	-1.7981841	0.00126 2074	0.04813 731	-1.8409713	0.002528 884	0.07719 037
Omd	- 1.80211 915	-1.8141924	5.59E-11	3.29E-08	-1.7900459	5.3E-10	0.00000 0344
Ccn5	- 1.79744 015	-1.8848737	0.00000 036	0.00007 43	-1.7100066	0.000587 529	0.02983 252
Tnfsf11	- 1.77168 825	-1.7817771	2.83E-10	0.00000 0135	-1.7615994	0.000000 708	0.00017 3961
9130024F 11Rik	- 1.71870 875	-1.6625888	0.00021 043	0.01325 189	-1.7748287	0.000005 47	0.00088 8564

Phex	- 1.71221 49	-1.6726963	1.1E-30	1.26E-26	-1.7517335	1.04E-27	9.45E-24
Alpl	- 1.68139 075	-1.6729202	1.13E-10	5.87E-08	-1.6898613	1.53E-10	0.00000 0121
Satb2	- 1.64613 565	-1.6000494	1.45E-10	7.37E-08	-1.6922219	6.86E-11	6.57E-08
Zbtb8b	- 1.53977 445	-1.367571	0.00284 5929	0.08166 055	-1.7119779	0.000206 601	0.01397 205
5830444B 04Rik	- 1.50985 595	-1.4824227	0.00011 1296	0.00828 3277	-1.5372892	0.003051 269	0.08659 701
Tnn	- 1.44537 48	-1.4456929	0.00000 373	0.00053 256	-1.4450567	0.000005 02	0.00083 0355
Gm32618	- 1.44223 265	-1.2424423	0.00000 504	0.00067 5685	-1.642023	0.001860 151	0.06401 953
Bcan	- 1.43330 365	-1.3483104	1.06E-08	0.00000 338	-1.5182969	0.000000 2	0.00005 87
Ccl27a	- 1.41939 42	-1.4567356	0.00001 23	0.00137 3936	-1.3820528	0.000071 2	0.00617 4384
Cilp2	- 1.41835 6	-1.4189963	0.00005 88	0.00492 1841	-1.4177157	0.000320 366	0.01892 289
Vdr	- 1.40630 015	-1.4341261	1.49E-08	0.00000 448	-1.3784742	0.000000 869	0.00020 5354
Pax9	- 1.40432 955	-1.3920039	0.00008 01	0.00638 5501	-1.4166552	0.001455 368	0.05530 122
Hsd11b1	- 1.38890 07	-1.4236239	0.00029 8262	0.01700 08	-1.3541775	0.001693 786	0.06089 598
Sgms2	- 1.37876 83	-1.37918	9.59E-19	4.4E-15	-1.3783566	6.69E-21	3.04E-17
Mkx	- 1.33043 995	-1.3789488	0.00000 051	0.00009 9	-1.2819311	6.7E-10	0.00000 0392

Cfh	- 1.32824 97	-1.3088834	2.05E-10	0.00000 01	-1.347616	1.66E-10	0.00000 0126
Kazald1	- 1.32361 32	-1.3108019	8.46E-11	4.81E-08	-1.3364245	3.45E-10	0.00000 0241
Btla	- 1.30721 17	-1.3664404	0.00003 08	0.00288 1882	-1.247983	0.002903 435	0.08410 716
Sp7	- 1.29649 135	-1.3132916	1.61E-10	8.04E-08	-1.2796911	4.75E-09	0.00000 227
Sost	- 1.29459 74	-1.3144981	0.00007 7	0.00620 0355	-1.2746967	0.000570 939	0.02917 563
Slc41a2	- 1.29140 44	-1.2646792	0.00074 7454	0.03326 971	-1.3181296	0.001174 364	0.04747 562
Lpar3	- 1.28507 815	-1.2734163	0.00000 0389	0.00007 97	-1.29674	0.000014 6	0.00185 9035
Mamdc2	- 1.26590 86	-1.2662714	9.66E-16	2.01E-12	-1.2655458	5.88E-13	8.22E-10
Ctsk	- 1.24498 245	-1.2523772	1.49E-14	1.89E-11	-1.2375877	1.75E-13	2.89E-10
Tmem147 os	- 1.24479 625	-1.1041633	0.00088 1555	0.03728 309	-1.3854292	0.001279 538	0.05016 67
Loxl4	- 1.24468 29	-1.1951167	0.00111 4419	0.04373 059	-1.2942491	0.000544 188	0.02845 133
Col8a1	- 1.24153 885	-1.2391378	0.00000 0743	0.00013 6319	-1.2439399	0.000001 18	0.00025 5052
Enpp6	- 1.23793 25	-1.2343553	0.00168 2835	0.05898 413	-1.2415097	0.000272 557	0.01675 122
Tmem169	- 1.23111 135	-1.1473036	0.00008 36	0.00662 7874	-1.3149191	0.000611 737	0.03049 177
Cfap74	- 1.21963 41	-1.2217042	0.00005 59	0.00476 7654	-1.217564	0.000474 266	0.02560 194

Snca	- 1.20686 735	-1.2182888	0.00136 1456	0.05049 946	-1.1954459	0.001991 442	0.06674 308
Col22a1	- 1.19337 64	-1.1711	3.87E-08	0.00001 04	-1.2156528	0.000000 979	0.00021 9799
Bmp8a	- 1.18137 19	-1.2150456	0.00013 4553	0.00965 7248	-1.1476982	0.000779 533	0.03563 132
Pik3r5	- 1.17668 99	-1.1648215	0.00010 7165	0.00805 4237	-1.1885583	0.001575 115	0.05814 979
Slc13a5	- 1.16426 135	-1.2091865	3.31E-08	0.00000 936	-1.1193362	0.000004 16	0.00071 4514
Hbb-bt	- 1.16240 345	-1.0964851	0.00004 74	0.00409 1491	-1.2283218	0.000028	0.00312 7054
Entpd3	- 1.15629 875	-1.1880079	0.00010 7891	0.00805 5945	-1.1245896	0.000048 3	0.00454 6774
Ccdc106	- 1.15017 565	-1.1003853	0.00025 1077	0.01506 659	-1.199966	0.000188 221	0.01322 053
Fam167b	- 1.14935 725	-1.1058543	0.00008 62	0.00678 8352	-1.1928602	0.001585 778	0.05827 975
Pappa	- 1.14548 39	-1.1472036	0.00172 4117	0.05973 277	-1.1437642	0.003715 973	0.09762 611
Rspo2	- 1.13642 43	-1.132777	0.00000 248	0.00037 2007	-1.1400716	0.000018 9	0.00227 4186
Grin3a	- 1.13015 77	-1.0890233	0.00000 478	0.00065 9173	-1.1712921	0.000009 05	0.00129 6826
Smad9	- 1.11791 17	-1.1072176	0.00090 3927	0.03774 267	-1.1286058	0.002663 165	0.07994 769
Tent5c	- 1.08794 64	-1.0842874	0.00098 6542	0.03991 278	-1.0916054	0.000873 543	0.03842 2
Podnl1	- 1.07624 735	-1.1141639	0.00040 6438	0.02146 722	-1.0383308	0.002511 076	0.07677 562

Vipr2	- 1.06756 185	-1.0069898	5.11E-08	0.00001 3	-1.1281339	0.000000 504	0.00013 2814
Runx2	- 1.05713 2	-1.125023	8.2E-09	0.00000 268	-0.989241	0.000087 7	0.00733 9017
Ccl9	- 1.05599 695	-1.0813727	2.35E-14	2.84E-11	-1.0306212	0.000015 6	0.00195 9501
Cd40	- 1.04959 785	-0.9729305	0.00072 6115	0.03276 998	-1.1262652	0.002122 379	0.06870 164
Hhip	- 1.04326 375	-1.0389872	0.00003 63	0.00331 1269	-1.0475403	0.000006 78	0.00103 681
Hbb-bs	- 1.04172 415	-1.0349662	0.00002 14	0.00218 268	-1.0484821	0.000021 3	0.00253 8051
Clec11a	- 1.03501 84	-1.0270489	0.00067 7951	0.03133 202	-1.0429879	0.000493 939	0.02638 541
Csrnp3	- 1.03258 295	-1.0571707	7.28E-09	0.00000 245	-1.0079952	0.000030 9	0.00332 971
Ifitm5	- 1.02994 065	-0.9976577	0.00066 2057	0.03083 411	-1.0622236	0.001083 4	0.04537 555
Mpeg1	- 1.02198 675	-0.9987476	0.00315 6571	0.08686 444	-1.0452259	0.002999 189	0.08578 812
Tnmd	- 1.00061 695	-1.0019806	0.00002 69	0.00259 5058	-0.9992533	0.000041 9	0.00403 3965

## Appendix 2:

**Table 2.S2 list of upregulated genes in rib cage RNA isolated from mutant embryos:**

Genes	Avg FC	log2FoldChange_fc	pvalue_fc	padj_fc	log2FoldChange_RSEM	pvalue_RSEM	padj_RSEM
Kprp	20.352 5713	27.3861933	2.38E-12	1.72E-09	13.3189493	0.00065 1622	0.0316 9599
Lce1d	20.325 8177	27.3834536	2.4E-12	1.72E-09	13.2681818	0.00068 3363	0.0328 8058
Lce1b	13.281 83315	13.7556011	0.0004 30015	0.0224 8578	12.8080652	0.00104 4049	0.0441 3894
2310050C 09Rik	13.178 0142	13.6816732	0.0004 61748	0.0236 2646	12.6743552	0.00117 802	0.0475 1781
Lce1g	12.897 51295	13.4085282	0.0005 98936	0.0286 6263	12.3864977	0.00152 2002	0.0568 5476
Lce1a1	12.883 2766	13.3958561	0.0000 0117	0.0001 98015	12.3706971	0.00000 0391	0.0001 06295
Flg	12.866 50905	13.0641787	0.0000 00029	0.0000 0843	12.6688394	0.00001 19	0.0015 9788
Lce1a2	12.714 2234	12.9262564	0.0002 27773	0.0140 1912	12.5021904	0.00137 3924	0.0529 5428

Lcelm	12.589 35125	12.6197337	0.0000 212	0.0021 71652	12.5589688	0.00000 914	0.0012 99504
Lcele	12.341 39905	12.9038612	0.0009 56893	0.0391 694	11.7789369	0.00257 0586	0.0778 1048
Lcelf	12.221 15045	13.0135656	0.0008 65384	0.0369 1485	11.4287353	0.00344 1898	0.0933 1595
Lcelj	12.145 8391	12.9355561	0.0009 29574	0.0385 3178	11.3561221	0.00365 2947	0.0965 9071
Lcell	12.047 15835	12.7083646	0.0011 42514	0.0446 9258	11.3859521	0.00356 503	0.0952 8297
Lcelh	11.903 09275	12.4718582	0.0014 11404	0.0518 4876	11.3343273	0.00371 8936	0.0976 2611
Lcelc	11.871 48875	11.5715573	0.0018 55371	0.0623 1631	12.1714202	0.00038 7476	0.0218 234
Lceli	10.898 35545	10.8639657	0.0029 4515	0.0832 4498	10.9327452	0.00153 2034	0.0571 1221
Gm48704	9.8602 397	9.7890698	0.0000 0113	0.0001 92139	9.9314096	0.00000 0687	0.0001 73476
Slurp1	8.7847 593	7.5841453	0.0021 54035	0.0685 791	9.9853733	0.00154 9016	0.0575 8933
Ly6m	8.5961 6625	8.688388	0.0000 0844	0.0010 34608	8.5039445	0.00001 88	0.0022 74186

Klk7	7.8620 351	7.8352714	0.0000 0535	0.0007 08453	7.8887988	0.00000 568	0.0009 14976
Il1a	7.8327 7925	7.3235368	0.0000 372	0.0033 69247	8.3420217	0.00024 4181	0.0157 7783
Ywhaq- ps1	7.7866 713	9.8089209	1.23E- 09	0.0000 00522	5.7644217	0.00021 956	0.0146 8467
Serpina12	7.5883 4845	7.4715347	0.0000 0154	0.0002 49801	7.7051622	0.00000 237	0.0004 49149
Pck1	7.5154 1745	7.7653653	0.0000 136	0.0014 86589	7.2654696	0.00000 172	0.0003 47394
Otop1	7.4346 466	7.9719797	0.0000 00205	0.0000 448	6.8973135	0.00001 55	0.0019 56857
Retn	7.2511 081	7.7044732	3.48E- 08	0.0000 0949	6.797743	0.00000 733	0.0010 73862
Plin1	7.0546 372	7.0027665	1.77E- 11	1.07E- 08	7.1065079	6.9E-10	0.0000 00392
Adipoq	6.8976 004	6.9279891	2.17E- 12	1.72E- 09	6.8672117	1.31E- 12	1.71E- 09
Cckar	6.8226 1875	6.9909919	1.93E- 08	0.0000 0574	6.6542456	0.00000 633	0.0009 84148
Gm12436	6.5304 099	6.3668157	0.0031 1539	0.0861 2706	6.6940041	0.00004 64	0.0044 20587

Il1f8	6.3088 811	6.4178829	0.0000 245	0.0024 3185	6.1998793	0.00006 33	0.0055 91281
Hal	6.0337 8565	6.1067226	0.0000 218	0.0022 16111	5.9608487	0.00000 177	0.0003 52655
Flg2	5.9569 906	6.089301	0.0016 36827	0.0580 8201	5.8246802	0.00203 8217	0.0670 6061
Cidec	5.7881 434	5.6465258	1.13E- 09	0.0000 00491	5.929761	2.09E- 15	5.44E- 12
Gm37496	5.6995 92	5.7973186	0.0001 02404	0.0078 5088	5.6018654	0.00088 0175	0.0384 9071
Cyp2b10	5.6606 5235	5.7613401	0.0002 1886	0.0137 4499	5.5599646	0.00316 3618	0.0882 7076
Acvr1c	5.6481	5.5068196	3.75E- 15	6.62E- 12	5.7893804	4.37E- 12	5.3E-09
Nccrp1	5.5852 0755	5.5516937	0.0007 60928	0.0336 0841	5.6187214	0.00055 1176	0.0284 8577
Tyrp1	5.4929 109	5.7005548	0.0000 132	0.0014 50154	5.285267	0.00044 7392	0.0243 6816
Acp7	5.4837 005	5.6984448	0.0016 12908	0.0573 2199	5.2689562	0.00232 4148	0.0734 7376
Il1f6	5.3206 5725	5.3665898	0.0029 60448	0.0833 785	5.2747247	0.00202 7102	0.0670 4918

Sowahd	5.1692 5075	5.1764184	6.92E- 08	0.0000 169	5.1620831	0.00004 76	0.0045 14084
Cdsn	5.1200 196	5.0812223	0.0001 17349	0.0085 66816	5.1588169	0.00009 96	0.0080 16144
Atp6v1c2	5.0945 652	5.280747	0.0006 97541	0.0320 5265	4.9083834	0.00074 8874	0.0346 6545
3300005 D01Rik	5.0815 347	4.9562737	0.0000 0143	0.0002 36011	5.2067957	0.00043 9851	0.0241 0169
Mrap	5.0256 8465	5.0939373	0.0000 00187	0.0000 421	4.957432	6.37E- 10	0.0000 00386
Gm49146	4.9942 159	4.1644862	0.0027 873	0.0804 7013	5.8239456	0.00054 7706	0.0284 5133
Gml	4.9091 1715	5.0710476	0.0000 305	0.0028 68415	4.7471867	0.00038 4312	0.0217 2757
Klb	4.8791 481	4.5876916	4.67E- 12	3.25E- 09	5.1706046	5.84E- 09	0.0000 0272
Crct1	4.8664 97	4.8674681	0.0024 33039	0.0746 6204	4.8655259	0.00247 8396	0.0763 9813
Abhd12b	4.7149 441	4.5927572	0.0000 596	0.0049 71123	4.837131	0.00157 8845	0.0581 4979
Slc26a9	4.6999 3145	4.4384737	0.0006 3602	0.0302 2473	4.9613892	0.00000 0308	0.0000 861

Mrgprb1	4.6925 824	4.1480294	0.0008 89135	0.0374 6625	5.2371354	0.00183 1968	0.0637 6098
Far2	4.6876 974	4.8558374	0.0000 111	0.0012 83832	4.5195574	0.00002 62	0.0029 7699
Nlrp10	4.6478 453	4.6304084	0.0005 30465	0.0259 8258	4.6652822	0.00041 0228	0.0228 2224
Klhdc7a	4.5805 4425	4.5523437	0.0000 101	0.0011 9624	4.6087448	0.00001 59	0.0019 77042
Plexd1	4.5522 0015	4.6657232	0.0000 572	0.0048 3995	4.4386771	0.00002 85	0.0031 45052
Sprr2d	4.5362 845	4.6095625	0.0031 35591	0.0863 908	4.4630065	0.00022 9703	0.0151 4044
Irs4	4.4852 986	4.4532733	2.26E- 30	1.72E- 26	4.5173239	4.06E- 25	2.46E- 21
Btc	4.3389 772	4.3729127	0.0005 79885	0.0279 2584	4.3050417	0.00082 801	0.0370 2366
Angptl8	4.3127 7565	3.534463	0.0000 247	0.0024 37666	5.0910883	0.00074 0794	0.0345 5521
Rnf225	4.2878 7765	4.2816694	0.0004 33429	0.0225 2946	4.2940859	0.00035 1547	0.0203 6734
Hnf4a	4.2591 8625	3.9228641	0.0001 46173	0.0102 156	4.5955084	0.00043 1128	0.0236 9509

Mrgprb2	4.1967 044	4.2496222	0.0000 112	0.0012 85985	4.1437866	0.00064 7815	0.0315 9533
Gpd1	4.1358 243	4.1109377	0.0000 00182	0.0000 414	4.1607109	0.00000 0119	0.0000 386
Gm11992	4.1247 957	4.1385771	0.0013 46673	0.0503 5854	4.1110143	0.00151 6837	0.0568 0532
Gm42711	4.0745 7865	3.9767112	0.0001 40601	0.0099 16896	4.1724461	0.00076 911	0.0354 1508
Capn12	3.8870 528	4.0241548	0.0000 975	0.0074 98565	3.7499508	0.00009 85	0.0079 99636
Aldob	3.8802 3615	4.1048811	0.0000 338	0.0031 15495	3.6555912	0.00253 6426	0.0772 1614
2010016I 18Rik	3.8485 235	3.8364251	0.0006 56418	0.0307 0831	3.8606219	0.00122 1625	0.0487 3641
Gm4316	3.8134 0115	4.4258848	0.0001 03709	0.0078 7738	3.2009175	0.00054 8946	0.0284 5133
2210017I 01Rik	3.7582 2135	3.7749554	0.0003 08339	0.0174 0903	3.7414873	0.00204 2193	0.0670 6061
Sdcbp2	3.7492 632	3.7525678	0.0003 58785	0.0192 6094	3.7459586	0.00049 2094	0.0263 8541
Gm26760	3.7262 687	3.8574517	0.0000 54	0.0046 1844	3.5950857	0.00221 2789	0.0708 7159

Fgf22	3.7229 0475	3.7385335	0.0009 89732	0.0399 4299	3.707276	0.00077 0909	0.0354 1508
Igsf21	3.6312 8555	3.5434316	4.36E- 08	0.0000 116	3.7191395	0.00000 0883	0.0002 05881
Cpn2	3.5973 3565	3.60874	0.0000 274	0.0026 31514	3.5859313	0.00206 3791	0.0675 2605
Serpina1b	3.4670 722	3.4745827	0.0016 53028	0.0583 8964	3.4595617	0.00008 58	0.0072 58082
Rnf227	3.4254 097	3.4839013	0.0004 52054	0.0233 3883	3.3669181	0.00035 8966	0.0207 3113
Itih4	3.4130 0205	3.6710996	0.0000 184	0.0019 18291	3.1549045	0.00201 9021	0.0670 466
Zfp92	3.3481 806	3.4562456	0.0000 475	0.0040 91491	3.2401156	0.00278 6735	0.0820 9397
Esy3	3.3378 5275	3.3859763	0.0021 06574	0.0675 3707	3.2897292	0.00200 9684	0.0669 6003
Slc6a20a	3.2923 828	3.2217784	0.0002 77213	0.0162 1058	3.3629872	0.00247 1064	0.0763 9813
Hsbp111	3.2586 82	3.2908986	0.0000 385	0.0034 51486	3.2264654	0.00028 5941	0.0174 5584
Atp6v1b1	3.2569 9425	3.4230658	0.0000 3	0.0028 39367	3.0909227	0.00068 5012	0.0328 8058

Fmo2	3.2311 4585	3.2173516	0.0025 82901	0.0772 6117	3.2449401	0.00183 603	0.0637 6098
Mrap2	3.2017 3795	3.0797176	0.0003 41145	0.0187 0829	3.3237583	0.00318 8293	0.0888 2301
Bhmt	3.1052 899	2.9144579	0.0003 58285	0.0192 6094	3.2961219	0.00141 171	0.0539 5342
Akr1cl	3.0611 416	3.1170383	0.0000 0498	0.0006 70935	3.0052449	0.00069 2256	0.0328 8125
Pnpla3	3.0170 0575	2.7524821	0.0006 64488	0.0308 3411	3.2815294	0.00173 5113	0.0614 6595
Heph1l	3.0074 051	2.9798429	0.0001 19114	0.0086 68078	3.0349673	0.00000 0163	0.0000 503
Mroh6	2.9561 657	2.9983611	0.0000 356	0.0032 59991	2.9139703	0.00078 7323	0.0357 8724
Lrat	2.9298 446	2.9010163	0.0000 0329	0.0004 73656	2.9586729	0.00010 8658	0.0086 31896
Galnt9	2.9038 035	2.7872472	0.0000 0214	0.0003 25028	3.0203598	0.00011 7083	0.0090 63732
Hcar1	2.8542 398	2.8725399	8.61E- 11	4.81E- 08	2.8359397	1.86E- 08	0.0000 0736
Mlxipl	2.8440 47	2.9609792	2.83E- 09	0.0000 0106	2.7271148	0.00001 34	0.0017 13876

Arg2	2.8360 254	2.4576105	0.0014 44612	0.0528 1475	3.2144403	0.00147 0872	0.0556 3014
Calml3	2.8181 812	2.8317579	0.0025 36426	0.0761 0275	2.8046045	0.00353 9861	0.0948 4115
Hoxc10	2.7944 559	2.6586413	0.0002 22541	0.0138 6225	2.9302705	0.00029 9599	0.0179 2866
Rnf223	2.7850 074	2.747549	0.0000 158	0.0016 79883	2.8224658	0.00011 4644	0.0089 12852
Lipe	2.7684 13	2.7428357	0.0000 685	0.0056 05773	2.7939903	0.00011 2498	0.0088 60069
Lnx1	2.7660 264	2.8952246	0.0025 29331	0.0759 8932	2.6368282	0.00016 9338	0.0120 8078
Plin4	2.7136 9335	2.7040548	0.0005 26579	0.0258 4746	2.7233319	0.00055 8101	0.0287 6195
Ikzf3	2.6968 9745	2.8068438	5.15E- 08	0.0000 13	2.5869511	0.00000 698	0.0010 49934
Sod3	2.6565 936	2.6539325	0.0003 81356	0.0202 8973	2.6592547	0.00047 7099	0.0256 7868
Slc16a5	2.6423 855	2.4595466	0.0029 15949	0.0828 0272	2.8252244	0.00313 4485	0.0882 7019
Aqp7	2.5960 1715	2.5872793	9.32E- 08	0.0000 223	2.604755	0.00000 438	0.0007 44519

Aadac	2.5893 093	2.1532871	0.0002 30627	0.0140 9777	3.0253315	0.00000 0757	0.0001 81216
Serpinb9b	2.5616 705	2.525865	0.0011 4672	0.0447 8067	2.597476	0.00074 578	0.0346 2516
C130021I 20Rik	2.5265 0135	2.4469513	0.0004 21707	0.0221 7152	2.6060514	0.00126 4163	0.0497 7846
Il1r2	2.4920 162	2.5428933	0.0003 52847	0.0191 2132	2.4411391	0.00246 1836	0.0763 9813
Ankef1	2.4780 2665	2.3003459	0.0000 0208	0.0003 17972	2.6557074	2.58E- 08	0.0000 0939
Hsd17b2	2.4483 2165	2.4755422	0.0002 75395	0.0161 869	2.4211011	0.00202 6201	0.0670 4918
Foxl1	2.4353 3095	2.4798607	0.0000 0079	0.0001 42525	2.3908012	0.00003 51	0.0036 29047
Foxg1	2.4318 389	2.2541518	0.0004 4317	0.0229 8367	2.609526	0.00065 5058	0.0317 7817
Phyhipl	2.4220 518	2.4771461	0.0000 444	0.0038 83427	2.3669575	0.00020 2591	0.0137 5197
Zic3	2.3698 2155	2.4776571	3.23E- 09	0.0000 0116	2.261986	0.00025 8932	0.0162 6508
Cxcl9	2.3608 36	2.6107696	0.0000 00533	0.0001 02736	2.1109024	0.00118 4542	0.0476 752

Slc39a8	2.2951 3285	2.3079251	0.0020 71749	0.0667 9425	2.2823406	0.00270 5607	0.0806 8918
Rilp	2.2366 021	2.2016348	0.0000 0998	0.0011 85207	2.2715694	0.00017 0795	0.0121 3715
Paqr7	2.2274 586	2.0887359	0.0026 59106	0.0786 5119	2.3661813	0.00132 0006	0.0513 1099
Ccdc65	2.2265 053	2.1765871	0.0033 18951	0.0895 0625	2.2764235	0.00300 5905	0.0858 4525
Cpsf4l	2.2201 349	2.0081152	0.0000 33	0.0030 61027	2.4321546	0.00039 8916	0.0222 6099
Gabra2	2.2013 0815	2.3163083	4.09E- 15	6.69E- 12	2.086308	1.34E- 08	0.0000 0567
Rpl3l	2.2012 0155	2.2048951	0.0000 0701	0.0008 99501	2.197508	0.00003 68	0.0036 8292
Ccr9	2.1444 6105	2.1088027	0.0002 34562	0.0142 6225	2.1801194	0.00174 3217	0.0614 6595
Trbc2	2.0950 222	1.8759478	0.0008 47173	0.0363 6656	2.3140966	0.00105 7945	0.0444 4834
Plcx2	2.0793 5665	2.0878162	0.0000 0103	0.0001 78238	2.0708971	0.00000 516	0.0008 45275
Adam11	2.0734 6295	2.2736079	1.5E-13	1.49E- 10	1.873318	4.73E- 09	0.0000 0227

A530016	2.0623	1.9767906	0.0000	0.0008	2.1478747	0.00003	0.0037
L24Rik	3265		0645	34891		76	01712
Il34	2.0615	2.0122371	0.0004	0.0224	2.1107754	0.00161	0.0587
	0625		30753	8578		2048	7031
Neat1	2.0016	1.9952553	0.0007	0.0334	2.0079968	0.00099	0.0421
	2605		52698	3815		2082	7507
Ybx2	2.0013	1.8861278	0.0000	0.0002	2.1166342	0.00005	0.0048
	81		0185	89221		23	32629
Gpat3	1.9913	1.9999996	0.0002	0.0140	1.982773	0.00034	0.0199
	863		28729	1912		3403	5907
Rassf10	1.9782	1.9605995	0.0004	0.0239	1.9958294	0.00081	0.0366
	1445		69692	794		1521	3324
Gm13652	1.9662	1.9886565	0.0001	0.0084	1.9438117	0.00218	0.0703
	341		14918	70283		417	2641
Thrsp	1.9595	1.961981	0.0000	0.0000	1.957113	0.00000	0.0000
	47		00034	094		0131	412
Kenk3	1.9591	1.9501468	1.33E-	0.0000	1.9682157	2.25E-	0.0000
	8125		09	00546		08	0852
C3	1.9473	2.0761501	6.15E-	0.0000	1.8185636	1.16E-	9.63E-
	5685		08	152		10	08
Prdm1	1.9440	1.9036359	0.0036	0.0954	1.9843645	0.00003	0.0036
	002		95174	9546		6	62811

Clstn3	1.9333 427	1.3821394	0.0000 964	0.0074 41744	2.484546	0.00000 0189	0.0000 562
6430571L 13Rik	1.9119 0185	1.8866024	0.0000 103	0.0012 08441	1.9372013	0.00008 79	0.0073 39017
Cox7a1	1.9091 736	1.9253261	0.0000 0147	0.0002 4042	1.8930211	0.00000 973	0.0013 61737
Grap	1.8638 517	1.4786206	0.0000 461	0.0040 06838	2.2490828	0.00276 9617	0.0819 2662
Xdh	1.8549 2565	2.0813313	0.0001 54875	0.0105 9759	1.62852	0.00084 5496	0.0375 1529
Pparg	1.8536 7675	1.8185845	9.06E- 11	4.95E- 08	1.888769	9.16E- 10	0.0000 00505
B3gnt3	1.8093 8095	1.8587475	5.74E- 09	0.0000 02	1.7600144	0.00003 67	0.0036 8292
Kcnj12	1.8043 5635	1.8232229	0.0000 232	0.0023 20433	1.7854898	0.00005 43	0.0049 61957
Gpt	1.8000 433	1.8279976	0.0000 00906	0.0001 60374	1.772089	0.00000 997	0.0013 84221
Adora3	1.7956 4055	1.7709309	0.0027 0211	0.0794 1085	1.8203502	0.00169 1359	0.0608 9598
Chdh	1.7551 147	1.7869305	0.0000 00757	0.0001 37759	1.7232989	0.00000 713	0.0010 63803

Slc22a4	1.7519 0305	1.7092691	0.0013 607	0.0504 9946	1.794537	0.00307 2523	0.0870 6439
Lrrc2	1.7372 5495	1.6650091	0.0013 89267	0.0512 8207	1.8095008	0.00071 3631	0.0335 4621
Arl5c	1.7279 906	1.4833157	0.0001 47424	0.0102 7177	1.9726655	0.00034 2079	0.0199 5907
Actn3	1.7255 521	1.7192544	0.0000 0156	0.0002 52128	1.7318498	0.00000 165	0.0003 40385
Tbc1d9	1.7079 0525	1.7195719	0.0000 0253	0.0003 7631	1.6962386	0.00000 676	0.0010 3681
Eef1a2	1.7036 759	1.7063967	0.0000 00216	0.0000 468	1.7009551	0.00000 0367	0.0001 01214
5430421F 17Rik	1.6935 111	1.7237862	7.37E- 12	4.97E- 09	1.663236	0.00000 151	0.0003 14999
Galnt15	1.6893 336	1.6999159	0.0000 372	0.0033 69247	1.6787513	0.00036 8298	0.0211 359
Clec12b	1.6578 292	1.5994105	0.0001 79331	0.0118 467	1.7162479	0.00060 9215	0.0304 9177
Lars2	1.6530 0105	1.669386	9.3E-15	1.25E- 11	1.6366161	2.37E- 14	4.79E- 11
Slc6a4	1.6336 9365	1.6284184	0.0000 0091	0.0001 60374	1.6389689	0.00004 04	0.0039 07067

Cyp4b1	1.5963 3255	1.6024281	2.14E- 09	0.0000 00833	1.590237	0.00000 117	0.0002 55052
Cyp11a1	1.5910 5525	1.6752349	0.0000 7	0.0056 87176	1.5068756	0.00169 1994	0.0608 9598
Pnpla2	1.5825 4805	1.5840779	0.0000 176	0.0018 49282	1.5810182	0.00002 88	0.0031 50931
Trarg1	1.5750 265	1.5246332	0.0000 318	0.0029 60995	1.6254198	0.00017 8579	0.0126 4086
Akr1c14	1.5711 499	1.5414275	1.13E- 15	2.16E- 12	1.6008723	1.99E- 13	3.02E- 10
Nat8l	1.5548 563	1.5631604	0.0000 163	0.0017 33554	1.5465522	0.00009 06	0.0074 87741
Car3	1.5190 2705	1.5097084	0.0000 587	0.0049 21841	1.5283457	0.00005 59	0.0050 56174
Fabp4	1.5088 0905	1.5051494	0.0000 0201	0.0003 08933	1.5124687	0.00000 257	0.0004 76244
Smtnl1	1.5052 82	1.5000823	0.0000 649	0.0053 31356	1.5104817	0.00012 4356	0.0095 4551
Hmgcs2	1.4795 1665	1.532397	2.13E- 16	5.43E- 13	1.4266363	1.59E- 08	0.0000 0656
Ptch2	1.4791 2335	1.4888302	0.0001 5694	0.0106 4363	1.4694165	0.00025 6598	0.0162 0844

Tmem52	1.4696 229	1.43096	0.0012 51805	0.0479 8518	1.5082858	0.00250 2182	0.0767 5997
4631405J 19Rik	1.4654 1445	1.5297984	0.0015 54481	0.0559 8067	1.4010305	0.00370 613	0.0976 2611
Map3k8	1.4623 103	1.3940992	0.0024 24735	0.0745 0696	1.5305214	0.00115 7505	0.0472 1373
Yod1	1.4618 7195	1.4574647	0.0004 09875	0.0215 9898	1.4662792	0.00069 0536	0.0328 8125
Ankrd23	1.4501 585	1.4422485	0.0006 99137	0.0320 5265	1.4580685	0.00003 6	0.0036 62811
Glb112	1.4318 3845	1.4885074	0.0001 13872	0.0084 20295	1.3751695	0.00133 6404	0.0517 2737
Abhd15	1.4296 767	1.5184467	0.0002 03311	0.0129 4582	1.3409067	0.00032 0374	0.0189 2289
Rpl39l	1.4135 462	1.273931	0.0007 32043	0.0329 0316	1.5531614	0.00120 1651	0.0481 5074
Paqr9	1.3897 44	1.3597375	0.0001 52165	0.0105 0626	1.4197505	0.00105 699	0.0444 4834
Mgst1	1.3799 0525	1.3241958	0.0006 62539	0.0308 3411	1.4356147	0.00086 3819	0.0381 4223
Pou4f1	1.3629 907	1.0364957	0.0016 0418	0.0571 8913	1.6894857	0.00353 1195	0.0947 4853

Marchf3	1.3524 732	1.3623696	0.0003 81489	0.0202 8973	1.3425768	0.00110 5549	0.0456 0577
Cidea	1.3506 979	1.349717	0.0013 85028	0.0512 0805	1.3516788	0.00196 9142	0.0664 5323
Slc15a2	1.3383 06	1.2250164	0.0003 18984	0.0177 909	1.4515956	0.00007 13	0.0061 74384
Xirp2	1.3155 2885	1.3366952	0.0004 31608	0.0224 8578	1.2943625	0.00151 0168	0.0567 6236
Grik3	1.3044 818	1.3271674	0.0000 0722	0.0009 14908	1.2817962	0.00183 0583	0.0637 6098
Ddo	1.2950 2755	1.2618105	0.0020 53039	0.0664 6026	1.3282446	0.00351 3706	0.0946 9829
Coq8a	1.2805 609	1.3183673	0.0001 8338	0.0120 4473	1.2427545	0.00025 2999	0.0161 8898
Ly6a	1.2736 6485	1.2855778	7.74E- 15	1.11E- 11	1.2617519	1.76E- 10	0.0000 00128
Nptx2	1.2726 2775	1.2802752	0.0001 16109	0.0085 03426	1.2649803	0.00245 0891	0.0763 9813
Maob	1.2625 9575	1.2475261	2.27E- 08	0.0000 0668	1.2776654	0.00000 0965	0.0002 1948
Irf4	1.2617 859	1.281588	0.0000 0178	0.0002 80178	1.2419838	0.00078 8846	0.0357 8724

C130080	1.2530	1.3423976	0.0000	0.0000	1.1636735	0.00000	0.0006
G10Rik	3555		00502	983		35	05997
Shox2	1.2493	1.3819611	7.51E-	6.62E-	1.1166596	0.00085	0.0378
	1035		13	10		4037	0205
Ephx2	1.2368	1.2296278	0.0000	0.0009	1.2440036	0.00006	0.0055
	157		0762	54817		33	91281
Agpat5	1.2321	1.2302633	0.0009	0.0377	1.2340071	0.00095	0.0411
	352		02307	4267		6558	3878
Elfn1	1.2281	0.9830118	0.0028	0.0823	1.4731884	0.00046	0.0250
	001		77226	4039		0503	0739
Slc19a2	1.2231	1.2150321	0.0015	0.0564	1.231191	0.00303	0.0863
	1155		73746	5537		7908	5254
Mpz	1.2188	1.2320024	1.14E-	7.29E-	1.2056129	7.38E-	6.71E-
	0765		11	09		11	08
Twist2	1.1857	1.202303	0.0000	0.0016	1.1691977	0.00022	0.0150
	5035		151	25166		7576	5479
Dnaic1	1.1843	1.1402862	0.0008	0.0369	1.2283937	0.00247	0.0763
	3995		66387	1485		8576	9813
Ckmt2	1.1802	1.1717901	0.0003	0.0177	1.1886611	0.00025	0.0161
	256		16598	009		362	8898
Grem2	1.1777	1.1659476	1.33E-	0.0000	1.1894928	1.75E-	0.0000
	202		09	00546		08	0708

Mettl21c	1.1531 574	1.1554526	0.0000 0849	0.0010 34608	1.1508622	0.00123 5117	0.0490 1789
Agt	1.1498 2895	1.1534606	0.0008 3829	0.0360 6878	1.1461973	0.00203 7133	0.0670 6061
Tlcd4	1.1493 125	1.0880474	0.0034 26024	0.0906 8678	1.2105776	0.00091 6235	0.0396 8608
Fam89a	1.1437 301	1.1615103	0.0001 49866	0.0104 1024	1.1259499	0.00170 8273	0.0609 3512
Cpt1b	1.1420 7	1.2294797	0.0001 13837	0.0084 20295	1.0546603	0.00195 3878	0.0661 9173
Asb11	1.1387 043	1.1573739	0.0001 39709	0.0098 84395	1.1200347	0.00207 7071	0.0677 6234
Prxl2a	1.1308 715	1.0753449	0.0002 40172	0.0144 8806	1.1863981	0.00001 85	0.0022 74186
Tst	1.1283 553	1.1239682	0.0005 50295	0.0268 3916	1.1327424	0.00172 1962	0.0613 0318
Plac9a	1.1248 672	0.5690647	0.0027 49277	0.0800 3165	1.6806697	0.00005 93	0.0053 12523
Phkg1	1.1226 0855	1.1443068	0.0000 382	0.0034 34069	1.1009103	0.00084 405	0.0375 1529
Map2	1.0997 317	1.0610452	0.0011 56087	0.0449 1693	1.1384182	0.00230 8761	0.0732 5948

Nt5c3	1.0985 4505	1.0879982	0.0007 59306	0.0336 0149	1.1090919	0.00080 4768	0.0364 1875
Apod	1.0976 1515	1.0409323	4.64E- 13	4.26E- 10	1.154298	1.03E- 10	8.91E- 08
NA	1.0899 9245	1.0893448	1.05E- 09	0.0000 00465	1.0906401	5.64E- 10	0.0000 00354
Tuba4a	1.0893 2195	1.0754957	0.0016 78	0.0589 8413	1.1031482	0.00208 7682	0.0679 4118
Serpinb1a	1.0879 7675	1.1482467	5.18E- 08	0.0000 13	1.0277068	0.00003 71	0.0036 83429
Fam131a	1.0810 1995	1.1107487	0.0012 70647	0.0483 1546	1.0512912	0.00165 7388	0.0599 4275
Perml	1.0808 0845	1.0757254	0.0001 06355	0.0080 19655	1.0858915	0.00008 52	0.0072 39915
Cmah	1.0668 729	1.0899198	0.0000 0715	0.0009 10107	1.043826	0.00007 81	0.0067 37658
N4bp211	1.0561 884	1.0239707	0.0032 19711	0.0881 7855	1.0884061	0.00315 9857	0.0882 7076
Scn4b	1.0556 323	1.0516957	0.0000 00636	0.0001 20471	1.0595689	0.00003 42	0.0035 71045
Mmp19	1.0520 7975	1.0356999	0.0000 0172	0.0002 73197	1.0684596	0.00002 68	0.0030 26722

Lgals4	1.0496 651	1.016736	0.0000 892	0.0070 02951	1.0825942	0.00123 2804	0.0490 1789
Srgn	1.0327 425	1.0536041	0.0003 3239	0.0183 5993	1.0118809	0.00041 7749	0.0230 9937
Ndrg2	1.0245 238	1.0458427	0.0022 54264	0.0710 7907	1.0032049	0.00322 2286	0.0894 9591
Chchd10	1.0234 5355	1.0152782	0.0018 44621	0.0621 8271	1.0316289	0.00197 7286	0.0664 8945

## Appendix 3:

**Table 2.S3 Statistical analysis of the upregulated genes biological processes**

Upregulated Genes Biological Processes	P-value
Peptide Cross-linking <i>Crc1, Lce1a1, Lce1a2, Lce1b, Sprr2d</i>	3.1E-18
Keratinocyte Differentiation <i>Crc1, Lce1a1, Lce1a2, Lce1b, Sprr2d</i>	2.8E-15
Lipid Metabolic Process <i>Agpat5, Hmgcs2, Angptl8, Apod, Cpt1b, Cidea, Cyp11a1, Ephx2, Far2, Pnpla2</i>	9.0E-8
Epidermis Development <i>Fig, Lce1f, Lce1h, Ptch2, Sprr2d</i>	2.8E-8
Oxidation-Reduction Process <i>Ddo, Chdh, Cyp11a1, Far2, Fmo2, Sod3, Tryp1</i>	7.9E-4
Triglyceride Catabolic Process <i>Lipe, Pnpla2, Pnpla3, Plin1</i>	8.7E-4
Regulation of Lipid Metabolic Process <i>Angptl8, Hnf4a, Irs4, Pparg,</i>	3.8E-3
Brown Fat Cell Differentiation <i>Adipoq, Fabp4, Mrap, Pparg</i>	4.1E-3
Negative Regulation of Smooth Muscle Cell Proliferation <i>Ndr2, Adipoq, Apod, Pparg</i>	5.7E-3
Positive Regulation of Fatty Acid Biosynthetic Process <i>Mixipl, Agt, Hnf4a</i>	7.7E-3